

TRANSVERSE RESUMMATION FOR DIRECT PHOTON PRODUCTION

Name: Christopher Edmond Fink
Department: Department of Physics
Major Professor: Joseph F. Owens
Degree: Doctor of Philosophy
Term Degree Awarded: Spring, 2001

Quantum Chromodynamics predicts radiative terms which, at low transverse momentum Q_T of an observed multi-particle system, can be large enough to threaten the legitimacy of a fixed-order perturbative treatment. We present a subtraction-style calculation which sums these terms to all orders for a direct photon plus jet final state, and show that the kinematic effect of such a resummation is significant even after integration over the jet. An improved matching algorithm is prescribed for the transition to the high- Q_T perturbative regime, and re-examination of the nonperturbative regime indicates that simple Gaussian parametrizations are to be favored, with coefficients that depend not on the photon-jet mass Q , but on the color structure of the initiated subprocess. Agreement with data is significantly improved, and the method is expected to have applicability in general for processes with steeply-falling spectra.

THE FLORIDA STATE UNIVERSITY
COLLEGE OF ARTS AND SCIENCES

TRANSVERSE RESUMMATION FOR DIRECT PHOTON
PRODUCTION

By
CHRISTOPHER EDMOND FINK

A Dissertation submitted to the
Department of Physics
in partial fulfillment of the
requirements for the degree of
Doctor of Philosophy

Degree Awarded:
Spring Semester, 2001

The members of the Committee approve the dissertation of Christopher Edmond Fink defended on March 23, 2001.

Joseph F. Owens
Professor Directing Dissertation

Jack Quine
Outside Committee Member

Howard Baer
Committee Member

Vasken Hagopian
Committee Member

Elbio Dagotto
Committee Member

For my parents Robert and Catherine, my brother David, and his wife Lynn.

ACKNOWLEDGEMENTS

This dissertation could not have been achieved without the support, patience, and guidance of Professor Joseph (Jeff) Owens. I am deeply indebted for his close personal interaction and concern. My sincere thanks to every member of the High Energy Group at Florida State University for making this doctoral study such an educational and enjoyable experience. I would like also to extend my sincere appreciation to Professor Howie Baer, Professor Vasken Hagopian, Professor Elbio Dagotto, and Professor Jack Quine for reviewing this manuscript. Finally, a special thanks to Professor Duncan Carlsmith at the University of Wisconsin, Madison, without whose encouragement I might have settled on a different line of work.

TABLE OF CONTENTS

List of Tables	vii
List of Figures	viii
Abstract	x
1. INTRODUCTION	1
1.1 QCD as a Quantum Field Theory	1
1.2 The Parton Model	4
1.3 The Perturbative Domain	6
1.4 The Need for Resummation	10
1.5 Goals and Outline of this Work	14
2. QCD PERTURBATION THEORY	17
2.1 The QCD Lagrangian	17
2.2 Feynman Rules for QCD	19
2.3 Renormalization	21
2.3.1 Motivation	21
2.3.2 Canonical Procedure	25
2.3.3 Counterterm Method	26
2.3.4 Application to QCD	30
2.4 Factorization	31
3. EARLY RESUMMATION SCHEMES	46
3.1 Origin of Terms in the Unresummed Distribution	46
3.2 Development of a Resummation Scheme	49
3.3 Application to QCD	53
3.4 Subleading Terms	59
4. THE CSS FORMALISM	61
4.1 Derivation	61
4.2 Extension to the Nonperturbative Region	70
4.3 The Sudakov Exponent at very low b	72

5. KT-SPACE RESUMMATION	74
5.1 Kimber, Martin, and Ryskin	75
5.2 Ellis and Veseli	76
6. DIRECT PHOTON PRODUCTION	81
6.1 Two-Body Final States	84
6.2 Three-Body Final States	89
6.2.1 Partial-fraction Three-Body matrix elements	91
6.2.2 Reduce Three-body Phase Space.	93
6.2.3 Define and Subtract Approximations.	95
6.2.4 Perform Approximations	101
6.2.5 Perform y_3 -Integrals.	106
6.2.6 Map to Photon-Jet space	109
6.2.7 Extract Poles in ϵ	111
6.3 Add Born, Virtual, and Counterterm Contributions.	114
6.4 Cancel Poles and Take $\epsilon \rightarrow 0$	114
6.5 Extract Resummation Parameters	116
6.6 Matching Resummed and Fixed-Order Results	121
7. RESULTS AND CONCLUSIONS	126
7.1 Photon p_T Distributions	126
7.1.1 Nonperturbative Parameter Choices	131
7.2 Other Parameter Choices	149
7.2.1 Scale Dependence	149
7.2.2 Jet Cone Width	149
7.3 Conclusions and Future Improvements	155
APPENDICES	
A. DIAGRAMS AND MATRIX ELEMENTS FOR NLO PHOTON HADROPRODUCTION	157
B. USEFUL INTEGRALS	170
C. DETAILED NLO RESULTS	182
D. THE MONTE CARLO METHOD IN HIGH ENERGY PHYSICS	194
REFERENCES	208
BIOGRAPHICAL SKETCH	213

LIST OF TABLES

2.1	Splitting function pieces.	43
4.1	Nonperturbative Parameters.	72
6.1	Soft limits of invariants.	102
6.2	$p_{\bar{a}} \cdot p_3 = 0$ collinear limits of invariants.	103
7.1	Anomaly at low Q_T	153

LIST OF FIGURES

1.1	Lowest Order (Born) Drell-Yan diagram, $ \mathcal{M} ^2 \sim [e^2]^2 \sim \alpha^2$.	8
1.2	Gluon Bremsstrahlung diagram, $ \mathcal{M} ^2 \sim [e^2 g]^2 \sim \alpha^2 \alpha_s$.	8
1.3	Compton diagram, $ \mathcal{M} ^2 \sim [e^2 g]^2 \sim \alpha^2 \alpha_s$.	9
1.4	Virtual Drell-Yan diagram, $ \mathcal{M} ^2 \sim [e^2 g^2]^2 \sim \alpha^2 \alpha_s^2$.	9
1.5	Intrinsic transverse momentum.	11
2.1	Feynman Rules for QCD.	20
2.2	Symmetry factors.	22
2.3	Building the full propagator.	24
2.4	Factorization of the hadronic interaction.	33
2.5	LO $q\bar{q} \rightarrow \gamma\gamma$ diagrams.	36
2.6	$q\bar{q} \rightarrow \gamma\gamma g$ diagrams.	37
2.7	$p_1 \cdot p_5 = 0$ collinear kinematics.	38
2.8	$q\bar{q} \rightarrow \gamma\gamma$ virtual diagrams.	45
3.1	A single radiated photon in the initial state.	47
3.2	Multiple radiated photons in the initial state.	49
3.3	Resummation brings the low- Q_T region under control.	52
3.4	Three regions of interest.	54
3.5	$pp \rightarrow \mu^+ \mu^- X$ resummed distribution.	58
6.1	\vec{p}_3 inside jet cone.	91
6.2	$p_{\bar{a}} \cdot p_3 = 0$ collinear kinematics.	103
6.3	Scale dependence of parton distributions.	122
6.4	Fixed-order perturbative result better at high Q_T .	123
7.1	$p\bar{p} \rightarrow \gamma + X$ at $\sqrt{S} = 1800\text{GeV}$.	128
7.2	$pBe \rightarrow \gamma + X$ at $\sqrt{S} = 38.7\text{GeV}$.	129
7.3	$pBe \rightarrow \gamma + X$ at $\sqrt{S} = 31.5\text{GeV}$.	130

7.4	k_T -space resummation : k_{Tlim} -dependence.	132
7.5	k_T -space resummation : \tilde{a} -dependence.	133
7.6	b -space resummation : reference distribution.	135
7.7	b -space resummation : g_1 dependence.	136
7.8	b -space resummation : g_2 dependence.	137
7.9	Adding Q -dependence to k_T -space NP form.	139
7.10	Removing Q -dependence from b -space NP form.	140
7.11	E605 b -space predictions, standard 2-parameter form.	142
7.12	E605 b -space predictions, w/out Q -dependence.	143
7.13	R209 b -space predictions, with and w/out Q -dependence.	144
7.14	E706 $\sqrt{S} = 31.5\text{GeV}$, with NP color dependence.	146
7.15	E706 $\sqrt{S} = 38.7\text{GeV}$, with NP color dependence.	147
7.16	D0 $\sqrt{S} = 1800\text{GeV}$, with NP color dependence.	148
7.17	Scale Dependence.	150
7.18	Q_T -distribution : Initial-state pieces.	151
7.19	Q_T -distribution : Final-state pieces.	152
7.20	Comparison of full and approximate jet definition results.	154
A.1	Basic couplings.	157
A.2	Leading order photon hadroproduction diagrams.	158
A.3	NLO direct photon Green's functions.	159
A.4	Time-ordered Feynman diagrams from (a) and (b)	167
A.5	Time-ordered Feynman diagrams from (c) and (d)	168
A.6	Virtual Contributions.	169
D.1	$\pi^- p \rightarrow \gamma\gamma X$ pair p_T distribution.	207

ABSTRACT

Quantum Chromodynamics predicts radiative terms which, at low transverse momentum Q_T of an observed multi-particle system, can be large enough to threaten the legitimacy of a fixed-order perturbative treatment. We present a subtraction-style calculation which sums these terms to all orders for a direct photon plus jet final state, and show that the kinematic effect of such a resummation is significant even after integration over the jet. An improved matching algorithm is prescribed for the transition to the high- Q_T perturbative regime, and re-examination of the nonperturbative regime indicates that simple Gaussian parametrizations are to be favored, with coefficients that depend not on the photon-jet mass Q , but on the color structure of the initiated subprocess. Agreement with data is significantly improved, and the method is expected to have applicability in general for processes with steeply-falling spectra.

CHAPTER 1

INTRODUCTION

1.1 QCD as a Quantum Field Theory

In particle physics we are continually searching for the most fundamental description of matter and the forces which govern its behavior. Those who wonder about the properties of macroscopic objects may now look to molecular and atomic physics; those who inquire about the structure of the atom may now be answered with the details of electrons and nuclei. In each case a multitude of types of matter has been replaced by a more fundamental set, the variety of types being replaced by a variety of ways these types can combine to form bound states. Concurrently, a unified description has arisen for many forces once thought disparate.

The situation is no different for the atomic nucleus or its inhabitants. In addition to radiation observed naturally, data on nuclear structure came from experimental probes of the nucleus, usually involving beams of particles known to be themselves structureless. As more energy was made available, the same method was used to probe individual nucleons (protons and neutrons). The mid-20th century saw a proliferation of new strongly-interacting particles (collectively known as *hadrons*) as the energy barrier for their discovery was crossed, and again it became natural to look for common properties (“good quantum numbers”), clues to a symmetry on a deeper level.

In 1963, motivated by the observation that the known hadronic families seemed to exhibit symmetries of a particular branch of mathematics known as *Lie groups*, Gell-Mann [1] and Zweig [2] proposed a model of hadronic structure based on a

limited assortment of sub-nucleonic constituents called *quarks*. Each quark came in a particular *flavor*, had fractional electric charge, and had a corresponding antimatter partner of opposite charge. Together, they were able to be combined in ways that reproduced the known subnuclear spectrum.

However, there was a spin-statistics problem. Systems of *fermions* (particles of half-integer spin, like the quark) must have wavefunctions which are totally antisymmetric under interchange of any two particles, while total symmetry is required of *boson* (integer-spin particle) collections. The quark model posited that all hadrons were quark (fermion) combinations, those of half-integral spin (the *baryons*, such as the proton and neutron), being composed of three quarks, and those of integral spin (i.e. *mesons*) composed of a quark and antiquark. Unfortunately, some of these combinations required symmetry in spin, space, and flavor, leading to a totally symmetric wavefunction. If the above compositions of baryons and mesons were correct, a new degree of freedom was required in which to properly perform the antisymmetrization [3].

A new type of charge, posited by Greenberg [4] and which eventually became known as *color* [5], thus solved the statistics problem. Again, group theory was instrumental (in this case a color $SU(3)$ fundamental representation). With three colors, hadrons could be properly antisymmetrized if each quark in a baryon was a different color, but those in mesons were of the same color. The quark model seemed to be rescued, despite the fact that no individual quarks, or any other “colored” states, had been seen in the laboratory. The lack of experimental evidence for anything but colorless states could be postulated as a rule (*color confinement*), but without an understanding of the forces present among quarks, such rules would remain baseless.

Classical theory described interaction at a distance in terms of fields, with forces that depended on the charges of the particles involved and the distance between them. Modern quantum theory, although maintaining use of the term

“field”, had replaced the concept with the (macroscopically equivalent) exchange of quanta, specific to the type of charge involved, which carried energy and momentum across the intervening distance. One theory of this type, Quantum Electrodynamics (QED), had already been successful in remodeling the electromagnetic interaction between charged particles (as well as all the known properties of light) in terms of intermediate, long-range bosons called *photons*.

It had also long been known that symmetries of field theories gave rise to conserved quantities, like charge and momentum. In particular, conservation of electric charge in the coupled system of photons and charged particles was shown to be a consequence of the symmetry of the theory with respect to certain local *gauge* transformations, performed simultaneously on all fields. As the quarks had not only electric but color charge, both of which were expected to be conserved, it was natural to look for gauge bosons of the color force. However, unlike the electromagnetic interaction, this force was known to become **weaker** at higher momentum transfer; that is, the individual quarks behave more like free particles [6–7]. This property, *asymptotic freedom*, was searched for in the known quantum field theories, and found eventually to be associated exclusively with those gauge theories in which the generators of the group symmetry do not commute; i.e. are *non-Abelian* [8–11].

Fritzsch and Gell-Mann proposed, then, that the group symmetry of a non-Abelian gauge field be associated with color symmetry, and Quantum Chromodynamics (QCD) was born [12–13]. The gauge bosons of this theory, called *gluons*, have eight members, corresponding to the number of elements in the adjoint representation of the $SU(3)$ color group. They couple to the color charge of the quarks, binding them together within the hadron. Being non-Abelian in nature, they also carry the color charge themselves and thereby couple with one another (unlike the photons of QED, which are Abelian). Not only does this explain the strengthening of the strong force with distance, and consequently why we do not see any free quarks or gluons (collectively known as *partons*), but also has implications for the question

of color confinement.¹ Indeed, Wilson [15] has shown that, for sufficiently strong coupling, the only finite-energy asymptotic states of QCD are colorless. Any attempt to separate one parton from another results only in the creation of a quark/antiquark pair somewhere in the intervening distance, the resulting colorless states propagating outward as everyday hadrons. This is the process of “fragmentation” or *hadronization*.

1.2 The Parton Model

Asymptotic freedom brings with it benefits and constraints. The collision of two hadrons is an enormously complex problem, and cannot be solved exactly, as the component partons can interact in infinite combinations. First, as we are not able to directly observe individual partons, we do not *a priori* know the precise distribution of momentum among the quarks inside the nucleon, nor can we predict from first principles the number of each type represented at a given energy. Just as an electron is at all times surrounded by its own cloud of photons and electron-positron pairs produced by these photons, which tend to alter the effective charge seen by a neighboring charge, so too do the quarks constantly emit and reabsorb gluons, themselves producing a cloud of quark-antiquark pairs. Increasing the interaction energy only serves to probe deeper into the cloud, thus changing the effective distribution [16]. Thus we find that the best description we can achieve of the nucleon at high energy is, probabilistically, a set of continuous densities, one for each flavor/antiflavor, plus a gluon density. These *parton distribution functions* give the probability of finding a certain type of parton (quark flavor or gluon) at a certain momentum fraction and interaction energy within the nucleon. Although prediction of these densities is ultimately a non-perturbative endeavor, we **can** perturbatively derive the relationship between densities at different interaction

¹The term “parton”, coined by R.P. Feynman [14] before the advent of QCD (and in a purely dynamical context), has since been identified with its basic building blocks.

energies. Measurement of the densities at one energy thus provides predictions for the rest.

Secondly, if the final state of interest contains particular hadrons that are to come from partons involved in the scattering process, instead of attempting to describe quantitatively the mechanism by which this hadronization occurs, we can currently account for it only phenomenologically, by introducing a *fragmentation function* for each of these partons. In a manner analogous to the parton distribution functions, these give the probability that a certain hadron will be produced from the fragmenting parton, with a specific fraction of that parent's momentum. Both distribution functions and fragmentation functions must ultimately be measured by experiment.

The good news of asymptotic freedom, however, is that at small distances (and correspondingly high collision energies), the strong force decreases and the partons behave more like free particles [17]. This allows us to *factorize* what we can perturbatively describe (the interaction of free partons) from what we can't (distributions and fragmentation). In the *parton model* of high-energy hadronic collisions, the initial reaction takes place over such a small time scale that it becomes plausible to treat each hadron as a collection of free partons, each traveling in the same direction as the parent hadron, and only one of which takes place in any given "hard scattering". That is, one may calculate basic subprocesses involving one parton from each hadron, then sum incoherently over the contributions of all partons via convolution with the parton distribution functions. Similarly, the process of fragmentation is assumed to take place over a time scale much longer than the hard scattering, and can therefore also be treated independently. Thus a description of hadronic collisions is necessarily built up from both perturbative and non-perturbative pieces.

One of the conveniences the new quantum model allows is the schematic representation of a subprocess as a *Feynman diagram*, each fermion or boson being represented

by a line. Line intersections (*vertices*) can represent instances of absorption, emission, or pair production, depending on the direction of time. To each element of this picture a mathematical expression is assigned, in such a way that one can easily derive the correct expression for a subprocess: one simply draws its diagram, starts at one end, and follows the lines and vertices, writing down the corresponding factors in order. The result is called the *amplitude* for the reaction, and its magnitude squared is a measure of the probability that the incoming particles will interact in precisely this way to form the outgoing particles. Since it is the vertices at which the force is felt, the overall strength of the reaction and its probability for occurring become dependent upon the number of vertices in the diagram.

Of course, for a given set of external lines, there is an infinite number of diagrams that could be built. Each makes a contribution to the total probability for the reaction, in relation to its *order*, or exponent of the coupling strength. It becomes clear that if we hope to make meaningful predictions through this *perturbation theory*, this relation must be inverse, *i.e.* the coupling constant (unit of charge) used must be less than one. Otherwise, the diagrams with the largest contribution would be the ones with the most vertices, and we cannot analyze an infinite number of diagrams. With a small coupling constant, we can usually stop at first or second order, confident that the higher-order diagrams are of negligible contribution (an important exception will be discussed in Section 1.4).

1.3 The Perturbative Domain

Having a small coupling constant is not necessarily enough; if the coefficients of successive orders grow, we may lose the applicability of perturbation theory. Hence, while in many cases we are justified in calculating only to leading order (LO), to confirm the convergence of the series and provide corrections to the leading-order result, we must often look at the next-to-leading order (NLO) terms as well [18]. *Loop* diagrams, having the same external legs but more internal vertices, will of

course contribute, as will the release of *bremsstrahlung* radiation which inherently accompanies acceleration of charged particles. Thus *inclusive* data is considered (all events are kept which contain the desired final state particles, regardless of the detection of additional debris), and all contributing diagrams up to a given order are calculated.

As an example, we'll show the leading order (LO) and next-to-leading order (NLO) contributions to the production of a muon pair in hadronic collisions. At lowest order, there is but one contributing subprocess, proposed initially by Drell and Yan [19–20]. A quark from one hadron annihilates with an antiquark from the other to produce a vector boson (hereinafter chosen to be a photon), which subsequently decays to a muon-antimuon pair. The expansion so far consists of one term of second order in the electromagnetic coupling α , zeroth order in the strong coupling α_s (see fig. 1.1). Order $\alpha^2\alpha_s$ subprocesses include gluon bremsstrahlung from one of the incoming quarks (fig. 1.2), and quark-gluon scattering (fig. 1.3), which produces an additional quark in the final state. The exchange of a gluon between incoming quarks is a contribution of order $\alpha^2\alpha_s^2$ (fig. 1.4); its interference with the Born term, however, leads to an α_s^1 quantity. Photon bremsstrahlung or exchange is also a possibility, but these order α^3 processes are suppressed by the small size of α/α_s .²

As a rule, bremsstrahlung and loop terms contain various mathematical singularities as masses and momenta are taken to certain limits, but these divergences can all be removed consistently in the full theory, as they must to avoid the absurdity of an infinite cross section [21–24]. *Infrared* singularities arise from both bremsstrahlung and loop diagrams, in the limit of zero radiative energy, and cancel if these con-

²In the diagrams, solid lines denote quarks, wavy lines photons, and curly lines gluons. The coupling constants e (electromagnetic) and g (strong) are more commonly traded for the quantities $\alpha \equiv e^2/4\pi$, $\alpha_s \equiv g^2/4\pi$.

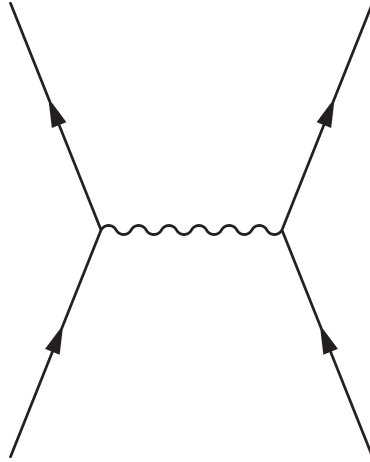


Figure 1.1. Lowest Order (Born) Drell-Yan diagram, $|\mathcal{M}|^2 \sim [e^2]^2 \sim \alpha^2$.

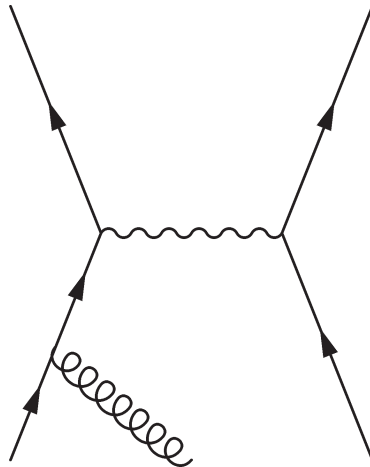


Figure 1.2. Gluon Bremsstrahlung diagram, $|\mathcal{M}|^2 \sim [e^2 g]^2 \sim \alpha^2 \alpha_s$.

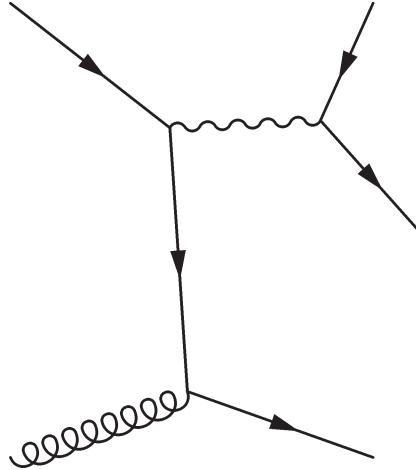


Figure 1.3. Compton diagram, $|\mathcal{M}|^2 \sim [e^2 g]^2 \sim \alpha^2 \alpha_s$.

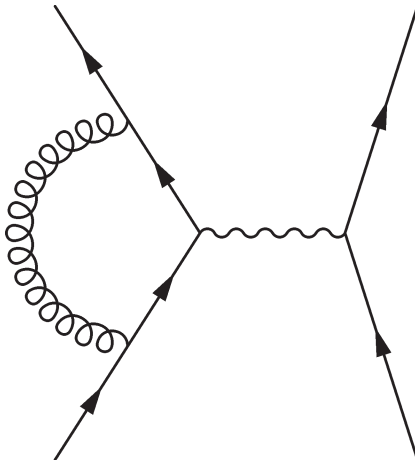


Figure 1.4. Virtual Drell-Yan diagram, $|\mathcal{M}|^2 \sim [e^2 g^2]^2 \sim \alpha^2 \alpha_s^2$.

tributions are both included. Loop diagrams also contain *ultraviolet* divergences at infinite loop momentum, and these are factored into a redefinition, or *renormalization* of the (unobservable) bare masses and couplings. The remaining class of divergence arises in the limit that bremsstrahlung radiation becomes parallel with the emitting particle. These *collinear* singularities are factored into a redefinition of the parton distribution functions (or *PDFs*, the probabilities that the colliding hadrons contain the relevant partons). In both renormalization and collinear factorization, the singularities (or *poles*) are accompanied at order α_s^n by a power series of logarithms involving an energy characteristic of the subprocess, *e.g.* the invariant mass Q of the muon-pair. In the *leading log approximation*, the largest of these logs at each order is summed over all orders and factored into the couplings and PDFs also, making them energy-dependent.³ As it has been shown that (for each parton species) the divergent logs arise in the same way for all processes with a large scale [25–27], once the new coupling and distributions are calculated, they are transportable in this approximation to other reactions. A lot of work is saved in the rough calculation of a new process, as only the Born subprocess need be derived, and the most dangerous higher-order terms accounted for by convoluting the Born term with the new coupling and parton distributions [28–29]. Further improvement comes, of course, with the inclusion of subleading higher-order terms, but as we shall see, even this may not be sufficient for processes which also involve a small scale.

1.4 The Need for Resummation

During the late 1970’s, the leading log approximation was applied to a number of processes [30], although we will focus here on muon pair production. In addition

³These energies are historically called *scales* (the collinear in particular being the *factorization* scale, which we’ll denote as M_f). One of the assumptions of the early, or “naïve”, parton model was that the parton distributions should “scale with” the momentum of the parent hadron; i.e. should depend only on the momentum **fraction** involved. As we are here taking our picture of the hadron as a hierarchy (or cloud) of partons which we sample at an effective resolution $1/M_f$, and building it into a redefinition of the parton distributions, this is no longer a valid assumption, though we transfer the terminology.

to single-scale observations such as the invariant mass Q of muon pairs [27, 31–34], physicists looked at correlations between the muons, such as the transverse momentum imbalance, that is, the **total** Q_T of the pair (here and throughout the text, we’ll use “ Q_T ” to denote the transverse momentum of a system of two or more particles, and “ k_T ” or “ p_T ” for single particles). To a good first approximation, at relativistic speeds along a single beam line, the constituents of hadronic interactions present no transverse momentum relative to each other or the beam, and thus at Born level (just the Drell-Yan subprocess), there should be no imbalance, and we get a delta function at total $Q_T = 0$.⁴ The available data [37] indeed showed the cross section to be largest at $Q_T = 0$, falling off gradually (although still steeply) with increasing Q_T . This data being inclusive, the contribution at $Q_T \neq 0$ could be due to “recoil” of the pair against bremsstrahlung from the initial state partons, recoil against a final-state quark in the quark-gluon “Compton” subprocess described above, or some nonperturbative, “intrinsic” p_T of the incoming partons (see figure 1.5) . The former having not yet been calculated, it was unclear how much of a contribution was to be ascribed to each of these effects, and the approach varied among researchers.

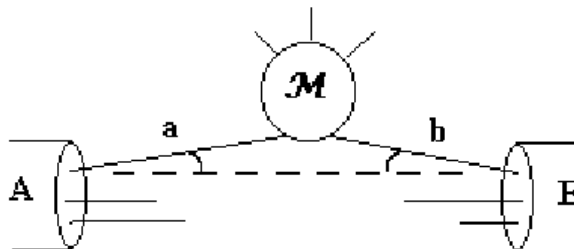


Figure 1.5. Intrinsic transverse momentum.

⁴Indeed, the “naïve” parton model takes this as a starting point; the current “effective constituents” interpretation recognizes that there are no natural cutoffs that would limit the transverse momenta of partons relative to their parent hadrons, and hence we’re led to the idea of “intrinsic” parton p_T [35–36].

A leading log calculation with simple Drell-Yan as the Born term admitted only intrinsic p_T , and thus some attempted a description solely through p_T -scaling of the parton distribution functions [38–39]. This would “smear” the zero- Q_T delta function into a more physical, Gaussian shape, and it was hoped that the amount of intrinsic p_T needed would be small. This turned out not to be the case [40]. When in fact the next-to-leading order bremsstrahlung and Compton subprocesses were calculated, although the large- Q_T region seemed to be sufficiently accounted for, an unacceptable low- Q_T prediction remained. Some authors simply left their results as valid only in the high- Q_T region [41–42]. Others, notably Altarelli, Parisi, and Petronzio, were able to devise a model of intrinsic p_T which also brought the low- Q_T distribution under control [29, 43]. The average intrinsic p_T required, however, was still a matter of phenomenology, not derivation. In the same way that the factorization and renormalization scale dependences of a leading-log calculation are reduced when next-to-leading (and higher) contributions are added, higher-order calculations were needed which focused on transverse momentum effects.

It was recognized that the incoming quarks could radiate any number of undetectable gluons, if the “jets” of hadrons thus produced had energies less than the trigger threshold, and that this additional, *soft* radiation could collectively influence the transverse recoil of the observed final state. An initial attempt to attack these contributions was undertaken in 1978 by Dokshitzer, D’Yakanov and Troyan (DDT) [44], who showed that in the soft limit, a pattern emerged as one went to higher orders. Careful inclusion of n gluons into the final state shows that even after the cancellation of the infrared divergence at $Q_T = 0$, there remains a series of logarithms at order n in the strong coupling of the form ⁵

⁵The “+” designation can here be thought of as a simple reminder that the pole at $Q_T = 0$ is removed. Later, in Section 2.4, we’ll introduce “plus-distributions” more formally. Neither these logs nor the leading order delta function at $Q_T = 0$ are sufficiently physical representations of an actual Q_T -distribution; their combination into such a representation is the goal of *resummation*.

$$\frac{1}{Q_T^2} \sum_{m=0}^{2n-1} [\ln(Q^2/Q_T^2)]_+^m. \quad (1.1)$$

At first glance, more gluons seems to make the problem worse. At high Q_T (close to the mass Q), these contributions are small. At low Q_T , however, we have a two scale problem, the contributions of which may easily overwhelm the smallness of α_s^n . The convergence of a perturbative expansion is thus thrown into doubt. Furthermore, as was shown by Altarelli, Ellis, and Martinelli (1979) [33], this is the case no matter how you define the parton distribution functions.

That a pattern existed, however, with at least the largest ($m = 2n - 1$) logs sharing a common coefficient across orders, allowed DDT to *resum* this tier of logarithms over all orders, yielding a finite result at $Q_T = 0$. Their method, flawed by a lack of regard for the conservation of momentum among the emitted gluons, was improved upon by Parisi and Petronzio in 1979 [45–46]. The new procedure used the momentum-conserving delta function to Fourier transform the cross section into impact parameter space, perform the sum there, and transform back to momentum space. The amount of intrinsic p_T needed to reproduce the data was drastically reduced, though the extremely low- Q_T region still required some such nonperturbative help.

A later analysis (1981) by Collins and Soper [47] for the reverse Drell-Yan process uncovered a systematic way to include subleading logs, thus improving the perturbatively-tractable region, and provided a model for non-perturbative effects, allowing the prediction to extend to even smaller transverse momenta. In 1984, Altarelli, Ellis, Greco, and Martinelli [48], along with Collins, Soper and Sterman [49], reapplied this formalism to the general case of intermediate vector boson production in hadronic collisions, and it became evident that reduction of the required intrinsic p_T was linked in large part to systematic addition of further tiers of subleading logs. This reflected the fact that ultimately both intrinsic and recoil

contributions derive from parton interactions, whether internal or external to the unobservable “dissociation” of the hadron.

1.5 Goals and Outline of this Work

Although the bulk of resummation work has been devoted to Drell-Yan and other intermediate vector boson processes, the methods have recently been shown beneficial in the prediction of other processes with steeply-falling transverse momentum spectra [50]. These include double jet (*dijet*) production [51] and direct double photon production [52–53].

The study of hadronic photon production is important for a number of reasons. Single photon production, due to its leading-order dependence on the gluon content of the incoming hadrons, serves as a good test of our knowledge of these densities. By comparing the results of single and double photon production, the strong coupling may be evaluated. Finally, in the ongoing search for the Higgs, theory predicts a two photon decay, making precise calculation of the direct reactions necessary for elimination of background events.

However, the focus of most of the literature has been on observed systems of two or more particles; less well-known is the effect of resummed soft radiation on single-particle p_T spectra. This is not surprising, as the resummed logarithms arise naturally only when asking questions about the properties of multi-particle systems. Any transverse “kick” from unobserved radiation, though, should distribute itself among the observed particles, and it is only natural to ask about this distribution as well. In this dissertation we apply the current resummation techniques intermediately to a direct photon plus jet final state, and show that the kinematic effect on the photon p_T is significant even after integration over the jet.

This requires that we keep track of more variables, and, unlike many previous calculations, refrain from integrating over them analytically. This is beneficial from an experimental standpoint as well. In order to extract useful signals in practice,

it is sometimes necessary to make kinematic cuts on the detected particles. These cuts may not be expressible analytically at the parton level, where the integrations need to be done, as there is usually a complicated mapping among the associated variables. A multitude of convoluted holes may appear in the partonic phase space, thus making of little versatility formulae in which the relevant variables have already been integrated over a continuous, predetermined range. In addition, jet definitions, detector acceptances, and kinematic cuts are often changed, necessitating full recalculation of analytic predictions.

We will handle experimental cuts by performing the required integrals via a Monte Carlo approach. By taking advantage of the method's ability to calculate Jacobians automatically, changes in applied cuts are easily accommodated, and added benefits include the ability to calculate any number of observables simultaneously [54–55]. Precedence has been set for the application of Monte Carlo to photon physics, as Bailey, Owens, and Ohnemus [50, 56] performed such studies in the early 1990's, incorporating a synthesis of NLO analytic and Monte Carlo methods to predict the photon p_T distribution. Inclusion of soft gluon effects is the focus of the current work, with the expectation that the resultant method will have applicability to other single-particle predictions.

In Chapter 2, the fundamentals of QCD perturbation theory are presented, starting with the development of the Lagrangian and the Feynman rules for calculating subprocess matrix elements. We discuss the singularities that arise in different types of diagrams, and the manner in which they disappear in the full theory via the process of renormalization. Finally, we describe the QCD hard scattering formalism, which combines the perturbatively calculable matrix elements with the experimentally determined parton distributions to arrive at predictions for observable quantities.

Chapters 3, 4, and 5 together present the evolution of current techniques for the resummation of those large residual logarithms which arise naturally in perturbation theory, but are problematic for its convergence. Chapter 3 motivates a statement

of the problem and offers the first attempts at a solution. Chapter 4 describes the efforts of Collins, Soper, and Sterman to derive a more comprehensive picture, and solution via a transform to impact-parameter space. Chapter 5 reviews both the manner in which this formalism may be analytically simplified and its connection with the idea of intrinsic parton transverse momentum.

Using the diagrams and corresponding matrix elements of Appendix A, in Chapter 6 we begin the process of calculating the pieces of a NLO direct photon (plus jet) cross section. Contributions from three-body final states are approximated in the singular regions of phase space, and these approximations are both subtracted from the original (to provide one finite piece) and added to the virtual two-body terms (which are singular but of the opposite sign) to provide another finite piece. Along the way, we perform a number of analytical integrations, collected for reference in Appendix B. Casting these finite pieces in a form congruent to that of the NLO expansion of our resummation scheme, we then simply read off the coefficients of the original resummed form. Detailed calculational results are presented in Appendix C. Finally, we present a method for matching the resummed and perturbative results at the boundary between their regions of applicability.

Crucial to the versatility of this calculation is the use of Monte Carlo techniques for performing remaining integrals, and a short treatise on these techniques is included in Appendix D. With the resulting FORTRAN program (available upon request), we produce physical predictions for the single direct photon p_T spectrum at a variety of energies; these results, and general conclusions, are presented in Chapter 7. Observations on the form of the nonperturbative parametrization are also discussed there.

CHAPTER 2

QCD PERTURBATION THEORY

2.1 The QCD Lagrangian

We begin by constructing the QCD Lagrangian, from which the equations of motion and scattering matrix follow. The Einstein summation convention will be used throughout, in which repeated indices are to be summed over.

The quarks will be represented by Fermi-Dirac fields $\psi_{f,i}(x)$ of flavor f , color i , and mass m_f . Such fields obey the Dirac equation, and so for a system of free quarks we would have but

$$\mathcal{L}_q = \bar{\psi}_{f,i} [i\gamma^\mu \partial_\mu - m_f] \psi^{f,i} . \quad (2.1)$$

Here the flavor index f runs over the number of flavors N_f , while the color index i (and later, j) runs over the number of colors N_c . Once we impose local $SU(N_c)$ gauge invariance, the existence of gauge boson fields (the gluons) $A_\mu^a(x)$ becomes necessary, as we must replace the gradient ∂_μ with the covariant derivative $D_\mu = \partial_\mu \delta^{ij} + ig(T_a)^{ij} A_\mu^a$. There are $N_c^2 - 1$ such fields, corresponding to the number of elements in the adjoint representation of the symmetry group, and we'll use the indices $\{a, b, c\}$ to distinguish them. The generators T_a form a basis for the Lie algebra of the $SU(N_c)$ symmetry group, and obey the commutation relations

$$[T_a, T_b] = if_{abc} T_c \quad (2.2)$$

$$\{T_a, T_b\} = \frac{\delta_{ab}}{3} + d_{abc}T_c . \quad (2.3)$$

The f_{abc} are totally antisymmetric, and are called the *structure constants* of the group. The d_{abc} are totally symmetric.

Now that we have gluons, we need to include a kinetic term for these fields which preserves local $SU(N_c)$ invariance. With field strength tensors given by

$$F_{\mu\nu}^a = \partial_\mu A_\nu^a - \partial_\nu A_\mu^a + gf_{abc}A_\mu^b A_\nu^c , \quad (2.4)$$

a suitable construction is simply

$$\mathcal{L}_g = -\frac{1}{4}F_a^{\mu\nu}F_{\mu\nu}^a . \quad (2.5)$$

In contrast to the photons of QED, an Abelian theory, the gluons of QCD couple to each other, as indicated by the third term in equation 2.4. As in QED, however, the boson fields as currently written have extra, unphysical degrees of freedom. We can get rid of these by imposing a *gauge-fixing* condition, and there are many options, not all of which preserve relativistic covariance. The *Lorentz* condition, $\partial_\mu A_a^\mu = 0$, does however, and leads to the Lagrangian term

$$\mathcal{L}_{fix} = -\frac{1}{2\zeta} \left(\partial_\mu A_a^\mu \right)^2 . \quad (2.6)$$

Use of a covariant gauge is not, unfortunately, a sufficient constraint. The longitudinal polarization of the gluon fields remains, and if not dealt with can destroy the unitarity of scattering amplitudes. Fortunately, as was shown by Faddeev in 1967, one can couple a set of scalar *ghost* fields ϕ_a to the gluons in such a way as to cancel the unwanted degrees of freedom. As there are $N_c^2 - 1$ such degrees of freedom (one per gluon field), there must be the same number of ghost fields, although the coupling is not purely color-matched, as the required addition to the Lagrangian shows:

$$\mathcal{L}_{ghost} = -\partial_\mu \bar{\phi}^a (\partial^\mu \delta_{ab} + ig(T^c)_{ab} A_c^\mu) \phi^b . \quad (2.7)$$

The final QCD Lagrangian in a Lorentz gauge is thus given by the sum

$$\mathcal{L}_{QCD} = \mathcal{L}_q + \mathcal{L}_g + \mathcal{L}_{fix} + \mathcal{L}_{ghost} . \quad (2.8)$$

2.2 Feynman Rules for QCD

By *quantizing* the fields in the above Lagrangian, we can derive quantum-mechanical amplitudes for particular field interactions and propagation from one point to another in spacetime. From these, physical predictions such as cross sections and decay rates can be found. Quantization is not a unique procedure, but all methods lead to the same physical predictions. In the traditional canonical operator formalism, the fields are identified with quantum operators which obey certain commutation relations. The Green functions from which a particular amplitude are built are calculated as vacuum expectation values of products of these operators at particular spacetime points. In the functional-integral approach, the Green functions are obtained by integrating the product of the fields over all their possible intermediate forms, with a Lagrangian-dependent weight. A further method is that of stochastic averaging, in which the fields are identified as stochastic variables and the Green functions averages of field products in equilibrium.

In momentum space, the Feynman diagrams for QCD and their corresponding Green functions are shown in figure fig:feynrule. Indices i and j run over the N_c colors, indices a through d (as well as all a_i) will denote the $N_c^2 - 1$ members of the adjoint representation of color $SU(N_c)$, Greek letters μ and ν (as well as all μ_i) are 4-vector indices, and momenta will be labeled by p_i and k_i . Spin and polarization indices are given as λ . In the denominator of the propagator factors, it is customary to add a small imaginary amount $i\epsilon$ in order to satisfy causal boundary conditions, but this will be ignored for clarity. There is some freedom in assigning factors of i

and minus signs with these diagrams; the particular convention used here is that of Muta [57].

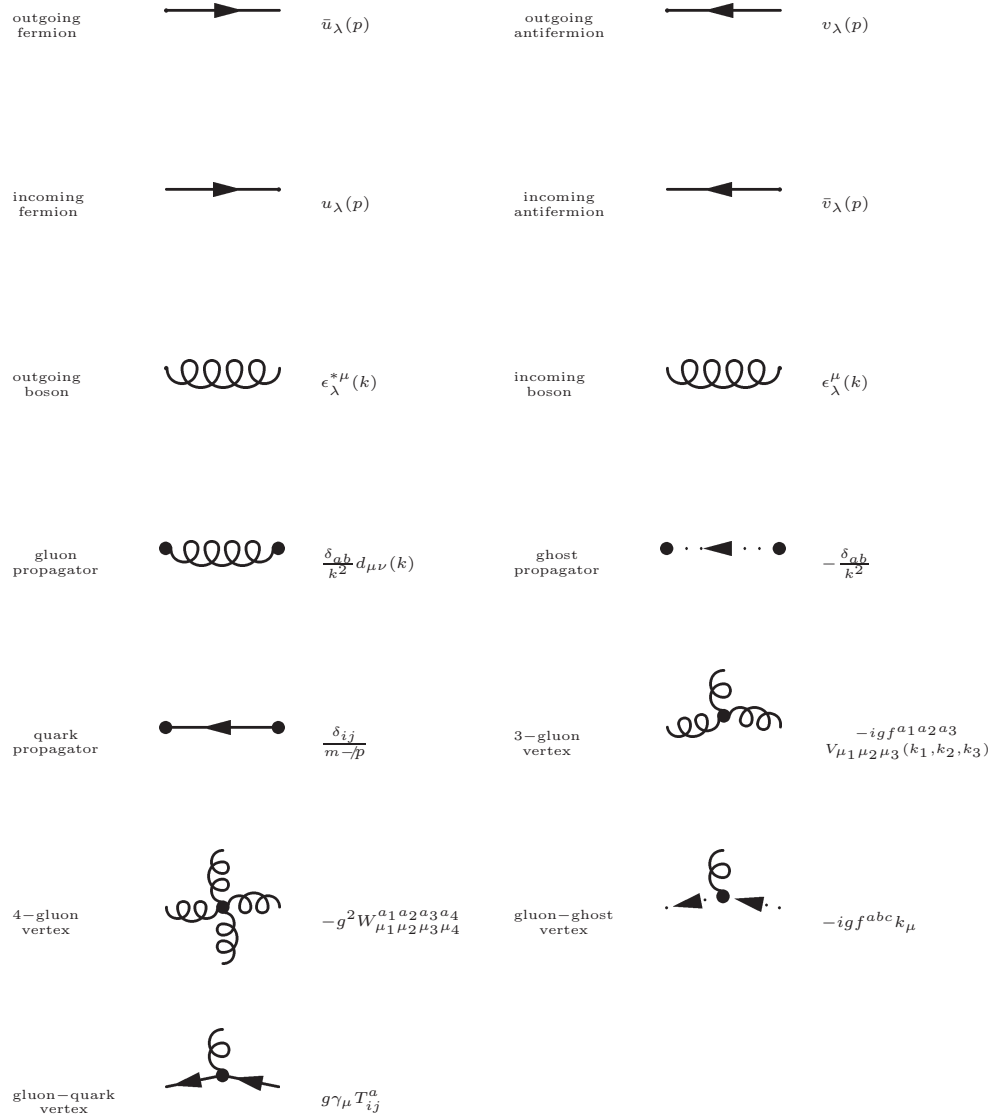


Figure 2.1. Feynman Rules for QCD.

The functions $d_{\mu\nu}$, $V_{\mu_1 \mu_2 \mu_3}$, and $W_{\mu_1 \mu_2 \mu_3 \mu_4}^{a_1 a_2 a_3 a_4}$ are given below:

$$\begin{aligned}
d_{\mu\nu}(k) &\equiv g_{\mu\nu} - (1 - \alpha) \frac{k_\mu k_\nu}{k^2} \\
V_{\mu_1\mu_2\mu_3}(k_1, k_2, k_3) &\equiv (k_1 - k_2)_{\mu_3} g_{\mu_1\mu_2} + (k_2 - k_3)_{\mu_1} g_{\mu_2\mu_3} + (k_3 - k_1)_{\mu_2} g_{\mu_3\mu_1} \\
W_{\mu_1\mu_2\mu_3\mu_4}^{a_1a_2a_3a_4} &\equiv (f^{13,24} - f^{14,32}) g_{\mu_1\mu_2} g_{\mu_3\mu_4} + (f^{12,34} - f^{14,23}) g_{\mu_1\mu_3} g_{\mu_2\mu_4} \\
&+ (f^{13,42} - f^{12,34}) g_{\mu_1\mu_4} g_{\mu_3\mu_2} ,
\end{aligned} \tag{2.9}$$

in which $f^{ij,kl}$ denotes the combination

$$f^{ij,kl} \equiv f^{a_i a_j a} f^{a_k a_l a} \tag{2.10}$$

and the Minkowski metric (in D dimensions) is taken to be

$$g_{\mu\nu} \equiv \delta_{\mu 0} \delta_{\nu 0} - \sum_{i=1}^{D-1} \delta_{\mu i} \delta_{\nu i} . \tag{2.11}$$

There are additional requirements when loops arise in diagrams. First of all, a ghost loop must be included whenever a closed fermion loop appears. Secondly, for all loops, the loop momentum k must be integrated over:

$$-i \int \frac{d^D k}{(2\pi)^D} ,$$

with fermion and ghost loops carrying an extra minus sign. Lastly, additional symmetry factors must be included for the types of diagrams shown in figure 2.2.

2.3 Renormalization

2.3.1 Motivation

In the calculation of the amplitude corresponding to a particular Feynman diagram containing internal (*virtual*) particles, there will necessarily be unobserved degrees of freedom which must be integrated over. For example, a diagram with two external legs and one loop will have two characteristic momenta, one (p^μ) for the external legs and one (k^ν) for an internal leg (or *propagator*) of the loop, the

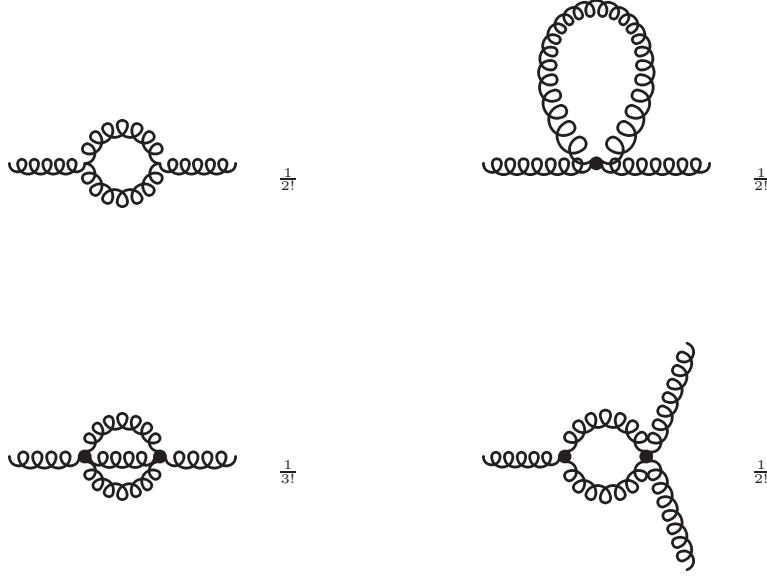


Figure 2.2. Symmetry factors.

other loop propagator momentum being fixed by momentum conservation. The loop momentum k^ν , being unobserved, must be integrated over, but by the uncertainty principle, it can be arbitrarily large as long as the “size” of the loop is correspondingly small. Thus the potential arises for the integral to diverge. Each propagator will contribute a power of 1 or 2 to the denominator of the integrand, thus lessening the degree of divergence, but if the dimension of the numerator is greater than that of the denominator, we will still have a problem. By the same token, if the rest mass of the loop particle is zero, there will be an infrared divergence at the low end of the integral, $k^\nu k_\nu = 0$.

As noted in Section 1.3, there are divergences even in purely tree-level graphs, and *regularization* is the general term used to describe the process by which divergences are parametrized and the amplitudes written as explicit functions of these parameters. Being arbitrary, such parameters must ultimately disappear in the prediction of any physical observable, but in the mathematical calculation thereof, we

can temporarily excuse their presence. One main class of regularization scheme is the *cutoff* method, in which ultraviolet integrals are stopped at some high scale or infrared divergences are avoided by introducing small masses. However, such techniques tend to destroy either the Lorentz invariance or the internal symmetries of the Lagrangian, and so are rarely used. More common is the method of *dimensional regularization*, in which integration over what would be a 4-dimensional momentum variable is analytically continued to a space of arbitrary dimension D , usually parametrized as $D = 4 - 2\epsilon$. The integral is now formally finite for $\epsilon > 0$, and the amplitude can be expressed as a function of ϵ . In the end, ultraviolet poles in the regularization parameter ϵ must either cancel or be absorbed into redefinitions of the observable masses and charges. This latter procedure, regardless of the means of regularization, is given the name *renormalization*.

The Lagrangian of a theory will be a function of the fields and “bare” parameters, such as masses m_0 and couplings e_0 . Derivation of the Feynman rules from such a Lagrangian will result in a set of “bare” Green functions, the simple propagators and vertices of the theory. Usually, the Lagrangian is written as a sum of terms, each of which corresponds to one of these functions. More complicated diagrams are built up from these, and can be grouped into two classes – those which have the same external legs as the bare diagrams and those that do not. Of the ones that do, some are single-particle-irreducible (simply-connected diagrams which have external propagators removed and which cannot be split into two by cutting one internal propagator). We denote these by the term “SPI”, and for vertices, this is all we have in this sub-class. For propagators there will be other diagrams, but these can be shown to be just combinations of the SPI diagrams. We’ll now define “full” propagators and vertices as sums of all diagrams with the same external legs as their corresponding bare diagrams. For vertices, this will then be the sum of all SPI vertex diagrams, while for propagators, we have to first sum the SPI propagators, and then link these sums in a geometric chain (see figure 2.3) [58]. We now have a set of full

Green functions, each in one-to-one correspondence with its bare counterpart. The remaining class of diagrams, those which don't have the same external legs as the bare versions, were still constructed from them, and so can be calculated now via the full Green functions, expanded to the appropriate order of the coupling.

$$\begin{aligned}
-i\Sigma(p, m_0) &\equiv \text{Diagram: a circle with two external lines pointing left} \\
&= \text{Diagram: a horizontal line with a cloud-like loop below it} + \text{Diagram: a horizontal line with a cloud-like loop above it} + \text{Diagram: a horizontal line with a circle inside a cloud-like loop} + \dots \\
\\
-i\bar{\Sigma}(p, m) &\equiv \text{Diagram: a shaded circle with two external lines pointing left} \\
&= \text{Diagram: a horizontal line with an arrow pointing left} + \text{Diagram: a circle with two external lines pointing left} + \text{Diagram: two circles in series with two external lines pointing left} + \dots \\
&= \frac{i}{\not{p} - m_0} + \frac{i}{\not{p} - m_0} \left(\frac{\Sigma(\not{p})}{\not{p} - m_0} \right) + \frac{i}{\not{p} - m_0} \left(\frac{\Sigma(\not{p})}{\not{p} - m_0} \right)^2 + \dots \\
&= \frac{i}{\not{p} - m_0 - \Sigma(\not{p})}
\end{aligned}$$

Figure 2.3. Building the full propagator.

In general, these Green functions will be UV-divergent, as they contain “clouds” of virtual activity. However, in a renormalizable theory, to each simple propagator or vertex there corresponds a characteristic quantity, potentially observable in the “full” case, unobservable in the “bare”. For propagators this is the mass; for vertices it is the coupling. The correspondence between the full and bare Green functions gives us a means of dealing with these divergences, as well as a physical picture of how higher

orders of virtual activity “shift” the masses and couplings from their bare values. The full Green functions emerge as divergent functions of the bare parameters, but if we define **observable** quantities such that the bare parameters are themselves divergent functions of the observables, then the Green functions can be rendered as finite functions of the observables.

2.3.2 Canonical Procedure

The exact process of renormalization depends on the theory under consideration, but (without getting into these details) one can describe, in a general way, the steps involved. We use one mass, coupling, and regulator for simplicity.

1. Compute the full functions Γ_i to a given order of the bare coupling e_0 , using a regulator Λ when necessary. One then has the functions $\Gamma_i(e_0, m_0, \Lambda, \{p_j\})$ to order N , and these are divergent as the regulator approaches some limit $\Lambda \rightarrow \Lambda_{lim}$. Here $\{p_j\}$ are the momenta of external legs.

2. Impose *renormalization conditions* to define the form of the renormalized Green functions at a particular scale $\mu = f(\{p_j\})$. These forms should contain a dependence on the renormalized couplings and masses $\{e, m\}$ and should be finite as $\Lambda \rightarrow \Lambda_{lim}$. Suitable forms are usually suggested by the bare Green functions themselves, *e.g.* the full propagator should be able to be brought into the same form as the bare propagator, the new, observable mass (now a complicated function of the bare parameters) taking the place of the bare mass (see figure 2.3). Imposition of such constraints on the Green functions Γ_i results in relations $e(e_0, m_0, \Lambda)$ and $m(e_0, m_0, \Lambda)$ between the renormalized and bare quantities.

3. Solve for the bare parameters $\{e_0, m_0\}$ and substitute into the functions Γ_i . The result is $\Gamma_i(e, m, \Lambda)$, which will be finite as $\Lambda \rightarrow \Lambda_{lim}$.

We’ll call this the **canonical** renormalization procedure, and it will always work in a renormalizable theory, yet is cumbersome at high orders N . An equivalent but better organized approach to the bookkeeping is provided by the **counterterm**

method, which anticipates the shift in parameter space by building it into the Lagrangian at the start.

2.3.3 Counterterm Method

1. Rescale the bare parameters (including the field strengths ψ_0) by introducing new, temporary unknowns Z_i , which relate them to their observable counterparts; i.e. $\psi = Z_\psi \psi_0$, $e = Z_e e_0$, etc.

2. Trade in these multiplicative unknowns Z_i for additive ones δ_i in such a way that, upon substitution of these expressions for the bare parameters into the Lagrangian, one reproduces the original Lagrangian (now in terms of the renormalized observables), plus additional *counterterms*. We'll refer to these pieces as \mathcal{L}_{CG} and \mathcal{L}_{CT} , respectively. The counterterms will have corresponding Feynman rules of their own.

3. Specify the renormalization conditions, again as desired relations of form between the unrenormalized and renormalized Green functions at scale μ .

4. Calculate the full functions using the rearranged Lagrangian. To a given order N , one will find the usual divergences from \mathcal{L}_{CG} , plus new divergences from the counterterms. However, we can now get these to cancel, as the set of unobservable shifts δ_i are free parameters. By adjusting these to maintain the renormalization conditions (which by construction define nonsingular amplitudes), we can consistently absorb the infinities of the theory into the bare parameters, leaving Green functions that are finite and dependent upon only the renormalized charges and masses.

The counterterms in \mathcal{L}_{CT} , with suitable renormalization conditions, are commonly said to “subtract off” the divergences of the “original” Lagrangian \mathcal{L}_{CG} , but there remains an ambiguity in this process, as one can always subtract an extra, arbitrary, finite amount as well. The size of this piece is, in general, related to the particular

renormalization conditions, and so together these two choices define a *renormalization scheme*. We will discuss the most commonly used schemes in a later section.

As an example, we take the renormalization of QED. The bare Lagrangian is as follows (we denote bare quantities by the subscript “0”):

$$\mathcal{L} = -\frac{1}{4}(F_0^{\mu\nu})^2 + \bar{\psi}_0(i\partial\!\!\!/ - m_0)\psi - e_0\bar{\psi}_0\gamma_\mu\psi_0A_0^\mu . \quad (2.12)$$

We now impose the following sets of rescalings and variable changes:

$$\begin{aligned} \psi_0 &= Z_2^{1/2}\psi \\ A_0^\mu &= Z_3^{1/2}A^\mu \\ e_0Z_2Z_3^{1/2} &= eZ_1 \end{aligned} \quad (2.13)$$

$$\begin{aligned} \delta_m &= Z_2m_0 - m \\ \delta_1 &= Z_1 - 1 \\ \delta_2 &= Z_2 - 1 \\ \delta_3 &= Z_3 - 1 , \end{aligned} \quad (2.14)$$

and thus transform the Lagrangian into a sum of two pieces, one of which resembles the original Lagrangian, the other provides the counterterms. The bare quantities and intermediate scaling factors disappear:

$$\begin{aligned} \mathcal{L} &= \mathcal{L}_{CG} + \mathcal{L}_{CT} \\ \mathcal{L}_{CG} &= -\frac{1}{4}(F^{\mu\nu})^2 + \bar{\psi}(i\partial\!\!\!/ - m)\psi - e\bar{\psi}\gamma_\mu\psi A^\mu \\ \mathcal{L}_{CT} &= -\frac{1}{4}\delta_3(F^{\mu\nu})^2 + \bar{\psi}(i\delta_2\partial\!\!\!/ - \delta_m)\psi - e\delta_1\bar{\psi}\gamma_\mu\psi A^\mu . \end{aligned} \quad (2.15)$$

For renormalization conditions, we use the following:

$$\begin{aligned}
\Sigma(\not{p} = m) &= 0 \\
\left. \frac{d\Sigma(\not{p})}{d\not{p}} \right|_{\not{p}=m} &= 0 \\
\Pi(q^2 = 0) &= 0 \\
\Gamma^\mu(\bar{p} = p) &= \gamma^\mu ,
\end{aligned} \tag{2.16}$$

where the amplitudes Γ^μ , Σ , and $\Pi^{\mu\nu} \equiv (g^{\mu\nu}q^2 - q^\mu q^\nu)\Pi$ denote the amputated full vertex, single-particle-irreducible (SPI) electron propagator element, and SPI photon propagator element, respectively. When calculated using the rearranged Lagrangian, which includes counterterms, each will, in general, be a function of the quantities $\{e, m, \delta_1, \delta_2, \delta_3, \delta_m, \not{p}, q\}$, and the regulator. Enforcing the above conditions then determines $\{\delta_1, \delta_2, \delta_3, \delta_m\}$.

As we have said, the precise conditions used are a matter of convention; the crucial point is that we define the full Green functions (and thus the renormalized masses and couplings) to (1) be finite, and (2) to take a certain form at some *renormalization scale* μ or set of scales. In the QED example above, we used a *momentum subtraction scheme*, in which the scale used depends on the Green function being renormalized. We could, however, have chosen a single scale, common to all amplitudes, *i.e.* $p^2 = -\mu^2$ and $q^2 = -\mu^2$. The counterterms then subtract only the divergent poles (*Minimal Subtraction*, or “*MS*”), or these plus standard constants *Modified Minimal Subtraction*, “ \overline{MS} ”). In this dissertation we will use the \overline{MS} convention.

Either way, we are left with renormalized Green’s functions G and couplings λ which, though finite, seem to depend upon a new parameter (μ) not present in the original, bare versions (G_0, λ_0). We know that these must be related by the (now calculable) rescalings Z_i ; for example, there must be a calculable function Z_G of the scaling factors Z_i such that

$$G(\mu, \lambda) = Z_G(\mu, \lambda)G_0(\lambda) . \tag{2.17}$$

However, we have calculated this relation to a fixed order N only. How can we generalize this to account for not only the poles but the associated scale dependent pieces $\ln^N \mu/p$ found at even higher orders? Specifically, if μ is taken large enough, how do we justify a perturbative expansion, unless the coupling $\sim \lambda^{2N}$ becomes correspondingly small? There must be a *Renormalization Group Equation* (RGE) which expresses the fact that a change in scale μ needs to be compensated in order to keep the bare Green's function (and the bare coupling) invariant. From equation 2.17:

$$\mu \frac{d}{d\mu} \frac{G}{Z_G} = 0 , \quad (2.18)$$

or

$$\left[\mu \frac{\partial}{\partial \mu} + \beta \frac{\partial}{\partial \lambda} + \gamma \right] G(\mu, \lambda) = 0 , \quad (2.19)$$

with

$$\beta(\lambda) \equiv \mu \frac{d\lambda}{d\mu} \quad (2.20)$$

$$\gamma(\lambda) \equiv -\frac{\mu}{Z_G} \frac{dZ_G}{d\mu} . \quad (2.21)$$

Equation 2.19 is known as the Callan-Symanzik equation [59–60]. The functions β and γ are unitless and must depend on the coupling only. Yet they describe the compensating shifts in coupling and field strengths (respectively) for a change in scale μ . So these strengths must themselves be functions of μ , and equations 2.20, 2.21 lead us to the perturbative form of this dependence. Here we simplified to a theory involving one field and one coupling; in general, there will be one γ for each field and one β for each coupling.

2.3.4 Application to QCD

Now that we've described the basics of renormalization, let's list the relations appropriate to QCD. As expected, they are somewhat more complicated. We'll use a superscript “0” to denote the bare quantities.

$$\begin{aligned}
g &= \mu^{-\epsilon} \frac{g^0}{\sqrt{Z_\alpha}} \\
m_j &= \frac{m_j^0}{Z_m} \\
\zeta &= \frac{\zeta^0}{Z_\zeta} \\
\psi_{q,i}(x) &= \frac{\mu_r^\epsilon}{\sqrt{Z_{2F}}} \psi_{q,i}^0(x) \\
A_\mu^a(x) &= \frac{\mu_r^\epsilon}{\sqrt{Z_{3YM}}} A_\mu^{a0}(x) \\
\phi_a(x) &= \frac{\mu_r^\epsilon}{\sqrt{\tilde{Z}_3}} \phi_a^0(x) \\
(g\bar{\psi}A\psi)(x) &= \frac{\mu_r^{2\epsilon}}{Z_{1F}} (g\bar{\psi}A\psi)^0(x) .
\end{aligned} \tag{2.22}$$

The *running coupling* $\alpha_s \equiv g^2/4\pi$ is a solution of the Callan-Symanzik equation 2.20, and comes out (to two loops) as

$$\alpha_s(\mu) = \frac{2\pi}{b \ln(\mu^2/\Lambda^2)} \left[1 - \frac{2c}{b} \frac{\ln[\ln(\mu^2/\Lambda^2)]}{\ln(\mu^2/\Lambda^2)} + O[\ln^{-2}(\mu^2/\Lambda^2)] \right] , \tag{2.23}$$

in which

$$\begin{aligned}
b &\equiv \frac{11N_C - 2N_F}{6} \\
c &\equiv \frac{1}{8b} \left[\frac{34}{3} N_C^2 - \frac{13}{3} N_C N_F + \frac{N_F}{N_C} \right] .
\end{aligned} \tag{2.24}$$

As expected, this exhibits the property of asymptotic freedom – at large μ , the coupling α_s decreases.

2.4 Factorization

With a renormalized theory, one can begin to calculate physical quantities and compare these predictions with experimental measurements. For a particular set of initial-state (incoming) reactants $\{a, b\}$ and final-state products $\{c, d\}$ (*e.g.*), one uses the Feynman rules to calculate an amplitude \mathcal{M}_i for each topologically unique way this reaction can occur. Quantum mechanics then dictates that the probability for the reaction is proportional to the squared sum of these amplitudes:

$$\sum_i |\mathcal{M}_i|^2 = \sum_i \mathcal{M}_i^* \mathcal{M}_i . \quad (2.25)$$

In addition, the squared amplitude refers to (and is a function of) particular values of the particle momenta $\{p_a^\mu, p_b^\mu, p_c^\mu, p_d^\mu\}$. That is, the reaction rate per unit time into volume element $d^3p_c d^3p_d$ is given by

$$\sum_i |\mathcal{M}_i|^2 \frac{d^3p_c}{(2\pi)^3 2p_c^0} \frac{d^3p_d}{(2\pi)^3 2p_d^0} (2\pi)^4 \delta^4(p_a^\mu + p_b^\mu - p_c^\mu - p_d^\mu)$$

and one must integrate over this *phase space* in order to obtain the full reaction rate. Note that a delta function is included to conserve momentum.

In the case of hadronic interactions, the initial state particles will be partons, one from each hadron. By the collinear geometry of the interaction, the parton momenta are known up to fractions x_a and x_b of the incoming hadron momenta, and the *cross section* (an experimentally measurable quantity) for two partons, of flavors a and b , with these momenta, to produce the given final state, is found by dividing the above reaction rate by a flux factor $2w(\hat{s}, m_a, m_b)$, in which $\hat{s} \equiv (p_a^\mu + p_b^\mu)^2$ and

$$w(x, y, z) \equiv \sqrt{x^2 + y^2 + z^2 - 2xy - 2xz - 2yz} . \quad (2.26)$$

For all but the heaviest quarks, we can take the parton masses to be zero (relative to the hadronic center of mass energy S), and $w(\hat{s}, m_a, m_b) \rightarrow \hat{s} = x_a x_b S$. The

partonic cross section for a particular $2 \rightarrow 2$ particle subprocess is thus given by the product

$$d\hat{\sigma} = \frac{\sum_i |\mathcal{M}_i|^2}{2\hat{s}} d^4\Gamma_2, \quad (2.27)$$

in which the 2-body phase space factor is

$$d^4\Gamma_2 = \frac{d^3p_c}{(2\pi)^3 2p_c^0} \frac{d^3p_d}{(2\pi)^3 2p_d^0} (2\pi)^4 \delta^4(p_a^\mu + p_b^\mu - p_c^\mu - p_d^\mu). \quad (2.28)$$

The partonic cross section is perturbatively calculable to any order N if one is willing to calculate the required amplitudes. However, it is not yet useful in practice. First, the above cross section pertains to partons of definite flavor, color, spin, and momentum fraction. In any real hadronic interaction, a multitude of partonic flavors will contribute, at all momenta and with all possible color and spin values. Spin and color averages are abbreviated by a line over the squared amplitude sum, e.g. $\overline{\sum}$. However, we do not *apriori* know the momentum or flavor distribution of partons inside hadrons, nor do we have a deterministic model for the hadronization of final state partons. We are forced to find a way of *factorizing* the reaction into component steps, some of which are dealt with perturbatively, the rest requiring effective parametrizations and experimental input (see figure 2.4).

In the *parton model* of high-energy hadronic collisions, the initial reaction takes place over such a small time scale that it becomes plausible to treat each hadron as a collection of free partons, each travelling in the same direction as the parent hadron, and only one of which takes place in any given “hard scattering”. That is, one may calculate basic subprocesses involving one parton from each hadron, then sum incoherently over the contributions of all partons. Similarly, the process of hadronization is assumed to take place over a time scale much longer than the hard scattering, and can therefore also be treated independently.

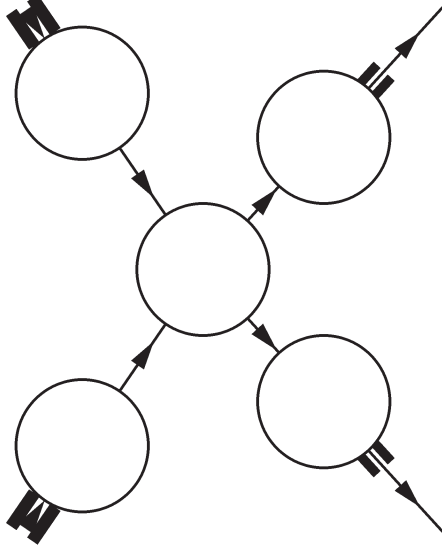


Figure 2.4. Factorization of the hadronic interaction.

Thus, we can assign to each initial state hadron a set of parton distribution functions $q_{i/I}$ ¹, and, if we are looking at particular hadrons in the final state, to each final-state parton a given probability $D_{H/h}$ to fragment into a state containing the desired hadron. The physically realizable cross section for the reaction is then obtained by weighting the subprocess cross section $d\hat{\sigma}$ with these distribution and fragmentation functions, evaluated for particular flavors and at particular fractions of the parent (or daughter) hadrons' momenta, then summing over all flavors and momentum fractions:

$$d\sigma^{(AB \rightarrow CD)} = \sum_{a,b,c,d} \int_0^1 dx_a \int_0^1 dx_b q_{a/A}(x_a) q_{b/B}(x_b) d\hat{\sigma}^{(ab \rightarrow cd)} D_{c/C}(z_c) D_{d/D}(z_d) . \quad (2.29)$$

¹Parton distributions are variously denoted in the literature by q_f or G_f (where f is the flavor), or f_q (where q is the flavor).

If suitable parametrizations of the distribution and fragmentation functions are made at the outset, these quantities may be fit to known cross section data and used in subsequent calculations.

In the process of calculating $d\hat{\sigma}$ to higher orders, two main classes of diagrams arise. First there are vertex and propagator modifications, in which extra connections are made between the legs of a diagram, without changing the number of external legs. These produce *ultraviolet* (UV) and *infrared* (IR) singularities (or “poles”) at the upper and lower limits of loop momentum, and in the previous section we have seen that the UV poles may be regulated and absorbed into the masses and couplings of the theory. The second class of diagrams involve the emission of an extra particle into the final state, and also give rise to IR singularities. Some of these arise in gauge boson emission at zero boson momentum, and cancel the IR poles from virtual contributions [24]. As well, there are *collinear* singularities at zero angle between the daughter and parent particle.

The collinear singularities, arising as they do from the inability to distinguish a bare parton from one accompanied by a number of collinear partons, get moved into a redefinition of the distribution and fragmentation functions, usually accompanied by logarithms of a momentum scale characteristic of the subprocess. The evolution of these quantities is now dependent upon the change in momentum transfer at which they are sampled, a result quantified for distribution functions by Altarelli and Parisi [28], and for the fragmentation functions by Owens and Uematsu [61].

At order N relative to the leading order, there can be as many as N extra radiated partons, any or all of which may be collinear. We thus find a power series of logarithmic divergences at the NLO and higher orders. In the *leading log approximation*, only the logarithm of highest power at each order is retained. Iteration of the evolution equations effectively sums the collinear logarithms to solve for the distribution and fragmentation functions, with the original momentum of parametrization as reference point. The leading log approximation dictates that we

can now simply use the modified coupling, distribution, and fragmentation functions with the Born matrix element. A number of calculations have been carried out in this way [63–65].

To show how singularity cancellation and factorization works, we’ll look at a simple example, that of double photon production. We won’t be looking for particular hadrons in the final state, so no fragmentation functions will enter into our calculation.

The ‘Born’ (leading order) subprocess cross section is calculated using the diagrams shown in figure 2.5. All contributions have already been regulated using dimensional regulation, with $\epsilon = (4 - D)/2$. To order α^2 , we have

$$d\sigma_0 = \frac{\sum_f}{2S} \int_0^1 \frac{dx_a}{x_a} \int_0^1 \frac{dx_b}{x_b} H(x_a, x_b) d^D\Gamma_2 \bar{\Sigma} |\mathcal{M}|_0^2, \quad (2.30)$$

where the luminosity function H (which contains the parton distributions q_f), the squared, summed and averaged matrix element $\bar{\Sigma} |\mathcal{M}|_0^2$, and the 2-body phase space factor $d^D\Gamma_2$ are given as follows:

$$H(x_a, x_b) = q_{f/A}(x_a) q_{\bar{f}/B}(x_b) + (f \rightarrow \bar{f}) \quad (2.31)$$

$$\bar{\Sigma} |\mathcal{M}|_0^2 = \frac{1}{2} \frac{1}{3^2} \frac{1}{2^2} 8N_C (4\pi)^2 \mu^{4\epsilon} \alpha^2 Q_f^4 (1 - \epsilon) \left[(1 - \epsilon) \left(\frac{\hat{t}}{\hat{u}} + \frac{\hat{u}}{\hat{t}} \right) - 2\epsilon \right] \quad (2.32)$$

$$d^D\Gamma_2 = \frac{1}{8\pi} \left(\frac{4\pi}{\hat{s}} \right)^\epsilon \frac{[v(1-v)]^{-\epsilon}}{\Gamma(1-\epsilon)} dv. \quad (2.33)$$

Note here that the phase space factor has been simplified by use of the momentum-conserving delta function, and becomes dependent only upon a single variable $v = \frac{1}{2}(1 + \cos \theta_3)$, where θ_3 is the angle \vec{p}_3 makes with \vec{p}_1 in the partonic center-of-mass frame. The *Mandelstam* variables $\{\hat{s}, \hat{t}, \hat{u}\}$ are then given by $\hat{s} = x_a x_b S$, $\hat{t} = -(1-v)\hat{s}$, $\hat{u} = -v\hat{s}$.

In a leading log calculation, we would stop here, take $\epsilon \rightarrow 0$ (as there are no divergences), and evaluate the distribution functions at a factorization scale M_f



Figure 2.5. Leading order diagrams for $q\bar{q} \rightarrow \gamma\gamma$.

characteristic of the subprocess (perhaps the mass $Q = \sqrt{\hat{s}}$ of the photon pair). If this leading-order term had contained a dependence on the running strong coupling α_s , we would evaluate this, too, at a renormalization scale μ , usually taken to be equal to the factorization scale. In fact, we will be adding higher-order terms, so the strong coupling will show up in the final result.

At next-to-leading order, two things happen. First, we will have contributions from tree diagrams in which a gluon is radiated from one of the quark legs ² Second, we will have virtual diagrams in which a gluon is radiated and reabsorbed, so that there are still only two particles in the final state. Of course, emission and reabsorption amounts to two QCD vertices, whereas the tree diagrams only contribute one, so if we're working to NLO only, we keep only the interference terms between the Born and virtual amplitudes.

The tree diagrams for $q(p_1)\bar{q}(p_2) \rightarrow \gamma(p_3)\gamma(p_4)g(p_5)$ are shown in figure 2.6, and their contribution is as follows:

$$d\sigma_1 = \frac{\sum_f}{2S} \int_0^1 \frac{dx_1}{x_1} \int_0^1 \frac{dx_2}{x_2} H(x_1, x_2) d^D\Gamma_3 \bar{\Sigma} |M|_1^2, \quad (2.34)$$

where here

²We will also have contributions in which a gluon initiates the process, and a quark appears in the final state, but we'll ignore these for the sake of this argument.

$$H(x_1, x_2) = q_{f/A}(x_1)q_{\bar{f}/B}(x_2) + (f \rightarrow \bar{f}) \quad (2.35)$$

$$\bar{\Sigma}|M|_1^2 = \frac{1}{2} \frac{1}{3^2} \frac{1}{2^2} 16 N_C (4\pi)^3 \mu^{6\epsilon} \alpha^2 \alpha_s Q_f^4 \frac{M_1(p_3^\mu, p_5^\mu, x_1, x_2, \epsilon)}{(p_5^0 \sin \theta_5)^2} \quad (2.36)$$

$$\begin{aligned} d^D \Gamma_3 &= \frac{(2\pi)^{4\epsilon-5}}{4} \left[2(4\pi)^{-\epsilon} \frac{\Gamma(1-\epsilon)}{\Gamma(1-2\epsilon)} \right]^2 \delta(p_4^2) \\ &\times (p_3^0)^{1-2\epsilon} \sin^{1-2\epsilon} \theta_3 \sin^{-2\epsilon} \phi_3 dp_3^0 d\theta_3 d\phi_3 \\ &\times (p_5^0)^{1-2\epsilon} \sin^{1-2\epsilon} \theta_5 \sin^{-2\epsilon} \phi_5 dp_5^0 d\theta_5 d\phi_5 . \end{aligned} \quad (2.37)$$

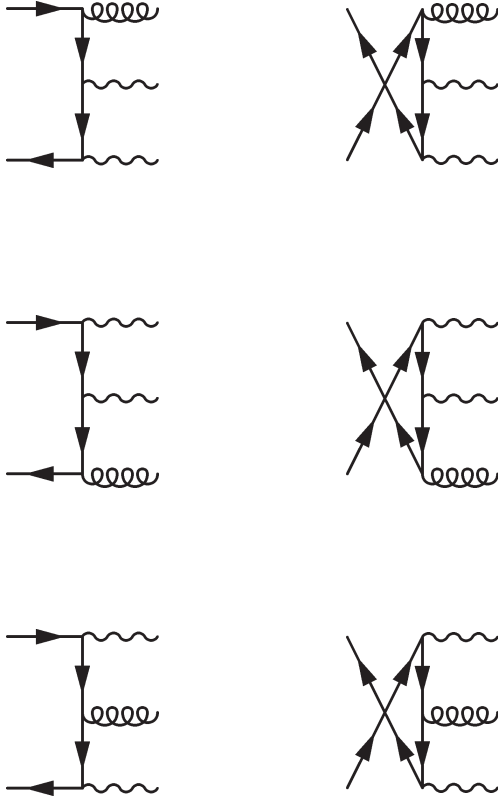


Figure 2.6. Diagrams for $q\bar{q} \rightarrow \gamma\gamma g$.

The function $M_1(p_3^\mu, p_5^\mu, x_1, x_2, \epsilon)$ is a complicated one, and this makes integrating over the extra gluon (p_5^μ) difficult. As we are here interested only in the singularity structure, we will make an approximation. In the limit that the gluon becomes collinear with an incoming quark ($\vec{p}_5 \parallel \vec{p}_1$, *e.g.*), its momentum, as well as that of the daughter quark (p_a^μ , which enters the subprocess) are related to the parent in terms of a simple fraction z . That is, $p_5^\mu = (1 - z)p_1^\mu$ and $p_a^\mu = zp_1^\mu$. The matrix element simplifies, the integrals become easy, and the remaining phase space is that of a two-body final state.

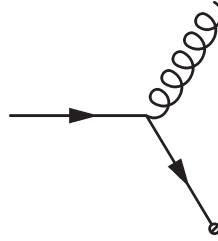


Figure 2.7. $p_1 \cdot p_5 = 0$ collinear kinematics.

In short, the matrix element factorizes into a Born term describing a $2 \rightarrow 2$ subprocess, and a *splitting function* \hat{P}'_{qq} describing the probability for a quark to split into a collinear quark-gluon pair. This latter function is independent of the particular subprocess, as long as it contains an incoming quark. Of course, we get a pole from the collinear singularity, and an important multiplicative factor. The result, in $D = 4 - 2\epsilon$ dimensions, is:

$$H(x_a/z, x_b) \rightarrow q_{f/A}(x_a/z)q_{\bar{f}/B}(x_2) + (f \rightarrow \bar{f}) \quad (2.38)$$

$$\bar{\Sigma}|M|_1^2 \rightarrow \bar{\Sigma}|M|_0^2 \frac{8(4\pi)\alpha_s\mu^{2\epsilon}}{\hat{s}\sin^2\theta_5} \frac{z}{(1-z)} \hat{P}'_{qq}(z) \quad (2.39)$$

$$d^D\Gamma_3 \rightarrow d^D\Gamma_2 \frac{-1}{\epsilon} \left(\frac{4\pi}{\hat{s}} \right)^\epsilon \frac{\Gamma(1-\epsilon)}{\Gamma(1-2\epsilon)} \frac{\hat{s}}{(4\pi)^2} \frac{dz}{4} \frac{(1-z)^{1-2\epsilon}}{z^{3-2\epsilon}}, \quad (2.40)$$

which gives the cross section

$$\begin{aligned} d\sigma_1 &= \frac{\sum_f}{2S} \int_0^1 \frac{dx_a}{x_a} \int_0^1 \frac{dx_b}{x_b} d^D\Gamma_2 \bar{\Sigma} |M|_0^2 \\ &\times \frac{-1}{\epsilon} \frac{\alpha_s}{2\pi} \left(\frac{4\pi\mu^2}{\hat{s}} \right)^\epsilon \frac{\Gamma(1-\epsilon)}{\Gamma(1-2\epsilon)} \int_{x_a}^1 \frac{dz}{z} \left[\frac{z}{1-z} \right]^{2\epsilon} H(x_a/z, x_b) \hat{P}'_{qq}(z, \epsilon). \end{aligned} \quad (2.41)$$

Here $\hat{P}'_{qq}(z, \epsilon)$ is the aforementioned splitting function, pertinent to the process $q \rightarrow qg$, where the quark on the right-hand side is involved in the QCD subprocess. This function will always appear in such a collinear limit, regardless of the subprocess, and has the form

$$\hat{P}'_{qq}(z, \epsilon) = C_F \left[\frac{1+z^2}{1-z} - \epsilon(1-z) \right]. \quad (2.42)$$

Unfortunately, there is also a soft pole here at $z = 1$. We'd like to separate this so we can focus on the purely collinear contribution. We start by adding and subtracting, under the z -integral, the $z \rightarrow 1$ limit of $H(x_a/z, x_b) \hat{P}'_{qq}(z, \epsilon)$. Remembering that all of this multiplies the collinear $\frac{-1}{\epsilon}$ pole, we have

$$\begin{aligned} \frac{-1}{\epsilon} \int_{x_a}^1 \frac{dz}{z} \left(\frac{z}{1-z} \right)^\epsilon &\left[H(x_a/z, x_b) \hat{P}'_{qq}(z, \epsilon) - \frac{2C_F H(x_a, x_b)}{1-z} \right] \\ &- \int_{x_a}^1 \frac{dz}{z} \left(\frac{z}{1-z} \right)^\epsilon \frac{2C_F H(x_a, x_b)}{1-z}. \end{aligned} \quad (2.43)$$

This allows us to express the first integrand (which is finite as $z \rightarrow 1$) in terms of a *plus-distribution*, a handy notational device which is defined upon convolution with a smooth function. We will have plenty of use for these in subsequent chapters, as well. Here, the plus-distribution $(1-z)_+$ is defined over a function $f(z)$ as

$$\int_0^1 dz \frac{f(z)}{(1-z)_+} \equiv \int_0^1 dz \frac{f(z) - f(1)}{1-z}. \quad (2.44)$$

The first term in equation 2.43 then works out to

$$\frac{-1}{\epsilon} \int_{x_a}^1 \frac{dz}{z} H(x_a/z, x_b) P_{qq}^+(z) + \frac{C_F H(x_a, x_b)}{\epsilon} \left[2 \ln \frac{1-x_a}{x_a} + \frac{3}{2} \right] + \mathcal{O}(1)$$

where P_{qq}^+ is the plus-distribution form of the ϵ -independent qq splitting function:

$$P_{qq}^+ \equiv C_F \left[\frac{1+z^2}{(1-z)_+} + \frac{3}{2} \delta(1-z) \right]; \quad (2.45)$$

the second term becomes

$$\frac{2C_F H(x_a, x_b)}{\epsilon} \left[\frac{1}{2\epsilon} - \ln \frac{1-x_a}{x_a} + \mathcal{O}(\epsilon) \right].$$

This operation splits $d\sigma_1$ into two contributions, the first of which we'll call $d\sigma_{coll}$ and the latter $d\sigma_{soft}$. The same terms arise, of course, when we look at the limit in which the gluon is radiated from the other incoming leg; in that case we'll be looking at terms involving $H(x_a, x_b/z)$. When we put everything together, we'll add in these contributions.

Meanwhile, the (renormalized) virtual contribution is:

$$d\sigma_{virt} = \frac{\sum_f}{2S} \int_0^1 \frac{dx_a}{x_a} \int_0^1 \frac{dx_b}{x_b} H(x_a, x_b) d^D \Gamma_2 \bar{\Sigma} |M|_v^2, \quad (2.46)$$

where

$$\bar{\Sigma} |M|_v^2 = \bar{\Sigma} |M|_0^2 \left[-\frac{2C_F}{\epsilon^2} - \frac{3C_F}{\epsilon} + \mathcal{O}(1) \right] \frac{\alpha_s}{2\pi} \left(\frac{4\pi\mu^2}{\hat{s}} \right)^\epsilon \frac{\Gamma(1-\epsilon)}{\Gamma(1-2\epsilon)}. \quad (2.47)$$

The virtual diagrams are shown in figure 2.8.

In all, then, we have one LO and three NLO contributions, which all add to give:

$$d\sigma = \frac{\sum_f}{2S} \int_0^1 \frac{dx_a}{x_a} \int_0^1 \frac{dx_b}{x_b} d^D \Gamma_2 \bar{\Sigma} |M|_0^2 H(x_a, x_b) \times \left[1 + \frac{1}{\epsilon} \frac{\alpha_s}{2\pi} \left(\frac{4\pi\mu^2}{\hat{s}} \right)^\epsilon \frac{\Gamma(1-\epsilon)}{\Gamma(1-2\epsilon)} [\Pi_{coll} + \Pi_{soft} + \Pi_{virt}] \right], \quad (2.48)$$

where

$$\begin{aligned}\Pi_{coll} &= - \int_{x_a}^1 \frac{dz}{z} \frac{H(x_a/z, x_b)}{H(x_a, x_b)} P_{qq}^+(z) - \int_{x_b}^1 \frac{dz}{z} \frac{H(x_a, x_b/z)}{H(x_a, x_b)} P_{qq}^+(z) \\ &+ 2C_F \ln \frac{1-x_a}{x_a} \frac{1-x_b}{x_b} + 3C_F + \mathcal{O}(\epsilon)\end{aligned}\quad (2.49)$$

$$\Pi_{soft} = 2C_F \left[\frac{1}{\epsilon} - \ln \frac{1-x_a}{x_a} \frac{1-x_b}{x_b} + \mathcal{O}(\epsilon) \right] \quad (2.50)$$

$$\Pi_{virt} = -\frac{2C_F}{\epsilon} - 3C_F + \mathcal{O}(\epsilon) . \quad (2.51)$$

One can see by inspection that, as predicted, all the poles cancel except those associated with convolutions over splitting functions. However, if we were to redefine our quark distributions such that

$$q_f(x, M_f^2) \equiv q_f(x) - \frac{1}{\epsilon} \frac{\alpha_s}{2\pi} \left(\frac{4\pi\mu^2}{M_f^2} \right)^\epsilon \frac{\Gamma(1-\epsilon)}{\Gamma(1-2\epsilon)} \int_x^1 \frac{dz}{z} q_f(x/z) P_{qq}^+(z) , \quad (2.52)$$

then we could absorb the remaining divergence into the distribution functions. The remaining NLO contributions would come solely from the finite $\mathcal{O}(\epsilon)/\epsilon = \mathcal{O}(1)$ remainders, we could take $\epsilon \rightarrow 0$ everywhere, and the distribution functions (as well as the running coupling, to this order) would then be evaluated at a factorization scale M_f , characteristic to the observed system (in our case, \hat{s}).

$$d\sigma = \frac{\sum_f}{2S} \int_0^1 \frac{dx_a}{x_a} \int_0^1 \frac{dx_b}{x_b} d^4\Gamma_2 \bar{\Sigma} |M|_0^2 H(x_a, x_b, M_f) \left[1 + \frac{\alpha_s(M_f)}{2\pi} \mathcal{O}(1) \right] . \quad (2.53)$$

This reflects the interpretation noted above, that a parton which participates in a subprocess is in fact a component of (a component of a component of...) the parent hadron, and at higher energies, we resolve more and more components. Of course, we have here shown only the first term in such an expansion; at higher orders (more splittings) we must absorb terms with more poles, higher orders of the coupling, and more complicated splitting factors.

Furthermore, we have shown only the $q \rightarrow qq$ splitting function (boldface type referring to the parton participating in the subprocess). In general, there are splitting functions for $q \rightarrow gq$, $g \rightarrow q\bar{q}$, and $g \rightarrow gg$.

The above redefinition is in fact a combination of two separate reorganizations; the first absorbs the poles (and an arbitrary constant), the second relates to energy dependence. Expanding the order α_s factor above, we find

$$\Delta q_f(x) = \frac{\alpha_s}{2\pi} \int_x^1 \frac{dz}{z} q_f(x/z) P_{qq}^+(z) \left[\frac{-1}{\epsilon} - \ln 4\pi + \gamma_E + \ln \frac{M_f^2}{\mu^2} - \mathcal{O}(1) \right], \quad (2.54)$$

where we have included the $\frac{\mathcal{O}(\epsilon)}{\epsilon} = \mathcal{O}(1)$ terms from 2.48; that is, the entire remainder. γ_E is the Euler constant, $\simeq 0.577216$.

We can now absorb the pole and as much of the finite remainder as we like into a new distribution function $\bar{q}_f(x)$. In the **DIS** scheme, everything is absorbed but the energy log:

$$\bar{q}_f(x) = q_f(x) + \frac{\alpha_s}{2\pi} \int_x^1 \frac{dz}{z} q_f(x/z) P_{qq}^+(z) \left[\frac{-1}{\epsilon} - \ln 4\pi + \gamma_E - \mathcal{O}(1) \right]. \quad (2.55)$$

In the $\overline{\text{MS}}$ scheme, only the factor $\frac{-1}{\epsilon} - \ln 4\pi + \gamma_E$ is subtracted:

$$\bar{q}_f(x) = q_f(x) + \frac{\alpha_s}{2\pi} \int_x^1 \frac{dz}{z} q_f(x/z) P_{qq}^+(z) \left[\frac{-1}{\epsilon} - \ln 4\pi + \gamma_E \right]. \quad (2.56)$$

In this dissertation, we will be using the $\overline{\text{MS}}$ scheme exclusively.

Either way, the energy scale logarithm which remains is just as ubiquitous as the constants $-\ln 4\pi + \gamma_E$ we have already absorbed, so we continue with the further redefinition

$$q_f(x, M_f) \equiv \bar{q}_f + \Delta q_f(x, M_f), \quad (2.57)$$

where

Table 2.1. Splitting function pieces.

ij	ρ_{ij}^0	$\hat{\rho}_{ij}^+$	ρ_{ij}^δ	ρ_{ij}^1
qq	C_F	$\frac{1+z^2}{(1-z)_+}$	$\frac{3}{2}\delta(1-z)$	$-(1-z)$
qg	$\frac{1}{2(1-\epsilon)}$	$z^2 + (1-z)^2$	0	-1
gq	C_F	$\frac{1+(1-z)^2}{z_+}$	$\frac{3}{2}\delta(z)$	$-z$
gg	$2N_C$	$\frac{z}{(1-z)_+} + \frac{1-z}{z} + z(1-z)$	$\frac{11-\frac{2}{3}N_f}{12}\delta(1-z)$	0
γq	Q_f^2	$\frac{1+(1-z)^2}{z_+}$	$\frac{3}{2}\delta(z)$	$-z$

$$\Delta q_f(x, M_f) = \frac{\alpha_s}{2\pi} (\ln M_f^2 - \ln \mu^2) \int_x^1 \frac{dz}{z} q_f(x/z) P_{qq}^+(z) . \quad (2.58)$$

In the limit of infinitesimal change of scale, and taking into account the other possible splitting functions, we are led to the aforementioned *Altarelli-Parisi* equations:

$$\frac{dq_f(x, M^2)}{d \ln M^2} = \frac{\alpha_s}{2\pi} \int_x^1 \frac{dz}{z} \left[q_f(x/z, M^2) P_{qq}^+(z) + q_g(x/z, M^2) P_{qg}^+(z) \right] \quad (2.59)$$

$$\frac{dq_g(x, M^2)}{d \ln M^2} = \frac{\alpha_s}{2\pi} \int_x^1 \frac{dz}{z} \left[q_f(x/z, M^2) P_{gq}^+(z) + q_g(x/z, M^2) P_{gg}^+(z) \right] . \quad (2.60)$$

For reference, Table 2.1 lists the terms involved in first-order splitting functions; the conventions used in this dissertation are:

1. The most general version is $P_{ij}^{+'} \equiv \rho_{ij}^0 \left[\hat{\rho}_{ij}^+ + \rho_{ij}^\delta + \epsilon \rho_{ij}^1 \right]$, where flavor i is the daughter, j the parent.
2. Non-plus-distribution versions are obtained from the above by simply removing the “+”-signs.
3. “Primed” functions include the ϵ -coefficient ρ^1 , non-primed functions do not.

4. “Hatted” functions do not include ρ^δ .

5. $P_{ij}^1 \equiv \rho_{ij}^0 \rho_{ij}^1$ includes only the coefficient of ϵ .

Examples (flavor labels suppressed):

$$\begin{aligned}
\hat{P} &= \rho^0 \hat{\rho} \\
P &= \rho^0 (\hat{\rho} + \rho^\delta) \\
\hat{P}^+ &= \rho^0 \hat{\rho}^+ \\
P^+ &= \rho^0 (\hat{\rho}^+ + \rho^\delta) \\
\hat{P}' &= \rho^0 (\hat{\rho} + \epsilon \rho^1) \\
P' &= \rho^0 (\hat{\rho} + \rho^\delta + \epsilon \rho^1) \\
\hat{P}'^+ &= \rho^0 (\hat{\rho}^+ + \epsilon \rho^1)
\end{aligned} \tag{2.61}$$

Thus we can derive the scale dependence of the parton distributions, and take into account the leading dependence at higher orders by iteratively solving the Altarelli-Parisi equations. Just as in the case of renormalization, a full solution requires that at some scale M_0 we **measure** the distributions by comparison with experiment. Use of the new distributions in cross section calculations now requires only that we calculate, but then drop (subtract) collinear poles (and attendant finite pieces appropriate to the chosen factorization scheme).

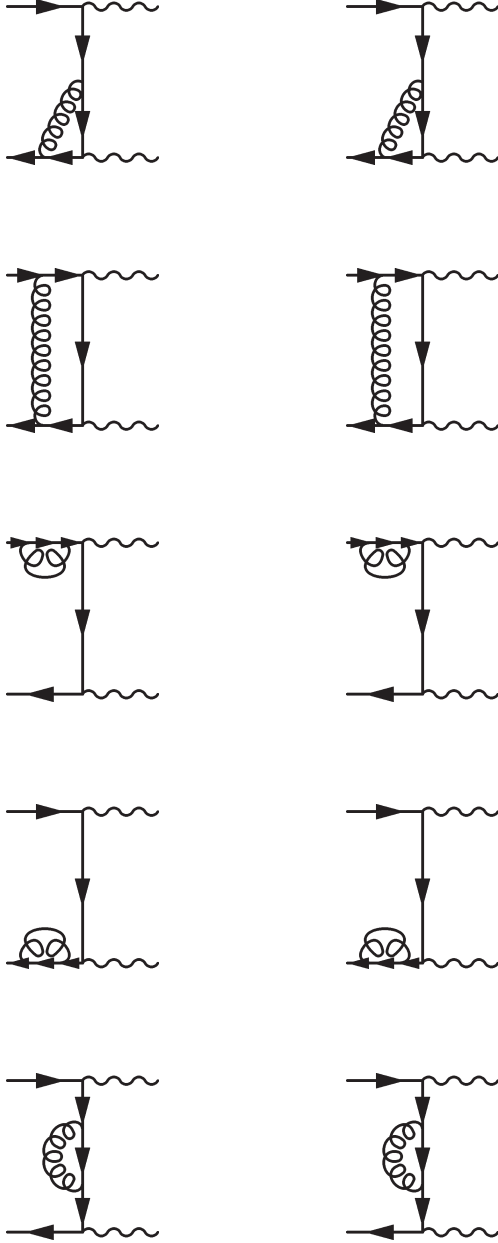


Figure 2.8. Virtual diagrams for $q\bar{q} \rightarrow \gamma\gamma$.

CHAPTER 3

EARLY RESUMMATION SCHEMES

3.1 Origin of Terms in the Unresummed Distribution

Here we will look at how the relevant logarithms arise for the QED process $e^+e^- \rightarrow \mu^+\mu^-$. We will then describe the evolution of a viable resummation method, and apply it finally to the more complicated QCD process $pp \rightarrow \mu^+\mu^- + X$.

As discussed in Section 1.4, if we define $Q^2 \equiv (p_{\mu^+}^\nu + p_{\mu^-}^\nu)^2$ as the mass (squared) of the observed muon pair, and $Q_T^2 = (\vec{p}_{T\mu^+} + \vec{p}_{T\mu^-})^2$ the transverse momentum (squared) of the pair, calculation of the leading-order contribution to a process of this type results in a delta-function at $Q_T^2 = 0$. That is, the Q_T -distribution is of the form

$$\frac{1}{\sigma_0} \frac{d\sigma}{dQ^2 dQ_T^2} = \delta(Q_T^2) \quad (3.1)$$

where $\sigma_0 \equiv d\sigma/dQ^2$.

In the relativistic limit, adding a single radiated boson to one of the incoming fermions modifies the matrix element thus:

$$\mathcal{M}u(p) \rightarrow \frac{-g\mathcal{M}\not{p}'\not{\epsilon}(k)u(p)}{p'^2} = \frac{-g\mathcal{M}(\not{p} - \not{k})\not{\epsilon}(k)u(p)}{(p - k)^2}. \quad (3.2)$$

Here $\mathcal{M}u(p)$ is the Born matrix element, p is the incoming electron momentum, and k is the momentum of the emitted massless boson, which we take to be a photon (see figure 3.1). For a high-mass muon pair, we may take the soft radiation limit (k

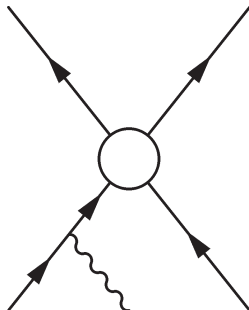


Figure 3.1. A single radiated photon in the initial state.

small relative to p), and ignore terms involving k in the numerator of equation 3.2. This leaves us with the *factorized* form

$$\mathcal{M}' = \frac{g\mathcal{M}\not{p}\not{\epsilon}u(p)}{2p \cdot k} \rightarrow g\mathcal{M}\frac{p \cdot \epsilon}{p \cdot k}u(p) . \quad (3.3)$$

By momentum conservation, $Q_T^2 = k_T^2 \sim (p \cdot k)^2$, and we find a *radiative correction* of order α to the Born cross section:

$$\frac{1}{\sigma_0} \frac{d\sigma}{dQ^2 dQ_T^2} = \delta(Q_T^2) + \frac{\alpha}{2\pi Q_T^2} (\ln(Q^2/Q_T^2) + O(1)) . \quad (3.4)$$

This cross section obviously diverges as $Q_T \rightarrow 0$ (see figure 3.3, dot-dashed line), a result of the soft and collinear divergences encountered when, respectively, the photon is either emitted with zero energy or is emitted in the same direction as the incident electron. In either case, $p \cdot k = 0$. In a full calculation, these divergences (or *poles*), will be cancelled by the contribution of other diagrams, and the remainder is usually described by means of a “*plus*”-distribution; that is, a distribution the value of which at any part of the domain is meaningful only when convoluted with another smooth function (see Section 2.4 for one example).

In our case we have a divergent function $\nu(Q_T)$ given by

$$\nu(Q_T) = \frac{1}{Q_T^2}(\ln(Q^2/Q_T^2) + O(1)) . \quad (3.5)$$

We wish to separate off the singularities at $Q_T^2 = 0$, which will be cancelled, and retain a function $\nu_+(Q_T)$ which is finite and integrable over the entire range of Q_T^2 , *i.e.* $0 \leq Q_T^2 \leq Q^2$. That is, we want

$$\nu(Q_T^2) \rightarrow \nu_+(Q_T^2) + \text{singularities}, \quad (3.6)$$

with the plus-distribution ν_+ defined as follows:

$$\int_0^{Q^2} dQ_T^2 \nu_+(Q_T) f(Q_T) \equiv \int_0^{Q^2} dQ_T^2 \nu(Q_T) [f(Q_T) - f(0)] . \quad (3.7)$$

At $Q_T^2 = 0$, $f(Q_T) - f(0) = 0$ and the integral is defined, even if the shape of $\nu_+(Q_T)$ is non-physical (like the Born term delta function). We will thus rewrite equation 3.4 in the form

$$\begin{aligned} \frac{1}{\sigma_0} \frac{d\sigma}{dQ^2 dQ_T^2} &= \delta(Q_T^2) + \frac{\alpha}{2\pi} \nu_+(Q_T) \\ \nu_+(Q_T) &\equiv \left[\frac{\ln Q^2/Q_T^2}{Q_T^2} \right]_+ + \left[\frac{O(1)}{Q_T^2} \right]_+ . \end{aligned} \quad (3.8)$$

If we now consider multiple radiated photons (see figure 3.2), we find that the matrix element—and thus the cross section—also factorizes in this soft approximation; that is, for n -photon emission we obtain a matrix element of the form

$$\mathcal{M} \frac{g^n}{n!} \prod_{i=1}^n \frac{p \cdot \epsilon}{p \cdot k_i} , \quad (3.9)$$

and a cross section

$$\frac{1}{\sigma_0} \frac{d^n \sigma}{dQ^2 dQ_T^2} = \frac{(\alpha/2\pi)^n}{n!} \prod_{i=1}^n \int_0^{Q_T^2} \nu_+(k_{T_i}^2) dk_{T_i}^2 \delta^2(\vec{Q}_T - \sum_{i=1}^n \vec{k}_{T_i}) , \quad (3.10)$$

where $\nu_+(k_{T_i}^2)$ is the first-order contribution for a single photon (here $\left[\frac{\ln Q^2/k_{T_i}^2}{k_{T_i}^2} \right]_+ + \left[\frac{O(1)}{k_{T_i}^2} \right]_+$), and the factor $n!$ arises from the indistinguishability of the emitted photons.

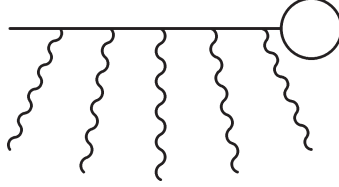


Figure 3.2. Multiple radiated photons in the initial state.

3.2 Development of a Resummation Scheme

We have seen how the series of large logarithms (equation 1.1) arises at each order in α . A first attempt at an all-orders result would naturally be to sum over just the largest log at each order. Our cross section contains a momentum-conserving delta function, but given the presence of $n!$, ignoring this function will allow us to directly form an exponentiation in momentum space. We now have completely independent photon emissions. If, as we have assumed so far, each has a relatively small transverse momentum, limited by that of the muon pair (Q_T), when we sum over all orders:

$$\begin{aligned}
\frac{1}{\sigma_0} \frac{d\sigma}{dQ^2 dQ_T^2} &= \frac{d}{dQ_T^2} \sum_{n=1}^{\infty} \frac{(\alpha/2\pi)^n}{n!} \prod_{i=1}^n \int_0^{Q_T^2} \nu_+(k_{T_i}^2) dk_{T_i}^2 \\
&= \frac{d}{dQ_T^2} \sum_{n=1}^{\infty} \frac{(\alpha/2\pi)^n}{n!} \left[\int_0^{Q_T^2} \nu_+(k_T^2) dk_T^2 \right]^n \\
&= \frac{d}{dQ_T^2} \left[e^{\frac{\alpha}{2\pi} \int_0^{Q_T^2} \nu_+ dk_T^2} - 1 \right], \tag{3.11}
\end{aligned}$$

we find, for $\nu_+(k_T^2) = \left[\frac{\ln(\hat{s}/k_T^2) + O(1)}{k_T^2} \right]_+$, the result

$$\begin{aligned}
\frac{1}{\sigma_0} \frac{d\sigma}{dQ^2 dQ_T^2} &= \frac{d}{dQ_T^2} \left[e^{-\frac{\alpha}{4\pi} \ln^2(Q^2/Q_T^2) - \frac{\alpha}{2\pi} \ln(Q^2/Q_T^2)} \right] \\
&= \frac{\alpha}{2\pi Q_T^2} \left[\ln \frac{Q^2}{Q_T^2} + O(1) \right] e^{-\frac{\alpha}{4\pi} \ln^2(Q^2/Q_T^2) - \frac{\alpha}{2\pi} \ln(Q^2/Q_T^2)}, \tag{3.12}
\end{aligned}$$

in which we have used the fact that the coefficient of our plus-distribution is constant:

$$\begin{aligned}
\int_0^{Q_T^2} \nu_+(k_T^2) dk_T^2 &= \int_0^{Q^2} \nu_+(k_T^2) dk_T^2 - \int_{Q_T^2}^{Q^2} \nu(k_T^2) dk_T^2 \\
&\equiv \int_0^{Q^2} \nu(k_T^2)(1-1) dk_T^2 - \int_{Q_T^2}^{Q^2} \nu(k_T^2)(1) dk_T^2 \\
&= 0 - \frac{1}{2} \ln^2 \frac{Q^2}{Q_T^2} - O(\ln \frac{Q^2}{Q_T^2}) .
\end{aligned} \tag{3.13}$$

This method was first attempted in 1978 by Dokshitzer, D'yakonov, and Troyan (DDT) [44].¹ It gives, as we see in figure 3.3 (dashed line), an exponential *Sudakov suppression* of the Q_T distribution as $Q_T^2 \rightarrow 0$. This effect is a consequence of the neglect of momentum-conservation among the emitted bosons, effectively imposing the condition that all of them have zero k_T in order for a zero- Q_T muon pair to be produced. The exceedingly small phase space for n bosons to be produced, all with near-zero k_T at the same time, leads to the suppression. We know, however, that this cannot be correct. It should be possible for two or more bosons of non-negligible \vec{k}_T to be emitted and still maintain a zero total \vec{Q}_T .

A subsequent analysis by Parisi and Petronzio [45–46] kept the factorized form for $d^n\sigma$, but also kept the full momentum-conserving delta function and first-order contribution. This time, the exponentiation develops automatically in impact-parameter (\vec{b}) space. The delta function can be rewritten as a Fourier transform in this space:

$$\delta^2(\vec{Q}_T - \sum_i \vec{k}_{Ti}) = \frac{1}{(2\pi)^2} \int d^2b e^{-i\vec{b} \cdot (\vec{Q}_T - \sum_i \vec{k}_{Ti})} . \tag{3.14}$$

The cross section for n -boson emission then becomes a Fourier transform and inverse-transform, with the exponentiation sandwiched inbetween. To start,

$$\frac{1}{\sigma_0} \frac{d^n\sigma}{dQ^2 dQ_T^2} = \frac{1}{(2\pi)^2} \frac{(\alpha/2\pi)^n}{n!} \int d^2b e^{-i\vec{b} \cdot (\vec{Q}_T - \sum_i \vec{k}_{Ti})} \prod_{i=1}^n \int \nu_+(k_{Ti}^2) d^2k_{Ti}$$

¹Actually, they resummed only the leading logs, $m = 2n - 1$. We include the $O(1)$ terms here as well.

$$\begin{aligned}
&= \frac{1}{(2\pi)^2} \int d^2b \frac{e^{-i\vec{b}\cdot\vec{Q}_T}}{n!} \left[\int e^{i\vec{b}\cdot\vec{k}_T} \frac{\alpha}{2\pi} \nu_+(k_T^2) d^2k_T \right]^n \\
&= \frac{1}{(2\pi)^2} \int d^2b e^{-i\vec{b}\cdot\vec{Q}_T} \frac{\left[\frac{\alpha}{2\pi} \tilde{\nu}_+(b) \right]^n}{n!}, \tag{3.15}
\end{aligned}$$

where $\tilde{\nu}_+(b)$ is the transform of $\nu_+(k_T)$ in impact parameter space.

The next step is clear. Summing over the contributions from all numbers of photons, and including the δ -function at $Q_T = 0$, Parisi and Petronzio arrived at

$$\begin{aligned}
\frac{1}{\sigma_0} \frac{d\sigma}{dQ^2 dQ_T^2} &= \frac{1}{(2\pi)^2} \int d^2b e^{-i\vec{b}\cdot\vec{Q}_T} \left[\sum_{n=1}^{\infty} \frac{1}{n!} \left[\frac{\alpha}{2\pi} \tilde{\nu}_+(b) \right]^n + 1 \right] \\
&= \frac{1}{(2\pi)^2} \int d^2b e^{-i\vec{b}\cdot\vec{Q}_T} e^{\frac{\alpha}{2\pi} \tilde{\nu}_+(b)}, \tag{3.16}
\end{aligned}$$

where the last exponential on the right is sometimes denoted by $\tilde{\sigma}$. The prescription is, then, a Fourier transform of an exponentiated transform of the next-to-leading order (NLO) perturbative result. For our simple QED example, this latter transform is

$$\begin{aligned}
\tilde{\nu}_+(b) &= \int d^2k_T e^{i\vec{b}\cdot\vec{k}_T} \left[\frac{\ln(Q^2/k_T^2) + O(1)}{k_T^2} \right]_+ \\
&= \int_0^{2\pi} d\phi \int_0^{Q^2} \frac{dk_T^2}{2} (e^{i\vec{b}\cdot\vec{k}_T} - 1) \left[\frac{\ln(Q^2/k_T^2) + O(1)}{k_T^2} \right], \tag{3.17}
\end{aligned}$$

where the upper limit on k_T has been relaxed relative to DDT and the plus-distribution definition 3.7 again used. In the high- b limit, this goes as $\tilde{\nu}(b) \simeq -\ln^2(1 + b^2 Q^2)$, giving

$$\frac{1}{\sigma_0} \frac{d\sigma}{dQ^2 dQ_T^2} \Big|_{Q_T^2=0} \sim \int_0^\infty db^2 e^{-\frac{\alpha}{2\pi} \ln^2(1+b^2 Q^2)} \simeq \frac{e^{\pi/2\alpha}}{Q^2} = \text{constant}. \tag{3.18}$$

The Sudakov suppression disappears, and one regains a finite, non-zero cross section at $Q_T = 0$ (see figure 3.3, solid line).

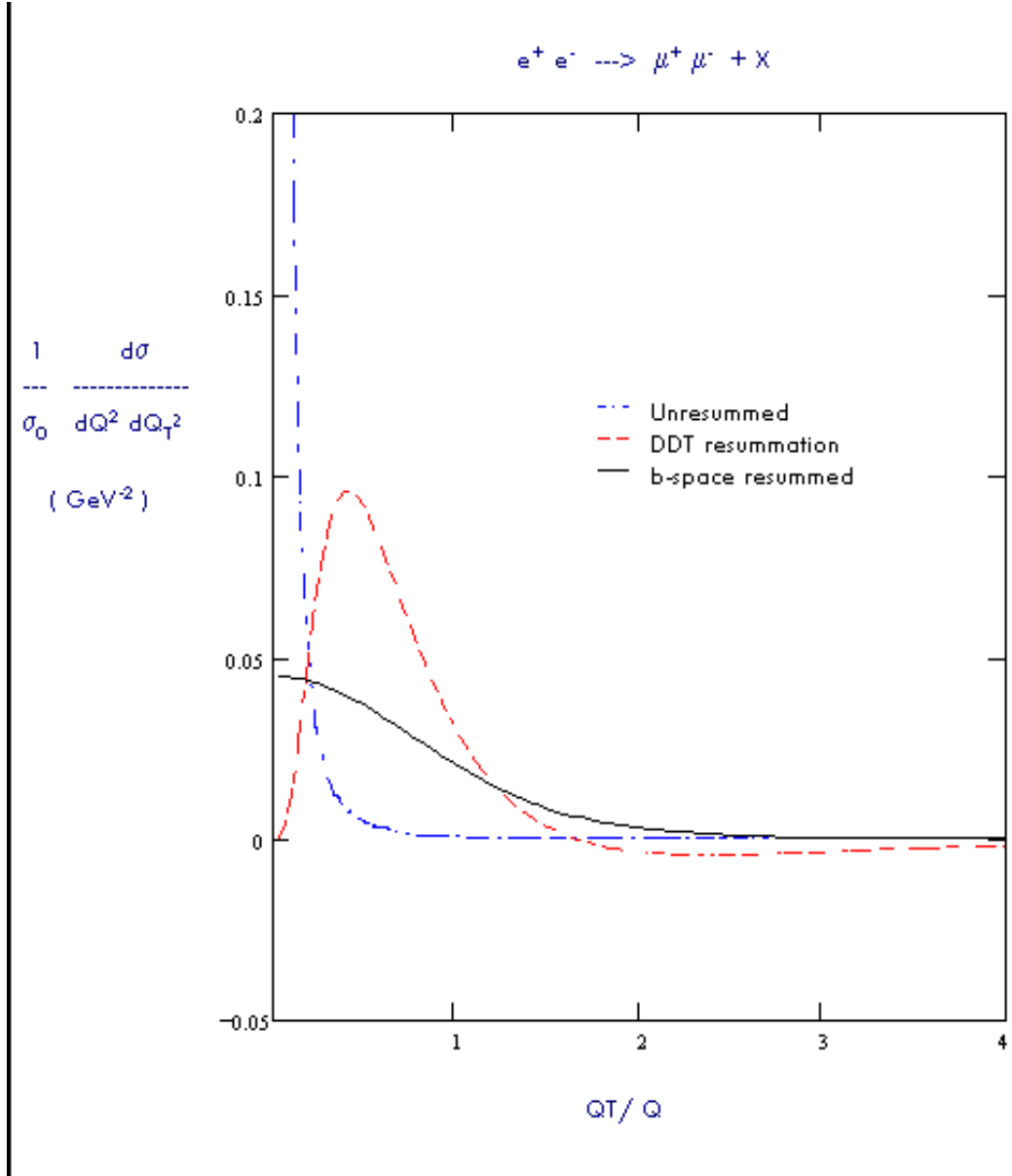


Figure 3.3. Resummation brings the low- Q_T region under control.

Resummation thus allows one to include the effects of multiple soft boson radiation to all orders, while keeping the low- Q_T region under control. The original perturbative prediction, necessarily unphysical as a result of the delta-functions and plus-distributions which dictated its bookkeeping, nevertheless was integrable:

$$\frac{1}{\sigma_0} \frac{d\sigma}{dQ^2} = \int_0^{Q^2} dQ_T^2 \left\{ \delta(Q_T^2) + \left[\frac{\ln Q^2/Q_T^2}{Q_T^2} \right]_+ + \left[\frac{O(1)}{Q_T^2} \right]_+ \right\} = 1 \quad (3.19)$$

Resummation maintains the normalization while providing a more physical model of the shape over the allowed Q_T range. Effectively, the delta function at $Q_T = 0$ is smeared by the combined recoil of multiple emissions, each of which may add or subtract from the transverse momentum of the observed muon pair.² It is worth noting, though, that although the perturbative and DDT results had an implied kinematic cutoff at $Q_T = Q$ (and in the case of DDT resummation a similar restraint on the k_T of each emitted boson), no such requirement was built into this final resummed result, and one must integrate over all Q_T to recover the correct normalization. In other words, while 3-momentum conservation was observed, energy conservation was not.

Imposition of such a constraint, if done smoothly, would tend to reduce the smearing effect, but it is not the only effect yet to be included. There remains the possibility (especially in QCD applications) that the incoming reactants may have an “intrinsic” transverse momentum, a nonperturbative effect which would again broaden the spectrum. Finally, there is the expectation that, due to the approximations which allow the above-described exponentiation to work, the correct shape of the distribution at higher Q_T (close to Q) would be better described by the original perturbative result, as the logs in that region do not overwhelm the expansion parameter. A proper description of transverse momentum spectra will necessarily be a delicate balance of perturbative, nonperturbative, and resummation effects (see figure 3.4), and in the chapters to come these will all be explored.

3.3 Application to QCD

Parisi and Petronzio applied their method to a QCD example, $pp \rightarrow \mu^+ \mu^- + X$, and compared the result with data. Due to the differing structure of the theory,

²The average transverse “kick” given to the system, $\langle Q_T \rangle$, will be a useful quantity to study in what follows.

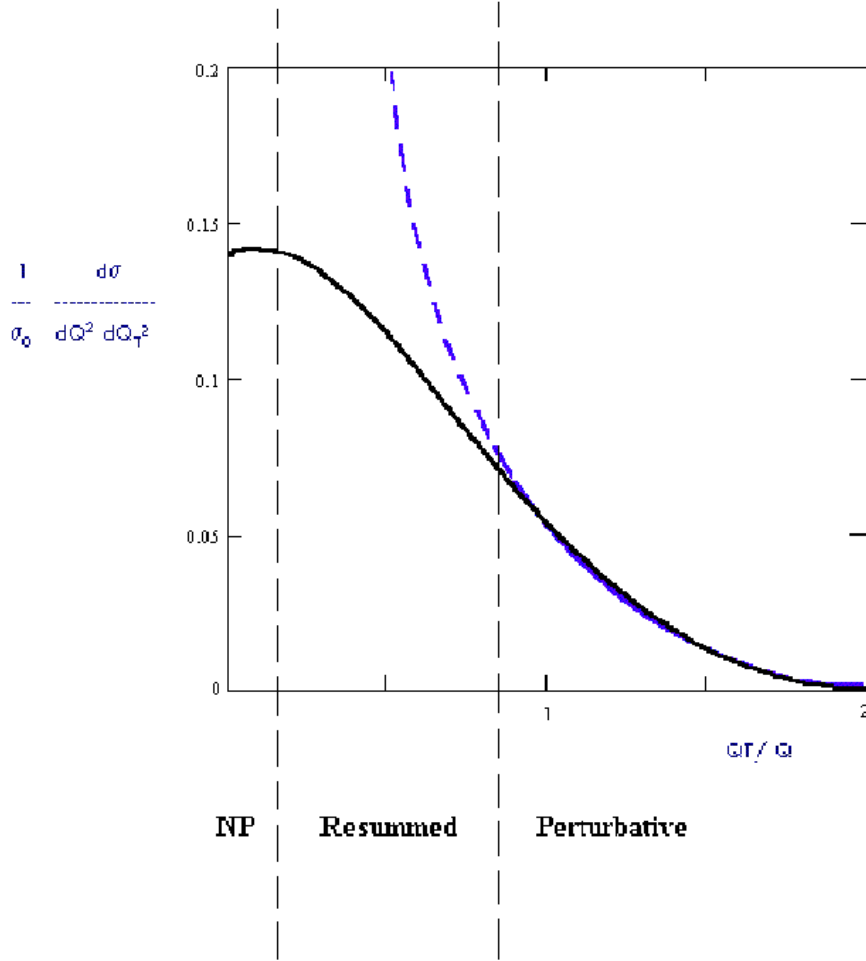


Figure 3.4. Three regions of interest.

there are details present here which do not apply to the QED case. Some of these are irrelevant to their argument and will be ignored. Others constitute new features of the procedure, or pitfalls that would otherwise constrain its effectiveness, and these will be discussed.

The structure of the resummed calculation is the same as that of the previous section (equation 3.16), although here the desired quantity is

$$E \frac{d^3\sigma}{d^3Q_T} \Big|_{y=0}^{\text{resummed}} = \frac{1}{\pi} \frac{d^3\sigma}{dQ_T^2 dQ dy} \Big|_{y=0}^{\text{res}}$$

$$\equiv \frac{\sigma_0}{(2\pi)^2} \int d^2b \, e^{-i\vec{b}\cdot\vec{Q}_T} e^{\Delta(b)} , \quad (3.20)$$

where the free variables are not only the mass Q and transverse momentum Q_T of the muon pair, but also the rapidity y (although they look only at the $y = 0$ region).

³ The “Sudakov” exponent Δ is still a transform to b -space, but as it contains the effects of higher-order corrections which now depend not on the QED coupling but the running QCD coupling $\alpha_s(k_T)$, the latter cannot in general be pulled out of the integral. There is instead

$$\Delta(b) = \int d^2k_T e^{i\vec{b}\cdot\vec{k}_T} \frac{\alpha_s(k_T^2)}{2\pi} \nu_+(k_T^2) , \quad (3.21)$$

in which ν_+ , like the Born cross section σ_0 , is defined by the unresummed perturbative result after cancellation of the poles:

$$\frac{1}{\pi} \frac{d^3\sigma}{dk_T^2 dQ dy} \Big|_{y=0} = \sigma_0 [\delta(k_T^2) + \frac{\alpha_s(k_T^2)}{2\pi} \nu_+(k_T^2)] . \quad (3.22)$$

The structure of the subprocess diagrams is the same as well, in that to leading order there is but fermion-antifermion annihilation, leading to an intermediate vector boson, which subsequently decays to the muon pair. At next-to-leading order, radiation from the initial state is included. The relevant diagrams have already been shown in the Introduction, figures 1.1, 1.2, 1.4. ⁴

Here, the fundamental interacting particles are the quarks which make up the colliding protons, and so parametrizations of these parton densities will necessarily be required. In the low- Q_T approximation to which the resummation formalism applies, it can be shown that these partons’ momentum fractions depend solely upon the rapidity of the muon pair and its mass relative to the center-of-mass energy of

³ $y = \frac{1}{2} \ln(q^0 + q^3)/(q^0 - q^3)$, where $q^\mu = p_{\mu-}^\mu + p_{\mu+}^\mu$.

⁴For simplicity, the Compton process of figure 1.3, in which a quark from one proton interacts with a gluon from the other, will not be considered here. The absence of a soft pole in this case leads only to subleading terms which are either also present in $q\bar{q}$ annihilation or which the current formalism has no mechanism to express. These terms will be discussed later in this chapter, and in Chapter 4.

the proton-proton system \sqrt{S} . In this center-of-mass frame, the two momentum fractions are

$$x_b^a = \frac{Q}{\sqrt{S}} e^{\pm y} , \quad (3.23)$$

and σ_0 will necessarily include sums over contributing flavors of the form

$$\sum_f Q_f^2 q_f^{\text{P}}(x_a) \bar{q}_f^{\text{P}}(x_b) ,$$

in which Q_f is the charge and q_f the density of flavor f . The sum extends over flavors and ant flavors, and color and spin sums must, of course, also be taken into account.

The details had also been calculated by Altarelli, *et.al.* (1978) [29], among others, and showed the expected logarithms of Q/Q_T . The difference, relative to the rough model of the previous section, is that in practice the coefficients of these logarithms are particular to the subprocess under study. For Drell-Yan production these are $2C_F$ and $-3C_F$, where $C_F = 4/3$ is a factor arising from the color structure involved. Specifically, the details are:

$$\begin{aligned} \nu_+(k_T^2) &= 2C_F \left[\frac{\ln Q^2/k_T^2}{k_T^2} \right]_+ - 3C_F \left[\frac{1}{k_T^2} \right]_+ \\ \sigma_0 &= \frac{16\alpha^2}{9QS} \sum_f Q_f^2 q_f^{\text{P}}(x_a) \bar{q}_f^{\text{P}}(x_b) . \end{aligned} \quad (3.24)$$

Before this calculation could be compared to data, a potential problem in the transform to b -space needed to be circumnavigated. This transform involves an integral over the range $0 \leq k_T^2 \leq Q^2$, but the running coupling $\alpha_s(k_T^2)$ diverges at the small scale Λ :

$$\alpha_s(k_T^2) = \frac{12\pi}{(33 - 2N_f) \ln(k_T^2/\Lambda^2)} . \quad (3.25)$$

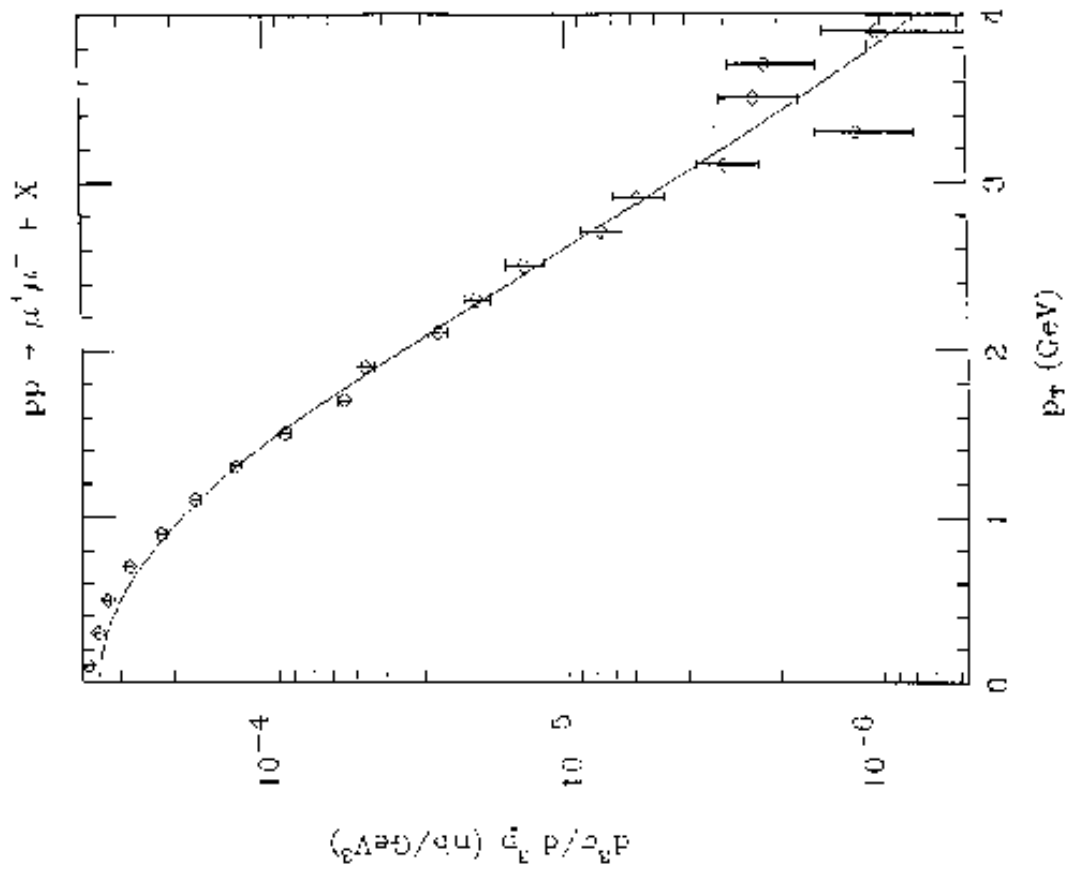
This problem was avoided by replacing k_T^2/Λ^2 with $(k_T^2 + M^2)/\Lambda^2$, where M is some scale greater than Λ , but small enough that at large k_T the replacement doesn't affect the result.

Parisi and Petronzio then dealt with the possibility that the annihilating partons might carry an intrinsic transverse momentum. This would be a small effect, observable only at very low Q_T of the pair, and would tend to “smear” the resulting low- Q_T distribution further, as the additional momentum could either add to or subtract from that provided by the radiative effects. This is most easily incorporated in impact space by tacking on a multiplicative factor to the b -space integrand:

$$e^{\Delta(b)} \rightarrow e^{\Delta(b)} e^{-\frac{1}{4}b^2 \langle p_T^2 \rangle_{\text{int}}} . \quad (3.26)$$

The Gaussian width is controlled by $\langle p_T^2 \rangle_{\text{int}}$, the average intrinsic p_T^2 assigned to the incoming partons. By damping out the high- b region, the effect of the “high-frequency” components is reduced and the momentum distribution softened somewhat, as necessary. This is a simple example of a “nonperturbative parametrization” which was to be more fully developed in later years, as the following chapter will show.

Utilizing the scale-dependent distribution functions of the CTEQ collaboration [66], and with the small values $\langle p_T^2 \rangle_{\text{int}} = 1.2 \text{ GeV}^2$ and $M^2 = 1.25 \text{ GeV}^2$, one can achieve close agreement with the data of reference [37] (see figure 3.5). Here $S = 750 \text{ GeV}^2$, $Q^2 = 56 \text{ GeV}^2$, and a conversion factor $C \simeq 389 \text{ nbarn GeV}^2$ was applied to show the results in units nb GeV^{-2} . At higher center-of-mass energies, nonperturbative effects are dwarfed by perturbative ones, the results approach independence of the phenomenological parameters, and the amount of intrinsic p_T needed to reproduce the data is considerably less.



$\langle p_{T \text{ in}}^2 \rangle = 1.2 \text{ GeV}^2$
 $\Lambda = 0.177 \text{ GeV}$
 $y = 0.0$
 $K_{\text{factor}} = 1.5227$
 $Q \text{ dep ON}$
 CTEQ LL PDF
 $N = 90$
 $\# \text{ Flavors} = 4$
 $M^2 = 1.25 \text{ GeV}^2$
 $Q^2 = 56 \text{ GeV}^2$
 $S = 750 \text{ GeV}^2$

© Data , Yoh, et. al. (1978)

Figure 3.5. $pp \rightarrow \mu^+ \mu^- X$ resummed distribution.

3.4 Subleading Terms

One final note: not all next-to-leading order terms have been included in this calculation. For both the gluon-radiative and Compton contributions, there exist remnants of collinear pole cancellations which go as $(\frac{1}{Q_T^2})_+$ times convolutions of parton densities with splitting functions. These, along with other finite terms, are not handled in the method of Parisi and Petronzio, which is focused primarily on consolidating the most singular terms.

In 1984, Altarelli, Ellis, Greco, and Martinelli (AEGM) [48] revisited the b -space formalism with the goal of including these terms. To start, they recast the calculation within the framework of the *subtraction method*, which not only performs the resummation operation upon low- Q_T approximations of the NLO terms, but then subtracts these approximations from the NLO terms to create additional finite pieces without double-counting.

In addition to these, AEGM found a way to include the collinear remnants mentioned above. Specifically, after transforming to b -space, there are terms of the form

$$\begin{aligned} q_f(x, \mu^2) &+ \frac{\alpha_s}{2\pi} \left[\ln \frac{Q_{Tmax}^2}{\mu^2} + \int_0^{Q_{Tmax}^2} d^2 Q_T e^{i\vec{b} \cdot \vec{Q}_T} \left(\frac{1}{Q_T^2} \right)_+ \right] [q_f(x, \mu^2) \circ P_{f\bar{f}}(z)] \\ &+ \frac{\alpha_s}{2\pi} [q_f(x, \mu^2) \circ C_f(z)] , \end{aligned} \quad (3.27)$$

in which $q_f(x, \mu^2)$ is a parton density of flavor f , evaluated at momentum fraction x and scale μ . $P_{f\bar{f}}(z)$ is an appropriate splitting function, and $C_f(z)$ contains other finite terms. The symbol $[q_f \circ P]$ refers to a convolution of the parton density with the function P (similarly for $[q_f \circ C]$):

$$q_f(x, \mu^2) \circ P_{f\bar{f}}(z) \equiv \sum_{\bar{f}} \int_x^1 \frac{dz}{z} q_{\bar{f}}\left(\frac{x}{z}, \mu^2\right) P_{f\bar{f}}(z) . \quad (3.28)$$

By defining a new factorization scale

$$\ln M_f^2 \equiv \ln Q_{Tmax}^2 + \int_0^{Q_{Tmax}^2} d^2 Q_T e^{i\vec{b} \cdot \vec{Q}_T} \left(\frac{1}{Q_T^2} \right)_+ , \quad (3.29)$$

they were able to absorb the remaining plus-distribution terms into the parton densities via rescalings

$$q_f(x, M_f^2) = q_f(x, \mu^2) + \frac{\alpha_s(\mu^2)}{2\pi} \ln \frac{M_f^2}{\mu^2} \sum_{\tilde{f}} \int_x^1 \frac{dz}{z} q_{\tilde{f}}\left(\frac{x}{z}, \mu^2\right) P_{f\tilde{f}}(z) . \quad (3.30)$$

The remaining $[q_f \circ C]$ convolutions were left alone (and not exponentiated), although they too were now evaluated at the new scale M_f^2 . As it turns out, $M_f \sim b_0/b$, which is the value suggested almost concurrently by the work of Collins, Soper, and Sterman (CSS), who used renormalization methods to solidify the theoretical basis of the b -space formalism, and extend it in a systematic way to include subleading tiers of logarithms. We will study the CSS work in more detail in Chapter 4.

CHAPTER 4

THE CSS FORMALISM

4.1 Derivation

In 1984, Collins, Soper, and Sterman (CSS) used renormalization group methods to arrive at an improved resummation scheme, one which not only preserves momentum conservation, but which can be made increasingly more precise as additional terms are calculated [49]. Although derived for Drell-Yan processes, the result is, in principle, generally applicable to all two-scale processes.

It will be helpful here to recall a bit of the physical picture: at leading order, two partons (one from each incoming hadron) collide and produce a measured final state, of mass Q and transverse momentum Q_T . In the case of Drell-Yan production, this final state is a pair of leptons. As the incoming partons are assumed to be collinear with each other and the hadronic beam, if no other particles are observed, there is nothing for the system to recoil against, and one predicts that Q_T will equal zero. Similarly, by energy conservation, the mass of the system of colliding partons (as measured in the same frame) must also have been Q , each parton contributing a fraction of this energy.

In general, of course, other particles are generated from this partonic collision, and one can go to higher orders in perturbation theory to predict more accurately the Q_T -dependence as measured in the lab. As noted in Chapter 3, these predictions are plausible, without modification, at high- Q_T , but in the limit $Q_T \ll Q$, the biggest contributions come from cases in which the additional particles are either too soft to

individually detect or are themselves nearly collinear with one or the other incoming parton. Resummation is then required for a complete description.

Fortunately, in this limit the long-distance (low energy) and short-distance (high energy) phenomena become roughly independent of one another, and one can expect a factorization of the cross-section as follows:

$$\begin{aligned}
\sigma_S &\sim \int d^2 k_{Ta} \int d^2 k_{Tb} \int d^2 k_{TS} \delta^2(\vec{Q}_T - \sum_i \vec{k}_{Ti}) \\
&\times J_a\left(\frac{p_a^0}{\mu}, \frac{k_{Ta}}{\mu}, g(\mu)\right) J_b\left(\frac{p_b^0}{\mu}, \frac{k_{Tb}}{\mu}, g(\mu)\right) \\
&\times S\left(\frac{k_{TS}}{\mu}, g(\mu)\right) H\left(\frac{p_a^0}{\mu}, \frac{p_b^0}{\mu}, \frac{Q}{\mu}, g(\mu)\right). \tag{4.1}
\end{aligned}$$

Here high-energy quantities such as Q and the parton energies $p_{a,b}^0$ organize themselves within a hard scattering factor H , while small, non-collinear transverse momenta k_{TS} contribute to a soft function S . Associated with each incoming parton (and the nearly collinear quanta k_{Ti} surrounding it) is a non-perturbative factor J_i , which remains dependent upon both low and high-energy quantities (k_{Ti} and p_i^0 respectively). For the transverse momenta shown, there is a delta-function included which relates their vector sum to the \vec{Q}_T of the observed system. The hard quantities are related to each other in a way: in the limit described, both p_a^0 and p_b^0 are expressible as simple fractions of Q . Thus the functions $J_{a,b}$ have an implicit dependence upon Q which will become important in what follows. Each function depends upon the QCD coupling strength $g(\mu)$ and its argument, the renormalization scale μ ; the fact that the cross section itself does not depend upon μ will also be of import.

Proof of such factorizations can be found, for example, in references [47, 67]; the particular choice of variables which express the high and low-energy scales is different, but the general argument is the same. The crucial point is that factorization, coupled with invariance of the cross section under certain

transformations, leads to renormalization group properties of the factored functions, and thus to exponentiation. An all-orders resummation of the leading terms is the end result, the corresponding leading coefficients determined by comparison with the perturbatively-calculated result at fixed order.

Equation 4.1 above is in the form of a multiple convolution; that is, only the matrix element, not the phase space, has factorized. Significant simplification arises after a Fourier transform to impact parameter space,

$$\int d^2 Q_T e^{i\vec{b} \cdot \vec{Q}_T} \delta^2(\vec{Q}_T - \sum_i \vec{k}_{Ti}) = e^{i\vec{b} \cdot \sum_i \vec{k}_{Ti}} = \prod_i e^{i\vec{b} \cdot \vec{k}_{Ti}} , \quad (4.2)$$

in which the impact parameter is the two-dimensional axial vector \vec{b} . Then, for each transverse momentum \vec{k}_{Ti} , one obtains

$$\int d^2 k_{Ti} e^{i\vec{b} \cdot \vec{k}_{Ti}} f(k_{Ti}) = f(b) . \quad (4.3)$$

This produces the simple product

$$\tilde{\sigma}_S(b, Q) = \tilde{J}_a\left(\frac{p_a^0}{\mu}, b\mu, g(\mu)\right) \tilde{J}_b\left(\frac{p_b^0}{\mu}, b\mu, g(\mu)\right) \tilde{S}(b\mu, g(\mu)) \tilde{H}\left(\frac{p_a^0}{\mu}, \frac{p_b^0}{\mu}, \frac{Q}{\mu}, g(\mu)\right) , \quad (4.4)$$

where the tilde above each function is a reminder of the transform that has taken place.

Taking the logarithmic derivative of both sides with respect to the large scale Q^2 , CSS arrived at

$$\frac{\partial \ln \tilde{\sigma}_S}{\partial \ln Q^2} = \frac{\partial \ln \tilde{J}_a}{\partial \ln Q^2} + \frac{\partial \ln \tilde{J}_b}{\partial \ln Q^2} + \frac{\partial \ln \tilde{H}}{\partial \ln Q^2} . \quad (4.5)$$

The logarithms of \tilde{J}_a and \tilde{J}_b now contain explicit dependences upon Q , and, as shown in references [47, 67–68], each derivative thereof contributes to two separate quantities, one a function of $b\mu$ and $g(\mu)$ only, the other a function of Q/μ and $g(\mu)$ only:

$$\frac{\partial \ln \tilde{J}_a}{\partial \ln Q^2} + \frac{\partial \ln \tilde{J}_b}{\partial \ln Q^2} = K(b\mu, g(\mu)) + G_J(Q/\mu, g(\mu)) . \quad (4.6)$$

As \tilde{H} doesn't depend on b , its derivative contributes only to a function of Q/μ and $g(\mu)$:

$$\frac{\partial \ln \tilde{H}}{\partial \ln Q^2} = G_H(Q/\mu, g(\mu)) . \quad (4.7)$$

Adding G_J and G_H to form a new function G , one arrives at

$$\frac{\partial \ln \tilde{\sigma}_S}{\partial \ln Q^2} = K(b\mu, g(\mu)) + G(Q/\mu, g(\mu)) . \quad (4.8)$$

CSS then made use of the fact that the cross section is independent of renormalization scale μ :

$$\frac{\partial}{\partial \ln Q^2} \frac{\partial \ln \tilde{\sigma}_S}{\partial \ln \mu} = \frac{\partial}{\partial \ln \mu} \frac{\partial \ln \tilde{\sigma}_S}{\partial \ln Q^2} = \frac{\partial}{\partial \ln \mu} [K + G] = 0 , \quad (4.9)$$

and so, since K and G share only a dependence on g , it must be that there exists some function γ such that

$$\frac{\partial K}{\partial \ln \mu} = -\frac{\partial G}{\partial \ln \mu} \equiv -\lambda(g(\mu)) . \quad (4.10)$$

All the b -dependence is in K , while all the Q -dependence is in G , and both can be independently scaled, since both satisfy their own evolution equations.

It will be instructive here to stop and see why this is important. In a perturbative calculation, after dealing with the soft and collinear poles, the cross section can be written as a sum of two series in $\alpha_s/2\pi$:

$$\sigma = \sum_{N=0}^{\infty} \left[\frac{\alpha_s(g(\mu))}{2\pi} \right]^N \left[\sigma_S^{(N)} + \sigma_R^{(N)} \right] , \quad (4.11)$$

in which the coefficients are either integrably divergent as $Q_T \rightarrow 0$ (here $\sigma_S^{(N)}$, the “singular” piece) or are zero in this limit and thus pose no threat to the convergence

of the expansion $(\sigma_R^{(N)})$, the “regular” piece).¹ The former series $(\sigma_S^{(N)})$ corresponds to the cross section we began with in equation 4.1, and we know something about its perturbative structure:

$$\begin{aligned} \sigma_S^{(N)} &= T_0^{(N)}(Q/\mu, g(\mu))\delta(\vec{Q}_T) \\ &+ \sum_{m=0}^{2N-1} T^{(N,m)}(Q/\mu, g(\mu)) \left[\frac{\ln^m(Q^2/Q_T^2)}{Q_T^2} \right]_+ . \end{aligned} \quad (4.12)$$

Here the “plus-distribution” $[]_+$ denotes a regularization such that

$$\begin{aligned} \int_0^{Q^2} dQ_T^2 \left[\frac{\ln^m(Q^2/Q_T^2)}{Q_T^2} \right]_+ f(Q_T) &\equiv \int_0^{Q^2} dQ_T^2 \left[\frac{\ln^m(Q^2/Q_T^2)}{Q_T^2} \right] [f(Q_T) - f(0)] \\ &\text{or} \\ \int_0^{p_T^2} dQ_T^2 \left[\frac{\ln^m(Q^2/Q_T^2)}{Q_T^2} \right]_+ &= -\frac{1}{m+1} \ln^{m+1}(Q^2/p_T^2) . \end{aligned} \quad (4.13)$$

CSS realized that, once the Fourier transform to b -space is performed, as in equation 4.4, the large logs of Q/Q_T become large logs of Qb , or equivalently, logs of Q/μ and $b\mu$:

$$\int d^2Q_T e^{-i\vec{Q}_T \cdot \vec{b}} \left[\frac{\ln^m(Q^2/Q_T^2)}{Q_T^2} \right]_+ \sim \sum_{n=0}^{m+1} \ln^n(Qb) . \quad (4.14)$$

Since these large logs occur, the expansion doesn’t converge, and one can’t even approximate $d\tilde{\sigma}_S$ well by the sum of the leading log terms ($m = 2N - 1$).

Fortunately, given the separability of these logarithms (as shown in equation 4.8) and the independent renormalization groups of K and G (equation 4.10), CSS were able to do something about this.² They scaled μ in K up to order $1/b$, and μ in G to order Q . Both the large logs of $b\mu$ in K and the logs of Q/μ in G then tended to 0.

¹This structure results from the use of the subtraction method (see Section 3.4). Asymptotic limits of the fixed-order result (that is, the logs of Q/Q_T) are subtracted to form $\sigma_R^{(N)}$, and then added back in to form $\sigma_S^{(N)}$ after pole-cancellation.

²The derivation to be embarked upon is rather involved, and the casual reader may wish to skip to equation 4.35.

In practice, this need not be exact, and CSS allowed for variation by using c_1/b and c_2Q , where c_1 and c_2 are both of order 1. The canonical choice for these constants is $c_1 = b_0 \equiv 2e^{-\gamma_E} \simeq 1.123$, $c_2 = 1$. From equation 4.10:

$$\begin{aligned} K(c_1, g(c_1/b)) - K(b\mu, g(\mu)) &= - \int_{\mu}^{c_1/b} \frac{d\bar{\mu}}{\bar{\mu}} \gamma(g(\bar{\mu})) \\ G(1/c_2, g(c_2Q)) - G(Q/\mu, g(\mu)) &= \int_{\mu}^{c_2Q} \frac{d\bar{\mu}}{\bar{\mu}} \gamma(g(\bar{\mu})) , \end{aligned} \quad (4.15)$$

and thus

$$\begin{aligned} [K(c_1, g(c_1/b)) + G(1/c_2, g(c_2Q))] &- [K(b\mu, g(\mu)) + G(Q/\mu, g(\mu))] \\ &= \int_{c_1^2/b^2}^{c_2^2Q^2} \frac{d\bar{\mu}^2}{\bar{\mu}^2} \frac{\gamma(g(\bar{\mu}))}{2} . \end{aligned} \quad (4.16)$$

Now, for any function $F(b, Q)$,

$$\frac{dF(b, Q)}{d(1/b^2)} = \frac{\partial F(b, Q)}{\partial \ln(1/b^2)} \frac{d \ln(1/b^2)}{d(1/b^2)} = \frac{1}{(1/b^2)} \frac{\partial F(b, Q)}{\partial \ln(1/b^2)} , \quad (4.17)$$

so

$$\begin{aligned} \int_{F(b, Q)}^{F(c_1/c_2Q, Q)} dF(\bar{b}, Q) &= F(c_1/c_2Q, Q) - F(b, Q) \\ &= \int_{1/b^2}^{c_2^2Q^2/c_1^2} \frac{d(1/\bar{b}^2)}{(1/\bar{b}^2)} \frac{\partial F(\bar{b}, Q)}{\partial \ln(1/\bar{b}^2)} . \end{aligned} \quad (4.18)$$

If one takes $F(b, Q) \equiv K(b\mu, g(\mu)) + G(Q/\mu, g(\mu))$, it follows that

$$\begin{aligned} K(b\mu) + G(Q/\mu) &= \frac{K(c_1\mu/c_2Q, g(\mu)) + G(Q/\mu, g(\mu))}{\int_{1/b^2}^{c_2^2Q^2/c_1^2} \frac{d(1/\bar{b}^2)}{(1/\bar{b}^2)} \frac{\partial [K(\bar{b}\mu) + G(Q/\mu)]}{\partial \ln(1/\bar{b}^2)}} , \end{aligned} \quad (4.19)$$

where

$$\frac{\partial[K(\bar{b}\mu) + G(Q/\mu)]}{\partial \ln(1/\bar{b}^2)} = \frac{\partial[K(c_1, g(c_1/\bar{b})) + G(1/c_2, g(c_2Q))]}{\partial \ln(1/\bar{b}^2)} + \frac{\gamma(g(c_1/\bar{b}))}{2}, \quad (4.20)$$

by equation 4.16 and the theorem

$$\frac{\partial}{\partial x} \int_a^x f(t) dt = f(x), \quad (4.21)$$

with $x \equiv c_1^2/\bar{b}^2$, $t \equiv \bar{\mu}^2$, and $a \equiv c_2^2Q^2$. Meanwhile,

$$\frac{\partial[K(c_1, g(c_1/\bar{b})) + G(1/c_2, g(c_2Q))]}{\partial \ln(1/\bar{b}^2)} = \beta(g(1/\bar{b}^2)) \frac{\partial K(c_1, g(1/\bar{b}^2))}{\partial g(1/\bar{b}^2)} \quad (4.22)$$

for $\beta(g(x)) \equiv \frac{dg(x)}{d \ln x}$, and

$$K(c_1\mu/c_2Q, g(\mu)) + G(Q/\mu, g(\mu)) = K(c_1, g(c_2Q)) + G(1/c_2, g(c_2Q)), \quad (4.23)$$

by equation 4.16 again, with $c_1/b \rightarrow c_2Q$.

Performing the change of variables $\bar{\mu} \equiv c_1/\bar{b}$ in the integral of equation 4.19:

$$\int_{1/b^2}^{c_2^2Q^2/c_1^2} \frac{d(1/\bar{b}^2)}{(1/\bar{b}^2)} \rightarrow \int_{c_1^2/b^2}^{c_2^2Q^2} \frac{d\bar{\mu}^2}{\bar{\mu}^2}, \quad (4.24)$$

CSS derived, in all,

$$K(b\mu, g(\mu)) + G(Q/\mu, g(\mu)) = - \int_{c_1^2/b^2}^{c_2^2Q^2} \frac{d\bar{\mu}^2}{\bar{\mu}^2} A(c_1, g(\bar{\mu})) - B(c_1, c_2, g(c_2Q)), \quad (4.25)$$

where

$$\begin{aligned} A(c_1, g(\bar{\mu})) &\equiv \frac{\gamma(g(\bar{\mu}))}{2} + \frac{1}{2} \beta(g(\bar{\mu})) \frac{\partial K(c_1, g(\bar{\mu}))}{\partial g(\bar{\mu})} \\ B(c_1, c_2, g(c_2Q)) &\equiv -[K(c_1, g(c_2Q)) + G(1/c_2, g(c_2Q))]. \end{aligned} \quad (4.26)$$

Thus, returning to equation 4.8,

$$\frac{\partial \ln \tilde{\sigma}_S(b, Q)}{\partial \ln Q^2} = - \int_{c_1^2/b^2}^{c_2^2 Q^2} \frac{d\bar{\mu}^2}{\bar{\mu}^2} A(c_1, g(\bar{\mu})) - B(c_1, c_2, g(c_2 Q)) , \quad (4.27)$$

where, since K, G, γ , and $\beta \partial K / \partial g$ all have perturbative expansions in α_s , so do A and B .

Treating equation 4.27 as an ordinary differential equation in $c_2 Q$ with a parameter b , CSS found the solution, and generated the Sudakov exponent, as follows. Separating variables and integrating both sides from c_1/b to $c_2 Q$ gives:

$$\begin{aligned} \int_{c_1/b}^{c_2 Q} d \ln \tilde{\sigma}_S(b, \bar{Q}) &= \ln \tilde{\sigma}_S(b, c_2 Q) - \ln \tilde{\sigma}_S(b, c_1/b) \equiv -S(b, Q) \\ \text{or} \\ \tilde{\sigma}_S(b, Q) &= \tilde{\sigma}_S(b, c_1/c_2 b) e^{-S(b, Q)} , \end{aligned} \quad (4.28)$$

where

$$S(b, Q) \equiv \int_{\ln(c_1/b)}^{\ln(c_2 Q)} d \ln(c_2 \bar{Q}) \left[\int_{c_1^2/b^2}^{c_2^2 \bar{Q}^2} \frac{d\bar{\mu}^2}{\bar{\mu}^2} A(\bar{\mu}) + B(c_2 \bar{Q}) \right] . \quad (4.29)$$

This Sudakov exponent can be simplified as follows. The first term,

$$\int_{\ln(c_1/b)}^{\ln(c_2 Q)} d \ln(c_2 \bar{Q}) \int_{c_1^2/b^2}^{c_2^2 \bar{Q}^2} \frac{d\bar{\mu}^2}{\bar{\mu}^2} A(\bar{\mu}) = 2 \int_{c_1/b}^{c_2 Q} \frac{d\bar{\mu}}{\bar{\mu}} \int_{c_1/b}^{\bar{\mu}} \frac{d\bar{\mu}'}{\bar{\mu}'} A(\bar{\mu}') , \quad (4.30)$$

followed by an integration by parts gives

$$\begin{aligned} \int &= 2 \ln \bar{\mu} \int_{c_1/b}^{\bar{\mu}} \frac{d\tilde{\mu}}{\tilde{\mu}} A(\tilde{\mu}) \Big|_{c_1/b}^{c_2 Q} - 2 \int_{c_1/b}^{c_2 Q} \frac{d\bar{\mu}}{\bar{\mu}} \ln \bar{\mu} A(\bar{\mu}) \\ &= 2 \ln c_2 Q \int_{c_1/b}^{c_2 Q} \frac{d\tilde{\mu}}{\tilde{\mu}} A(\tilde{\mu}) - 2 \ln c_1/b \int_{c_1/b}^{c_1/b} \frac{d\tilde{\mu}}{\tilde{\mu}} A(\tilde{\mu}) - 2 \int_{c_1/b}^{c_2 Q} \frac{d\bar{\mu}}{\bar{\mu}} \ln \bar{\mu} A(\bar{\mu}) \\ &= \int_{c_1^2/b^2}^{c_2^2 Q^2} \frac{d\bar{\mu}^2}{\bar{\mu}^2} \ln \left(\frac{c_2^2 Q^2}{\bar{\mu}^2} \right) A(\bar{\mu}) , \end{aligned} \quad (4.31)$$

while

$$\int_{\ln(c_1/b)}^{\ln(c_2 Q)} d\ln(c_2 \bar{Q}) B(c_2 \bar{Q}) = \frac{1}{2} \int_{c_1^2/b^2}^{c_2^2 Q^2} \frac{d\bar{\mu}^2}{\bar{\mu}^2} B(\bar{\mu}) , \quad (4.32)$$

and thus

$$S = \int_{c_1^2/b^2}^{c_2^2 Q^2} \frac{d\bar{\mu}^2}{\bar{\mu}^2} \left[\ln\left(\frac{c_2^2 Q^2}{\bar{\mu}^2}\right) A(\bar{\mu}) + B(\bar{\mu}) \right] . \quad (4.33)$$

Evaluating 4.4 with $Q = c_1/c_2 b$ gives the coefficient of the Sudakov exponential in equation 4.28. Pulling out the parton distributions from $\tilde{J}_{a,b}$ and rewriting the rest as separable functions $C_{i/\tilde{i}}$, CSS obtained :

$$\begin{aligned} \tilde{\sigma}_S(b, \mu) &= \sum_{\tilde{a}} \int_{x_1^0}^1 \frac{dx_1}{x_1} f_{\tilde{a}/A}(x_1, \mu) C_{a/\tilde{a}}(x_1^0/x_1, b, c_1/c_2, g(\mu)) \\ &\times \sum_{\tilde{b}} \int_{x_2^0}^1 \frac{dx_2}{x_2} f_{\tilde{b}/B}(x_2, \mu) C_{b/\tilde{b}}(x_2^0/x_2, b, c_1/c_2, g(\mu)) , \end{aligned} \quad (4.34)$$

for which they, in practice, set the scale $\mu = c_1/b$.

To regain a useful expression in Q_T -space, CSS performed the inverse Fourier transform on equation 4.28, added back in the finite remainders σ_R from equation 4.11, and arrived at their final result for the perturbative region

$$\sigma = \left\{ \frac{1}{2\pi^2} \int d^2 \vec{b} e^{i\vec{b} \cdot \vec{Q}_T} \tilde{\sigma}_S(b, c_1/c_2 b) e^{-S(b, Q)} \right\} + \sigma_F , \quad (4.35)$$

in which

$$S = \int_{c_1^2/b^2}^{c_2^2 Q^2} \frac{d\bar{\mu}^2}{\bar{\mu}^2} \left[\ln\left(\frac{c_2^2 Q^2}{\bar{\mu}^2}\right) A(\bar{\mu}) + B(\bar{\mu}) \right] \quad (4.36)$$

$$\sigma_F = \sum_{a,b} \int_{x_1^0}^1 \frac{dx_1}{x_1} \int_{x_2^0}^1 \frac{dx_2}{x_2} \sum_{N=1}^{\infty} \left[\frac{\alpha_s(\mu)}{2\pi} \right]^N \sigma_R^{(N)}(a, b, Q_T, Q, \mu, \frac{x_1^0}{x_1}, \frac{x_2^0}{x_2}) . \quad (4.37)$$

CSS resummation allows for the resummation of tiers of logarithms two at a time. That is, given the first N $\{A, B, C\}$ coefficients, one can resum the first $2N$

tiers of logarithms over all orders. Implicitly, there occurs a reorganization of the logs ($L \equiv \ln(Q/Q_T)$) such that successive orders grow by α_s as opposed to $\alpha_s L^2$:

$$\begin{aligned}
\sigma &\sim \alpha_s(L+1) \\
&+ \alpha_s^2 \left[(L^3 + L^2) + (L+1) \right] \\
&+ \alpha_s^3 \left[(L^5 + L^4) + (L^3 + L^2) + (L+1) \right] \\
&+ \dots \\
\rightarrow &\rightarrow \alpha_s \left[(L+1) + \alpha_s(L^3 + L^2) + \alpha_s^2(L^5 + L^4) + \dots \right] \\
&+ \alpha_s^2 \left[(L+1) + \alpha_s(L^3 + L^2) + \alpha_s^2(L^5 + L^4) + \dots \right] \\
&+ \alpha_s^3 \left[(L+1) + \alpha_s(L^3 + L^2) + \alpha_s^2(L^5 + L^4) + \dots \right] \\
&+ \dots
\end{aligned}$$

To obtain these coefficients, one expands the resummed form to the same order as one has calculated perturbatively, and compares this expansion with the asymptotic approximation of the perturbative result. Double-counting is avoided, as in the AEGM result, by use of the subtraction method. Furthermore, the C coefficients contain the unexponentiated subleading terms discussed in Section 3.4.

4.2 Extension to the Nonperturbative Region.

Strictly, the above result is valid only at low b ($b \ll 1/\Lambda_{QCD}$). At $b > \sim \frac{1}{\Lambda_{QCD}}$, the coefficients A and B in the Sudakov exponent become dependent not only on $\alpha_s(\bar{\mu})$ but on the parton masses in the form $m_f/\bar{\mu}$. A high enough impact parameter is reached that perturbation theory is not a valid description, and $\bar{\mu}$ is then allowed to go small enough that both $g(\bar{\mu})$ and $m_f/\bar{\mu}$ blow up. As Parisi and Petronzio have shown [45], $\tilde{\sigma}_S$ is dominated by $b \simeq \frac{1}{\Lambda_{QCD}} \left(\frac{Q}{\Lambda_{QCD}} \right)^{-0.41} \ll \frac{1}{\Lambda_{QCD}}$ for large Q/Q_T , but we don't with current technology obtain large enough Q to ignore the $b > \frac{1}{\Lambda_{QCD}}$

region. At low b , c_1/b and hence $\bar{\mu}$ stays high enough that both $m_f/\bar{\mu}$ and $g(\bar{\mu})$ are small, and one recovers the perturbative results above.

It is clear that some arrangements must be made to parametrize the effects of the nonperturbative region, while keeping the perturbative formalism in use in its region of applicability. CSS suggested the following: define a function

$$b^*(b) \equiv \frac{b}{\sqrt{1 + b^2/b_{max}^2}} , \quad (4.38)$$

which goes no higher than b_{max} . Use this b^* for evaluations of the perturbative $d\tilde{\sigma}_S$, and rewrite the full $d\tilde{\sigma}_S$ as

$$d\tilde{\sigma}_S(b) = d\tilde{\sigma}_S(b^*) \left[\frac{d\tilde{\sigma}_S(b)}{d\tilde{\sigma}_S(b^*)} \right] , \quad (4.39)$$

where the second factor is approximated by a parametrization in b .

Perhaps the easiest way to predict the form of such a parametrization is to return to equation 4.8 and directly integrate, starting at some minimum scale Q_0 at which one would deem a finite-order expansion in terms of $\alpha_s(Q_0)$ “sufficiently accurate” (*e.g.* $Q_0 = c_1/b_{max}$). Dividing by the result taken at $b = b^*$ yields a ratio of the form [69]

$$\frac{d\tilde{\sigma}_S(b)}{d\tilde{\sigma}_S(b^*)} = \exp \left[-h_K(b) \ln(Q^2/Q_0^2) - h_A(x_a^0, b) - h_B(x_b^0, b) \right] . \quad (4.40)$$

We will hereafter refer to the exponent above as the nonperturbative function S_{NP} . Like the parton distributions, the coefficient functions h are intended to be universal (generally applicable) and extractible from data. The one constraint is that $\exp(S_{NP}) \rightarrow 1$ as $b \rightarrow b^* \rightarrow 0$.

To date, sufficient data have not been taken to study the flavor dependence of the functions $h_{A,B}$, nor the dependence upon x_a^0 or x_b^0 individually. However, attempts have been made to fit simplified versions of the above form. Ladinsky and Yuan (LY)

[70] in 1994 and Landry, Brock, Ladinsky, and Yuan (LBLY) [71] in 1999 used the three-parameter form shown here:

$$S_{NP} = -g_2 b^2 \ln\left(\frac{Q}{2Q_0}\right) - g_1 b^2 - g_1 g_3 b \ln(100 x_a^0 x_b^0) . \quad (4.41)$$

A previous analysis by Davies, Webber, and Stirling (DWS) [72] in 1985 was made with a two-parameter form obtained by setting $g_3 = 0$ in the above. LBLY also studied the two-parameter form, and the results of all these efforts are collected in Table 4.1 below. In Chapter 7, we will provide evidence that a single-parameter, Q -independent form may agree better with data.

Table 4.1. Nonperturbative Parameters.

	DWS	LBLY	LY	LBLY
$g_1(GeV^2)$	0.40	0.24	0.11	0.15
$g_2(GeV^2)$	0.15	0.34	0.58	0.48
$g_3(GeV^{-1})$	N/A	N/A	-1.5	-0.58
$Q_0(GeV)$	2.0	1.6	1.6	1.6
$b_{max}(GeV^{-1})$	0.5	0.5	0.5	0.5
PDF	DO1	CTEQ3M	CTEQ2M	CTEQ3M
DATA	E288,R209	E288,R209, CDF-Z,E605	E288,R209, CDF-Z	E288,R209, CDF-Z,E605

In lieu of equation 4.35 then, the final CSS result can be written as:

$$d\sigma = \left\{ \frac{1}{2\pi^2} \int d^2\vec{b} e^{i\vec{b}\cdot\vec{Q}_T} d\tilde{\sigma}_S(b^*, c_1/c_2 b^*) e^{-S(b^*, Q)} e^{S_{NP}(b, Q)} \right\} + d\sigma_F . \quad (4.42)$$

4.3 The Sudakov Exponent at very low b .

Now, what about the very low- b region, where $c_1/b > c_2 Q$? Here there are no large logs, but one does not want the Sudakov exponent to change sign. In practice one may consider cutting off the exponent, that is, simply taking $\exp[-S(b)] \rightarrow \exp[0] = 1$

for this region. But will this preserve the proper normalization upon integration over Q_T ? Altarelli, *et. al.* (1984) [48] calculated the exact first-order result for the Sudakov form factor and arrived at

$$S(b, Q) = \frac{\alpha_s}{2\pi} \int_0^{Q^2} \frac{d\bar{\mu}^2}{\bar{\mu}^2} \left[A^{(1)} \ln\left(\frac{Q^2}{\bar{\mu}^2}\right) + B^{(1)} \right] (J_0(b\bar{\mu}) - 1) , \quad (4.43)$$

which by inspection has the desired property of becoming zero as $b \rightarrow 0$.

In the proposal of Ellis, *et. al.* (1997) [73], the CSS form for S is maintained, but new scales $\lambda(b)$ and $\mu(b)$, which never go above $c_2 Q$, are used as lower limits:

$$S(b, Q) = \int_{\lambda^2(b)}^{c_2^2 Q^2} \frac{d\bar{\mu}^2}{\bar{\mu}^2} \ln \frac{Q^2}{\bar{\mu}^2} A(\alpha_s(\bar{\mu})) + \int_{\mu^2(b)}^{c_2^2 Q^2} \frac{d\bar{\mu}^2}{\bar{\mu}^2} B(\alpha_s(\bar{\mu})) . \quad (4.44)$$

To agree with the Altarelli result, these scales must be defined such that

$$\begin{aligned} \int_{\lambda}^{c_2 Q} \frac{dx}{x} \ln \frac{c_2 Q}{x} &= \frac{1}{2} \ln^2 \frac{c_2 Q}{\lambda} = \int_0^{c_2 Q} \frac{dx}{x} \ln \frac{c_2 Q}{x} [1 - J_0(bx)] , \\ \int_{\mu}^{c_2 Q} \frac{dx}{x} &= \ln \frac{c_2 Q}{\mu} = \int_0^{c_2 Q} \frac{dx}{x} [1 - J_0(bx)] , \end{aligned} \quad (4.45)$$

and so must be

$$\begin{aligned} \mu(b) &= Q \exp\left\{-\int_0^Q \frac{dx}{x} (1 - J_0(bx))\right\} \\ \lambda(b) &= Q \exp\left\{-\left[\int_0^Q \frac{dx}{x} \ln(Q/x) (1 - J_0(bx))\right]^{\frac{1}{2}}\right\} . \end{aligned} \quad (4.46)$$

At large b , λ and μ both $\rightarrow \sim b_0/b$, in agreement with CSS.

CHAPTER 5

KT-SPACE RESUMMATION

As successful as the CSS formalism has been, it is not necessarily easy to put into practice. Performing Fourier transforms numerically is a slow process, requiring many samplings of the parton distributions to achieve a prediction for a single Q_T value. The impact parameter integral formally extends to $b = \infty$, but of course one must in practice halt the integration at some b_{max} , and either drop the rest or introduce an asymptotic expansion [74]. Moreover, the differing treatment of asymptotic pieces between resummed and subtracted versions can affect their cancellation, leading to unphysical behavior at large- Q_T . One must take pains to smoothly yield to the ordinary perturbative result in this region. It would be nice if one could perform the Fourier transform analytically, or avoid it altogether.

A number of authors have undertaken this task, building on the foundation laid by Dokshitzer, D'yakonov and Troyan (DDT) [44, 75]. Their central result is essentially that of equation 3.12, in a more general two-scale form:

$$\frac{d\sigma}{dQ^2 dQ_T^2 dy} = \frac{d\hat{\sigma}}{dQ^2 dy} \sum_{a,b} \frac{d}{dQ_T^2} \left[f_a(x_a, Q_T) T_a(Q^2, Q_T^2) f_b(x_b, Q_T) T_b(Q^2, Q_T^2) \right], \quad (5.1)$$

where the momentum fractions and Sudakov exponents are

$$x_b^a = \frac{Q}{\sqrt{S}} e^{\pm y} \quad (5.2)$$

$$T_b^a = \exp \left[- \int_{Q_T^2}^{Q^2} \frac{d\lambda^2}{\lambda^2} \frac{\alpha_s(\lambda^2)}{2\pi} \left(A_b^a \ln \frac{Q^2}{\lambda^2} + B_b^a \right) \right]. \quad (5.3)$$

5.1 Kimber, Martin, and Ryskin

In 1999, Kimber, Martin, and Ryskin [76] revisited the theory behind the DDT equation, and reinterpreted it in terms of k_T -dependent parton distributions $f(x, k_T, Q)$, e.g.:

$$f_a(x_a, k_a, Q) = \frac{\partial}{\partial \lambda^2} [f_a(x_a, \lambda) T_a(\lambda, Q)] \Big|_{\lambda=k_a}. \quad (5.4)$$

That is, the perturbative terms encompassed in the Sudakov exponential T_a are combined with standard distributions $f_a(x_a, \lambda)$ to form new, *unintegrated* parton distributions, describing partons with transverse momentum \vec{k}_a at sampling energy $k_a \leq Q$.

The DDT form is then obtained by application of the *strong-ordering condition* to the convolution over f_a and f_b . The Q_T -dependence being now described by a single luminosity function \mathcal{L}_{ab} :

$$\frac{d\sigma}{dQ^2 dQ_T^2 dy} = \frac{d\hat{\sigma}}{dQ^2 dy} \sum_{a,b} \mathcal{L}_{ab}(x_a, x_b, Q_T, Q), \quad (5.5)$$

with

$$\mathcal{L}_{ab} = \int f_a(x_a, k_a, Q) f_b(x_b, k_b, Q) \delta^2(\vec{k}_a + \vec{k}_b - \vec{Q}_T) \frac{d^2 k_a}{k_a^2} \frac{d^2 k_b}{k_b^2} \frac{1}{\pi}, \quad (5.6)$$

application of strong-ordering allows only one of the off-shell partons to contribute at a time. That is, either $k_a \ll k_b \simeq Q_T$ or $k_b \ll k_a \simeq Q_T$. In the first case, the delta function collapses to $\delta^2(\vec{k}_b - \vec{Q}_T)$, while in the second case one gets $\delta^2(\vec{k}_a - \vec{Q}_T)$. Summing over both possibilities yields

$$\mathcal{L}_{ab}(x_a, x_b, Q_T, Q) = \frac{d}{d\lambda^2} [f_a(x_a, \lambda) T_a(\lambda, Q) f_b(x_b, \lambda) T_b(\lambda, Q)] \Big|_{\lambda=Q_T}, \quad (5.7)$$

which reproduces equation 5.1.

Note that since $T_{a,b}(x_{a,b}, Q, Q) = 1$, it follows that integrating the luminosity up to scale Q recovers the standard luminosity :

$$\int_0^{Q^2} dQ_T^2 \mathcal{L}_{ab}(x_a, x_b, Q_T, Q) = f_a(x_a, Q) f_b(x_b, Q) , \quad (5.8)$$

and in particular,

$$\int_0^{Q^2} \frac{dk_i^2}{k_i^2} f_i(x_i, k_i, Q) = f_i(x_i, Q) . \quad (5.9)$$

5.2 Ellis and Veseli

In 1997, R.K. Ellis and S. Veseli (EV) came up with a similar extension of the DDT result, while maintaining the improvements of the CSS formalism [77]. They did so by successfully performing the CSS b -space Fourier transform analytically, for the first three tiers of logarithms. Starting with the purely perturbative CSS result

$$\frac{d\sigma}{dQ^2 dy dQ_T^2} = \sum_{a,b} \frac{\hat{\sigma}_0}{2} \int_0^\infty db b J_0(Q_T b) e^{-S(b,Q)} \acute{f}_a(x_a, \frac{b_0}{b}) \acute{f}_b(x_b, \frac{b_0}{b}) , \quad (5.10)$$

in which $\acute{f}_{a,b}$ are the convolutions over finite, unresummed $C_{i/\tilde{i}}$ corrections

$$\begin{aligned} \acute{f}_a(x_a, \frac{b_0}{b}) &\equiv \sum_{\tilde{a}} \int_{x_a}^1 \frac{dz}{z} f_{\tilde{a}/A}(x_a/z, b_0/b) C_{a/\tilde{a}}(z, b_0/b) \\ \acute{f}_b(x_b, \frac{b_0}{b}) &\equiv \sum_{\tilde{b}} \int_{x_b}^1 \frac{dz}{z} f_{\tilde{b}/B}(x_b/z, b_0/b) C_{b/\tilde{b}}(z, b_0/b) , \end{aligned} \quad (5.11)$$

EV defined a fixed scale ratio $t \equiv Q^2/S$ and used the rapidity y to write

$$\begin{aligned} \frac{d\sigma}{dt dQ_T^2} &= \int_0^1 dx_a \int_0^1 dx_b \delta(t - x_a x_b) \int dy \delta(y - \frac{1}{2} \ln \frac{x_a}{x_b}) \frac{d\sigma(t, y, Q_T)}{dt dy dQ_T^2} \\ &= \int_0^1 dx_a \int_0^1 dx_b \delta(t - x_a x_b) \frac{d\sigma(t, x_a/x_b, Q_T)}{dt dy dQ_T^2} . \end{aligned} \quad (5.12)$$

Then, after substitution of equation 5.10, they took the N th moment with respect to t :

$$\begin{aligned}
\Sigma(N) &\equiv \int dt \, t^N \frac{d\sigma}{dt dQ_T^2} \\
&= \sum_{a,b} \frac{\hat{\sigma}_0}{2} \int_0^\infty db \, b J_0(Q_T b) e^{-S(b,Q)} \\
&\quad \cdot \left[\int_0^1 dx_a x_a^N f_a(x_a, \frac{b_0}{b}) \right] \left[\int_0^1 dx_b x_b^N f_b(x_b, \frac{b_0}{b}) \right] \\
&\equiv \sum_{a,b} \frac{\hat{\sigma}_0}{2} \int_0^\infty db \, b J_0(Q_T b) e^{-S(b,Q)} \tilde{f}_a(N, \frac{b_0}{b}) \tilde{f}_b(N, \frac{b_0}{b}) . \tag{5.13}
\end{aligned}$$

The modified parton density moments \tilde{f}_i evolve according to

$$\begin{aligned}
\frac{d\tilde{f}_i(N, \mu)}{d \ln \mu^2} &= \gamma'_N \tilde{f}_i(N, \mu) , \quad \text{or} \\
\tilde{f}_i(N, b_0/b) &= \tilde{f}_i(N, Q) \exp \left[- \int_{b_0^2/b^2}^{Q^2} \frac{d\mu^2}{\mu^2} \gamma'_N \right] , \tag{5.14}
\end{aligned}$$

in which the γ'_N are $\alpha_s(\mu)$ -dependent anomalous dimensions. After defining $x \equiv Q_T b$, this allowed EV to reorganize the cross-section moment as

$$\Sigma(N) = \frac{\hat{\sigma}_0}{2} \frac{H_N(Q)}{Q_T^2} \int_0^\infty dx \, x J_0(x) e^{\mathcal{U}_N(x, Q_T, Q)} , \tag{5.15}$$

where $H_N(Q) \equiv \sum_{a,b} \tilde{f}_a(N, Q) \tilde{f}_b(N, Q)$ and

$$\begin{aligned}
\mathcal{U}_N(x, Q_T, Q) &= - \int_{b_0^2 Q_T^2 / x^2}^{Q^2} \frac{d\mu^2}{\mu^2} \left[A \ln \frac{Q^2}{\mu^2} + B + 2\gamma'_N \right] \\
&\equiv \sum_{n=1}^\infty \sum_{m=0}^{n+1} \left[\frac{\alpha_s(Q^2)}{2\pi} \right]^n \ln^m \frac{Q^2 x^2}{Q_T^2 b_0^2} {}_n D_m . \tag{5.16}
\end{aligned}$$

That is, the new parameters ${}_n D_m$ are directly calculable from the CSS parameters $\{A_i, B_i\}$. With the relation

$$\frac{d}{dx} [x J_1(x)] = x J_0(x) , \tag{5.17}$$

equation 5.15 can now be integrated by parts, with the result

$$\Sigma(N) = \frac{\hat{\sigma}_0}{2} \frac{H_N(Q)}{Q_T^2} \left[x J_1(x) e^{\mathcal{U}_N} \Big|_0^\infty - \int_0^\infty dx x J_1(x) \frac{d e^{\mathcal{U}_N}}{dx} \right]. \quad (5.18)$$

Due to the rapid damping of $\exp(\mathcal{U}_N)$ and $J_1(x)$ as $x \rightarrow \infty$, one can ignore the boundary term; and, using

$$\frac{x}{Q_T^2 dx} = \frac{x}{Q_T^2} \frac{1}{b d Q_T} = \frac{2}{d Q_T^2}, \quad (5.19)$$

exhibit the similarity to the DDT formula:

$$\Sigma(N) = -\frac{d}{d Q_T^2} \left\{ \hat{\sigma}_0 H_N(Q) \int_0^\infty dx J_1(x) e^{\mathcal{U}_N(x, Q_T, Q)} \right\}. \quad (5.20)$$

In fact, were it not for the logs of x/b_0 in \mathcal{U}_N , one would have the standard Sudakov exponent, containing only logs of Q^2/Q_T^2 , which are, of course, the important ones.

For this reason, EV split these off and defined a remainder \mathcal{R}_N . First, they defined an integrand $\tilde{\mathcal{R}}_N$ via

$$\begin{aligned} \mathcal{U}_N(x, Q_T, Q) &= \exp \left[\sum_{n=1}^\infty \sum_{m=0}^{n+1} \left[\frac{\alpha_s}{2\pi} \right]^n \ln^m \frac{Q^2 x^2}{Q_T^2 b_0^2} {}^n D_m \right] \\ &\equiv \exp \left[\sum_{n=1}^\infty \sum_{m=0}^{n+1} \left[\frac{\alpha_s}{2\pi} \right]^n \ln^m \frac{Q^2}{Q_T^2} {}^n D_m \right] + \tilde{\mathcal{R}}_N(x, Q_T, Q) \\ &= \mathcal{U}_N(b_0, Q_T, Q) + \tilde{\mathcal{R}}_N(x, Q_T, Q), \end{aligned} \quad (5.21)$$

where

$$\begin{aligned} \tilde{\mathcal{R}}_N(x, Q_T, Q) &\equiv \exp \left[\sum_{n=1}^\infty \sum_{m=0}^{n+1} \left[\frac{\alpha_s}{2\pi} \right]^n \ln^m \frac{Q^2 x^2}{Q_T^2 b_0^2} {}^n D_m \right] \\ &\quad - \exp \left[\sum_{n=1}^\infty \sum_{m=0}^{n+1} \left[\frac{\alpha_s}{2\pi} \right]^n \ln^m \frac{Q^2}{Q_T^2} {}^n D_m \right]. \end{aligned} \quad (5.22)$$

Then, since \mathcal{U}_N no longer depends on x , and $\int_0^\infty dx J_1(x) = 1$, equation 5.20 becomes

$$\Sigma(N) = -\frac{d}{d Q_T^2} \left\{ \hat{\sigma}_0 H_N(Q) e^{\mathcal{U}_N(b_0, Q_T, Q)} + \mathcal{R}_N(Q_T, Q) \right\}, \quad (5.23)$$

where

$$\mathcal{R}_N(Q_T, Q) \equiv \hat{\sigma}_0 H_N(Q) \int_0^\infty dx J_1(x) \tilde{\mathcal{R}}_N(x, Q_T, Q) . \quad (5.24)$$

Using equations 5.14 and 5.16, the Sudakov exponent is defined:

$$\begin{aligned} H_N(Q) e^{\mathcal{U}_N(b_0, Q_T, Q)} &= H_N(Q_T) e^{-S(b \rightarrow b_0/Q_T, Q)} \\ &= \sum_{a,b} \left[\int_0^1 dx_a x_a^N \dot{f}_a(x_a, Q_T) \right] \left[\int_0^1 dx_b x_b^N \dot{f}_b(x_b, Q_T) \right] e^{-S(b_0/Q_T, Q)} , \end{aligned} \quad (5.25)$$

at which point the inverse transformation back to Q -space becomes easy. Comparison of equations 5.25 and 5.13 leads to Ellis and Veseli's final result in the perturbative regime

$$\frac{d\sigma}{dQ^2 dy dQ_T^2} = \sum_{a,b} \hat{\sigma}_0 \frac{d}{dQ_T^2} \left[\dot{f}_a(x_a, Q_T) \dot{f}_b(x_b, Q_T) e^{-S(b_0/Q_T, Q)} \right] + \Sigma^{-1} \left(\frac{d\mathcal{R}_N(Q_T, Q)}{dQ_T^2} \right) , \quad (5.26)$$

where Σ^{-1} denotes the inverse transform $N \rightarrow Q$, and the Sudakov exponent becomes the same as in the b -space formalism (equation 4.36), except that the lower limit b_0^2/b^2 is replaced by Q_T^2 . By using known integrals of $J_1(x) \ln^m \frac{x}{b_0}$, Ellis and Veseli were able to prove that the remainder term \mathcal{R} contributes no more importantly than the NNNL series of logarithms, that is, those corresponding to the CSS $B^{(2)}\alpha_s^2$ terms.

One still requires a prescription for dealing with the very lowest Q_T values, for which perturbation theory doesn't hold. As in the CSS paper, this is handled by including a non-perturbative function F_{NP} , this time of Q_T , while sampling the Sudakov exponent and parton distributions at a scale which never goes below a limiting value Q_{Tlim} . To maintain proper normalization, while affecting only the small- Q_T region, Ellis and Veseli chose the following parametrization:

$$F_{NP}(Q_T) = 1 - e^{-\tilde{a}Q_T^2} , \quad (5.27)$$

$$Q_{T*}^2 = Q_T^2 + Q_{Tlim}^2 \exp\left[-\frac{Q_T^2}{Q_{Tlim}^2}\right]. \quad (5.28)$$

The resummed piece then becomes:

$$\frac{d\sigma_S}{dQ^2 dy dQ_T^2} = \sum_{a,b} \hat{\sigma}_0 \frac{d}{dQ_T^2} \left[f_a(x_a, Q_T^*) f_b(x_b, Q_T^*) e^{-S(Q_T^*, Q)} F_{NP}(Q_T) \right], \quad (5.29)$$

where

$$S(Q_T, Q) = \int_{Q_T^2}^{Q^2} \frac{d\bar{\mu}^2}{\bar{\mu}^2} \left[\ln\left(\frac{Q^2}{\bar{\mu}^2}\right) A(\bar{\mu}) + B(\bar{\mu}) \right]. \quad (5.30)$$

This can be used with the same perturbative remainder σ_F as in equation 4.37. Transforming to b -space is avoided, drastically improving the speed of numerical implementations, although the method remains susceptible to pathologies at high- Q_T , especially at fixed-target energies, as explained further in Section 6.6.

CHAPTER 6

DIRECT PHOTON PRODUCTION

Here we begin the process of putting together a consistent, resummed, next-to-leading order (NLO) description of single photon hadroproduction.¹ However, the resummation prescriptions described in Chapters [3,4,5] all describe how to reorganize logarithms of Q^2/Q_T^2 , where Q and Q_T are properties of the kinematics of a **pair** of observed particles. In predicting the cross section for inclusive direct photon production, we are, in the end, concerned only with the properties of the photon, so if we want to include the effects of resummation we must, as an intermediate step, define a second potentially observed particle for application of these prescriptions. Fortunately, kinematics requires there to be a second final-state particle at leading order anyway. To NLO, the required Feynman diagrams involve up to two additional particles in the final-state (besides the photon). At the subprocess level these are either quarks or gluons; by the time they reach the detector they have fragmented into hadronic *jets*, so named because each has very little transverse spread about its original partonic vector. That is, the hadrons into which each parton fragments are concentrated within a narrow “cone” about the parent parton’s direction.

If one is ultimately unconcerned with precisely what kinds of hadrons are produced (as in our case), then even if one could identify each type within a particular jet, one would be ignoring (summing over) this information, so in our calculation we need only keep track of the kinematics of the jet itself (or, equivalently, the parent

¹All relevant diagrams and matrix elements are collected in Appendix A.

parton); the fractional probabilities of particular fragmentations all sum to one by definition.

That said, we are left with the following question: our NLO calculation consists not just of $2 \rightarrow 2$ -body leading order (LO) contributions (for which assignment of the jet is unambiguous), but also $2 \rightarrow 3$ -body contributions involving a photon and **two** potential jets. To which do we pair with the photon and apply the resummation formalism?

The answer is **both**, in turn, but in the following way. Experimentally, if the jets are far enough apart in direction as to be distinguishable, we can define the “pair” to be the photon plus the jet of greater transverse momentum. Given that the experiment cannot tell which parton initiated that jet, however, our calculation must consider both possibilities. And, in the instance in which the jets are **not** distinguishable, our calculation must treat the resulting kinematics as that of a **single** jet. Each experiment has its own criteria for distinguishability, the details of which are important only if the final predictions include explicit jet characteristics. As this will not be of concern to us, our calculation can consider any nonzero separation distinguishable.

Thus, in addition to subprocess matrix elements \mathcal{M} and phase-space factors $d\Gamma$ (both of which are given in terms of subprocess momenta $\{p_i^\mu\}$), the ingredients of our calculation should also include a *jet definition*, that is, a set of delta-functions the job of which is to define the jet variables p_j^μ and pair variables $q^\mu \equiv p_\gamma^\mu + p_j^\mu$ in terms of these subprocess momenta.

The photon (p_γ^μ), of course, can be unambiguously associated with one of the outgoing subprocess momenta $\{p_1^\mu, p_2^\mu, p_3^\mu\}$ (we’ll choose p_1^μ). However, after application of momentum conservation, many of the variables included in $\{p_1^\mu, p_2^\mu, p_3^\mu\}$ will not be free but expressible only in terms of other variables in the set. Depending on the contribution being calculated, the most convenient remaining set for evaluation of that contribution may not include p_1^μ , and thus carrying around explicit definitions

for both the photon and jet would help keep track of their properties in terms of the free subprocess variables. In the end, integration over the phase space $d\Gamma$ then yields a cross section in terms of the desired jet and/or pair observables. For the sake of clarity we will suppress these delta-functions in what follows.

The result of this chapter will be a collection of singularity-free pieces which, when added, give an unresummed, NLO cross section for $\gamma + jet$ production, but which are also organized such that their assignment to CSS-style resummation coefficients is self-evident. It is then a simple matter to use these coefficients in a resummed calculation, and integrate over the jet numerically. Indeed a FORTRAN program, switchable between NLO and resummed output, has been written concurrently with this dissertation, and is available upon request.

The attempt is made throughout to keep as many free variables as possible, consistent with the requirements of divergence cancellation and infrared safety. This is required in order to account for kinematic recoil of the photon-jet system against the soft radiation.

A word on notation: the 4-momentum of particle i will be represented by p_i^μ throughout. The energy of such a particle is p_i^0 , while the magnitude and direction of 3-momentum are $|\vec{p}_i|$ and \hat{p}_i , respectively. We use massless particles exclusively, for which $|\vec{p}_i| = p_i^0$. The transverse momentum, $|\vec{p}_i| \sin \theta_i$ will hereafter be noted as simply p_i , while the rapidity is y_i . If we need to refer to the *vector* transverse momentum of particle i , we will denote this as \vec{p}_{Ti} . Dot-products of 4-vectors, usually represented using Greek indices and the Einstein summation convention, as in $p_i^\mu p_{j\mu}$, will for the sake of clarity be shown as $p_i \cdot p_j$. Both describe the quantity $p_i^0 p_j^0 - p_i^1 p_j^1 - p_i^2 p_j^2 - p_i^3 p_j^3$. The following table, valid for massless particles, should help to clarify our notation:

$$p_i^0 = |\vec{p}_i| = p_i \cosh y_i$$

$$\begin{aligned}
p_i^1 &= |\vec{p}_i| \sin \theta_i \cos \phi_i = p_i \cos \phi_i \\
p_i^2 &= |\vec{p}_i| \sin \theta_i \sin \phi_i = p_i \sin \phi_i \\
p_i^3 &= |\vec{p}_i| \cos \theta_i = p_i \sinh y_i .
\end{aligned} \tag{6.1}$$

6.1 Two-Body Final States

The two-body phase space in arbitrary dimension $D = 4 - 2\epsilon$ is

$$d^D \Gamma_2 = \frac{d^{D-1} p_1}{2p_1^0 (2\pi)^{D-1}} \frac{d^{D-1} p_2}{2p_2^0 (2\pi)^{D-1}} (2\pi)^D \delta^D(p_a^\mu + p_b^\mu - p_1^\mu - p_2^\mu) , \tag{6.2}$$

where the incoming parton vectors $\{p_a^\mu, p_b^\mu\}$ are, in the hadronic C.M., given in terms of the momentum fractions $\{x_a, x_b\}$ as follows:

$$\begin{aligned}
p_a^\mu &= x_a \frac{\sqrt{S}}{2} (1, 0, \dots, 0, 1) \\
p_b^\mu &= x_b \frac{\sqrt{S}}{2} (1, 0, \dots, 0, -1) .
\end{aligned} \tag{6.3}$$

For a given matrix element \mathcal{M}_i , the corresponding 2-body cross section is written as an integral over these momentum fractions, weighted by the squared matrix element (suitably summed and averaged over final and initial spins and colors), the phase-space factor, and a luminosity function \mathcal{L} which gives the probabilities of finding incoming partons with those momenta inside the parent hadrons. Thus the cross section for subprocess i is written:

$$d^D \sigma_i = \int_0^1 dx_a \int_0^1 dx_b d^D \Gamma_2 \mathcal{L}_i(x_a, x_b) \overline{\sum} |\mathcal{M}_i|^2 , \tag{6.4}$$

in which the luminosity is a function of the relevant parton densities $\{q_f^A, q_f^B\}$ inside hadrons A and B :

$$\mathcal{L}_i(x_a, x_b) \equiv \frac{\sum_{f, \tilde{f}} q_f^A(x_a) q_{\tilde{f}}^B(x_b)}{2x_a x_b S} . \tag{6.5}$$

The indices f and \tilde{f} each run over all flavors of partons relevant to subprocess i (here the gluon, as well as all quarks and antiquarks, are considered “flavors”).

Thus, *e.g.*, for the $qg \rightarrow \gamma q$ subprocess the sum is simply $\sum_f q_f^A(x_a)q_g^B(x_b)$, in which f ranges over quark flavors and ant flavors. We will sometimes refer to this sum, for a given subprocess i , as $H_i(x_a, x_b)$.

It should be noted that charge factors, denoted in this work by Q_f , are present at photon/quark vertices, and, as they depend on the quark flavor f , need to be included in the sum. Each gives the value of the relevant quark's electromagnetic charge in units of the proton charge ($+e$). As they arise in the matrix element, each $\overline{\sum}|\mathcal{M}|_i^2$ above should properly have a subscript $f\tilde{f}$, and the summation symbol $\sum_{f\tilde{f}}$ should be placed outside \mathcal{L} . For clarity, we take these abbreviations to be understood in what follows. Actually, we will no longer refer to the matrix element as a whole; each can be written as the product of factors

$$\overline{\sum}|\mathcal{M}|_i^2 = \omega_{2\gamma}[K'T'_{f\tilde{f}}(v)]_i, \quad (6.6)$$

in which $\omega_{2\gamma} \equiv 2(4\pi)^2\alpha\alpha_s C_F \mu^{4\epsilon}$ is independent of the particular subprocess and $K'T'_{f\tilde{f}}(v)$ gives the angular dependence as a function of $v \equiv e^{y_1}/(e^{y_1} + e^{y_2})$. This, of course, **is** dependent upon the particular subprocess, and upon the quark charges involved. The “primes” denote ϵ -dependence; when ϵ is taken to zero, the primes will disappear.

We may now begin to simplify matters by integrating over some of the unneeded variables in $d^D\Gamma_2$. Breaking down the p_1^μ factor as

$$\begin{aligned} \frac{d^{D-1}p_1^\mu}{2p_1^0}\delta^D(p_a^\mu + p_b^\mu - p_1^\mu - p_2^\mu) &= \frac{dy_1}{2}\delta(p_1^+ - X^+)\delta(p_1^- - X^-) \\ &\times d^{D-2}\vec{p}_{T1}\delta^{D-2}(\vec{p}_{T1} - \vec{X}_T) \\ &= \frac{dy_1}{S}\delta(x_a - \chi_a)\delta(x_b - \chi_b)d^{D-2}\vec{p}_{T1}\delta^{D-2}(\vec{p}_{T1} - \vec{X}_T), \end{aligned} \quad (6.7)$$

where

$$\begin{aligned}
X^\mu &\equiv p_a^\mu + p_b^\mu - p_2^\mu \\
\chi_a &= \frac{p_2}{\sqrt{S}}(e^{y_1} + e^{y_2}) \\
\chi_b &= \frac{p_2}{\sqrt{S}}(e^{-y_1} + e^{-y_2}) ,
\end{aligned} \tag{6.8}$$

we can integrate over x_a, x_b , and \vec{p}_{T1} , which has the effect that $d^D\Gamma_2$ becomes

$$d^D\Gamma_2 = \frac{2\pi dy_1}{S} \frac{d^{D-1}p_2}{2p_2^0(2\pi)^{D-1}} . \tag{6.9}$$

Since we'll require (at most) a transverse momentum, rapidity, and azimuthal angle for each particle, we can further reduce our variables as follows. Again, note that here and throughout this dissertation, we will abbreviate single-particle transverse momenta as $p_i \equiv |\vec{p}_i| \sin \theta_i$:

$$\begin{aligned}
\frac{d^{D-1}p_2}{2p_2^0(2\pi)^{D-1}} &= \frac{|\vec{p}_2|^{D-3}}{2(2\pi)^{D-1}} d|\vec{p}_2| \sin^{D-3} \theta_2 d\theta_2 d^{D-3}\phi_2 \\
&= \frac{p_2^{D-3} dp_2 dy_2 d^{D-3}\phi_2}{2(2\pi)^{D-1}} ,
\end{aligned} \tag{6.10}$$

Of course, we could stop here, and leave our result in the following form:

$$d^D\sigma_i = \mathcal{L}(x_a, x_b) \omega_{2\gamma} [K' T'_{f\bar{f}}(v)]_i d^D\bar{\Gamma}_2 , \tag{6.11}$$

where

$$d^D\bar{\Gamma}_2 = \frac{dy_1 dp_2 dy_2 d^{D-3}\phi_2 p_2^{D-3}}{2S(2\pi)^{D-2}} . \tag{6.12}$$

However, to use this result for prediction of photon cross sections, it will be helpful to know what the associated photon variables $\{p_\gamma, y_\gamma, \phi_\gamma\}$ are in terms of the above. Since we are assigning the photon to p_1^μ and the jet to p_2^μ , we have the following:

$$p_\gamma = p_1 \quad p_j = p_2$$

$$\begin{aligned}
y_\gamma &= y_1 & y_j &= y_2 \\
\phi_\gamma &= \phi_2 + \pi & \phi_j &= \phi_2 .
\end{aligned}
\tag{6.13}$$

For a leading-order (LO) calculation, this is all that would be necessary, and the reader could simply plug in the $ab \rightarrow \gamma d$ matrix elements given in Appendix A.²

For a NLO calculation, however, in which the panorama of 2-body contributions includes virtual and counterterm pieces, as well as subtraction terms derived from 3-body asymptotic approximations, all with poles in ϵ , the constraint of infrared safety forces us to choose some common set of free **observable** quantities, in order that addition of these pieces will result in pole cancellation. We have four so far: $\{y_\gamma, p_j, y_j, \phi_j\}$, but in order to fully define two **independent** massless 4-vectors (as our formalism requires), we need six altogether. Specifically, in order to use the resummation procedures described earlier in this work, we will need the pair transverse momentum Q_T ; in order to incorporate smearing of the photon kinematics due to recoil, we will also need an additional angle, which we take to be the axial direction ϕ_q of the pair.

For the two-body contributions, of course, Q_T is zero, and ϕ_q is undefined. We will consequently tack on a factor

$$dQ_T \delta(Q_T) \frac{d^{D-3}\phi_q}{\int d^{D-3}\phi_q}$$

for these pieces, to supply the additional two degrees of freedom required.

Furthermore, there will be certain multiplicative factors common to all pieces, which will be convenient to express explicitly here. To that end, for our $ab \rightarrow \gamma d$ subprocesses, we take $D = 4 - 2\epsilon$, and define the following quantities:

$$d_\epsilon[\gamma j] \equiv dy_\gamma dp_j dy_j d^{1-2\epsilon}\phi_j dQ_T d^{1-2\epsilon}\phi_q$$

²QCD Bremsstrahlung diagrams also contribute to order $\alpha\alpha_s$; these will be discussed at the end of the section.

$$\kappa_i \equiv \frac{\alpha\alpha_s}{S} \frac{p_j}{\int d^{1-2\epsilon}\phi} \left(\frac{p_j}{2\pi\mu^2} \right)^{-2\epsilon} 4C_F [\mathcal{L}(x_a, x_b) K' T'_{f\bar{f}}(v)]_i, \quad (6.14)$$

through which one can show:

$$\begin{aligned} d\sigma_i^{\text{Born}} &= \mathcal{L}(x_a, x_b) \omega_{2\gamma} [K' T'_{f\bar{f}}(v)]_i d^D \bar{\Gamma}_2 \\ &\rightarrow d_\epsilon [\gamma j] \kappa_i \delta(Q_T). \end{aligned} \quad (6.15)$$

For a resummed result, the pair mass Q also requires definition; for these pieces it is $Q = \sqrt{x_a x_b S} = \sqrt{2p_j^2(1 + \cosh(y_1 - y_2))}$, as can easily be verified via the pair definition $q^\mu \equiv p_\gamma^\mu + p_j^\mu$.

Two-body Bremsstrahlung also contributes; here one final-state parton in a purely QCD subprocess (such as $q\bar{q} \rightarrow q\bar{q}$) fragments into hadronic material and an essentially collinear photon. The probability for this to occur is thus most conveniently described by *photon fragmentation functions* $D_{\gamma/q}(z)$ and $D_{\gamma/g}(z)$, each a function of the fraction z of the parent parton's momentum that is carried away by the photon. The transverse momentum imbalance between the photon and away-side jet in this case is not zero, but instead given by $Q_T = p_\gamma - p_j = (1 - z)p_j$.

There are 11 such subprocesses to consider (see Appendix A), and the cross section for subprocess i , in terms of the definitions 6.14, is:

$$\begin{aligned} d\sigma_i^{\text{Brem}} &= d_\epsilon [\gamma j] \kappa_i \frac{\alpha_s}{\alpha} \int_{z_{\min}}^1 dz \delta(Q_T - (1 - z)p_j) D_{\gamma/c}(z) \\ &= d_\epsilon [\gamma j] \kappa_i \frac{\alpha_s}{\alpha} \frac{1}{p_j} D_{\gamma/c} \left(\frac{p_j - Q_T}{p_j} \right) \theta((1 - z_{\min})p_j - Q_T), \end{aligned} \quad (6.16)$$

in which $D_{\gamma/c}(z)$ is the fragmentation function relevant to parton c in the subprocess ($ab \rightarrow cd$). Here a lower bound z_{\min} is included for the general case in which minimum photon energy constraints (*isolation cuts*) are experimentally imposed [50].

One would expect such processes to be of order $\alpha\alpha_s^2$; in fact, the $D_{\gamma/c}$ are of order α/α_s , and so one obtains overall $\mathcal{O}(\alpha\alpha_s)$ quantities. We use the leading-log fragmentation functions of reference [78]:

$$\begin{aligned}
D_{\gamma/q}^{\text{LL}}(z, \mu) &= \frac{F(\mu)}{z} \left[\frac{Q_q^2 (2.21 - 1.28z + 1.29z^2) z^{0.049}}{1 - 1.63 \ln(1 - z)} + 0.0020 (1 - z)^{2.0} z^{-1.54} \right] \\
D_{\gamma/g}^{\text{LL}}(z, \mu) &= \frac{F(\mu)}{z} \frac{0.194}{8} (1 - z)^{1.03} z^{-0.97} ,
\end{aligned} \tag{6.17}$$

where $F(z, \mu) = (\alpha/2\pi) \ln(\mu^2/\Lambda^2)$ with $\Lambda = 0.2\text{GeV}$.

At NLO, we will require first-order expansions of the parton distribution and fragmentation functions, in order to cancel collinear singularities which arise in three-body final states (see Section 2.4, in particular equation 2.52). In the \overline{MS} scheme, with common factorization scale M_f , these *counterterms* are as follows:

$$d\sigma_{a(i)}^{\text{CT}} = d_\epsilon[\gamma j] \kappa_i \beta_\epsilon \delta(Q_T) \sum_{\tilde{a}} \int_{x_a}^1 \frac{dz}{z} \frac{H(x_a/z, x_b)}{H(x_a, x_b)} \frac{P_{a/\tilde{a}}^+(z)}{\epsilon} \tag{6.18}$$

$$d\sigma_{b(i)}^{\text{CT}} = d_\epsilon[\gamma j] \kappa_i \beta_\epsilon \delta(Q_T) \sum_{\tilde{b}} \int_{x_b}^1 \frac{dz}{z} \frac{H(x_a, x_b/z)}{H(x_a, x_b)} \frac{P_{b/\tilde{b}}^+(z)}{\epsilon} \tag{6.19}$$

$$d\sigma_{1(i)}^{\text{CT}} = d_\epsilon[\gamma j] \kappa_i \beta_\epsilon \sum_q \frac{P_{\gamma q}^+(\tilde{z})}{\epsilon} , \tag{6.20}$$

where

$$\beta_\epsilon \equiv \frac{\alpha_s}{2\pi} \left(\frac{4\pi\mu^2}{M_f^2} \right)^\epsilon \frac{\Gamma(1 - \epsilon)}{\Gamma(1 - 2\epsilon)} . \tag{6.21}$$

In addition, there will be virtual diagrams, which contribute at NLO in the form

$$d\sigma_i^{\text{Virt}} = d_\epsilon[\gamma j] \kappa_i \beta_\epsilon \delta(Q_T) \left[\frac{A_v^2}{\epsilon^2} + \frac{A_v^1}{\epsilon} + A_v^0 + \frac{B^v}{T_0} \right]_i . \tag{6.22}$$

The virtual diagrams are shown in Appendix A; their parameters A_v^2, A_v^1, A_v^0, B^v are given in Appendix C.

6.2 Three-Body Final States

As a general guide we use the work of Ellis, Kunszt, and Soper [79–80]. These authors arrived at a general subtraction algorithm for calculating infrared-safe

quantities in hadron-hadron collisions. The process is as follows: We begin with the 3-body matrix elements for NLO single-photon production, as listed in Appendix A. These will have singularities in those regions of phase-space for which one of the final-state particles become soft or collinear with another particle. By the process of partial-fractioning, we can break these matrix elements into smaller pieces, each of which has at most two singular regions, one soft and one collinear. The potential singularities manifest themselves as quantities in the denominator which tend to zero in the singular regions of phase-space, but as the numerators simplify in these regions also, we can define approximate, simplified numerators which can be added and subtracted in **all** regions. Each partial-fractioned 3-body piece pairs with a subtracted approximate piece to form a function which is finite everywhere, while the leftover (added) approximations are dealt with separately. This is the essence of the *subtraction method*, as contrasted with the *Phase-Space-Slicing* (PSS) method, in which the singular regions of phase space are cut out and their effects added in later after simplification and analytical integration. A NLO inclusive single photon calculation using the PSS method, but without transverse-momentum resummation, was performed by Baer, Ohnemus, and Owens (1990) [56].

The leftover “subtraction” pieces contain all the singularities of the original 3-body piece, but are simpler to work with, as many angular dependences fall away. What is required is that the singularities be made **explicit** so they may be cancelled against virtual pieces or absorbed into distribution and fragmentation functions. It should not matter, for a given singular quantity, whether this end is achieved via integration in D -dimensions or via extraction in terms of a pole and accompanying plus-distribution. In the present calculation, we use the former method for all but the required six free variables, and handle poles in these variables with plus-distributions.

Once the Born terms and virtual contributions are added, and the poles taken care of, what remains is a completely finite NLO result. From this, one may

obtain parameters for use in a resummed version of the calculation by expanding the resummed form to NLO and comparing coefficients.

Crucial to the success of any such venture is the recognition that one of the vectors we intend to observe, namely that of the jet, is not uniquely defined in terms of the vectors we begin with (call them $\{p_1^\mu, p_2^\mu, p_3^\mu\}$). We may declare that p_1^μ be assigned to the photon, but it is an experimental reality that any jet we observe may correspond to either **or both** of the final-state partons emitted in our 3-body subprocesses (p_2^μ and p_3^μ). Any attempt to force a one-to-one correspondence will lead to uncanceled poles, which is another way of saying that the result wouldn't be *infrared-safe*. One must define the jet kinematics in such a way that if the final-state partons are together within a certain angular region, this is counted as a single jet (see figure 6.1). One practical consequence of this is that singularity cancellation can only be done after the free variables have been reduced to those of the photon and jet, not those of $\{p_1^\mu, p_2^\mu, p_3^\mu\}$.

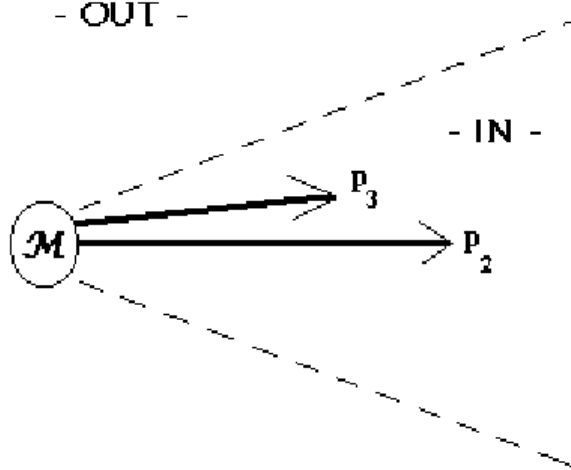


Figure 6.1. \vec{p}_3 inside jet cone.

6.2.1 Partial-fraction Three-Body matrix elements

Three-body phase space, in analogy with equation 6.2, is:

$$d^D \Gamma_3 = \frac{d^{D-1} p_1}{2p_1^0 (2\pi)^{D-1}} \frac{d^{D-1} p_2}{2p_2^0 (2\pi)^{D-1}} \frac{d^{D-1} p_3}{2p_3^0 (2\pi)^{D-1}} \times (2\pi)^D \delta^D(p_a^\mu + p_b^\mu - p_1^\mu - p_2^\mu - p_3^\mu), \quad (6.23)$$

while the squared, summed, and averaged matrix element (or partial-fractioned piece thereof) is denoted by $\overline{\sum} |\mathcal{M}|^2$, and is a function of all five momenta $\{p_a^\mu, p_b^\mu, p_1^\mu, p_2^\mu, p_3^\mu\}$.

As written, the final-state 4-vectors are allowed to range over all space, and there are then up to 12 potential singularities:

1. $p_1^\mu, p_2^\mu, p_3^\mu$ soft,
2. $p_1^\mu, p_2^\mu, p_3^\mu$ collinear with the beam in either direction, and
3. $p_1 \cdot p_2 = 0, p_1 \cdot p_3 = 0, p_2 \cdot p_3 = 0$ collinear singularities.

If we assign p_1^μ to the photon, and through cuts make sure it is never soft or collinear to the beam, this reduces us to 9 singularities. If we go further and declare p_3^μ to be that parton with the lowest transverse momentum (written as simply p_3), then the p_2^μ singularities disappear, providing we symmetrize our matrix elements with respect to $p_2^\mu \leftrightarrow p_3^\mu$. We will consequently define a symmetrized squared matrix element (note the tilde instead of a bar)

$$\widetilde{\sum} |\mathcal{M}|^2 \equiv \overline{\sum} |\mathcal{M}|^2 \left(p_a^\mu, p_b^\mu, p_1^\mu, p_2^\mu, p_3^\mu \right) + \overline{\sum} |\mathcal{M}|^2 \left(p_a^\mu, p_b^\mu, p_1^\mu, p_3^\mu, p_2^\mu \right), \quad (6.24)$$

and introduce a theta function $\theta(p_2 - p_3)$.

We are left with 5 singular regions, corresponding to p_3^μ being either soft or collinear with one of the other 4 particles. Since momentum conservation prohibits more than two of these from occurring at once (for nonzero photon p_T), the divergent terms with which we must deal will be at worst of the form

$$\frac{1}{p_m \cdot p_3 p_n \cdot p_3}.$$

This arrangement is singular in two different “collinear regions”. To simplify to only one collinear possibility, we may partial-fraction these terms as follows:

$$\frac{1}{p_m \cdot p_3 p_n \cdot p_3} = \frac{1}{p_3 \cdot (p_m + p_n)} \left[\frac{1}{p_m \cdot p_3} + \frac{1}{p_n \cdot p_3} \right]. \quad (6.25)$$

The factor $[p_3 \cdot (p_m + p_n)]^{-1}$ gives a singularity only when p_3^μ is soft, but if this turns out to be the case, then the simpler quantity p_3 will be zero as well, and within an already partial-fractioned term, it will be simpler to express the pole with p_3 .

So, in all, we can split each (symmetrized, summed and averaged) matrix element into four terms, each a product of an explicit $[p_3 p_m \cdot p_3]^{-1}$ singular factor and a general function of $\{p_1^\mu, p_2^\mu, p_3^\mu\}$:

$$\tilde{\Sigma} |\mathcal{M}|_{ab \rightarrow 123}^2 = \sum_{m=a,b,1,2} \frac{\Psi_m}{p_3 p_m \cdot p_3}, \quad (6.26)$$

in which, by virtue of equation 6.25, Ψ_m itself (and thus the cross section) can be written as a sum of terms

$$\Psi_m \equiv \sum_{n=a,b,1,2} \frac{\Psi_{mn}}{p_3 \cdot (p_m + p_n)}. \quad (6.27)$$

Refer to Appendix A for a list of the 3-body matrix elements which contribute. The Ψ_{mn} , however, will not be listed.

6.2.2 Reduce Three-body Phase Space.

The structure of the cross section is analogous to the two-body case:

$$d^D \sigma_3 = \int_0^1 dx_1 \int_0^1 dx_2 \mathcal{L}(x_1, x_2) \widetilde{\sum} |\mathcal{M}|_{ff}^2 d^D \Gamma_3 \theta(p_2 - p_3), \quad (6.28)$$

with the phase-space factor

$$d^D \Gamma_3 = \frac{d^{D-1} p_1}{2p_1^0 (2\pi)^{D-1}} \frac{d^{D-1} p_2}{2p_2^0 (2\pi)^{D-1}} \frac{d^{D-1} p_3}{2p_3^0 (2\pi)^{D-1}} (2\pi)^D \delta^D(p_a^\mu + p_b^\mu - p_1^\mu - p_2^\mu - p_3^\mu) , \quad (6.29)$$

but after the manipulations given in equations 6.7 and 6.10, we now find

$$d^D \Gamma_3 = \frac{2\pi dy_1}{S} \frac{d^{D-1} p_2}{2p_2^0 (2\pi)^{D-1}} \frac{d^{D-1} p_3}{2p_3^0 (2\pi)^{D-1}} \quad (6.30)$$

$$x_{\frac{1}{2}} \equiv \frac{1}{\sqrt{S}} (p_1 e^{\pm y_1} + p_2 e^{\pm y_2} + p_3 e^{\pm y_3}) . \quad (6.31)$$

in which

$$\begin{aligned} p_1 &\equiv \sqrt{p_2^2 + p_3^2 + 2p_2 p_3 \cos(\phi_2 - \phi_3)} \\ \phi_1 &\equiv \tan^{-1} \left(\frac{p_2 \sin \phi_2 + p_3 \sin \phi_3}{p_2 \cos \phi_2 + p_3 \cos \phi_3} \right) + \pi . \end{aligned} \quad (6.32)$$

We must now arrange our cross-section ingredients in a form which makes the function to be approximated explicit. We'll call this function \mathcal{F}_{mn} , corresponding to the partial-fractioned matrix element numerators defined in section 6.2.1. The phase space and singular factors will not be a part of this function, while the luminosity factor and Ψ_{mn} will. By analogy with equations 6.6 and 6.14, we'll also find it convenient to extract the overall factor $\omega_3 = 4(4\pi)^3 C_F \alpha \alpha_s^2 \mu^{6\epsilon}$ common to all our 3-body matrix elements, and define the new quantities

$$\begin{aligned} d_\epsilon[123] &\equiv dy_1 dp_2 dy_2 d\phi_2^{1-2\epsilon} dp_3 dy_3 d\phi_3^{1-2\epsilon} , \\ \chi(\epsilon) &\equiv \frac{\alpha \alpha_s^2 \mu^{2\epsilon}}{(2\pi)^2 S} \left(\frac{p_2}{2\pi\mu} \right)^{-2\epsilon} \left(\frac{p_3}{2\pi\mu} \right)^{-2\epsilon} p_2 p_3 4C_F , \end{aligned} \quad (6.33)$$

by which our partial-fractioned cross-section pieces can then be expressed as

$$d^D \sigma_{mn} = \frac{d_\epsilon[123] \chi(\epsilon)}{p_3 p_m \cdot p_3} \mathcal{F}_{mn} \theta(p_2 - p_3) , \quad (6.34)$$

with

$$\mathcal{F}_{mn}(p_1^\mu, p_2^\mu, p_3^\mu) \equiv \mathcal{L}(x_1, x_2) \frac{\Psi_{mn}}{\omega_3 p_3 \cdot (p_m + p_n)} . \quad (6.35)$$

Keep in mind, of course, that we will often refer to $d\sigma_m$ and \mathcal{F}_m , which are, by equation 6.27, sums over $d\sigma_{mn}$ and \mathcal{F}_{mn} , respectively.

Strictly speaking, the above is used only for the $m = \{a, b, 2\}$ contributions. The $m = 1$ contribution contains poles in the limit $\hat{p}_3 \rightarrow \hat{p}_1$, and we'd like to take advantage of the math already done for the $\hat{p}_3 \rightarrow \hat{p}_2$ case. Thus we begin by switching $1 \leftrightarrow 2$ in the phase space element $d\Gamma_3$ *only* (after approximation, we will switch back in the subtracted piece, in order to use the same Monte-Carlo event generator). Thus, in place of equations 6.33, we wind up with

$$\begin{aligned} d_\epsilon[213] &\equiv dy_2 dp_1 dy_1 d^{1-2\epsilon} \phi_1 dp_3 dy_3 d^{1-2\epsilon} \phi_3 \\ \tilde{\chi}(\epsilon) &\equiv \frac{\alpha \alpha_s^2 \mu^{2\epsilon}}{(2\pi)^2 S} \left(\frac{p_1}{2\pi\mu} \right)^{-2\epsilon} \left(\frac{p_3}{2\pi\mu} \right)^{-2\epsilon} p_1 p_3 4C_F \end{aligned} \quad (6.36)$$

in which x_1 and x_2 retain their usual definitions, but this time p_1 and ϕ_1 are fixed, while p_2^μ is a function of $\{y_2, p_1^\mu, p_3^\mu\}$:

$$\begin{aligned} p_2 &\equiv \sqrt{p_1^2 + p_3^2 + 2p_1 p_3 \cos(\phi_1 - \phi_3)} \\ \phi_2 &\equiv \tan^{-1} \left[\frac{p_1 \sin \phi_1 + p_3 \sin \phi_3}{p_1 \cos \phi_1 + p_3 \cos \phi_3} \right] + \pi . \end{aligned} \quad (6.37)$$

6.2.3 Define and Subtract Approximations

We'll now define the additions and subtractions of approximate versions of these functions \mathcal{F}_m . Each multiplies a factor $[p_3 p_m \cdot p_3]^{-1}$ which becomes singular in the regions in which p_3^μ either disappears altogether ($p_3^0 \rightarrow 0$, the **soft** region) or becomes collinear with particle m (the **collinear** region, $\hat{p}_m \cdot \hat{p}_3 \rightarrow 1$). The essence of the subtraction method is, as previously stated, to subtract off a simpler asymptotic approximation which retains the same pole structure. This “**subtracted piece**” (or

asymptotic piece) pairs with the original three-body partial-fractioned piece to form a function $d\sigma_m^{finite}$, finite everywhere in phase space, and which goes to zero as the singular regions are approached.

This process then, of course, requires us to add back in that which was subtracted; so our singularities re-enter our calculation, but now in a much simplified form. These “**subtraction pieces**” can now be analytically manipulated in order to extract their poles explicitly, these being subsequently cancelled by the addition of virtual and counterterm corrections.

In practice, since two types of poles exist in each original partial-fractioned piece, it is usually convenient to allow for two separate subtractions in order that each resulting subtraction piece contain only one type of pole. There is a further reason: as stated in Section 2.4, we expect the soft limits to reduce to known 2-body subprocess matrix elements, and the collinear limits to show up as these times convolutions of familiar splitting functions and luminosity factors. Thus for the $m = \{a, b\}$ (initial-state) terms, it will be convenient to have one version which fixes the direction of p_3^μ while taking p_3^0 to zero (the soft approximation), and another which takes $\hat{p}_3 \rightarrow \hat{p}_m$ (collinear). Then, to keep our soft singularities in one place and avoid double counting, we subtract the soft limit from our collinear piece.

The above is only a rough statement for the moment, however, as we did not leave ourselves with p_3^0 and \hat{p}_3 (the energy and direction) as free variables, but instead the set $\{p_3, y_3, \phi_3\}$. We must be more precise.

First of all, we eventually intend to integrate over y_3 , so we must be clear about the limits of this integral. Allowing y_3 to go to infinity in either direction, without a corresponding decrease in the magnitude $|\vec{p}_3|$, would at some point violate momentum conservation, as the momentum fractions of the incoming partons cannot exceed 1. In other words, when we take initial-state soft and collinear approximations (in which the transverse momentum p_3 necessarily tends to zero), we can do so only if these factors of p_3 stand alone; if p_3 multiplies some divergent function of y_3 , we must take

additional care. So far, we have not explicitly included these bounds, but we do so now in terms of restrictions on y_3 .

From equations 6.31 and 6.32, we have the momentum fractions

$$\begin{aligned} x_1 &= \frac{1}{\sqrt{S}}(p_1 e^{y_1} + p_2 e^{y_2} + p_3 e^{y_3}) \\ x_2 &= \frac{1}{\sqrt{S}}(p_1 e^{-y_1} + p_2 e^{-y_2} + p_3 e^{-y_3}) , \\ \text{where} \\ p_1 &\equiv \sqrt{p_2^2 + p_3^2 + 2p_2 p_3 \cos(\phi_2 - \phi_3)} . \end{aligned} \quad (6.38)$$

Restricting $x_{\frac{1}{2}} \leq 1$ is thus equivalent to the restrictions

$$\begin{aligned} y_3 &\leq \ln \frac{\sqrt{S} - p_1 e^{y_1} - p_2 e^{y_2}}{p_3} \\ y_3 &\geq -\ln \frac{\sqrt{S} - p_1 e^{-y_1} - p_2 e^{-y_2}}{p_3} . \end{aligned} \quad (6.39)$$

However, since the factors of p_3 in p_1 do not multiply exponentials of y_3 , these can be dropped in the low- p_3 limit, leaving

$$\begin{aligned} y_3 &\leq \ln \frac{(1 - x_a)\sqrt{S}}{p_3} \\ y_3 &\geq -\ln \frac{(1 - x_b)\sqrt{S}}{p_3} , \end{aligned} \quad (6.40)$$

in which x_a, x_b are the usual two-body fractions

$$x_{\frac{a}{b}} \equiv \frac{p_2}{\sqrt{S}}(e^{\pm y_1} + e^{\pm y_2}) . \quad (6.41)$$

In practice, we can ignore one or both of these limits if the relevant integrand is not singular as y_3 approaches infinity from that direction. Our initial-state soft pieces must therefore retain both limits, but our initial-state collinear pieces can ignore one of the limits, and in the case of final-state pieces, both limits are ignored.

So, although naïvely expecting our soft limit to be adequately represented by the conditions “ $p_3 \rightarrow 0$, y_3 and ϕ_3 fixed” ignores the fact that $p_3^0 = p_3 \cosh y_3$ does not necessarily go to zero if y_3 is taken large enough, now that we have finite limits on y_3 , these conditions make sense, and we will write our soft limits in the form

$$\mathcal{F}_m(p_3 = 0, y_3, \phi_3) \theta_a \theta_b ,$$

where θ_a and θ_b express the y_3 limits above:

$$\begin{aligned} \theta_a &\equiv \theta(\ln[(1 - x_a)\sqrt{S}/p_3] - y_3) , \\ \theta_b &\equiv \theta(y_3 + \ln[(1 - x_b)\sqrt{S}/p_3]) . \end{aligned} \tag{6.42}$$

Unfortunately, the same notation won’t work for the initial-state collinear terms. What we wish to express is that as p_3^μ becomes parallel with p_a^μ , for example, $p_3 \cdot p_a \sim p_3 e^{-y_3}$ and p_3 alone go to zero, while $p_3 \cdot p_b \sim p_3 e^{y_3}$ does not. The descriptions we will use are: ³

$$\begin{aligned} \mathcal{F}_a(p_3 e^{y_3}, p_3 e^{-y_3} = 0, \vec{p}_{T3} = \vec{0}) \theta_a \\ \mathcal{F}_b(p_3 e^{y_3} = 0, p_3 e^{-y_3}, \vec{p}_{T3} = \vec{0}) \theta_b , \end{aligned} \tag{6.43}$$

the soft limits of which are

$$\begin{aligned} \mathcal{F}_a(p_3 e^{y_3} = 0, p_3 e^{-y_3} = 0, \vec{p}_{T3} = \vec{0}) \theta_a \\ \mathcal{F}_b(p_3 e^{y_3} = 0, p_3 e^{-y_3} = 0, \vec{p}_{T3} = \vec{0}) \theta_b , \end{aligned} \tag{6.44}$$

and will be called *soft-collinear* limits. These will be subtracted from the collinear terms.

³Moving to light-cone coordinates $p_3^\mu \equiv \{p_3^+, p_3^-, \vec{p}_{T3}\}$, in which $p_3^+ \equiv (p_3^0 + p_3^3)/\sqrt{2} = p_3 e^{y_3}/\sqrt{2}$ and $p_3^- \equiv (p_3^0 - p_3^3)/\sqrt{2} = p_3 e^{-y_3}/\sqrt{2}$ would allow us to write our collinear limits more cleanly, but at the expense of additional notation. We will have to be content with the above descriptions.

For $m = a$, then, we have in the end these pieces:

$$d^D \sigma_a^{soft} \equiv \frac{d_\epsilon[123]\chi(\epsilon)}{p_3 p_a \cdot p_3} \theta(p_2 - p_3) \theta_a \theta_b \mathcal{F}_a(p_3 = 0, y_3, \phi_3) \quad (6.45)$$

$$\begin{aligned} d^D \sigma_a^{coll} &\equiv \frac{d_\epsilon[123]\chi(\epsilon)}{p_3 p_a \cdot p_3} \theta(p_2 - p_3) \theta_a \\ &\times \left[\mathcal{F}_a(p_3 e^{y_3}, p_3 e^{-y_3} = 0, \vec{p}_{T3} = \vec{0}) - \mathcal{F}_a(p_3 e^{y_3} = 0, p_3 e^{-y_3} = 0, \vec{p}_{T3} = \vec{0}) \right] \end{aligned} \quad (6.46)$$

$$\begin{aligned} d^D \sigma_a^{finite} &\equiv \frac{d_\epsilon[123]\chi(\epsilon)}{p_3 p_a \cdot p_3} \theta(p_2 - p_3) \\ &\times \left[\mathcal{F}_a(y_1, p_2, y_2, \phi_2, p_3, y_3, \phi_3) - \mathcal{F}_a(p_3 e^{y_3}, p_3 e^{-y_3} = 0, \vec{p}_{T3} = \vec{0}) \theta_a \right. \\ &+ \left. \mathcal{F}_a(p_3 e^{y_3} = 0, p_3 e^{-y_3} = 0, \vec{p}_{T3} = \vec{0}) \theta_a - \mathcal{F}_a(p_3 = 0, y_3, \phi_3) \theta_a \theta_b \right] \end{aligned} \quad (6.47)$$

Note that $d^D \sigma_a^{finite}$ is finite everywhere, so we can in fact take $\epsilon \rightarrow 0$ in this term, thus replacing $d_\epsilon[123]\chi(\epsilon)$ with the notations $d_0[123]\chi_0$ and $D = 4 - 2\epsilon \rightarrow 4$. Meanwhile, $d^D \sigma_a^{coll}$ has a collinear singularity but no soft ones, and $d^D \sigma_a^{soft}$ has both soft and collinear divergences. The sum $d\sigma^{soft} + d\sigma^{coll} + d\sigma^{finite} \sim \mathcal{F}(y_1, p_2, y_2, \phi_2, p_3, y_3, \phi_3)$, which is what we started with.

It will become evident in Section 6.2.5 that significant simplification of our y_3 integrals arises if we take advantage of the further breakdown $d\sigma_a = d\sigma_{ab} + d\sigma_{a2}$ for the soft pieces ($\{mn\} = \{a1, b1, 21\}$ do not occur via the arguments of section 6.2.1). In addition to $d\sigma_a^{finite}$, then, we have just defined three *subtraction pieces*, two soft (labeled $\{mn\} = \{ab, a2\}$) and one collinear. Analogous terms are similarly constructed for $m = b$.

The final-state pieces have their own organizational requirements, but thankfully are simpler as regards notation. For $m = 2$, we subtract the soft-collinear piece from the soft term instead, leaving it with no collinear poles.

$$\begin{aligned}
d^D \sigma_2^{soft} &\equiv \frac{d_\epsilon[123]\chi(\epsilon)}{p_3 p_2 \cdot p_3} \theta(p_2 - p_3) \\
&\times \left[\mathcal{F}_2(p_3 = 0, y_3, \phi_3) - \mathcal{F}_2(p_3 = 0, y_3 = y_2, \phi_3 = \phi_2) \right] \quad (6.48)
\end{aligned}$$

$$d^D \sigma_2^{coll} \equiv \frac{d_\epsilon[123]\chi(\epsilon)}{p_3 p_2 \cdot p_3} \theta(p_2 - p_3) \mathcal{F}_2(p_3, y_3 = y_2, \phi_3 = \phi_2) \quad (6.49)$$

$$\begin{aligned}
d^4 \sigma_2^{finite} &\equiv \frac{d_0[123]\chi_0}{p_3 p_2 \cdot p_3} \theta(p_2 - p_3) \\
&\times \left[\mathcal{F}_2(y_1, p_2, y_2, \phi_2, p_3, y_3, \phi_3) - \mathcal{F}_2(p_3, y_3 = y_2, \phi_3 = \phi_2) \right. \\
&\quad \left. + \mathcal{F}_2(p_3 = 0, y_3 = y_2, \phi_3 = \phi_2) - \mathcal{F}_2(p_3 = 0, y_3, \phi_3) \right]. \quad (6.50)
\end{aligned}$$

Again, it will be useful to break the $m = 2$ soft piece into two partial-fractioned terms $\{mn\} = \{2a, 2b\}$.

For $m = 1$, we will worry about a collinear piece only, as it can be shown that there are no soft poles:

$$d^D \sigma_1^{coll} \equiv \frac{d_\epsilon[213]\tilde{\chi}(\epsilon)}{p_1 \cdot p_3} \theta(p_2 - p_3) \mathcal{F}_1(p_3, y_3 = y_1, \phi_3 = \phi_1) \quad (6.51)$$

$$\begin{aligned}
d^4 \sigma_1^{finite} &\equiv \frac{d_0[123]\chi_0}{p_1 \cdot p_3} \theta(p_2 - p_3) \\
&\times \left[\mathcal{F}_1(y_1, p_2, y_2, \phi_2, p_3, y_3, \phi_3) - \mathcal{F}_1(p_3, y_3 = y_1, \phi_3 = \phi_1) \right]. \quad (6.52)
\end{aligned}$$

Note that, as promised, we have switched back to $p_1^\mu \leftrightarrow p_2^\mu$ in the phase space of $d^D \sigma_1^{finite}$ in order to take advantage of one common event generator in our Monte Carlo program.

In all, we have ten subtraction pieces; six correspond to soft singularities and are labeled $\{mn\} = \{ab, ba, a2, b2, 2a, 2b\}$. The other four correspond to the legs with which p_3^μ may be collinear, and these are labeled $m = \{a, b, 1, 2\}$. The next section is devoted to performing the approximations herein defined.

6.2.4 Perform Approximations

Since the \mathcal{F}_m , like the squared matrix elements from which they are derived, are given in terms of invariant dot-products $p_i \cdot p_j$, we must first see what these look like in terms of our free variables $\{y_1, p_2, y_2, \phi_2, p_3, y_3, \phi_3\}$.

$$\begin{aligned}
2p_a \cdot p_b &= x_1 x_2 S \\
2p_a \cdot p_1 &= x_1 \sqrt{S} p_1 e^{-y_1} \\
2p_a \cdot p_2 &= x_1 \sqrt{S} p_2 e^{-y_2} \\
2p_a \cdot p_3 &= x_1 \sqrt{S} p_3 e^{-y_3} \\
2p_b \cdot p_1 &= x_2 \sqrt{S} p_1 e^{y_1} \\
2p_b \cdot p_2 &= x_2 \sqrt{S} p_2 e^{y_2} \\
2p_b \cdot p_3 &= x_2 \sqrt{S} p_3 e^{y_3} \\
2p_1 \cdot p_2 &= 2p_1 p_2 [\cosh(y_1 - y_2) - \cos(\phi_1 - \phi_2)] \\
2p_1 \cdot p_3 &= 2p_1 p_3 [\cosh(y_1 - y_3) - \cos(\phi_1 - \phi_3)] \\
2p_2 \cdot p_3 &= 2p_2 p_3 [\cosh(y_2 - y_3) - \cos(\phi_2 - \phi_3)] , \tag{6.53}
\end{aligned}$$

in which

$$\begin{aligned}
x_1 &= \frac{1}{\sqrt{S}} \left(p_1 e^{\pm y_1} + p_2 e^{\pm y_2} + p_3 e^{\pm y_3} \right) \\
p_1 &= \sqrt{p_2^2 + p_3^2 + 2p_2 p_3 \cos(\phi_2 - \phi_3)} \\
\phi_1 &= \tan^{-1} \frac{p_2 \sin \phi_2 + p_3 \sin \phi_3}{p_2 \cos \phi_2 + p_3 \cos \phi_3} . \tag{6.54}
\end{aligned}$$

In the soft limit, $p_3 \rightarrow 0$ while y_3 and ϕ_3 remain fixed. We then obtain $p_1 \rightarrow p_2$ and $\{x_1, x_2\} \rightarrow \{x_a, x_b\}$, where

$$x_a^b = \frac{p_2}{\sqrt{S}} (e^{\pm y_1} + e^{\pm y_2}) , \tag{6.55}$$

leading to the soft limits expressed in Table 6.1, in which the $ab \rightarrow 12$ subprocess invariants $\hat{s}, \hat{t}, \hat{u}$ are given (for massless particles) as

Table 6.1. Soft limits of invariants.

$2p_a \cdot p_b = \hat{s}$			
$2p_a \cdot p_1 = -\hat{t}$	$2p_b \cdot p_1 = -\hat{u}$		
$2p_a \cdot p_2 = -\hat{u}$	$2p_b \cdot p_2 = -\hat{t}$	$2p_1 \cdot p_2 = \hat{s}$	
$2p_a \cdot p_3 = 0$	$2p_b \cdot p_3 = 0$	$2p_1 \cdot p_3 = 0$	$2p_2 \cdot p_3 = 0$

$$\begin{aligned}\hat{s} &= 2p_a \cdot p_b = 2p_1 \cdot p_2 \\ &= x_a x_b S = 2p_2^2 (1 + \cosh(y_1 - y_2))\end{aligned}\tag{6.56}$$

$$\begin{aligned}\hat{t} &= -2p_a \cdot p_1 = -2p_b \cdot p_2 \\ &= -x_a \sqrt{S} p_2 e^{-y_1} = -p_2^2 (1 + e^{y_2 - y_1})\end{aligned}\tag{6.57}$$

$$\begin{aligned}\hat{u} &= -2p_a \cdot p_2 = -2p_b \cdot p_1 \\ &= -x_a \sqrt{S} p_2 e^{-y_2} = -p_2^2 (1 + e^{y_1 - y_2}) .\end{aligned}\tag{6.58}$$

In fact, for 2-body subprocesses, these invariants are not independent. For massless participants, \hat{t} and \hat{u} can be written in terms of \hat{s} and a single angular variable v :

$$\begin{aligned}\hat{t} &= -(1 - v)\hat{s} \\ \hat{u} &= -v\hat{s} \\ v &\equiv \frac{1}{2}(1 + \cos \theta_1) = \frac{e^{y_1}}{e^{y_1} + e^{y_2}} .\end{aligned}\tag{6.59}$$

In this way, we can show that, as expected, the soft limits $\mathcal{F}_m(p_3 = 0, y_3, \phi_3)$ reduce to products of 2-body matrix elements $T'_{f\bar{f}}(v)$ and luminosity functions $\mathcal{L}(x_a, x_b)$. The denominators will retain certain y_3, ϕ_3 dependences after approximation, and we will integrate over these in what follows.

As an example of how the **collinear** limits are taken, we look at the case in which a gluon is radiated from one of the incoming legs of a subprocess, as in the diagram below. As the gluon (here p_3^μ) becomes collinear with the parent quark p_a^μ , its

momentum, as well as that of the daughter quark (p_a^μ , which enters the subprocess) are related to the parent in terms of a simple fraction z . That is, $p_3^\mu = (1 - z)p_a^\mu$ and $p_a^\mu = zp_a^\mu$:

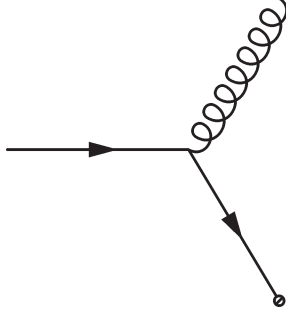


Figure 6.2. $p_{\tilde{a}} \cdot p_3 = 0$ collinear kinematics.

The functions to be approximated, \mathcal{F}_m , are in general functions of the invariants $p_i \cdot p_j$, where $\{i, j\} = \{\tilde{a}, b, 1, 2, 3\}$ for a three-body scattering $p_a^\mu + p_b^\mu \rightarrow p_1^\mu + p_2^\mu + p_3^\mu$.

⁴ In the collinear limit of massless particles, however, these invariants reduce to functions of z and the subprocess invariants (see Table 6.2).

Table 6.2. $p_{\tilde{a}} \cdot p_3 = 0$ collinear limits of invariants.

$2p_{\tilde{a}} \cdot p_b = \frac{\hat{s}}{z}$		
$2p_{\tilde{a}} \cdot p_1 = -\frac{\hat{t}}{z}$	$2p_b \cdot p_1 = -\hat{u}$	
$2p_{\tilde{a}} \cdot p_2 = -\frac{\hat{u}}{z}$	$2p_b \cdot p_2 = -\hat{t}$	$2p_1 \cdot p_2 = \hat{s}$
$2p_{\tilde{a}} \cdot p_3 = 0$	$2p_b \cdot p_3 = \frac{1-z}{z}\hat{s}$	$2p_1 \cdot p_3 = -\frac{1-z}{z}\hat{t} \quad 2p_2 \cdot p_3 = -\frac{1-z}{z}\hat{u}$

The fraction z is not arbitrary; its value in terms of our free variables is, as it should be, given by the $\{p_3 e^{y_3}, p_3 e^{-y_3} = 0, \hat{p}_3 = 0\}$ limit of the ratio $x_a/x_{\tilde{a}}$:

⁴Labeling of the partons involved in a collinear splitting can be confusing. Having started with the 3-body labels $ab \rightarrow 123$, it would seem appropriate to leave the parent label unchanged (e.g. a), and add a tilde to the daughter (e.g. \tilde{a}). The convention, however, is that the parent always carries the tilde.

$$z_a \equiv \frac{x_a}{x_{\bar{a}}} = \frac{x_a}{x_1} \rightarrow \frac{x_a \sqrt{S}}{x_a \sqrt{S} + p_3 e^{y_3}} . \quad (6.60)$$

One can easily verify that in the soft-collinear limit, when $p_3 e^{y_3}$ itself goes to zero, $z \rightarrow 1$ and the invariants in Table 6.2 reduce to those in Table 6.1.

For the $m = 1$ collinear contribution, p_3^μ becomes collinear with p_1^μ , and their sum balances p_2^μ . A new momentum fraction \tilde{z} is thus defined via $p_1 = \tilde{z}(p_1 + p_3)$, and the momenta of the incoming partons becomes the $\{y_3, \phi_3\} \rightarrow \{y_1, \phi_1\}$ limit of $x_{\frac{1}{2}}$, namely

$$\tilde{x}_b^a = \frac{(p_1 + p_3)}{\sqrt{S}}(e^{\pm y_1} + e^{\pm y_2}) \quad (6.61)$$

(see equations 6.31, 6.36). For $m = 2$, we have the $\{y_3, \phi_3\} \rightarrow \{y_2, \phi_2\}$ limits

$$\begin{aligned} \bar{z} &\equiv \frac{p_2}{p_2 + p_3} \\ \bar{x}_b^a &\equiv \frac{(p_2 + p_3)}{\sqrt{S}}(e^{\pm y_1} + e^{\pm y_2}) . \end{aligned} \quad (6.62)$$

In this way, all collinear \mathcal{F}_m can be shown to factorize into two functions, a splitting function \hat{P}'_{ij} which depends on only the relevant momentum fraction z , and a two-body matrix element $T'_{ff}(v)$ characteristic of the subprocess but independent of the earlier splitting.

Adding up the contributions to each $d^D \sigma_m^{soft}$ and $d^D \sigma_m^{coll}$ from all our 3-body matrix elements, and grouping by 2-body subprocess i (see Appendix A for a list), we can finally write out our subtraction pieces as follows. With the definitions (see equations 6.33, 6.38, 6.41, 6.42, 6.59):

$$\begin{aligned} x_b^a &\equiv \frac{p_2}{\sqrt{S}}(e^{\pm y_1} + e^{\pm y_2}) \\ v &\equiv \frac{e^{y_1}}{e^{y_1} + e^{y_2}} \end{aligned}$$

$$\begin{aligned}
x_2 &\equiv \frac{1}{\sqrt{S}}(p_1 e^{\pm y_1} + p_2 e^{\pm y_2} + p_3 e^{\pm y_3}) \\
p_1 &\equiv \sqrt{p_2^2 + p_3^2 + 2p_2 p_3 \cos(\phi_2 - \phi_3)} \\
p_a^\mu &\equiv \frac{x_a}{x_1} p_a^\mu = x_a \frac{\sqrt{S}}{2} (1 \quad 0 \quad 0 \quad 1) \\
p_b^\mu &\equiv \frac{x_b}{x_2} p_b^\mu = x_b \frac{\sqrt{S}}{2} (1 \quad 0 \quad 0 \quad -1) \\
\theta_a &\equiv \theta(\ln[(1 - x_a)\sqrt{S}/p_3 - y_3]) \\
\theta_b &\equiv \theta(y_3 + \ln[(1 - x_b)\sqrt{S}/p_3]) \\
d_\epsilon[123] &\equiv dy_1 dp_2 dy_2 d\phi_2^{1-2\epsilon} dp_3 dy_3 d\phi_3^{1-2\epsilon} \\
\chi(\epsilon) &\equiv \frac{\alpha_s^2 \mu^{2\epsilon}}{(2\pi)^2 S} \left(\frac{p_2}{2\pi\mu}\right)^{-2\epsilon} \left(\frac{p_3}{2\pi\mu}\right)^{-2\epsilon} p_2 p_3 4C_F, \tag{6.63}
\end{aligned}$$

our soft pieces become, for subprocess i :

$$d\sigma_{ab(i)}^{\text{soft}} = \frac{d_\epsilon[123]\chi(\epsilon)}{p_a \cdot p_3} \left[\psi_{ab}^0 \mathcal{L}(x_a, x_b) K' T'_{f\bar{f}}(v) \right]_i \frac{p_a \cdot p_b}{p_a \cdot p_3 + p_b \cdot p_3} \theta_a \theta_b \tag{6.64}$$

$$d\sigma_{ba(i)}^{\text{soft}} = \frac{d_\epsilon[123]\chi(\epsilon)}{p_b \cdot p_3} \left[\psi_{ba}^0 \mathcal{L}(x_a, x_b) K' T'_{f\bar{f}}(v) \right]_i \frac{p_a \cdot p_b}{p_a \cdot p_3 + p_b \cdot p_3} \theta_a \theta_b \tag{6.65}$$

$$d\sigma_{a2(i)}^{\text{soft}} = \frac{d_\epsilon[123]\chi(\epsilon)}{p_a \cdot p_3} \left[\psi_{a2}^0 \mathcal{L}(x_a, x_b) K' T'_{f\bar{f}}(v) \right]_i \frac{p_a \cdot p_2}{p_a \cdot p_3 + p_2 \cdot p_3} \theta_a \theta_b \tag{6.66}$$

$$d\sigma_{b2(i)}^{\text{soft}} = \frac{d_\epsilon[123]\chi(\epsilon)}{p_b \cdot p_3} \left[\psi_{b2}^0 \mathcal{L}(x_a, x_b) K' T'_{f\bar{f}}(v) \right]_i \frac{p_b \cdot p_2}{p_b \cdot p_3 + p_2 \cdot p_3} \theta_a \theta_b \tag{6.67}$$

$$d\sigma_{2a(i)}^{\text{soft}} = \frac{d_\epsilon[123]\chi(\epsilon)}{p_2 \cdot p_3} \left[\psi_{2a}^0 \mathcal{L}(x_a, x_b) K' T'_{f\bar{f}}(v) \right]_i \left[\frac{p_2 \cdot p_a}{p_a \cdot p_3 + p_2 \cdot p_3} - \frac{p_2}{p_3} \right] \tag{6.68}$$

$$d\sigma_{2b(i)}^{\text{soft}} = \frac{d_\epsilon[123]\chi(\epsilon)}{p_2 \cdot p_3} \left[\psi_{2b}^0 \mathcal{L}(x_a, x_b) K' T'_{f\bar{f}}(v) \right]_i \left[\frac{p_2 \cdot p_b}{p_b \cdot p_3 + p_2 \cdot p_3} - \frac{p_2}{p_3} \right], \tag{6.69}$$

in which the $[K' T'_{f\bar{f}}(v)]_i$ are given in Appendix A and

$$[\psi_{mn}^0]_i = [\psi_{nm}^0]_i = (2C_F - N_C) \delta_{mq} \delta_{nq} + N_C (1 - \delta_{mq} \delta_{nq}). \tag{6.70}$$

As an example, for the subprocess $q\bar{q} \rightarrow \gamma g$, $\psi_{ab}^0 = \psi_{ba}^0 = 2C_F - N_C$, as both $m = a$ and $n = b$ refer to quarks, while $\psi_{\{a2, 2a, b2, 2b\}}^0$ all equal N_C for this subprocess.

With the further definitions (see equations 6.36, 6.60, 6.61, 6.62)

$$\begin{aligned}
z_a &\equiv \frac{x_a \sqrt{S}}{x_a \sqrt{S} + p_3 e^{y_3}} \\
z_b &\equiv \frac{x_b \sqrt{S}}{x_b \sqrt{S} + p_3 e^{-y_3}} \\
\tilde{z} &\equiv \frac{p_1}{p_1 + p_3} \\
\tilde{x}_b^a &\equiv \frac{(p_1 + p_3)}{\sqrt{S}} (e^{\pm y_1} + e^{\pm y_2}) \\
d_\epsilon[213] &\equiv dy_2 dp_1 dy_1 d^{1-2\epsilon} \phi_1 dp_3 dy_3 d^{1-2\epsilon} \phi_3 \\
\tilde{\chi}(\epsilon) &\equiv \frac{\alpha \alpha_s^2 \mu^{2\epsilon}}{(2\pi)^2 S} \left(\frac{p_1}{2\pi\mu} \right)^{-2\epsilon} \left(\frac{p_3}{2\pi\mu} \right)^{-2\epsilon} p_1 p_3 4C_F \\
\bar{z} &\equiv \frac{p_2}{p_2 + p_3} \\
\bar{x}_b^a &\equiv \frac{(p_2 + p_3)}{\sqrt{S}} (e^{\pm y_1} + e^{\pm y_2}) ,
\end{aligned} \tag{6.71}$$

we find the collinear contributions:

$$\begin{aligned}
d\sigma_{a(i)}^{\text{coll}} &= \frac{d_\epsilon[123]\chi(\epsilon)}{p_a \cdot p_3} [\mathcal{L}(x_a, x_b) K' T'_{f\bar{f}}(v)]_i \theta_a \\
&\times \sum_{\tilde{a}} \left[\frac{\mathcal{L}(x_a/z_a, x_b)}{\mathcal{L}(x_a, x_b)} \hat{P}'_{a\tilde{a}}(z_a) - \frac{2C(a)z_a}{1-z_a} \delta_{g3} \right]
\end{aligned} \tag{6.72}$$

$$\begin{aligned}
d\sigma_{b(i)}^{\text{coll}} &= \frac{d_\epsilon[123]\chi(\epsilon)}{p_b \cdot p_3} [\mathcal{L}(x_a, x_b) K' T'_{f\bar{f}}(v)]_i \theta_b \\
&\times \sum_{\tilde{b}} \left[\frac{\mathcal{L}(x_a, x_b/z_b)}{\mathcal{L}(x_a, x_b)} \hat{P}'_{b\tilde{b}}(z_b) - \frac{2C(b)z_b}{1-z_b} \delta_{g3} \right]
\end{aligned} \tag{6.73}$$

$$d\sigma_{1(i)}^{\text{coll}} = \frac{d_\epsilon[213]\tilde{\chi}(\epsilon)}{p_1 \cdot p_3} [\mathcal{L}(\tilde{x}_a, \tilde{x}_b) K' T'_{f\bar{f}}(v)]_i \sum_q \hat{P}'_{\gamma q}(\tilde{z}) \tag{6.74}$$

$$d\sigma_{2(i)}^{\text{coll}} = \frac{d_\epsilon[123]\chi(\epsilon)}{p_2 \cdot p_3} [\mathcal{L}(\bar{x}_a, \bar{x}_b) K' T'_{f\bar{f}}(v)]_i \sum_{\tilde{d}} \hat{P}'_{d\tilde{d}}(\bar{z}) . \tag{6.75}$$

Here $\delta_{g3} = 1$ if the radiated third particle is a gluon; otherwise $\delta_{g3} = 0$.

6.2.5 Perform y_3 -Integrals.

We will now integrate analytically over the rapidity y_3 . This process will introduce further new notation, but as the functional form of these integrals is shared by more

than one subtraction term, the net increase in clarity should render the abbreviations forgivable.

To start, the notation we're currently using for our free, unobservable phase-space differentials is $d_\epsilon[123]$. After integration over y_3 it may be easiest to simply write

$$d_\epsilon[123 - y_3] \equiv dy_1 dp_2 dy_2 d\phi_2^{1-2\epsilon} dp_3 d\phi_3^{1-2\epsilon} . \quad (6.76)$$

Next, we'll see that for our initial-state subtraction terms, the limits on y_3 (as shown in the functions θ_a and θ_b) will appear in the final result. These limits will be written as

$$y_{3m}^{a,b} \equiv \ln[(1 - x_{a,b})\sqrt{S}/p_3] , \quad (6.77)$$

and will provide us, eventually, with the logs of Q_T we expect.

The integrals we'll need are performed in Appendix B; the results are as follows:

$$I_{ab}^s(x) \equiv \int_{-y_{3m}^b}^{y_{3m}^a} dy_3 \frac{e^{\pm y_3}}{e^{\pm y_3} + x e^{\mp y_3}} = (y_{3m}^a - \frac{1}{2} \ln x) \pm \frac{1}{2} \ln \left[\frac{1 + x^{\pm 1} e^{-2y_{3m}^a}}{1 + x^{\mp 1} e^{-2y_{3m}^b}} \right] \quad (6.78)$$

$$\begin{aligned} I_{a2}^s(x) &\equiv \int_{-y_{3m}^b}^{y_{3m}^a} dy_3 \frac{e^{\pm(y_3 - y_2)}}{x e^{\mp(y_3 - y_2)} + \cosh(y_3 - y_2) - \cos(\phi_3 - \phi_2)} \\ &= \pm \ln \left[\frac{(1 + 2x)^{\pm 1} e^{-2(y_{3m}^a - y_2)} + 1}{(1 + 2x)^{\mp 1} e^{-2(y_{3m}^b + y_2)} + 1} \right] \\ &+ 2(\pi - \alpha(x)) \cot \alpha(x) - \ln(1 + 2x) + 2(y_{3m}^a \mp y_2) \end{aligned} \quad (6.79)$$

$$\begin{aligned} I_{2a}^s(x) &\equiv \int_{-\infty}^{\infty} dy_3 \frac{1}{\cosh(y_3 - y_2) - \cos(\phi_3 - \phi_2)} \\ &\times \left[\frac{x}{x e^{\mp y_3} + \cosh(y_3 - y_2) - \cos(\phi_3 - \phi_2)} \right] \\ &= \ln(1 + 2x) + 2(\pi - (\phi_3 - \phi_2)) \cot(\phi_3 - \phi_2) - 2(\pi - \alpha(x)) \cot \alpha(x) \end{aligned} \quad (6.80)$$

$$I_2^c \equiv \int_{-\infty}^{\infty} \frac{dy_3}{\cosh(y_3 - y_2) - \cos(\phi_3 - \phi_2)} = \frac{2(\pi - (\phi_3 - \phi_2))}{\sin(\phi_3 - \phi_2)} \quad (6.81)$$

$$I_a^c \equiv \int_{-\infty}^{y_{3m}^a} dy_3 \frac{p_3 z_a}{x_a \sqrt{S} e^{-y_3}} \left[\frac{H(x_a/z_a, x_b)}{H(x_a, x_b)} \hat{P}'_{aa}(z_a) - \frac{2C(a)}{1 - z_a} \delta_{g3} \right]$$

$$= \int_{x_a}^1 \frac{dz_a}{z_a} \left[\frac{H(x_a/z_a, x_b)}{H(x_a, x_b)} \hat{P}'_{a\bar{a}}(z_a) - \frac{2C(a)}{1-z_a} \delta_{g3} \right] \quad (6.82)$$

$$\begin{aligned} I_b^c &\equiv \int_{-y_{3m}^b}^{\infty} dy_3 \frac{p_3 z_b}{x_b \sqrt{S} e^{y_3}} \left[\frac{H(x_a, x_b/z_b)}{H(x_a, x_b)} \hat{P}'_{b\bar{b}}(z_b) - \frac{2C(b)}{1-z_b} \delta_{g3} \right] \\ &= \int_{x_b}^1 \frac{dz_b}{z_b} \left[\frac{H(x_a, x_b/z_b)}{H(x_a, x_b)} \hat{P}'_{b\bar{b}}(z_b) - \frac{2C(b)}{1-z_b} \delta_{g3} \right], \end{aligned} \quad (6.83)$$

in which we've abbreviated

$$\begin{aligned} \cos \alpha(x) &\equiv \frac{\cos(\phi_3 - \phi_2)}{\sqrt{1+2x}} \\ H(x_1, x_2) &\equiv 2x_1 x_2 S \mathcal{L}(x_1, x_2). \end{aligned} \quad (6.84)$$

The subtraction terms then become:

$$d\sigma_{ab(i)}^{\text{soft}} = d_\epsilon [123 - y_3] \chi(\epsilon) \left[\psi_{ab}^0 \mathcal{L}(x_a, x_b) K' T'_{f\bar{f}}(v) \right]_i \frac{2}{p_3^2} I_{ab}^s \left(\frac{x_a}{x_b} \right) \quad (6.85)$$

$$d\sigma_{ba(i)}^{\text{soft}} = d_\epsilon [123 - y_3] \chi(\epsilon) \left[\psi_{ba}^0 \mathcal{L}(x_a, x_b) K' T'_{f\bar{f}}(v) \right]_i \frac{2}{p_3^2} I_{ba}^s \left(\frac{x_b}{x_a} \right) \quad (6.86)$$

$$d\sigma_{a2(i)}^{\text{soft}} = d_\epsilon [123 - y_3] \chi(\epsilon) \left[\psi_{a2}^0 \mathcal{L}(x_a, x_b) K' T'_{f\bar{f}}(v) \right]_i \frac{1}{p_3^2} I_{a2}^s \left(\frac{x_a \sqrt{S} e^{-y_2}}{2p_2} \right) \quad (6.87)$$

$$d\sigma_{b2(i)}^{\text{soft}} = d_\epsilon [123 - y_3] \chi(\epsilon) \left[\psi_{b2}^0 \mathcal{L}(x_a, x_b) K' T'_{f\bar{f}}(v) \right]_i \frac{1}{p_3^2} I_{b2}^s \left(\frac{x_b \sqrt{S} e^{y_2}}{2p_2} \right) \quad (6.88)$$

$$d\sigma_{2a(i)}^{\text{soft}} = d_\epsilon [123 - y_3] \chi(\epsilon) \left[\psi_{2a}^0 \mathcal{L}(x_a, x_b) K' T'_{f\bar{f}}(v) \right]_i \frac{1}{p_3^2} \left[I_{2a}^s \left(\frac{x_a \sqrt{S} e^{-y_2}}{2p_2} \right) - I_2^c \right] \quad (6.89)$$

$$d\sigma_{2b(i)}^{\text{soft}} = d_\epsilon [123 - y_3] \chi(\epsilon) \left[\psi_{2b}^0 \mathcal{L}(x_a, x_b) K' T'_{f\bar{f}}(v) \right]_i \frac{1}{p_3^2} \left[I_{2b}^s \left(\frac{x_b \sqrt{S} e^{y_2}}{2p_2} \right) - I_2^c \right] \quad (6.90)$$

$$d\sigma_{a(i)}^{\text{coll}} = d_\epsilon [123 - y_3] \chi(\epsilon) [\mathcal{L}(x_a, x_b) K' T'_{f\bar{f}}(v)]_i \frac{2}{p_3^2} \sum_{\bar{a}} I_{\bar{a}}^c \quad (6.91)$$

$$d\sigma_{b(i)}^{\text{coll}} = d_\epsilon [123 - y_3] \chi(\epsilon) [\mathcal{L}(x_a, x_b) K' T'_{f\bar{f}}(v)]_i \frac{2}{p_3^2} \sum_{\bar{b}} I_{\bar{b}}^c \quad (6.92)$$

$$d\sigma_{1(i)}^{\text{coll}} = d_\epsilon [213 - y_3] \tilde{\chi}(\epsilon) [\mathcal{L}(\tilde{x}_a, \tilde{x}_b) K' T'_{f\bar{f}}(v)]_i \frac{I_2^c}{p_1 p_3} \sum_q \hat{P}'_{\gamma q}(\tilde{z}) \quad (6.93)$$

$$d\sigma_{2(i)}^{\text{coll}} = d_\epsilon [123 - y_3] \chi(\epsilon) [\mathcal{L}(\bar{x}_a, \bar{x}_b) K' T'_{f\bar{f}}(v)]_i \frac{I_2^c}{p_2 p_3} \sum_{\bar{d}} \hat{P}'_{d\bar{d}}(\bar{z}). \quad (6.94)$$

6.2.6 Map to Photon-Jet space

It's now time to translate to a common set of observables $\{y_\gamma, p_j, y_j, \phi_j, Q_T, \phi_q\}$ so that Born, virtual, counterterm, and subtraction terms may all be added and poles cancelled. As stated in Section 6.2, the poles in ϵ will not cancel unless this is done first.

For the initial-state contributions $m = \{a, b\}$, we simply have $\{y_1, p_2, y_2, \phi_2\} \rightarrow \{y_\gamma, p_j, y_j, \phi_j\}$ as in the two-body case, but as we have a non-zero p_3 which contributes transverse momentum to the pair, we take $p_3 \rightarrow Q_T$ and $\phi_3 \rightarrow \phi_q - \pi$. As this affects the photon transverse momentum, we also list the smeared dependent variables

$$\begin{aligned} p_\gamma &= \sqrt{p_j^2 + Q_T^2 + 2p_j Q_T \cos(\phi_j - \phi_q - \pi)} \\ \phi_\gamma &= \tan^{-1} \left(\frac{p_j \sin \phi_j + Q_T \sin \phi_q}{p_j \cos \phi_j + Q_T \cos \phi_q} \right) + \pi . \end{aligned} \quad (6.95)$$

The final-state soft pieces $\{mn\} = \{2a, 2b\}$ will not be resummed, so we could approximate the kinematics as well as the weights, and simply set $Q_T = 0$ here. Unfortunately, this would require an analytic integration over ϕ_3 (namely $\int d^{1-2\epsilon} \phi_3 (\pi - \alpha) \cot \alpha$), and our lack of a closed form for such an expression makes it difficult to explicitly show the cancellation of poles. As these terms describe radiation which, in general, falls outside the jet cone, and thus contributes to the Q_T of the photon-jet pair, it will be more natural to treat these terms in the same way as the $\{mn\} = \{a2, b2\}$ pieces above.

For the $m = 2$ collinear term, we unquestionably have zero Q_T , and due to the collinear configuration of particles 2 and 3, they are counted as a single jet of transverse momentum $p_2 + p_3$. With the definition of \bar{z} used earlier, we can take

$$\int dp_2 dp_3 \rightarrow p_j dp_j d\bar{z} , \quad (6.96)$$

while $\{y_1, y_2, \phi_2\} \rightarrow \{y_\gamma, y_j, \phi_j\}$ and $p_\gamma = p_j$, $\phi_\gamma = \phi_j + \pi$. As we now have purely $2 \rightarrow 2$ kinematics for this piece, ϕ_q is undefined, and so we (as in the two-body case)

include a factor $d^{1-2\epsilon}\phi_q/\int d^{1-2\epsilon}\phi_q$. The integrations over ϕ_3 and \bar{z} must be done analytically.

Finally, for the $m = 1$ collinear term, we do have a nonzero $Q_T = p_3$, and $p_j = p_2$ as in the initial-state pieces. However, as we have switched $p_1^\mu \leftrightarrow p_2^\mu$ in the phase space for calculational simplicity, p_2 is no longer a free variable. Instead we have its approximation $p_j = p_1 + p_3$. Thus we write $p_1(\equiv p_\gamma) \rightarrow p_j - p_3 = p_j - Q_T$. The splitting functions will continue to be expressed in terms of the momentum fraction \tilde{z} , where now $\tilde{z} = (p_j - Q_T)/p_j$. As for the rest of the variables, $\{y_1, y_2\} \rightarrow \{y_\gamma, y_j\}$ and $\phi_1(\equiv \phi_\gamma) \rightarrow \phi_j + \pi$, while $\phi_3 \rightarrow \phi_q - \pi$ as in the initial-state terms.

After performing the above operations, we can split each χ and $\tilde{\chi}$ factor into three pieces. The first, κ_i , will be common to all contributions (2-body and subtraction), the second, β_ϵ , common to all higher-order contributions, and the third, χ_{fac} , will be expanded through the balance of the relevant contribution. With the definitions:

$$\begin{aligned}
d_\epsilon[\gamma j] &\equiv dy_\gamma dp_j dy_j d^{1-2\epsilon}\phi_j dQ_T d^{1-2\epsilon}\phi_q \\
x_b^a &\equiv \frac{p_j}{\sqrt{S}}(e^{\pm y_\gamma} + e^{\pm y_j}) \\
\kappa_i &\equiv \frac{\alpha_s}{S} \frac{p_j}{\int d^{1-2\epsilon}\phi} \left(\frac{p_j}{2\pi\mu^2}\right)^{-2\epsilon} 4C_F[\mathcal{L}(x_a, x_b)K'T'_{f\bar{f}}(v)]_i \\
\beta_\epsilon &\equiv \frac{\alpha_s}{2\pi} \left(\frac{4\pi\mu^2}{M_f^2}\right)^\epsilon \frac{\Gamma(1-\epsilon)}{\Gamma(1-2\epsilon)} \\
\chi_{\text{fac}} &\equiv \frac{\Gamma(1-2\epsilon)}{\Gamma^2(1-\epsilon)} \left(\frac{M_f^2}{p_j^2}\right)^\epsilon,
\end{aligned} \tag{6.97}$$

in which M_f is the factorization scale, we can now write all our subtraction pieces in the form:

$$d\sigma_{(i)} = d_\epsilon[\gamma j]\kappa_i\beta_\epsilon\Gamma_{(i)}, \tag{6.98}$$

where

$$\Gamma_{ab(i)}^{\text{soft}} = \chi_{\text{fac}}\psi_{ab(i)}^0 \frac{2}{Q_T} \left(\frac{p_j^2}{Q_T^2}\right)^\epsilon I_{ab}^s\left(\frac{x_a}{x_b}\right) \tag{6.99}$$

$$\Gamma_{ba(i)}^{\text{soft}} = \chi_{\text{fac}} \psi_{ba(i)}^0 \frac{2}{Q_T} \left(\frac{p_j^2}{Q_T^2} \right)^\epsilon I_{ba}^s \left(\frac{x_b}{x_a} \right) \quad (6.100)$$

$$\Gamma_{a2(i)}^{\text{soft}} = \chi_{\text{fac}} \psi_{a2(i)}^0 \frac{1}{Q_T} \left(\frac{p_j^2}{Q_T^2} \right)^\epsilon I_{a2}^s \left(\frac{1}{2(1-v)} \right) \quad (6.101)$$

$$\Gamma_{b2(i)}^{\text{soft}} = \chi_{\text{fac}} \psi_{b2(i)}^0 \frac{1}{Q_T} \left(\frac{p_j^2}{Q_T^2} \right)^\epsilon I_{b2}^s \left(\frac{1}{2v} \right) \quad (6.102)$$

$$\Gamma_{2a(i)}^{\text{soft}} = \chi_{\text{fac}} \psi_{2a(i)}^0 \frac{1}{Q_T} \left(\frac{p_j^2}{Q_T^2} \right)^\epsilon \left[I_{2a}^s \left(\frac{1}{2(1-v)} \right) - I_2^c \right] \quad (6.103)$$

$$\Gamma_{2b(i)}^{\text{soft}} = \chi_{\text{fac}} \psi_{2b(i)}^0 \frac{1}{Q_T} \left(\frac{p_j^2}{Q_T^2} \right)^\epsilon \left[I_{2b}^s \left(\frac{1}{2v} \right) - I_2^c \right] \quad (6.104)$$

$$\Gamma_{a(i)}^{\text{coll}} = \chi_{\text{fac}} \frac{2}{Q_T} \left(\frac{p_j^2}{Q_T^2} \right)^\epsilon \sum_{\bar{a}} I_{\bar{a}}^c \quad (6.105)$$

$$\Gamma_{b(i)}^{\text{coll}} = \chi_{\text{fac}} \frac{2}{Q_T} \left(\frac{p_j^2}{Q_T^2} \right)^\epsilon \sum_{\bar{b}} I_{\bar{b}}^c \quad (6.106)$$

$$\Gamma_{1(i)}^{\text{coll}} = \chi_{\text{fac}} \frac{I_2^c}{p_j} [\tilde{z}(1-\tilde{z})]^{-2\epsilon} \sum_q \hat{P}'_{\gamma q}(\tilde{z}) \quad (6.107)$$

$$\Gamma_{2(i)}^{\text{coll}} = \chi_{\text{fac}} \delta(Q_T) \frac{\int d^{1-2\epsilon} \phi_3 I_2^c(\phi_3)}{\int d^{1-2\epsilon} \phi_3} \int d\bar{z} [\bar{z}(1-\bar{z})]^{-2\epsilon} \sum_{\bar{d}} \hat{P}'_{d\bar{d}}(\bar{z}) . \quad (6.108)$$

6.2.7 Extract Poles in ϵ

Toward this end, we notice that for most contributions, the poles reside purely at $Q_T = 0$, and can be extracted with the help of:

$$\int_0^{p_j} \frac{dQ_T}{Q_T} \left(\frac{p_j^2}{Q_T^2} \right)^\epsilon f(Q_T) = \int_0^{p_j} dQ_T \left[\left(\frac{1}{Q_T} \right)_+ - \frac{\delta(Q_T)}{2\epsilon} \right] f(Q_T) \quad (6.109)$$

$$\begin{aligned} \int_0^{p_j} \frac{dQ_T}{Q_T} \left(\frac{p_j^2}{Q_T^2} \right)^\epsilon 2y_{3m}^i f(Q_T) &= \int_0^{p_j} dQ_T \left[\ln \left(\frac{(1-x_i)^2 S}{p_j^2} \right) \left[\left(\frac{1}{Q_T} \right)_+ - \frac{\delta(Q_T)}{2\epsilon} \right] \right. \\ &\quad \left. - 2 \left(\frac{\ln Q_T/p_j}{Q_T} \right)_+ + \frac{\delta(Q_T)}{2\epsilon^2} \right] f(Q_T) \end{aligned} \quad (6.110)$$

whereas for the $m = 2$ collinear piece, there are poles at $\bar{z} = 1$ and $\phi_3 = \phi_j + \pi$. We then need:

$$\bar{\mathcal{Z}}(q) \equiv \sum_{\bar{d}} \int_{\frac{1}{2}}^1 d\bar{z} [\bar{z}(1-\bar{z})]^{-2\epsilon} \hat{P}'_{d\bar{q}}(\bar{z})$$

$$\simeq C_F \left[-\frac{1}{\epsilon} - \frac{3}{2} + \epsilon \left(\frac{2\pi^2}{3} - \frac{13}{2} \right) \right] \quad (6.111)$$

$$\begin{aligned} \bar{\mathcal{Z}}(g) &\equiv \sum_{\bar{d}} \int_{\frac{1}{2}}^1 d\bar{z} [\bar{z}(1-\bar{z})]^{-2\epsilon} \hat{P}'_{dg}(\bar{z}) \\ &\simeq N_C \left[-\frac{1}{\epsilon} - \frac{11}{6} + \epsilon \left(\frac{2\pi^2}{3} - \frac{67}{9} \right) \right] + N_f \left[\frac{1}{3} + \frac{23}{18}\epsilon \right] \end{aligned} \quad (6.112)$$

$$\begin{aligned} \mathcal{Z}_2^c &\equiv \int d^{1-2\epsilon} \phi_3 I_2^c(\phi_3) / \int d^{1-2\epsilon} \phi \\ &= -\frac{16^{-\epsilon}}{\epsilon} \frac{\Gamma^4(1-\epsilon)}{\Gamma^2(1-2\epsilon)}. \end{aligned} \quad (6.113)$$

Finally, the $m = 1$ collinear piece has nonzero Q_T (implicit in our definition of \tilde{z}) and therefore dependence upon a defined pair angle ϕ_q . Unlike the $m = 2$ collinear case, then, integration over the function I_2^c is not independent of our free variables, and we must extract its $\phi_q = \phi_j + \pi$ pole in the sense of a distribution as follows:

$$\int d^{1-2\epsilon} \phi_q I_2^c(\phi_q) = \int d^{1-2\epsilon} \phi_q \left[\frac{2(\pi - \Delta\phi)}{\sin \Delta\phi} [1 - \cos \Delta\phi] - \frac{1}{\epsilon} \right], \quad (6.114)$$

with $\Delta\phi \equiv \text{MOD}(\|\phi_q - \phi_j - \pi\|/\pi)$.

This brings us, finally, to:

$$\begin{aligned} \Gamma_{ab(i)}^{\text{soft}} &= \psi_{ab(i)}^0 \left[\ln \frac{(1-x_a)^2 S x_b}{x_a p_j^2} \left[\left(\frac{1}{Q_T} \right)_+ - \frac{\delta(Q_T)}{2\epsilon} \right] \right. \\ &\quad \left. - 2 \left(\frac{\ln Q_T/p_j}{Q_T} \right)_+ + \frac{\delta(Q_T)}{2\epsilon^2} + \frac{1}{Q_T} \left(\frac{p_j^2}{Q_T^2} \right)^\epsilon \ln \left[\frac{1 + \frac{x_a}{x_b} e^{-2y_{3m}^a}}{1 + \frac{x_b}{x_a} e^{-2y_{3m}^b}} \right] \right] \chi_{\text{fac}} \end{aligned} \quad (6.115)$$

$$\begin{aligned} \Gamma_{ba(i)}^{\text{soft}} &= \psi_{ba(i)}^0 \left[\ln \frac{(1-x_b)^2 S x_a}{x_b p_j^2} \left[\left(\frac{1}{Q_T} \right)_+ - \frac{\delta(Q_T)}{2\epsilon} \right] \right. \\ &\quad \left. - 2 \left(\frac{\ln Q_T/p_j}{Q_T} \right)_+ + \frac{\delta(Q_T)}{2\epsilon^2} - \frac{1}{Q_T} \left(\frac{p_j^2}{Q_T^2} \right)^\epsilon \ln \left[\frac{1 + \frac{x_a}{x_b} e^{-2y_{3m}^a}}{1 + \frac{x_b}{x_a} e^{-2y_{3m}^b}} \right] \right] \chi_{\text{fac}} \end{aligned} \quad (6.116)$$

$$\begin{aligned} \Gamma_{a2(i)}^{\text{soft}} &= \psi_{a2(i)}^0 \left[\left[2(\pi - \alpha_a) \cot \alpha_a - 2y_j + \ln \frac{(1-x_a)^2 S(1-v)}{(2-v)p_j^2} \right] \left[\left(\frac{1}{Q_T} \right)_+ - \frac{\delta(Q_T)}{2\epsilon} \right] \right. \\ &\quad \left. - 2 \left(\frac{\ln Q_T/p_j}{Q_T} \right)_+ + \frac{\delta(Q_T)}{2\epsilon^2} + \frac{1}{Q_T} \left(\frac{p_j^2}{Q_T^2} \right)^\epsilon \ln \left[\frac{1 + \frac{2-v}{1-v} e^{-2(y_{3m}^a - y_j)}}{1 + \frac{1-v}{2-v} e^{-2(y_{3m}^b + y_j)}} \right] \right] \chi_{\text{fac}} \end{aligned} \quad (6.117)$$

$$\begin{aligned} \Gamma_{b2(i)}^{\text{soft}} &= \psi_{b2(i)}^0 \left[\left[2(\pi - \alpha_b) \cot \alpha_b + 2y_j + \ln \frac{(1-x_b)^2 S v}{(1+v)p_j^2} \right] \left[\left(\frac{1}{Q_T} \right)_+ - \frac{\delta(Q_T)}{2\epsilon} \right] \right. \\ &\quad \left. - 2 \left(\frac{\ln Q_T/p_j}{Q_T} \right)_+ + \frac{\delta(Q_T)}{2\epsilon^2} - \frac{1}{Q_T} \left(\frac{p_j^2}{Q_T^2} \right)^\epsilon \ln \left[\frac{1 + \frac{v}{1+v} e^{-2(y_{3m}^a - y_j)}}{1 + \frac{1+v}{v} e^{-2(y_{3m}^b + y_j)}} \right] \right] \chi_{\text{fac}} \end{aligned} \quad (6.118)$$

$$\begin{aligned}\Gamma_{2a(i)}^{\text{soft}} &= \psi_{2a(i)}^0 \left[\left(\frac{1}{Q_T} \right)_+ - \frac{\delta(Q_T)}{2\epsilon} \right] \\ &\times \left[\ln \frac{2-v}{1-v} - 2(\pi - \Delta\phi) \frac{(1 - \cos \Delta\phi)}{\sin \Delta\phi} - 2(\pi - \alpha_a) \cot \alpha_a \right] \chi_{\text{fac}}\end{aligned}\quad (6.119)$$

$$\begin{aligned}\Gamma_{2b(i)}^{\text{soft}} &= \psi_{2b(i)}^0 \left[\left(\frac{1}{Q_T} \right)_+ - \frac{\delta(Q_T)}{2\epsilon} \right] \\ &\times \left[\ln \frac{1+v}{v} - 2(\pi - \Delta\phi) \frac{(1 - \cos \Delta\phi)}{\sin \Delta\phi} - 2(\pi - \alpha_b) \cot \alpha_b \right] \chi_{\text{fac}}\end{aligned}\quad (6.120)$$

$$\Gamma_{a(i)}^{\text{coll}} = \sum_{\tilde{a}} I_{\tilde{a}}^c \left[\left(\frac{2}{Q_T} \right)_+ - \frac{\delta(Q_T)}{\epsilon} \right] \chi_{\text{fac}} \quad (6.121)$$

$$\Gamma_{b(i)}^{\text{coll}} = \sum_{\tilde{b}} I_{\tilde{b}}^c \left[\left(\frac{2}{Q_T} \right)_+ - \frac{\delta(Q_T)}{\epsilon} \right] \chi_{\text{fac}} \quad (6.122)$$

$$\Gamma_{1(i)}^{\text{coll}} = [\tilde{z}(1 - \tilde{z})]^{-2\epsilon} \sum_q \hat{P}'_{\gamma q}(\tilde{z}) \left[\frac{2(\pi - \Delta\phi)}{\sin \Delta\phi} [1 - \cos \Delta\phi] - \frac{1}{\epsilon} \right] \frac{\chi_{\text{fac}}}{p_j} \quad (6.123)$$

$$\Gamma_{2(i)}^{\text{coll}} = \delta(Q_T) \bar{\mathcal{Z}}(d) \mathcal{Z}_2^c \chi_{\text{fac}} \quad (6.124)$$

where the d in $\bar{\mathcal{Z}}(d)$ is the type of parton (q or g) on leg d (for subprocess $ab \rightarrow \gamma d$), and

$$\begin{aligned}v &\equiv \frac{e^{y_\gamma}}{e^{y_\gamma} + e^{y_j}} \\ \cos \alpha_a &\equiv \cos \Delta\phi \sqrt{\frac{1-v}{2-v}} \\ \cos \alpha_b &\equiv \cos \Delta\phi \sqrt{\frac{v}{1+v}} \\ y_j &= \ln \frac{x_a(1-v)}{x_b v} \\ \Delta\phi &\equiv \text{MOD}(\|\phi_q - \phi_j - \pi\|/\pi) .\end{aligned}\quad (6.125)$$

Note that in $\Gamma_{ab,ba,a2,b2}^{\text{soft}}$, there exist complicated logarithms of the form

$$\ln \left[\frac{1 + x e^{-2y_{3m}^a}}{1 + \frac{1}{x} e^{-2y_{3m}^b}} \right] .$$

Since these tend to zero as $Q_T \rightarrow 0$, we can drop them for the sake of simplicity. This amounts to a redefinition of our asymptotic form, and is valid as long as we get

rid of these terms in the finite piece also. This has been done in the Monte Carlo program.

6.3 Add Born, Virtual, and Counterterm Contributions.

We may now add in the two-body pieces from Section 6.1:

$$d\sigma_i^{\text{Born}} = d_\epsilon[\gamma j] \kappa_i \delta(Q_T) \quad (6.126)$$

$$d\sigma_i^{\text{Virt}} = d_\epsilon[\gamma j] \kappa_i \beta_\epsilon \Gamma_{\text{Virt}(i)} \quad (6.127)$$

$$d\sigma_{a(i)}^{\text{CT}} = d_\epsilon[\gamma j] \kappa_i \beta_\epsilon \Gamma_{a(i)}^{\text{CT}} \quad (6.128)$$

$$d\sigma_{b(i)}^{\text{CT}} = d_\epsilon[\gamma j] \kappa_i \beta_\epsilon \Gamma_{b(i)}^{\text{CT}} \quad (6.129)$$

$$d\sigma_{1(i)}^{\text{CT}} = d_\epsilon[\gamma j] \kappa_i \beta_\epsilon \Gamma_{1(i)}^{\text{CT}} , \quad (6.130)$$

where

$$\Gamma_{\text{Virt}(i)} = \delta(Q_T) \left[\frac{A_v^2}{\epsilon^2} + \frac{A_v^1}{\epsilon} + A_v^0 + \frac{B^v}{T_0} \right]_i \quad (6.131)$$

$$\Gamma_{a(i)}^{\text{CT}} = \delta(Q_T) \sum_{\tilde{a}} \int_{x_a}^1 \frac{dz}{z} \frac{H(x_a/z, x_b)}{H(x_a, x_b)} \frac{P_{a\tilde{a}}^+(z)}{\epsilon} \quad (6.132)$$

$$\Gamma_{b(i)}^{\text{CT}} = \delta(Q_T) \sum_{\tilde{b}} \int_{x_b}^1 \frac{dz}{z} \frac{H(x_a, x_b/z)}{H(x_a, x_b)} \frac{P_{b\tilde{b}}^+(z)}{\epsilon} \quad (6.133)$$

$$\Gamma_{1(i)}^{\text{CT}} = \sum_q \frac{P_{\gamma q}^+(\tilde{z})}{\epsilon p_j} . \quad (6.134)$$

and the virtual parameters A_v^2, A_v^1, A_v^0, B^v are given in Appendix C.

6.4 Cancel Poles and Take $\epsilon \rightarrow 0$

For simplicity of notation, we allow the virtual and counterterm pieces to share $\{mn\}$ designations of their own, and write the sum

$$\sum_{mn} \Gamma_{mn(i)} \equiv \Gamma_{\text{Virt}(i)} + \Gamma_{ab(i)}^{\text{soft}} + \Gamma_{ba(i)}^{\text{soft}} + \Gamma_{a2(i)}^{\text{soft}} + \Gamma_{b2(i)}^{\text{soft}} + \Gamma_{2a(i)}^{\text{soft}} + \Gamma_{2b(i)}^{\text{soft}}$$

$$+ \Gamma_{a(i)}^{\text{coll}} + \Gamma_{b(i)}^{\text{coll}} + \Gamma_{2(i)}^{\text{coll}} + \Gamma_{1(i)}^{\text{coll}} + \Gamma_{a(i)}^{\text{CT}} + \Gamma_{b(i)}^{\text{CT}} + \Gamma_{1(i)}^{\text{CT}} , \quad (6.135)$$

which should now be finite. The full NLO result is then

$$d\sigma = d\sigma^{\text{sing}} + d\sigma^{\text{finite}} , \quad (6.136)$$

with $d\sigma^{\text{finite}}$ given by the finite corrections of equations [6.47, 6.50, 6.52], and

$$d\sigma^{\text{sing}} = \sum_i d_\epsilon[\gamma j] \kappa_i \left[\delta(Q_T) + \beta_\epsilon \sum_{mn} \Gamma_{mn(i)} \right] . \quad (6.137)$$

After pole cancellation, of course, we can take $\epsilon \rightarrow 0$, and

$$\begin{aligned} d_\epsilon[\gamma j] &\rightarrow dy_\gamma dp_j dy_j d\phi_j dQ_T d\phi_q \\ \kappa_i &\rightarrow \frac{\alpha\alpha_s}{S} \frac{p_j}{2\pi} 4C_F [\mathcal{L}(x_a, x_b) K T_{f\bar{f}}(v)]_i \\ \beta_\epsilon &\rightarrow \frac{\alpha_s}{2\pi} . \end{aligned} \quad (6.138)$$

With the exception of the $m = 1$ Bremsstrahlung pieces, which we will handle separately, each Γ_{mn} can be written in the form (subprocess label i suppressed)

$$\begin{aligned} \Gamma_{mn} &\equiv \delta(Q_T) \left(\frac{{}_2\Gamma_{mn}}{\epsilon^2} + \frac{{}_1\Gamma_{mn}}{\epsilon} \right) + \delta(Q_T) {}_\delta C_{mn} \\ &+ \delta(Q_T) \left[\sum_{\bar{a}} \int_{x_a}^1 \frac{dz}{z} \frac{H(x_a/z, x_b)}{H(x_a, x_b)} {}_{\bar{a}} C_{mn}(z) \right. \\ &+ \left. \sum_{\bar{b}} \int_{x_b}^1 \frac{dz}{z} \frac{H(x_a, x_b/z)}{H(x_a, x_b)} {}_{\bar{b}} C_{mn}(z) \right] \\ &- 4A_{mn} \left[\frac{\ln Q_T/Q}{Q_T} \right]_+ + 2B_{mn} \left[\frac{1}{Q_T} \right]_+ \\ &+ \left[\frac{2}{Q_T} \right]_+ \left[{}_a D_{mn} \sum_{\bar{a}} \int_{x_a}^1 \frac{dz}{z} \frac{H(x_a/z, x_b)}{H(x_a, x_b)} P_{a\bar{a}}^+(z) \right. \\ &+ \left. {}_b D_{mn} \sum_{\bar{b}} \int_{x_b}^1 \frac{dz}{z} \frac{H(x_a, x_b/z)}{H(x_a, x_b)} P_{b\bar{b}}^+(z) \right] , \end{aligned} \quad (6.139)$$

the coefficients of which are given in Appendix C. Note (there) that the sum of all ${}_2\Gamma_{mn}$ coefficients is zero, as required, as is the sum of ${}_1\Gamma_{mn}$ coefficients. Also note

that logs of Q_T/p_j have been expanded into logs of Q_T/Q plus logs of Q/p_j in order to anticipate comparison with the expansion of the resummed form.

6.5 Extract Resummation Parameters

Each resummation formalism described in the text has, as parameters, a set of functions which depend on the particular process under study. In the b -space formalism, these parameters are A , B , $C_{a/\bar{a}}$, and $C_{b/\bar{b}}$, and we have seen in Chapter 5 that these same parameters can be used for resummation in k_T -space. Now that we have a set of finite terms which together constitute the cross section to a fixed order (here NLO), we have the material necessary to calculate these parameters.

This can be done in a couple of ways, each of which involves an expansion of the resummed form to the same order in α_s as our perturbative result, followed by identification of A , B , $C_{a/\bar{a}}$, and $C_{b/\bar{b}}$ in the expansion with corresponding coefficients in that perturbative result.

However straightforward this procedure may sound, it is not without its complications. Although the b -space and k_T -space resummed expressions are formally finite at $Q_T = 0$ (even without the non-perturbative parametrizations), this convergence is inextricably tied to the all-orders nature of the Sudakov exponentiation. Attempts to expand either result directly, to a fixed order, will lead to expressions which are unregulated at zero Q_T .

For the b -space formalism, one way to resolve this is to “meet the expansion halfway” by comparing the Fourier transform of the NLO result to an expansion of just the b -space integrand. Our starting point is equation 4.35, minus the finite correction:

$$d\sigma_S^{pert} = \frac{1}{2\pi^2} \int d^2\vec{b} e^{i\vec{b}\cdot\vec{Q}_T} d\tilde{\sigma}^S(b) e^{-S(b,Q)} . \quad (6.140)$$

The C parameters live inside $d\tilde{\sigma}^S$, and can be expanded to NLO in α_s . Since we seek a form in which the partons are sampled at the same energy as in the NLO

expression, we must also expand the parton distributions $f_{a,b}(b_0/b)$ into $f_{a,b}(M_f)$ plus appropriate convolutions over splitting functions P^+ . The resulting expansion of $d\tilde{\sigma}^S$ takes the form:

$$\begin{aligned}
d\tilde{\sigma}^S &\simeq \sum_{a,b} \left[f_{a/A}(x_a, M_f) f_{b/B}(x_b, M_f) \right. \\
&+ \frac{\alpha_s}{2\pi} \sum_{\tilde{a}} \int_{x_a}^1 \frac{dz}{z} f_{\tilde{a}/A}(x_a/z, M_f) f_{b/B}(x_b, M_f) \left(C_{a/\tilde{a}}^{(1)}(z) - 2 \ln \frac{M_f b}{b_0} P_{a\tilde{a}}^+(z) \right) \\
&+ \left. \frac{\alpha_s}{2\pi} \sum_{\tilde{b}} \int_{x_b}^1 \frac{dz}{z} f_{a/A}(x_a, M_f) f_{\tilde{b}/B}(x_b/z, M_f) \left(C_{b/\tilde{b}}^{(1)}(z) - 2 \ln \frac{M_f b}{b_0} P_{b\tilde{b}}^+(z) \right) \right] \quad (6.141)
\end{aligned}$$

The A and B coefficients live inside the Sudakov exponential $S(b, Q)$, and can also be expanded to NLO in α_s . Performing the integral over μ in S , while keeping $\alpha_s(\mu) \simeq \alpha_s(M_f)$ to first order, yields logarithms of Qb/b_0 :

$$e^{-S(b, Q)} \simeq 1 - \frac{\alpha_s}{2\pi} \left[2A^{(1)} \ln^2 \frac{Qb}{b_0} + 2B^{(1)} \ln \frac{Qb}{b_0} \right]. \quad (6.142)$$

Multiplying these two expressions and keeping only terms of order 1 or α_s gives an expansion which can be compared with the Fourier transform of the NLO result. It is perhaps easiest to go back a few steps in our NLO derivation to directly transform the regulated $Q_T^{-1+2\epsilon} \ln^m Q_T/Q$ pieces, but the transforms over plus-distributions can be done as well. Either procedure yields the required logs of Qb/b_0 , so that identification of the resummation parameters can proceed. The following integrals are useful in this regard:

$$T_+(x) \equiv \int_0^x \frac{dt}{t} [J_0(t) - 1] + \int_x^\infty \frac{dt}{t} J_0(t) = \ln \frac{b_0}{x} \quad (6.143)$$

$$T_+^{\ln}(x) \equiv \int_0^x \frac{dt}{t} [J_0(t) - 1] \ln t + \int_x^\infty \frac{dt}{t} J_0(t) \ln t = \frac{1}{2} \ln \frac{b_0}{x} \left[2 \ln b_0 - \ln \frac{b_0}{x} \right] \quad (6.144)$$

Since our plus-distributions have been defined with the upper limit p_j , the Fourier transforms we would need are $T_+(bp_j)$ and $T_+^{\ln}(bp_j)$. These give logs of bp_j/b_0 , which

can be expanded into the required logs of bQ/b_0 , plus logs of p_j/Q . Since any finite upper limit to our Q_T -integrals is immaterial, the latter logs should cancel similar logs in the NLO result (those created when the plus-distributions were introduced).

That said, the actual method we will use to extract the resummation parameters is even simpler, and it relies on the fact that in the k_T -space formalism, the transform from b -space back to transverse momentum space has already been done. We still cannot directly compare a finite-order expansion, but we can integrate both the resummed form and the NLO expression up to some arbitrary limit, and *then* expand the former. Beginning with equation 5.26 (without the remainder term \mathcal{R}), we integrate on Q_T^2 up to some p_T^2 :

$$\begin{aligned} \int_0^{p_T^2} dQ_T^2 \sum_{a,b} \hat{\sigma}_0 \frac{d}{dQ_T^2} \left[\dot{f}_a(x_a, Q_T) \dot{f}_b(x_b, Q_T) e^{-S(Q_T, Q)} \right] = \\ \sum_{a,b} \hat{\sigma}_0 \left[\dot{f}_a(x_a, p_T) \dot{f}_b(x_b, p_T) e^{-S(p_T, Q)} - \dot{f}_a(x_a, 0) \dot{f}_b(x_b, 0) e^{-S(0, Q)} \right]. \end{aligned} \quad (6.145)$$

Since the Sudakov exponent goes like $S \sim \sum_m \ln^m Q/Q_T$, taking $Q_T \rightarrow 0$ kills the second term above, and we're left with only the first term, which, when expanded, gives

$$\begin{aligned} \int_0^{p_T^2} dQ_T^2 d\sigma^S \simeq \sum_{a,b} \hat{\sigma}_0 \left[f_{a/A}(x_a, M_f) f_{b/B}(x_b, M_f) \right. \\ + \frac{\alpha_s(M_f)}{2\pi} \sum_{\tilde{a}} \int_{x_a}^1 \frac{dz}{z} f_{\tilde{a}/A}\left(\frac{x_a}{z}, M_f\right) f_{b/B}(x_b, M_f) \left(C_{a/\tilde{a}}^{(1)}(z) - 2 \ln \frac{M_f}{p_T} P_{a\tilde{a}}^+(z) \right) \\ + \frac{\alpha_s(M_f)}{2\pi} \sum_{\tilde{b}} \int_{x_b}^1 \frac{dz}{z} f_{a/A}(x_a, M_f) f_{\tilde{b}/B}\left(\frac{x_b}{z}, M_f\right) \left(C_{b/\tilde{b}}^{(1)}(z) - 2 \ln \frac{M_f}{p_T} P_{b\tilde{b}}^+(z) \right) \\ \left. - \frac{\alpha_s(M_f)}{2\pi} \left[2A^{(1)} \ln^2 \frac{Q}{p_T} + 2B^{(1)} \ln \frac{Q}{p_T} \right] \right]. \end{aligned} \quad (6.146)$$

To this we must compare the integral of the NLO expression. As can be seen in equation 6.139, we'll need only three integrals to perform this task. They are:

$$\begin{aligned}
\int_0^{p_T} dQ_T \delta(Q_T) &= 1 \\
\int_0^{p_T} dQ_T \left[\frac{1}{Q_T} \right]_+ &= -\frac{1}{2} \ln \frac{M_f^2}{p_T^2} + \frac{1}{2} \ln \frac{M_f^2}{p_j^2} \\
&= -\frac{1}{2} \ln \frac{Q^2}{p_T^2} + \frac{1}{2} \ln \frac{Q^2}{p_j^2} \\
\int_0^{p_T} dQ_T \left[\frac{\ln Q_T/Q}{Q_T} \right]_+ &= \frac{1}{8} \ln^2 \frac{Q^2}{p_T^2} - \frac{1}{8} \ln^2 \frac{Q^2}{p_j^2}.
\end{aligned} \tag{6.147}$$

Note that the coefficients of the plus-distributions we've used are constant, and these distributions were defined with an upper limit p_j . The integral from 0 to p_j is therefore zero; the logs appearing in equations 6.147 arise solely from the integral from p_j to p_T .

Applying these expressions to equation 6.139, followed by comparison with equation 6.146, yields the following resummation parameters:

$$\begin{aligned}
A^{(1)} &= \sum_{mn} A_{mn} \\
B^{(1)} &= \sum_{mn} B_{mn} \\
C_{a/\bar{a}}^{(1)} &= \sum_{mn} \left[\delta_{a\bar{a}} \delta(1-z) \left(\frac{\delta C_{mn}}{2} + \frac{A_{mn}}{4} \ln^2 \frac{Q^2}{p_j^2} + \frac{B_{mn}}{2} \ln \frac{Q^2}{p_j^2} \right) + \bar{a} C_{mn} \right] \\
&\quad + \sum_{mn} P_{a\bar{a}}^+ \left[{}_a D_{mn} \ln \frac{M_f^2}{p_j^2} + (1 - {}_a D_{mn}) \ln \frac{M_f^2}{p_T^2} \right] \\
C_{b/\bar{b}}^{(1)} &= \sum_{mn} \left[\delta_{b\bar{b}} \delta(1-z) \left(\frac{\delta C_{mn}}{2} + \frac{A_{mn}}{4} \ln^2 \frac{Q^2}{p_j^2} + \frac{B_{mn}}{2} \ln \frac{Q^2}{p_j^2} \right) + \bar{b} C_{mn} \right] \\
&\quad + \sum_{mn} P_{b\bar{b}}^+ \left[{}_b D_{mn} \ln \frac{M_f^2}{p_j^2} + (1 - {}_b D_{mn}) \ln \frac{M_f^2}{p_T^2} \right].
\end{aligned} \tag{6.148}$$

Note that delegation of the A_{mn} , B_{mn} , and δC_{mn} coefficients to one or the other leg (a or b) is arbitrary; we have chosen to assign half to each leg. We choose in this dissertation to resum only initial-state (IS) pieces, and for these, ${}_a D_{mn} = {}_b D_{mn} = 1$, so the $\ln M_f^2/p_T^2$ term drops in the above. Final-state (FS) pieces are left in the NLO

form shown in the last section. From here on out, we will make a distinction among the following four types of contributions:

$$\begin{aligned} d\sigma &= d\sigma_{IS}^{sing} + d\sigma_{IS}^{finite} \\ &+ d\sigma_{FS}^{sing} + d\sigma_{FS}^{finite} . \end{aligned} \quad (6.149)$$

$d\sigma^{sing}$ are the (regulated) asymptotic approximations. $d\sigma^{finite}$ are the finite corrections (compare equation 6.136). Resummation will be performed on only the first term, and afterwards we will call it $d\sigma_{IS}^{Resum}$. The initial/final distinction cannot be applied to virtual terms; we make the choice to include them in $d\sigma_{IS}^{sing}$, where they show up in the CSS $C^{(1)}$ pieces.

Note also that in this transverse momentum space comparison, we again obtain the logs of Q/p_j mentioned above. As the δC_{mn} pieces already contain logs of p_j/M_f , addition of the new logarithms serves to produce p_j -independent $C^{(1)}$ -parameters, as expected. The new $D_{mn}P^+ \ln(M_f^2/p_j^2)$ terms also serve to cancel corresponding terms in ${}_a C_{mn}$ and ${}_b C_{mn}$.

Finally, a word on free variables: references to b -space and k_T -space resummed expressions usually assume the set of free variables $\{Q, y, Q_T, \phi_q, \cos \theta_{\text{CSS}}, \phi_{\text{CSS}}\}$, in which Q^2 and ϕ_q are the mass and azimuthal angle of the observed particle pair, and $\{\theta_{\text{CSS}}, \phi_{\text{CSS}}\}$ the direction of one of the particles in a specific 2-body rest frame. We, of course, are using a different set of variables, namely $\{y_\gamma, p_j, y_j, \phi_j, Q_T, \phi_q\}$, but given the existence of a nonsingular Jacobian between these two sets of variables (as there must be), there is sufficient justification to write the resummed result with either set of variables. ⁵

⁵Once the CSS coefficients are found, Monte-Carlo coding of the resummed piece proceeds as given by the CSS formalism, in which the upper limit on Q_T is the γj pair mass Q (which $= \sqrt{2p_j^2(1 + \cosh(y_\gamma - y_j))}$ in our variables), not the limit given by the theta function $\theta(p_j - Q_T)$ at NLO. The question of whether this constitutes double-counting, or is physically justified given the **multiple** emission being described, will be discussed in a future work.

6.6 Matching Resummed and Fixed-Order Results

Depending on the quality of the approximations used in defining the resumable asymptotic piece $d\sigma_{IS}^{sing}$, there is no guarantee that it will continue to be a useful quantity at high pair Q_T , either before or after resummation. In fact, it may even become negative: looking at the resummed k_T -space expression of equation 5.29, one can see that as Q_T gets bigger, both the Sudakov and non-perturbative exponentials tend to one, while their derivatives tend to zero. This leaves only a term proportional to the derivative of the parton distributions with respect to scale. According to the Altarelli-Parisi equations, this contribution (and thus $d\sigma_{IS}^{Resum}$) will be negative for all but the smallest momentum fractions (see figure 6.3).

On the other hand, the 3-body perturbative piece (that is, the unregulated NLO result) is fine in the high- Q_T region. The act of resumming its logs of Q/Q_T should only make a difference in the low- Q_T region.

One is thus forced to make a switch from the resummed piece $d\sigma_{IS}^{Resum}$ to the perturbative 3-body piece at some value of Q_T (see figure 6.4). The best method is still a matter of debate. Remember that in $d\sigma_{IS}^{finite}$ there live both the perturbative 3-body result and a 3-body asymptotic approximation thereof. The resummed piece is a regulated and exponentiated version of the latter, and if the resummation procedure leaves its high- Q_T behavior significantly unchanged from the asymptotic approximation on which it is based, there is hope that cancellation will occur between these pieces, leaving only the perturbative piece. If not, then this cancellation will require a little help.

Kauffman [81] proposed inclusion of a function $f(Q_T)$ to smoothly force this cancellation as Q_T becomes greater than some arbitrary *matching value* Q_T^{match} . That is,

$$d\sigma \simeq f(Q_T, Q_T^{match})(\text{Resummed} - \text{Asymptotic}) + \text{Perturbative} , \quad (6.150)$$

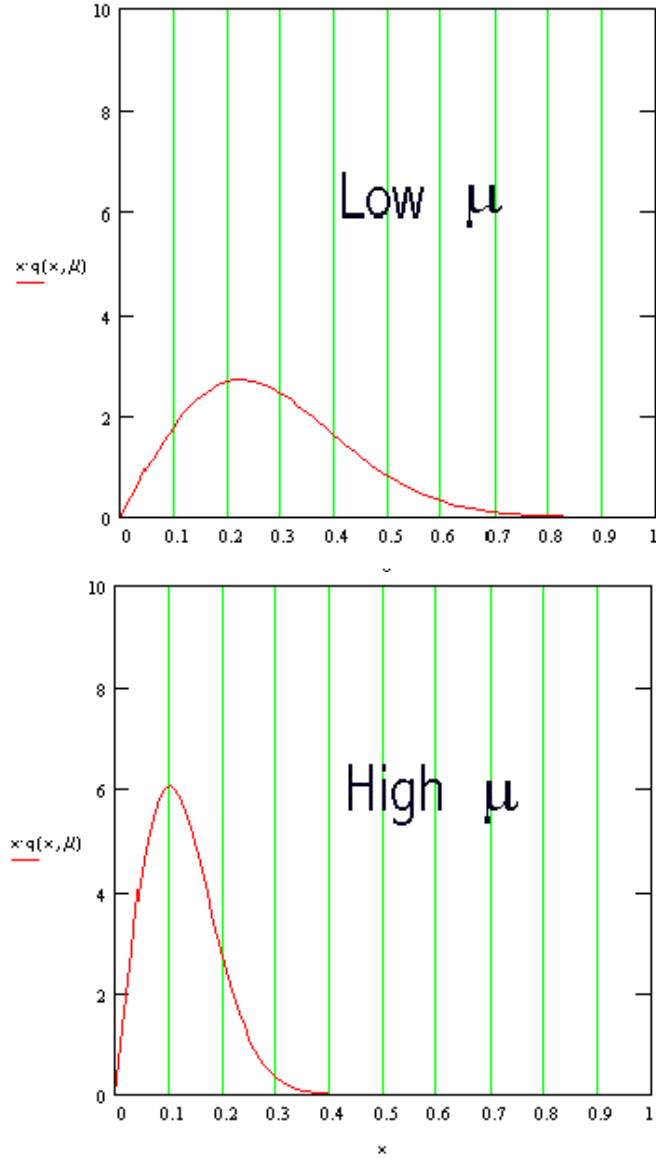


Figure 6.3. Scale dependence of parton distributions.

where, it was suggested, an appropriate function might be

$$f(Q_T, Q_T^{\text{match}}) = \frac{1}{1 + \left(\frac{Q_T}{Q_T^{\text{match}}}\right)^4} . \quad (6.151)$$

This allows all contributions to do their job at low Q_T , but shuts off the resummed and asymptotic contributions at high- Q_T .

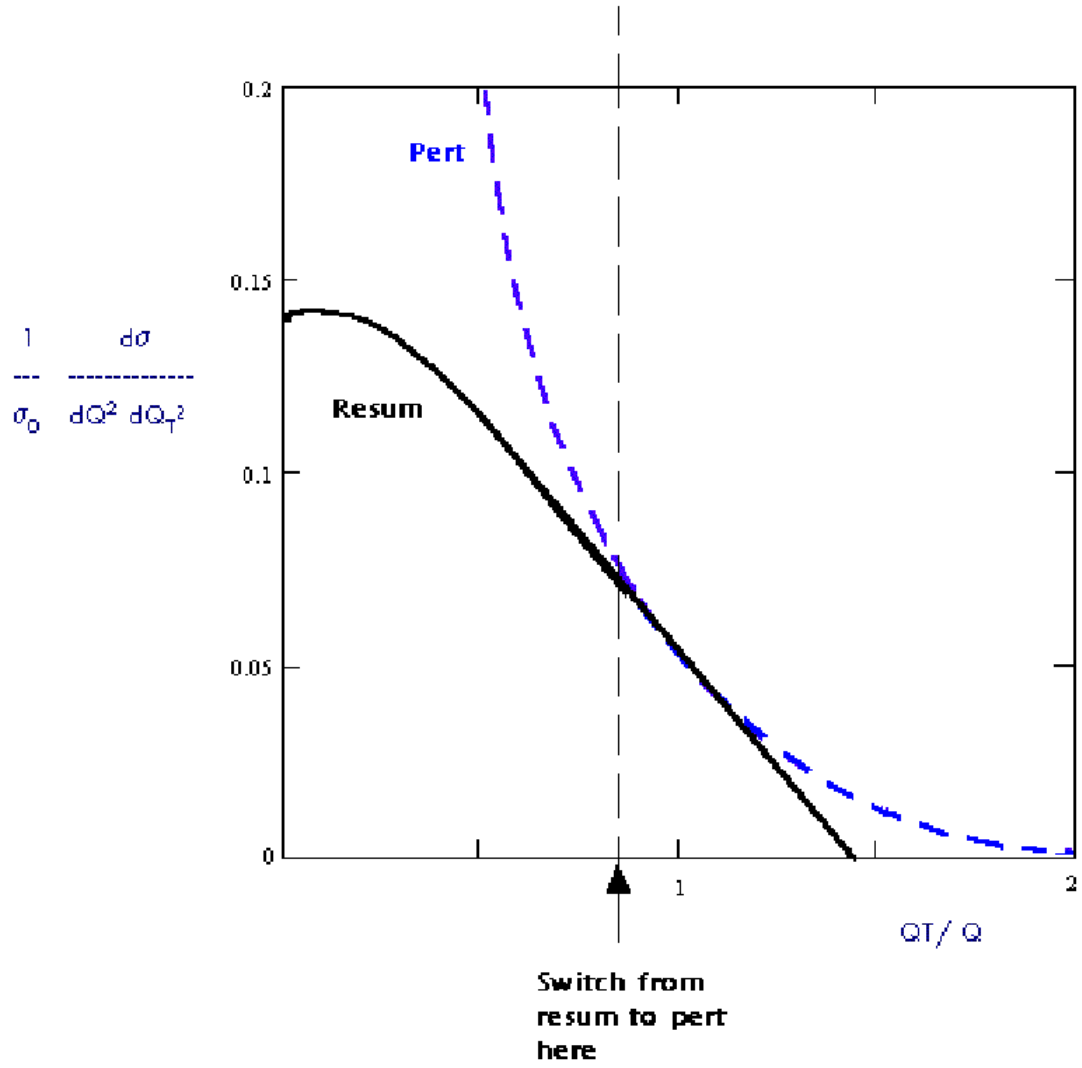


Figure 6.4. Fixed-order perturbative result better at high Q_T .

Of course, it remains to determine Q_T^{match} , and it is by no means certain that one particular value will suffice for all circumstances. If one's desired output is a single Q_T -distribution at fixed pair mass and rapidity, it may be easy to determine the optimum value by trial and error; better would be to histogram each piece separately and, after the full run, pick a Q_T -value at which the resummed and perturbative pieces most closely agree, then drop all higher- Q_T resummed and asymptotic contributions.

The procedure we will use in this dissertation allows the kinematics of the particular incoming state to determine the proper cutoff (as opposed to a fixed Q_T^{match}). However, it does so only by allowing one distribution to be binned at a time.

That is, we assume an output consisting of a single one-dimensional histogram, the ordinate of which we will here label x . Given a domain and step size in x , we have then a defined number N of bins in x .

1. For each x -bin, we construct a two dimensional array in Q and Q_T (up to $\sqrt{S}/2$ each). Thus in effect we have a 3-dimensional array in x , Q , and Q_T .
2. Proceeding with Monte-Carlo evaluation of $d\sigma^{\text{resum}}$, we fill this 3-D array with weights.
3. We then collapse (integrate over x) this array into a 2-D array in Q and Q_T only. For each Q -value, we start at $Q_T = 0$ and go up in Q_T until we see the x -integrated weight dip below zero. This will define a cutoff $Q_T^{\text{match}}(Q)$ for each value of Q . That is, for each Q , all bins above this Q_T -value are set to zero in the original 3-D array, for all x .
4. The original 3-D array may now be integrated over Q and Q_T to determine the proper $d\sigma_{IS}^{\text{Resum}}$ for each x .
5. The array of cutoffs $Q_T^{\text{match}}(Q)$ is now used in the subsequent evaluation of the 3-body weights ($d\sigma^{\text{finite}}$). As each 3-body point is generated, Q and Q_T are calculated for this point, and if $Q_T > Q_T^{\text{match}}$ for that Q , the asymptotic weight is not calculated, leaving only the perturbative.

This procedure, while it has its limitations, nevertheless respects the approximations in their regions of accuracy, while not forcing a unique matching Q_T .

However, for the sake of relative simplicity, we're not using the optimum cutoff criterion mentioned above, which would be to compare the resummed cross-section to the perturbative, and perform the cutoff at the Q_T value at which they most closely agree. This would require additional arrays and introduction of some sort of

tolerance parameter. It could be done, but the results we've been able to achieve with the present system don't reveal any need for the additional overhead.

In fact, at high enough hadronic-to-partonic energy ratios (low momentum fraction), the resummed piece goes smoothly to zero (without going negative) at high Q_T , and matching procedures of any sort are not required. The above procedure alters nothing in this case; by contrast, a fixed- Q_T^{match} procedure would kick in anyway.

CHAPTER 7

RESULTS AND CONCLUSIONS

7.1 Photon p_T Distributions

The direct photon p_T spectrum is probably the easiest test of our formalism, as there are data, and no correlations with jets to consider. We begin with results at collider energies, and end with lower energy fixed-target results. We use the k_T -space resummation formalism alone, at first, and use the nonperturbative parameters $\tilde{a} = 0.3\text{GeV}^{-2}$ and $k_{Tlim} = 4\text{GeV}$ for each subprocess. A discussion of these parameters, and why we may want to use different fits for different subprocesses, will follow in the next section.

In figure 7.1, we show four curves: The LO contribution, the NLO results, and finally resummed results using the k_T formalism, both with and without matching. Data are from the Fermilab D0 experiment [82]. The process studied is $p\bar{p} \rightarrow \gamma + X$ at $\sqrt{S} = 1800\text{GeV}$, with the photon rapidity constrained at $|y_\gamma| \leq 0.9$ and factorization scale $M_f = p_\gamma$, where p_γ is the transverse momentum of the photon. There is also an isolation cut on the photon, which rejects events with a jet of energy $p_j > 2\text{GeV}$ within $R \equiv \sqrt{(y_\gamma - y_j)^2 + (\phi_\gamma - \phi_j)^2} \leq 0.4$ of the photon.

In figure 7.2, we show the same four curves, this time at the lower energy $\sqrt{S} = 38.7\text{GeV}$, and for the quantity $E_\gamma d^3\sigma/d^3p_\gamma$, the invariant cross section, as opposed to $d^2\sigma/dp_\gamma dy_\gamma$. Data are from the Fermilab E706 experiment [83]. The process is $pBe \rightarrow \gamma + X$, with the photon rapidity constrained at $-1.0 \leq y_\gamma \leq 0.5$.

Notable here is the effect of our matching prescription (described in Section 6.6), which cuts out the poor high- Q_T behavior of the resummed and asymptotic

pieces. At $p_\gamma \approx 3\text{GeV}$, the incoming partons' momentum fractions are on the order $x \approx 2p_\gamma/\sqrt{S} \approx 0.2$, but as one approaches $p_\gamma \approx 6.5 \sim 12.0\text{GeV}$, these fractions reach $x \approx 0.4 \sim 0.8$, and in this range, the derivative of the parton distributions (which is dominant in the resummed piece at high- Q_T) is negative. In contrast, matching at the higher energy $\sqrt{S} = 1800\text{GeV}$ is not an issue, as the momentum fractions concerned rarely go above $x \approx 0.13$.

For completeness, we repeat the trials at the still lower energy $\sqrt{S} = 31.5\text{GeV}$ (see figure 7.3). Data here are also from the Fermilab E706 experiment [83]. The process is $pBe \rightarrow \gamma + X$, with the photon rapidity constrained at $|y_\gamma| \leq 0.75$. For all these curves, the factorization scale $M_f = p_\gamma$ is used, and the parton distributions are those of the CTEQ Collaboration, specifically CTEQ5M [84].

$p \bar{p} \rightarrow \gamma + X$ at $\sqrt{s}=1800$ GeV

$-0.9 < y_\gamma < 0.9$

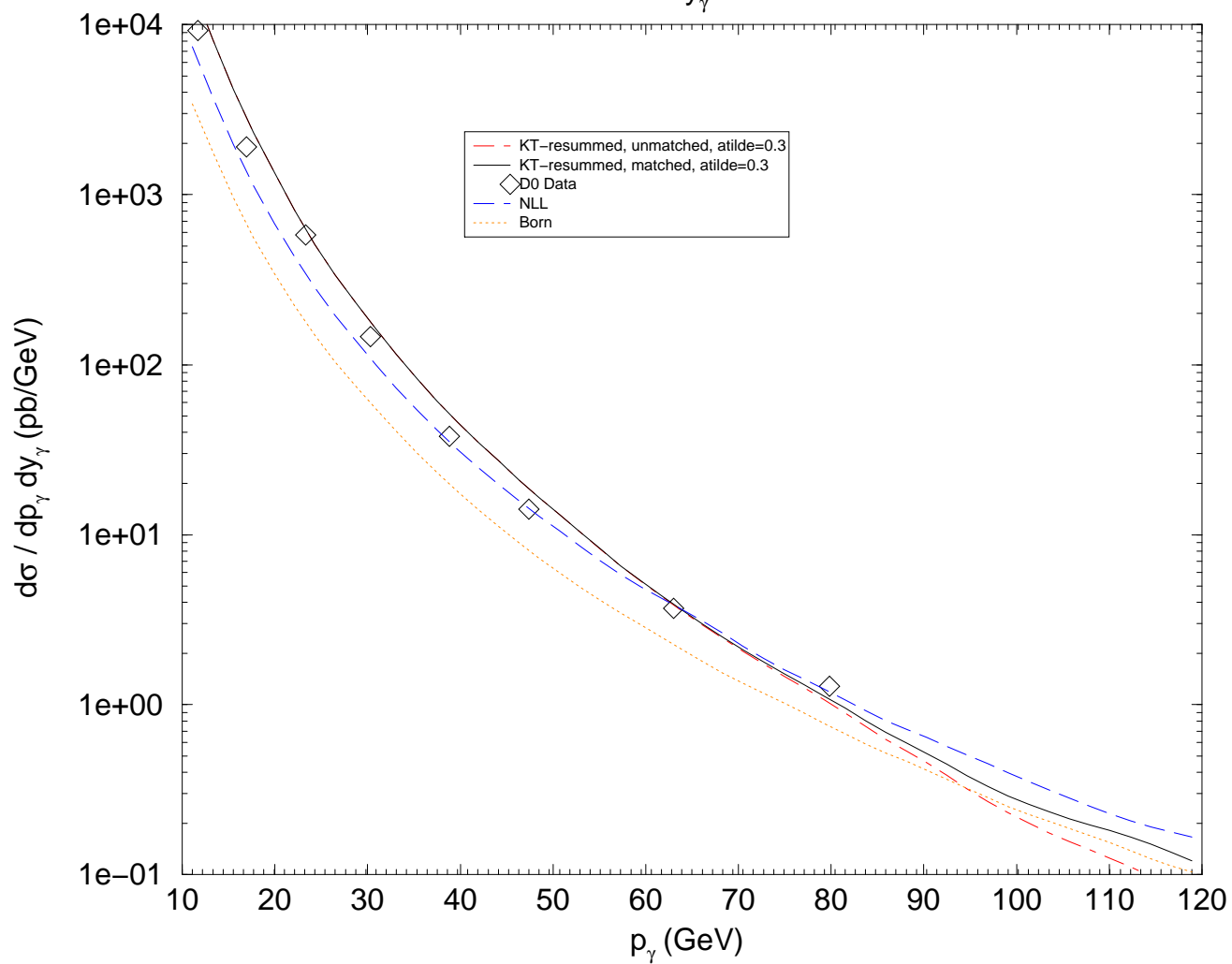


Figure 7.1. $p\bar{p} \rightarrow \gamma + X$ at $\sqrt{s} = 1800$ GeV.

$p \text{ Be} \rightarrow \gamma + X$ at $\sqrt{s}=38.7 \text{ GeV}$

$-1.0 < y_\gamma < 0.5$

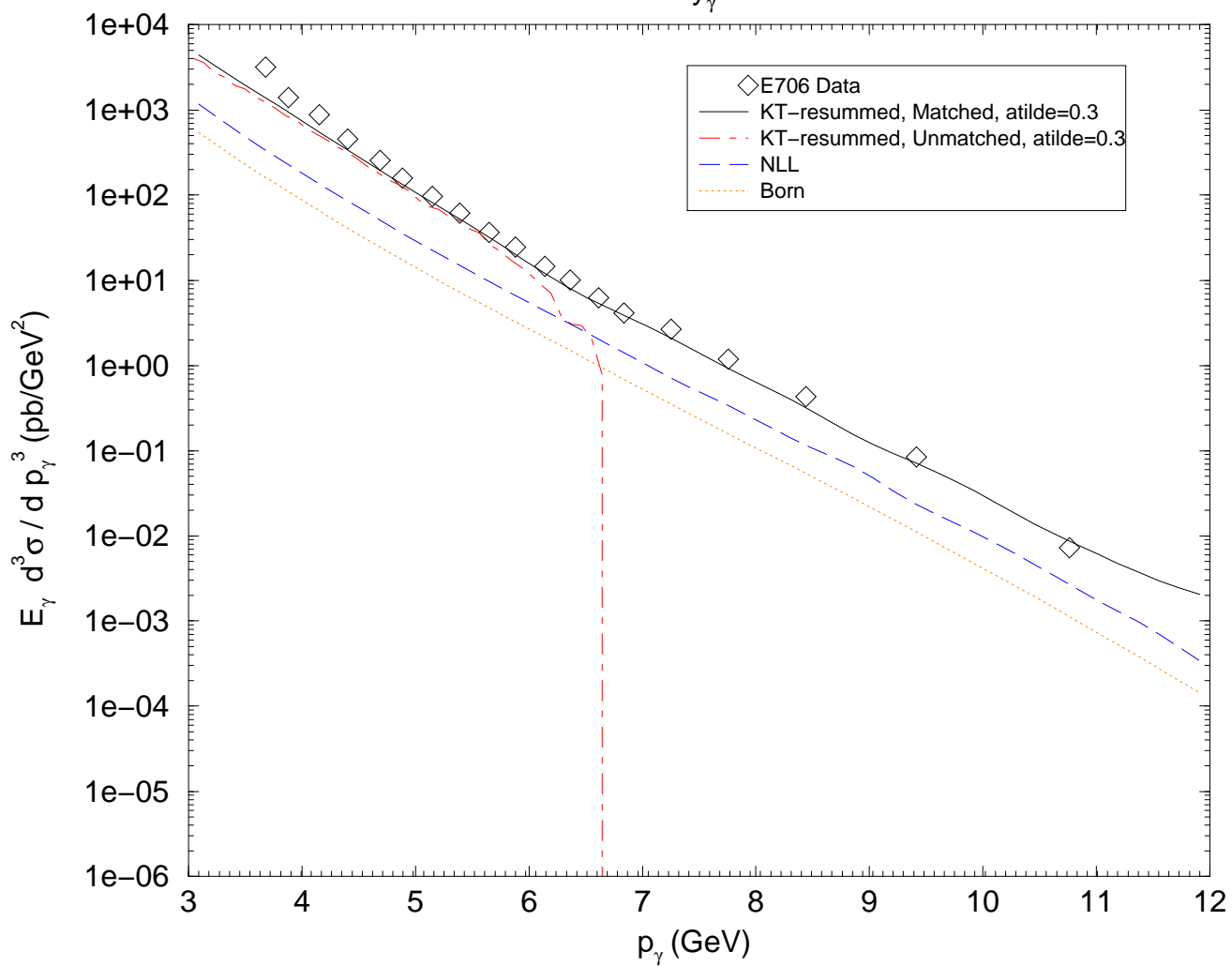


Figure 7.2. $p\text{Be} \rightarrow \gamma + X$ at $\sqrt{s} = 38.7 \text{ GeV}$.

$p \text{ Be} \rightarrow \gamma + X$ at $\sqrt{s}=31.5 \text{ GeV}$

$-0.75 < y_\gamma < 0.75$

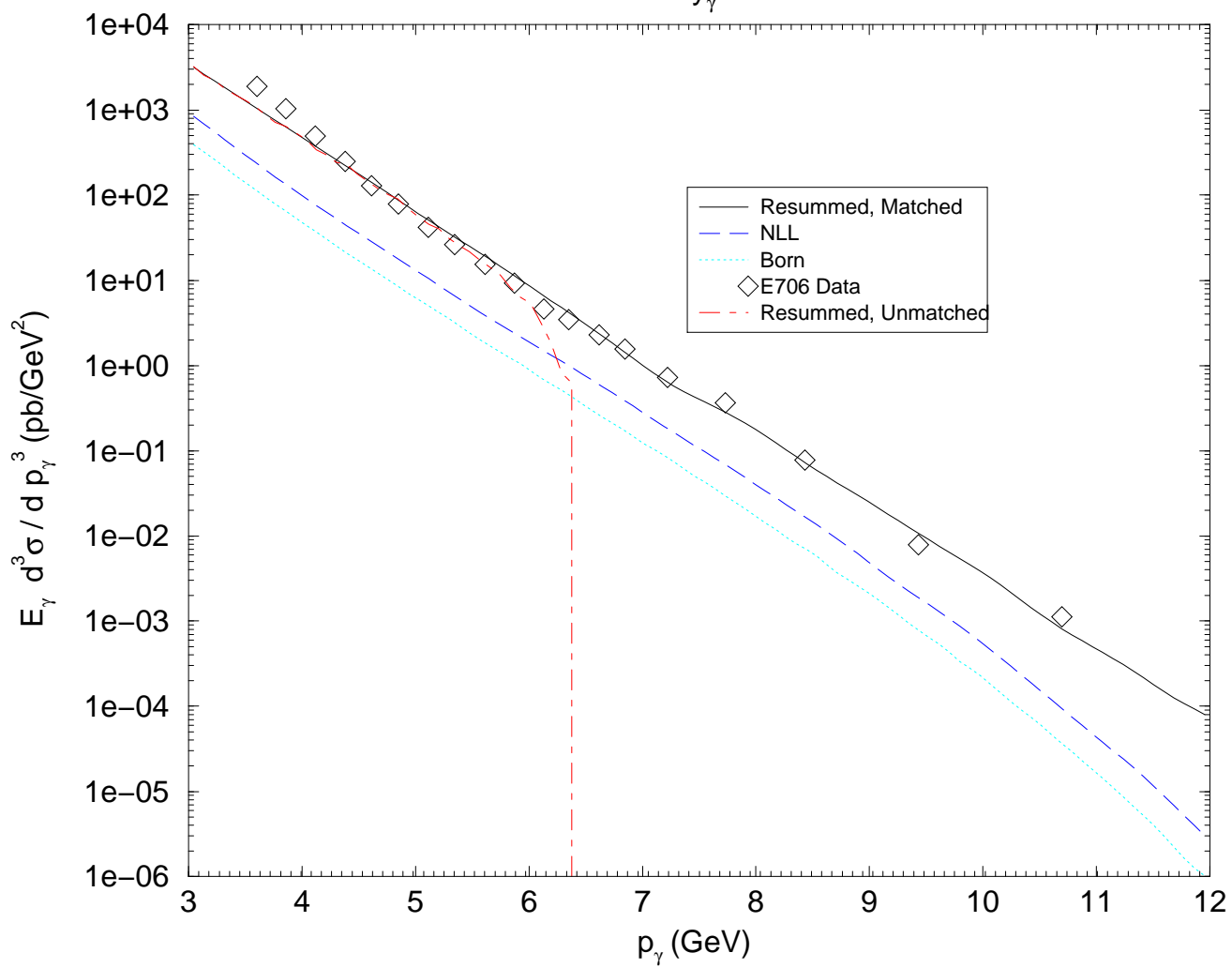


Figure 7.3. $p\text{Be} \rightarrow \gamma + X$ at $\sqrt{s} = 31.5 \text{ GeV}$.

7.1.1 Nonperturbative Parameter Choices

As the lower-energy results are much more sensitive to changes in the nonperturbative parameters, we focus exclusively on comparison with the E706 results at $\sqrt{S} = 31.5\text{GeV}$.

In the plots discussed above, the k_T -space resummation formalism was utilized exclusively. In accordance with the work of Ellis and Veseli [77], this includes a nonperturbative factor of the form

$$F_{NP}(Q_T) = 1 - e^{-\tilde{a}Q_T^2} . \quad (7.1)$$

Besides \tilde{a} , there is also a second nonperturbative parameter, k_{Tlim} , which controls the boundary between perturbative and nonperturbative regions. We use a value $k_{Tlim} = 4\text{GeV}$, but changes of up to 50% in this parameter have little effect, as can be seen in figure 7.4. Thus, for the balance of this argument, we will think of the k_T -space method as having effectively a single-parameter nonperturbative form.

Starting with a value of $\tilde{a} = 0.3\text{GeV}^{-2}$, figure 7.5 shows the effect of raising and lowering \tilde{a} as k_{Tlim} is held fixed. As can be seen here and in the previous plots, our initial value works well with available data, but the results are significantly dependent upon the precise value at low \sqrt{S} .

Figure 7.4. k_T -space resummation : k_{Tlim} -dependence.

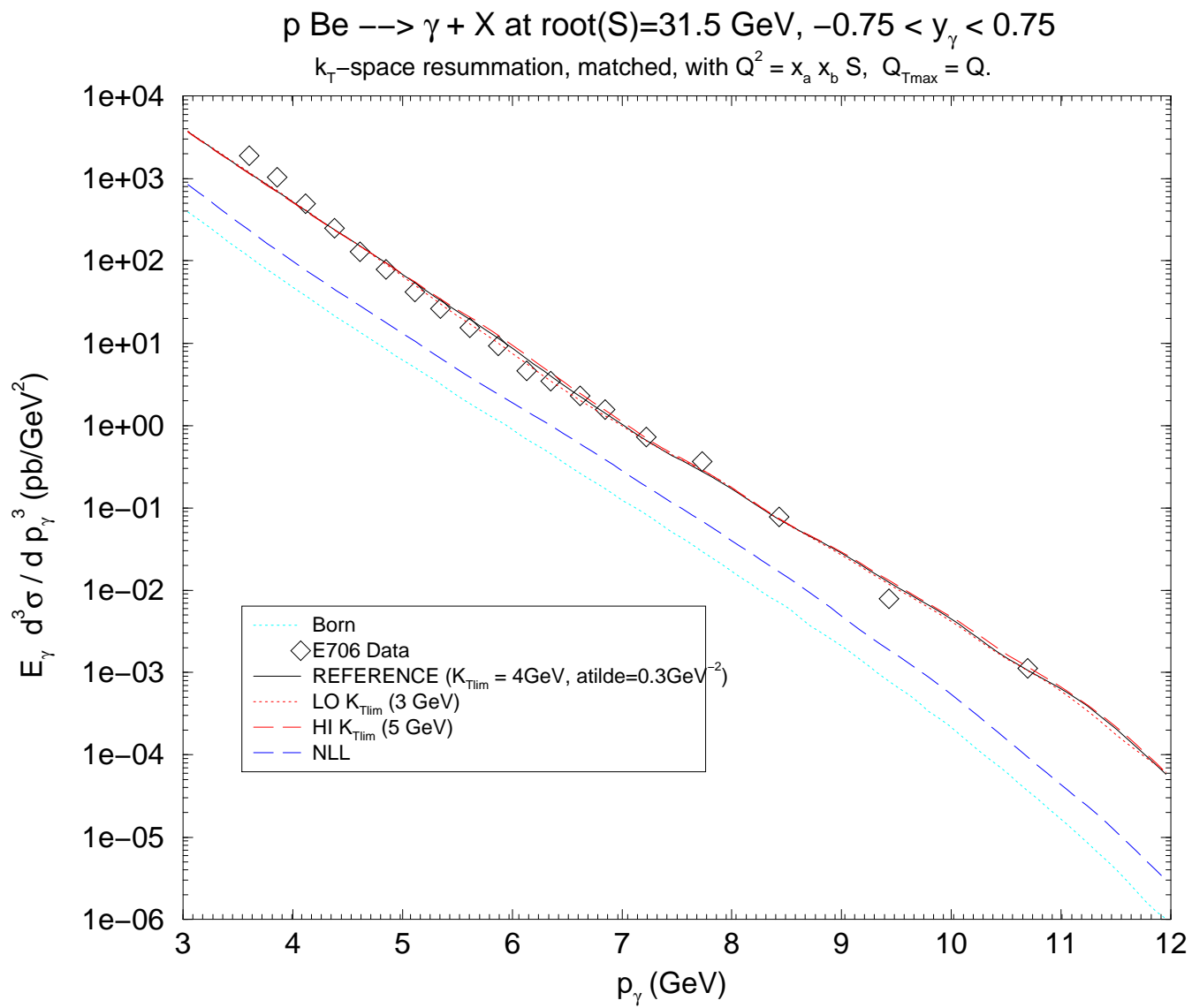
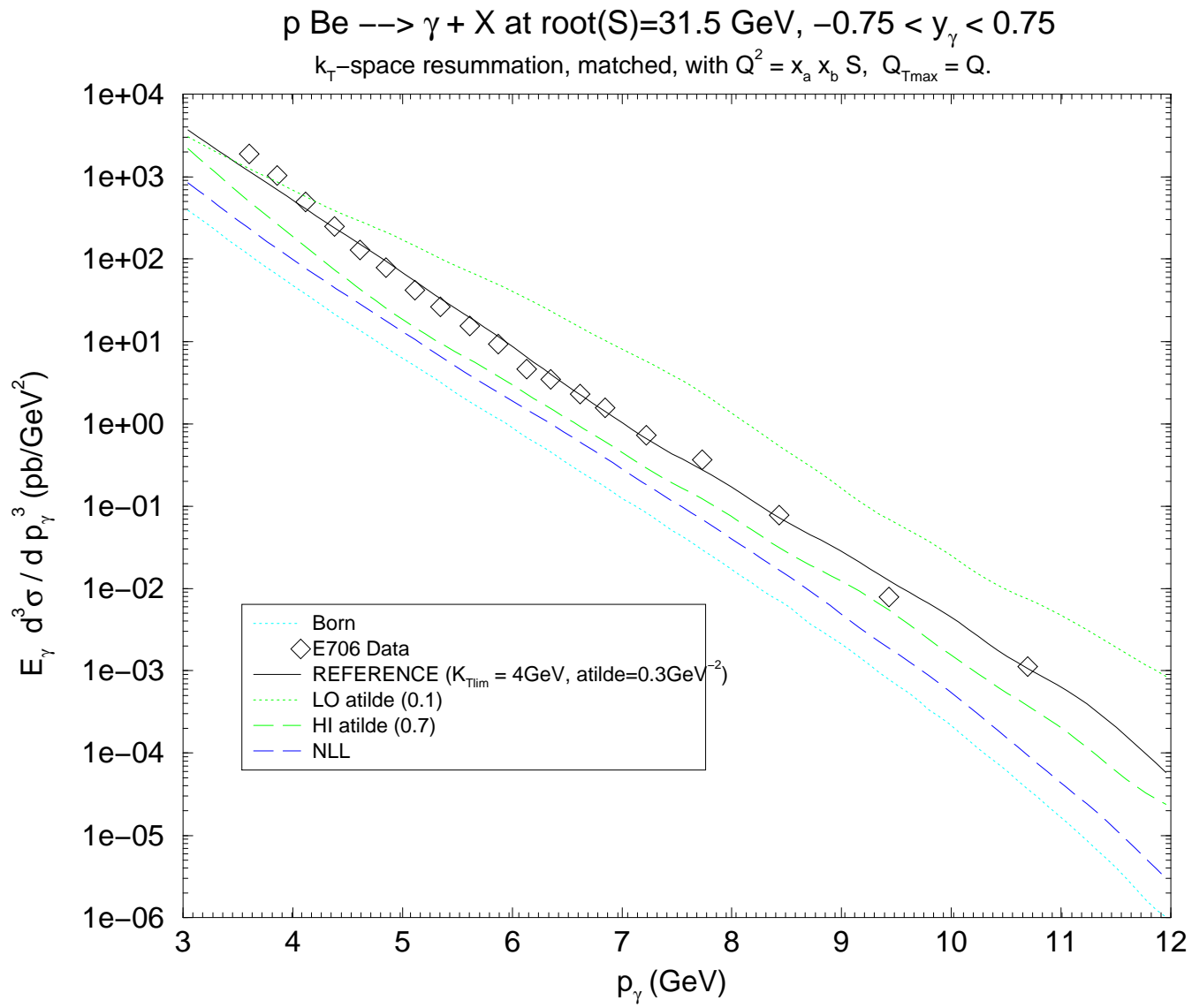


Figure 7.5. k_T -space resummation : $\tilde{\alpha}$ -dependence.



This being the case, it is important to compare these k_T -space results with the predictions given by the b -space formalism, the parameters of which are, ostensibly, better known. Using the b -space CSS formalism of Chapter 4, and the Sudakov parameters calculated in Chapter 6, figure 7.6 shows the Born, NLO, and resummed theoretical results compared with data. For the resummed curve, the 2-parameter nonperturbative model of Landry, Brock, Ladinsky, and Yuan (LBLY) [71] is used, with their best-fit parameters $g_1 = 0.24\text{GeV}^2$ and $g_2 = 0.34\text{GeV}^2$.

Figures 7.7 and 7.8 show, respectively, the result of altering g_1 and g_2 by 50% each. As can be seen from the parametrization

$$F_{NP}(b, Q) = \exp\left[-b^2\left(g_2 \ln \frac{Q}{2Q_0} + g_1\right)\right], \quad (7.2)$$

raising either g_1 or g_2 dampens out more of the high- b region, thereby broadening the Q_T spectrum, and consequently raising the average recoil momentum.

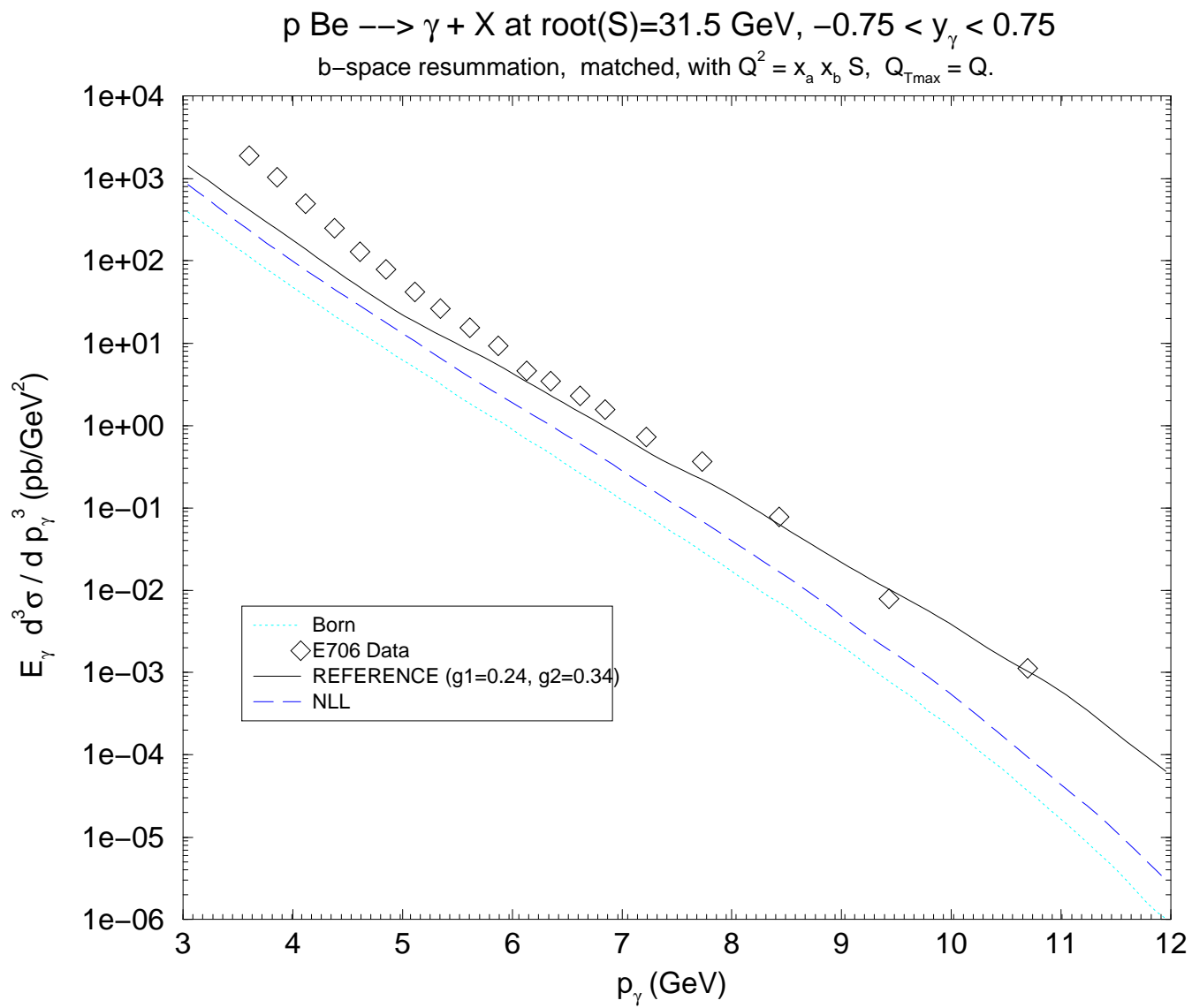


Figure 7.6. b -space resummation : reference distribution.

Figure 7.7. b -space resummation : g_1 dependence.

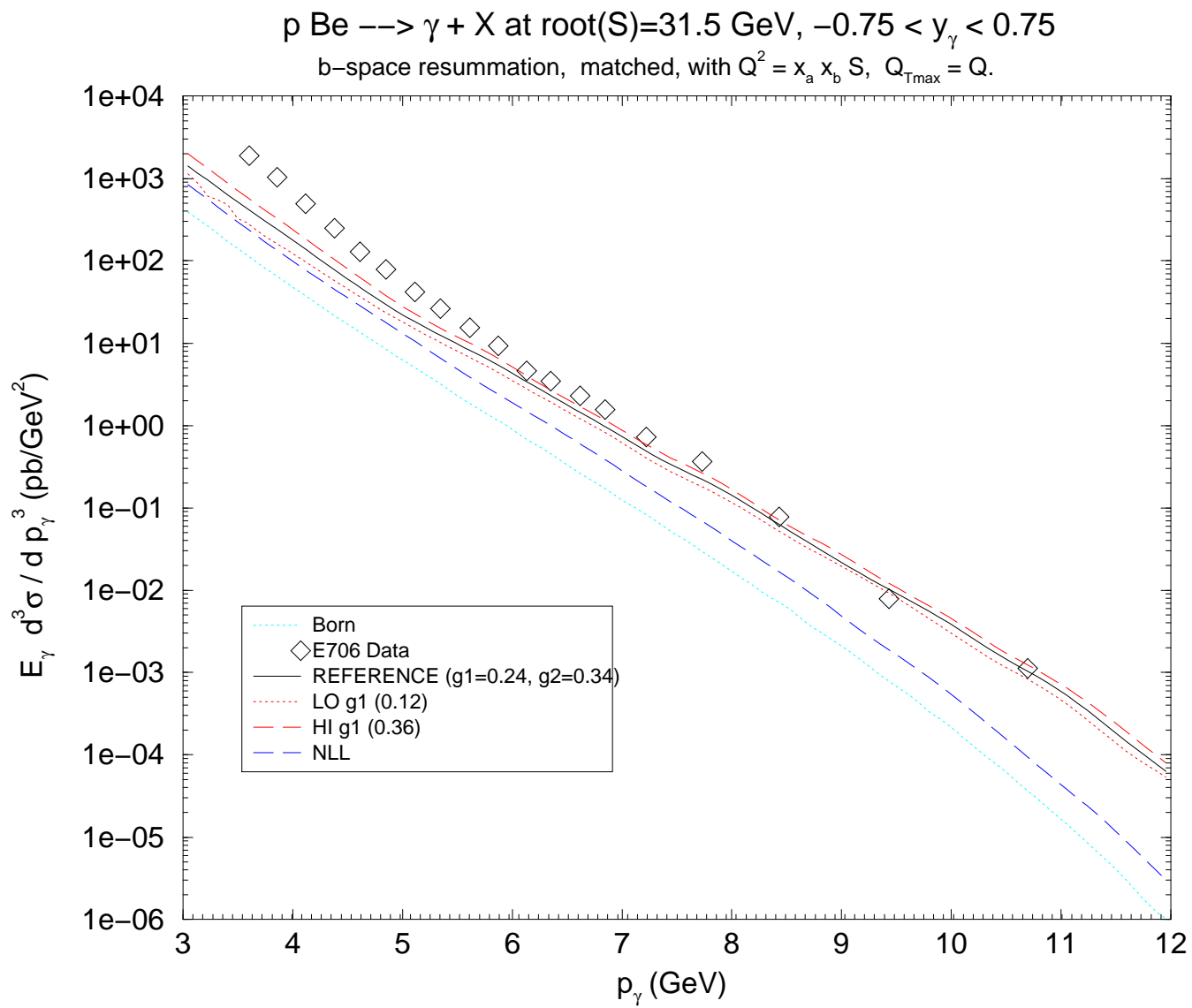
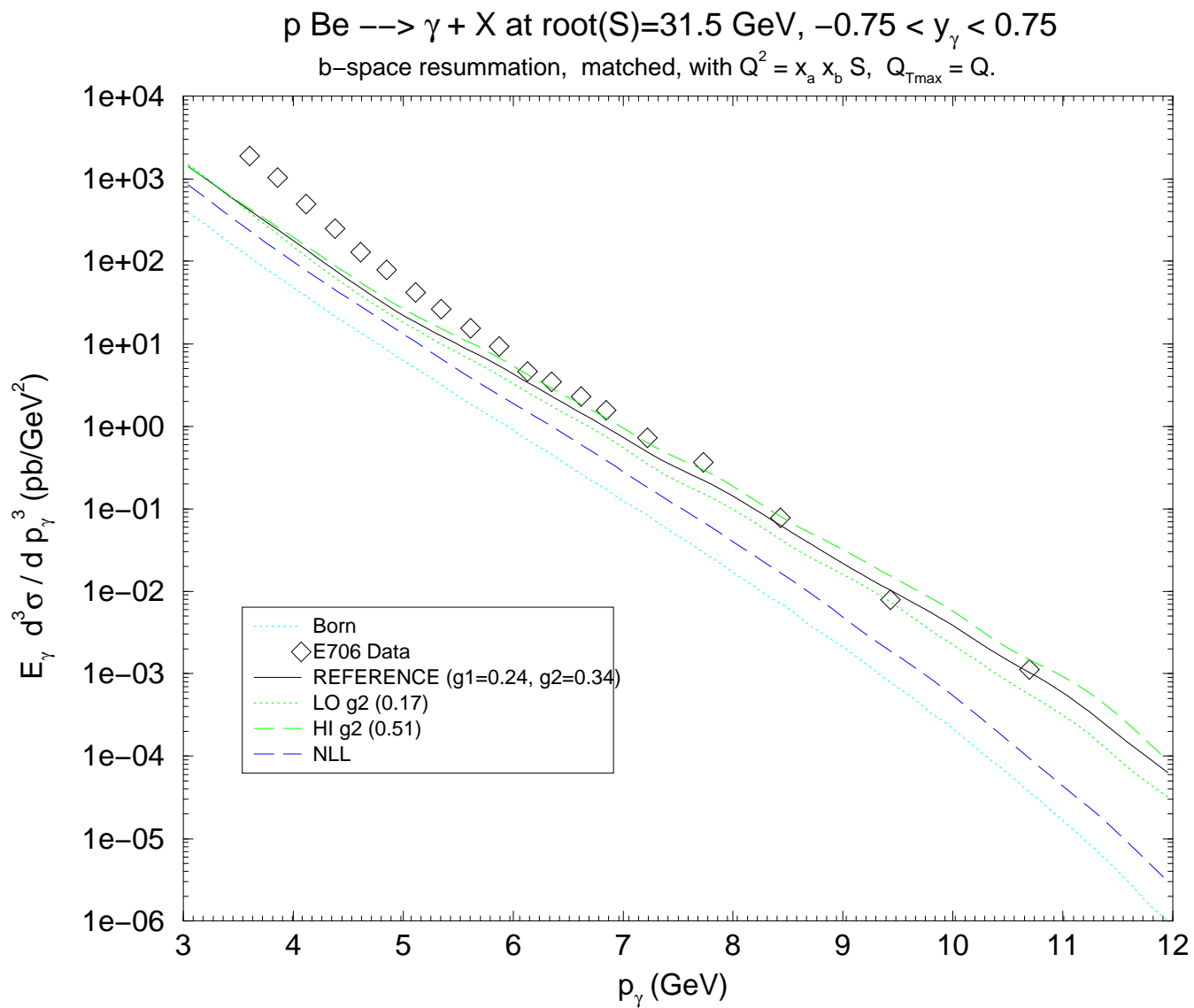


Figure 7.8. b -space resummation : g_2 dependence.



Unfortunately, none of these curves agrees as well with the data as does the single-parameter, Q -independent k_T -space result. The first question to be answered, then, is whether the difference lies entirely in the Q -dependence of the b -space parametrization. To do this, we first look at the approximate analytical relation between each parameter set and the average Q_T “kick” given to the system.

For example, in the b -space model, to first order in α_s we are resumming only the Born terms, and the b -dependence of the Fourier integrand is simply that of the nonperturbative exponential, which we write as simply $\exp(-gb^2)$. Then,

$$\begin{aligned}\frac{d\sigma}{dQ_T} &\sim \frac{2Q_T}{2\pi} \int d^2b e^{i\vec{b}\cdot\vec{Q}_T} e^{-gb^2} \\ &= 2Q_T \int db b J_0(bQ_T) e^{-gb^2} \\ &= \frac{Q_T}{g} e^{-Q_T^2/4g},\end{aligned}\tag{7.3}$$

which has a maximum at $\langle Q_T \rangle = \sqrt{2g}$.

In the k_T -space model, we have

$$\begin{aligned}\frac{d\sigma}{dQ_T} &\sim 2Q_T \frac{d}{dQ_T^2} [1 - e^{-\tilde{a}Q_T^2}] \\ &= 2Q_T \tilde{a} e^{-\tilde{a}Q_T^2},\end{aligned}\tag{7.4}$$

which peaks at $\langle Q_T \rangle = 1/\sqrt{2\tilde{a}}$. Equating these two results gives a simple relation $g\tilde{a} = 1/4$ which we can use to test the effect of the Q -dependence in g .

Figure 7.9 shows the result of a k_T -space run with $\tilde{a} = 1/(4g)$ superimposed upon a b -space run of the canonical two-parameter form $g(Q) = g_2 \ln \frac{Q}{2Q_0} + g_1$. One can see that adding the Q -dependence to \tilde{a} reproduces the b -space result. Conversely, as shown in figure 7.10, **removing** the Q -dependence by fixing $g = 1/(4\tilde{a})$ also results in agreement between the b and k_T -space formalisms.

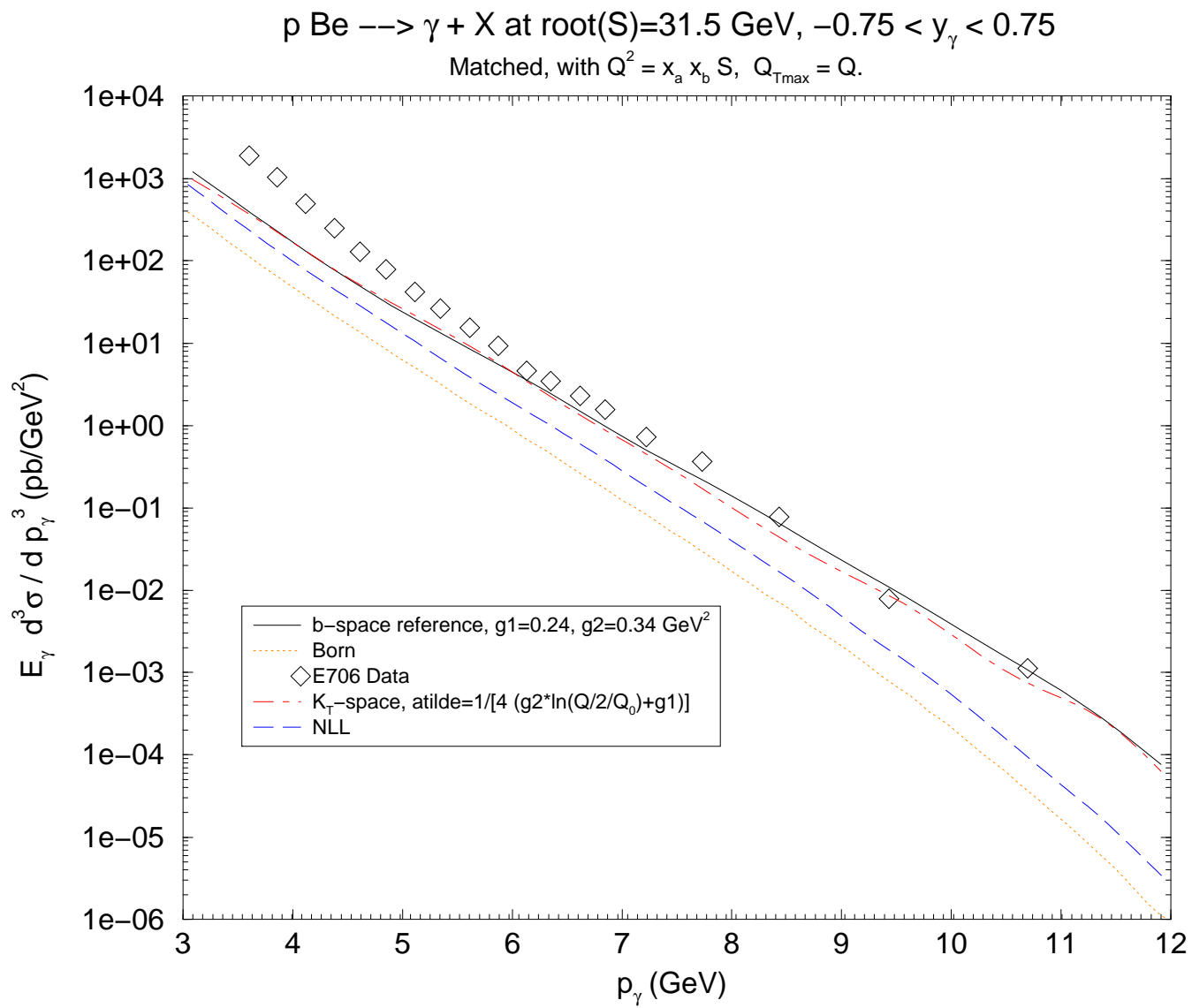


Figure 7.9. Adding Q -dependence to k_T -space NP form.

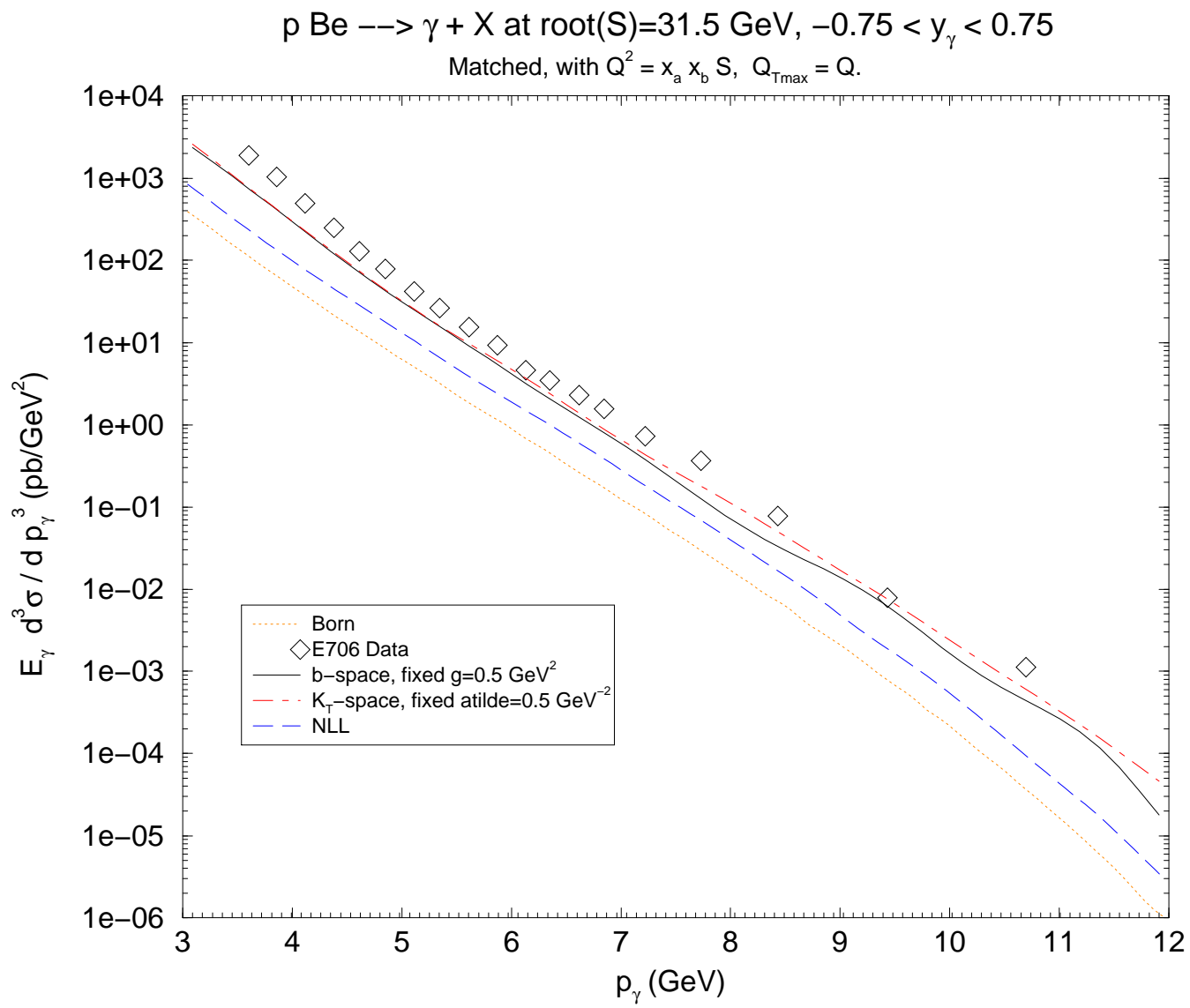


Figure 7.10. Removing Q -dependence from b -space NP form.

The next question is whether a Q -dependent form is truly required by the existing data, and for that to be answered we must look at the application of resummation methods to intermediate vector boson production, *e.g.* Drell-Yan processes, which comprise the bulk of the data upon which the current nonperturbative fits have been based.

By simply swapping out our direct photon CSS parameters $\{A_i, B_i, C_i\}$ for those calculated by Ellis, Ross, and Veseli [73] or Balázs and Yuan [85], we can begin comparing resummed theory to data for dimuon production, as was done in references [70–72] (see Section 4.2). Here we include only the resummed piece (which gives the bulk of the cross section in this region), not the finite corrections. Figure 7.11 shows an invariant cross section as a function of Q_T for various Q -bins. The data are from the E605 experiment [86], and the theory curves are the b -space resummed predictions using the two-parameter Q -dependent nonperturbative form. The values $g_1 = 0.24\text{GeV}^2$ and $g_2 = 0.34\text{GeV}^2$ are the result of the global fit performed by Landry, Brock, Ladinsky and Yuan (LBLY) [71], which considered data only out to $Q_T = 1.4\text{GeV}$.

However, as shown in figure 7.12, we find that using a single-parameter, Q -**independent** form, with $g_1 \simeq 0.5\text{GeV}^2$ and $g_2 = 0.0\text{GeV}^2$, produces a better fit to the shape of the cross section at every range of Q , especially in light of the 15% normalization uncertainty of the data. This is true also for the dimuon data of the R209 experiment [87], as shown in figure 7.13. These data have a normalization uncertainty of 10%, and were also used in the LBLY fit.

E605 pN $\rightarrow \mu^+ \mu^- + X$ at $\sqrt{s}=38.8$ GeV

b-space resum, 2-parameter reference: $(g_1, g_2)=(0.24, 0.34)$, $NORM=0.94$

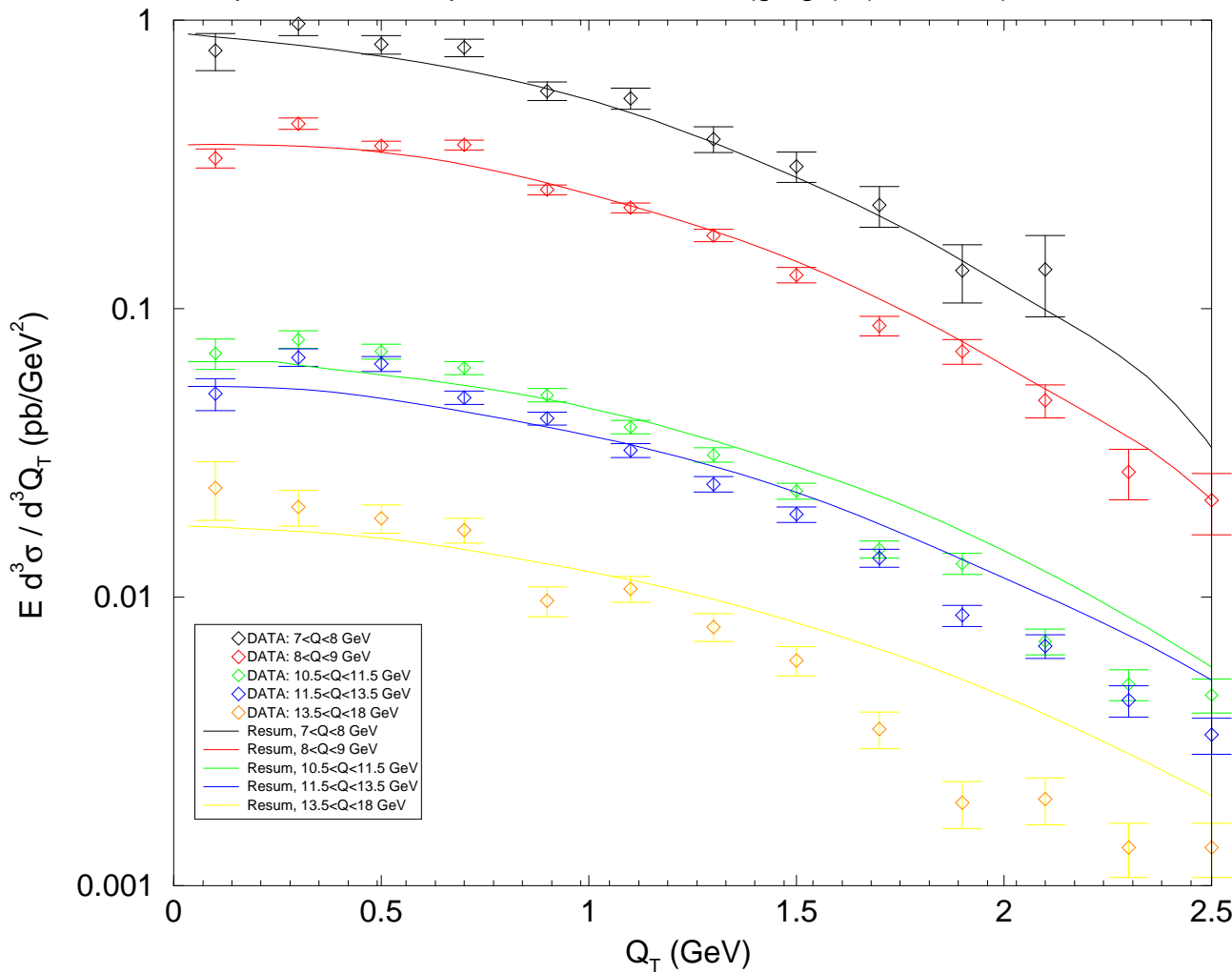


Figure 7.11. E605 b -space predictions, standard 2-parameter form.

E605 pN $\rightarrow \mu^+ \mu^- + X$ at $\sqrt{s}=38.8$ GeV

b-space resum, Fixed $g_1=0.53$, NORM=0.94

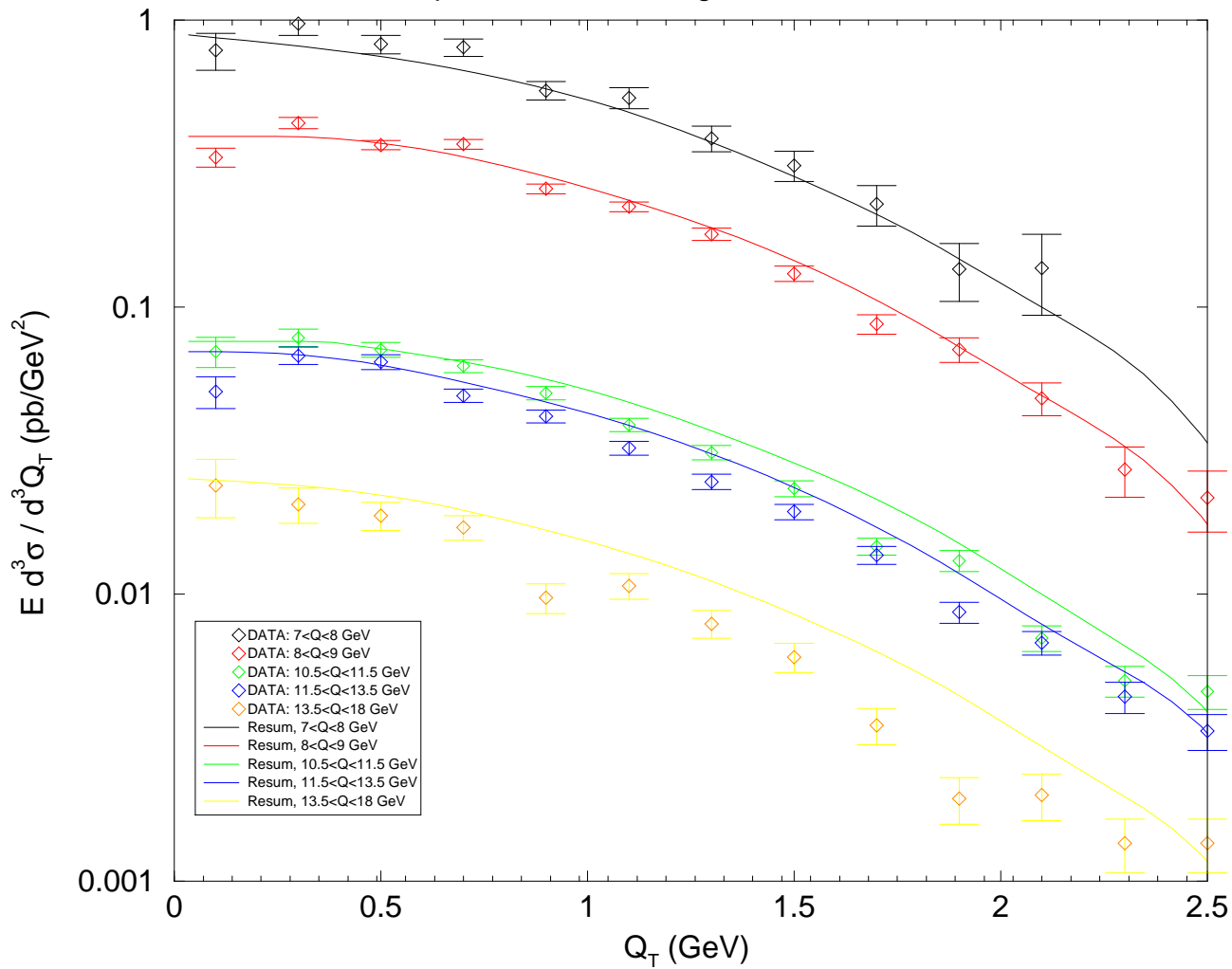


Figure 7.12. E605 b -space predictions, w/out Q -dependence.

R209 $pp \rightarrow \mu^+ \mu^- + X$ at $\sqrt{s}=62$ GeV

$5 < Q < 8$ GeV, b -space Resum

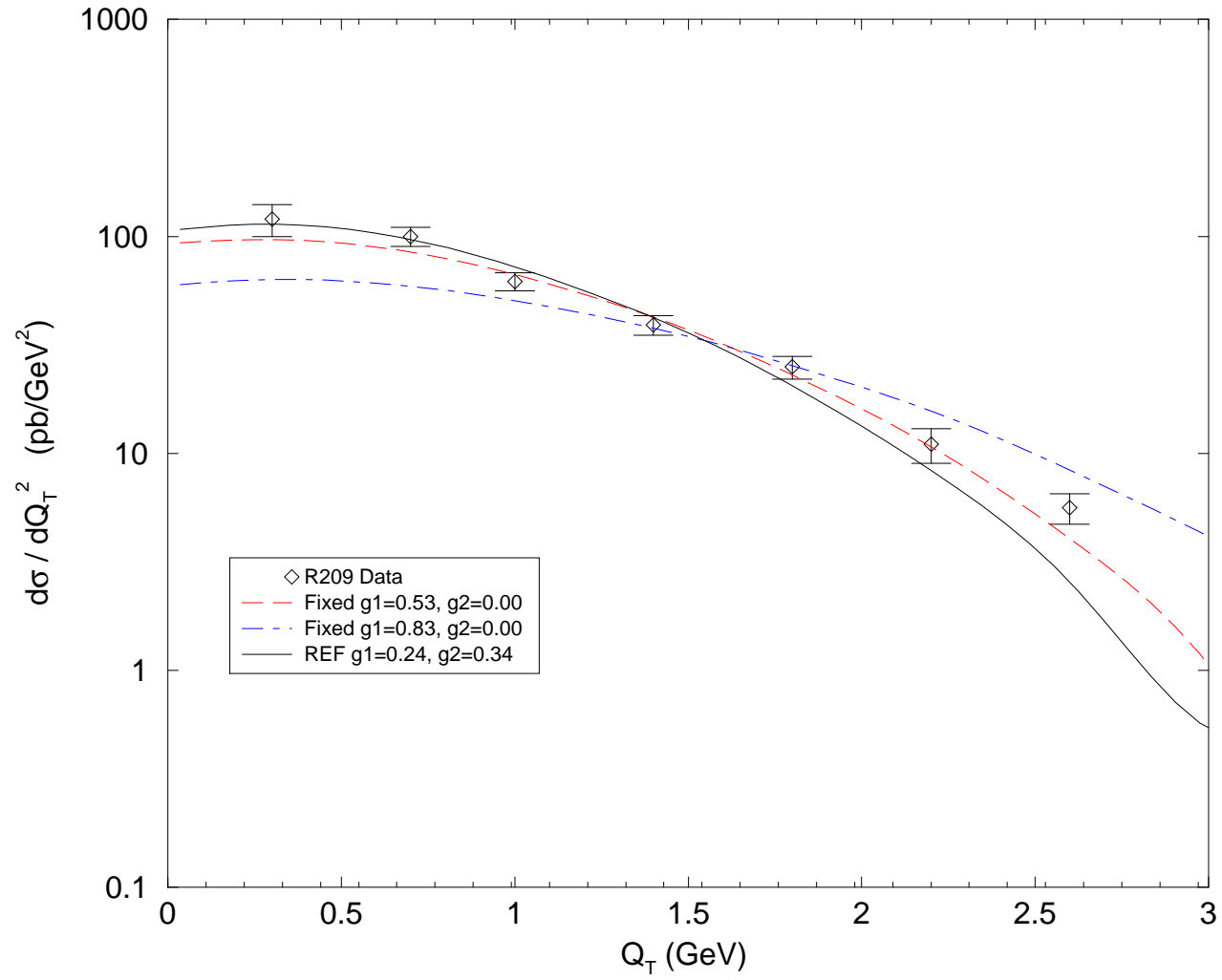


Figure 7.13. R209 b -space predictions, with and w/out Q -dependence.

As seen in the previous section, k_T -space resummation did well in describing direct photon data, as long as \tilde{a} was not too far from 0.3GeV^{-2} . The value of \tilde{a} which corresponds to a b -space parameter $g = 0.5\text{GeV}^2$, however, is $\tilde{a} \simeq 1/(4g) \simeq 0.5\text{GeV}^{-2}$. Drell-Yan dimuon production, however, has only quark annihilation subprocesses as Born terms, while direct photon production has gluon-induced Born-level terms, so it is possible that a color-structure-dependent nonperturbative form is required.

To check this, we repeat the direct photon predictions of the previous section, using single-parameter, Q -independent forms for both b and k_T -space resummations. For the $q\bar{q}$ contributions, we use $g = 0.5\text{GeV}^2$ and $\tilde{a} = 0.5\text{GeV}^{-2}$, and for the qg and gq contributions,

$$\begin{aligned}
g &= \frac{(C_F + N_C)}{2C_F} 0.5\text{GeV}^2 = 0.83\text{GeV}^2 \\
\text{and} \\
\tilde{a} &= 1/(4g) = 0.3\text{GeV}^{-2} .
\end{aligned} \tag{7.5}$$

The results, for E706 data at $\sqrt{S} = 31.5\text{GeV}$ and 38.7GeV , and for D0 data at $\sqrt{S} = 1800\text{GeV}$, are shown in figures 7.14, 7.15, and 7.16, respectively. The factorization scale is $M_f = p_\gamma$ for all plots. All show improved agreement with data for both b and k_T -space resummation procedures.

p Be $\rightarrow \gamma + X$ at $\sqrt{s}=31.5$ GeV

$-0.75 < y_\gamma < 0.75$

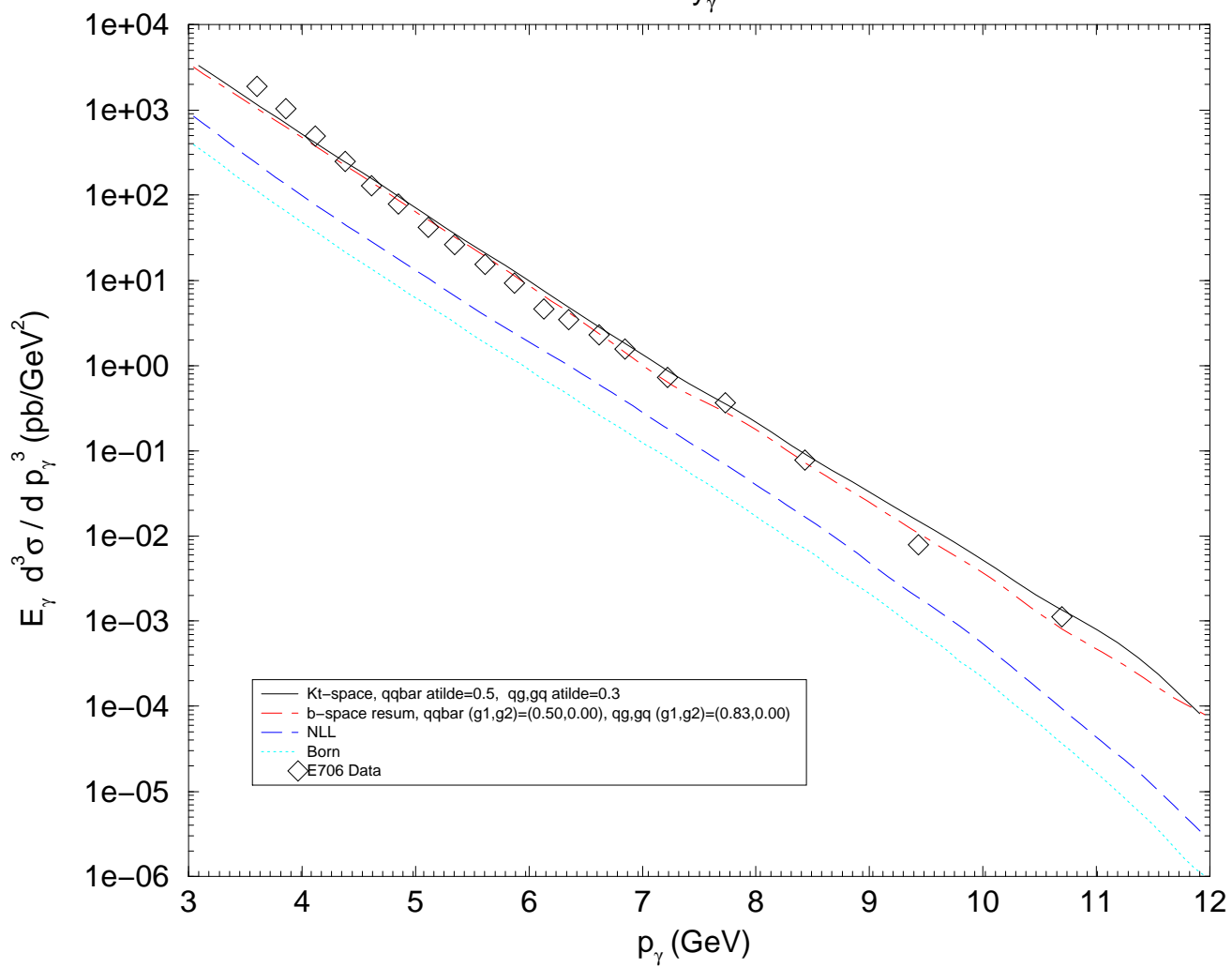


Figure 7.14. E706 $\sqrt{s} = 31.5$ GeV, with NP color dependence.

$p \text{ Be} \rightarrow \gamma + X \text{ at } \sqrt{s}=38.7 \text{ GeV}$

$-1.0 < y_\gamma < 0.5$

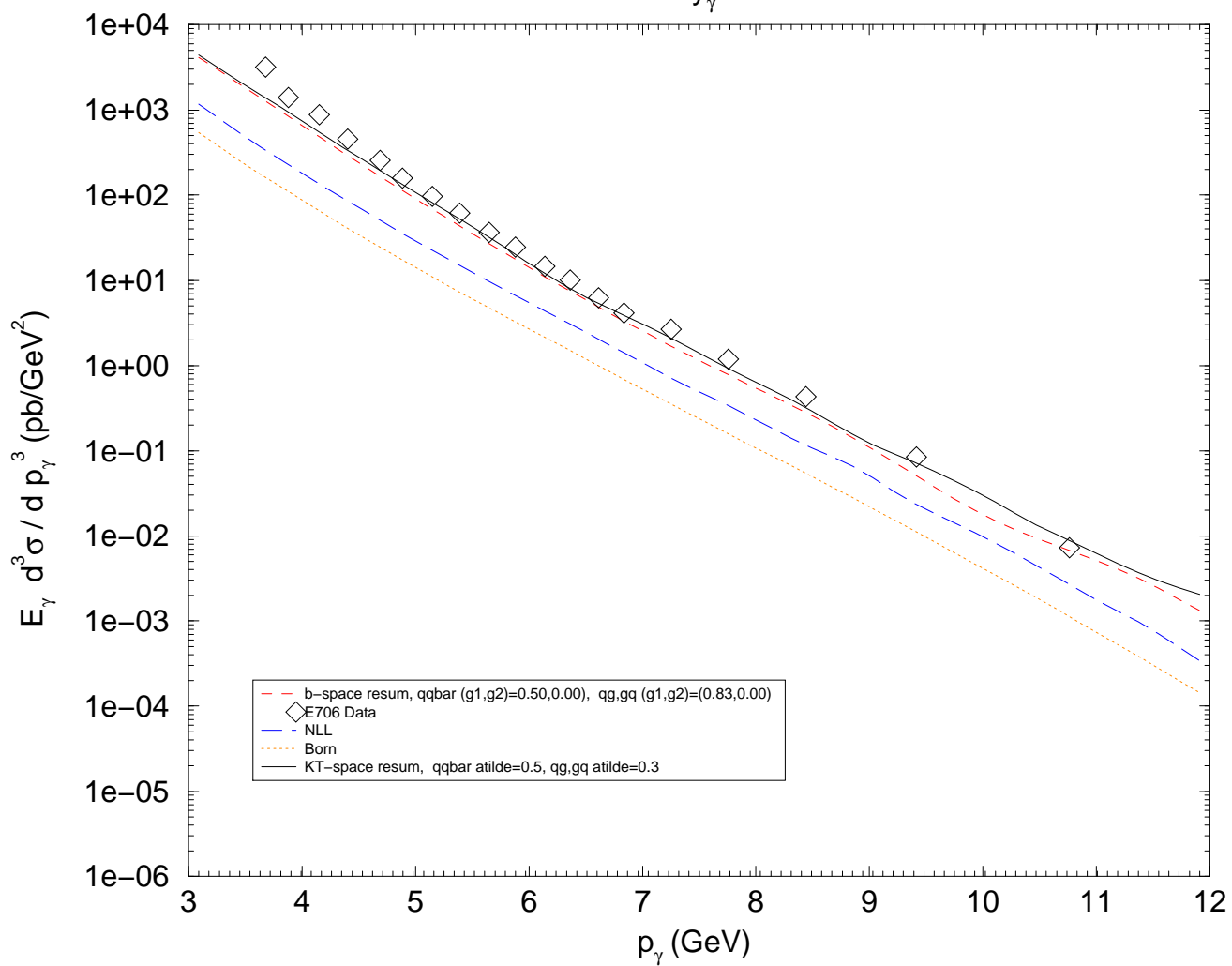


Figure 7.15. E706 $\sqrt{s} = 38.7 \text{ GeV}$, with NP color dependence.

$p \text{ pbar} \rightarrow \gamma + X$ at $\sqrt{s}=1800 \text{ GeV}$

$-0.9 < y_\gamma < 0.9$

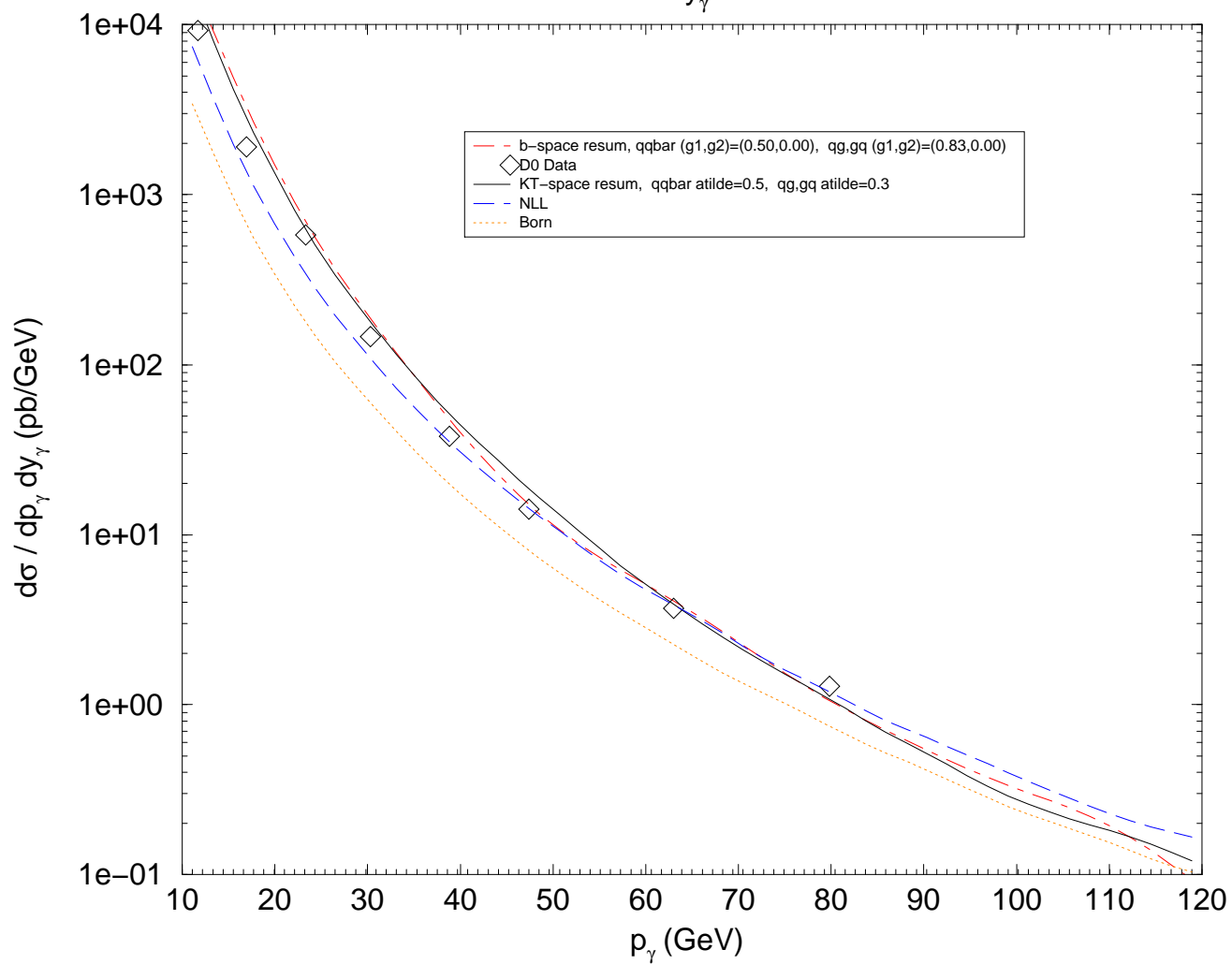


Figure 7.16. D0 $\sqrt{s} = 1800 \text{ GeV}$, with NP color dependence.

7.2 Other Parameter Choices

7.2.1 Scale Dependence

In a leading-order calculation, the Born terms are combined with energy-dependent couplings and distribution functions to produce a Leading-Log (LL) approximation. As discussed in Chapter 2, when next-to-leading order contributions are added, the dependence on renormalization and factorization scales should diminish. We check this by looking at photon p_T distributions in pBe collisions at a fixed target energy of 530GeV. We set the renormalization and factorization scales equal to each other, and run the LL and NLL calculations for $3 \leq p_\gamma \leq 12\text{GeV}$ at three values of this scale. When we're done, for each p_γ bin, we plot the difference between the low and high scales in ratio with the value at the middle scale. The NLL calculation should show smaller percent differences, and does, as shown in figure 7.17.

7.2.2 Jet Cone Width

The jet cone definition we have used counts two partons as belonging to the same jet if they are within an angular radius R of each other, this radius defined by [80]

$$r^2 = \left[(\Delta y)^2 + (\Delta \phi)^2 \right] \left(\frac{p_2}{p_2 + p_3} \right)^2. \quad (7.6)$$

However, our asymptotic pieces do not depend on this radius, as we have taken a fixed jet definition for each (see Chapter 6). The only possible dependence we have on this parameter comes via the three-body perturbative contribution, and then only through those observable quantities which are defined differently depending on whether or not the cone condition is met. For example, if we are looking at a photon p_γ spectrum, with cuts on the photon rapidity y_γ , we should see no dependence on the cone radius R , since $p_\gamma = \sqrt{p_2^2 + p_3^2 + 2p_2p_3 \cos(\phi_2 - \phi_3)}$ and $y_\gamma = y_1$ everywhere in phase space. However, if we are looking at a Q_T distribution, say, then raising R

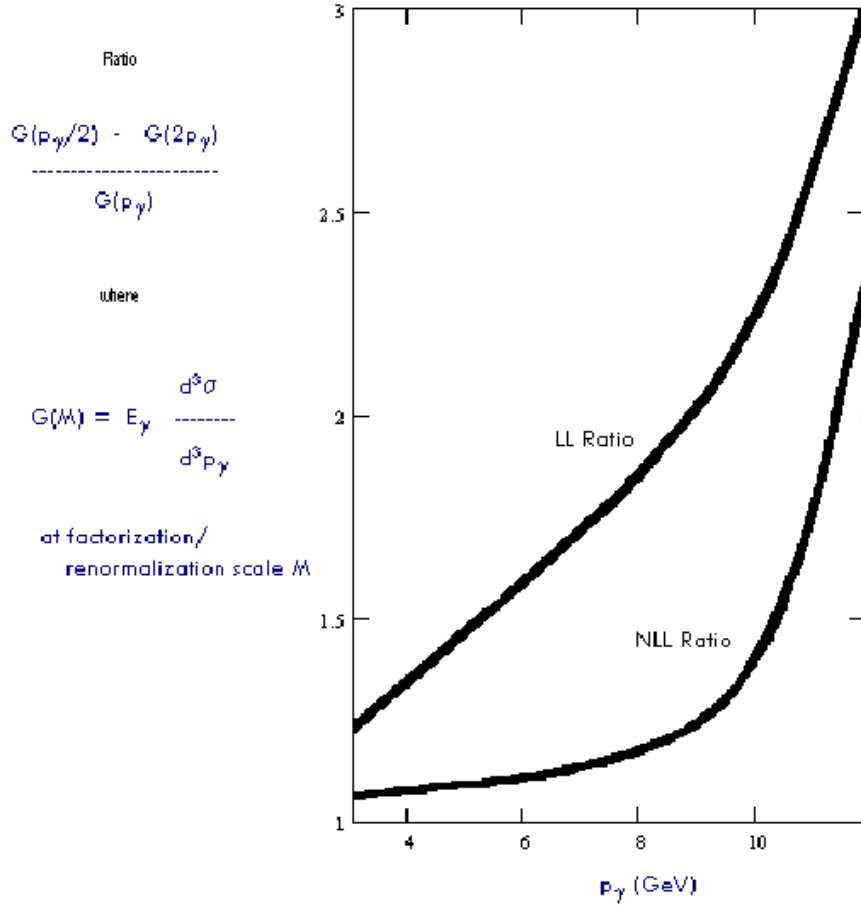


Figure 7.17. Scale Dependence.

should steepen the curve, since more weights are being binned as if the photon were recoiling against a single jet, *i.e.* at $Q_T = 0$.

Figures 7.18 and 7.19 show the cross section vs. Q_T for those pieces associated with initial and final-state singularities. In each, the perturbative, asymptotic, 2-body, finite (perturbative - asymptotic), and total are displayed. Here $R = 0.2$, $6.5 \leq Q \leq 7.5 \text{ GeV}$, $-0.75 \leq y_\gamma \leq 0.75$, $-0.3 \leq y_j \leq 0.3$, and the reaction is $pBe \rightarrow \gamma + j + X$.

p Be $\rightarrow \gamma + j + X$ at $\sqrt{s}=31.5$ GeV

Initial-State Pieces

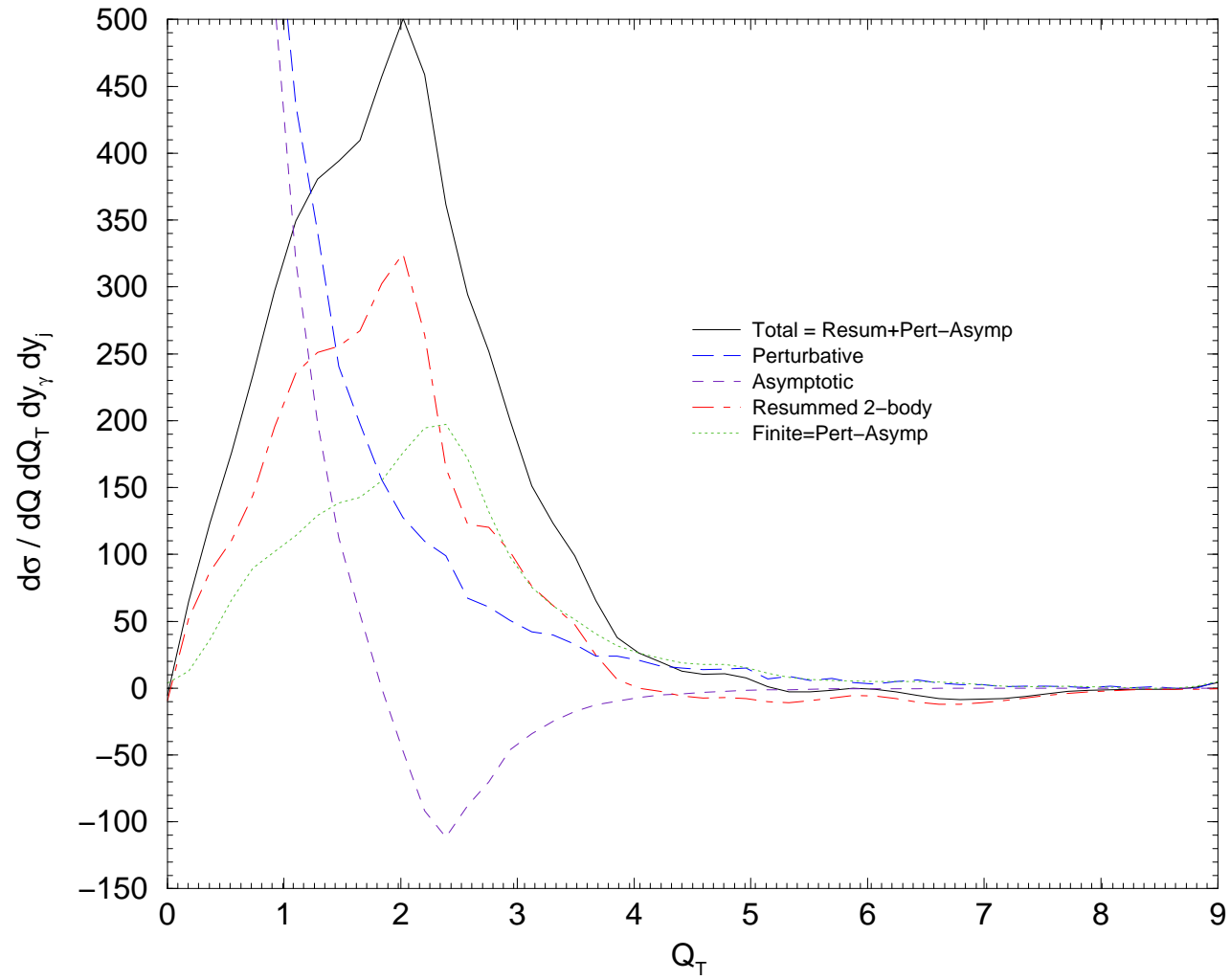


Figure 7.18. Q_T -distribution : Initial-state pieces.

$p \text{ Be} \rightarrow \gamma + j + X$
Final-State Pieces

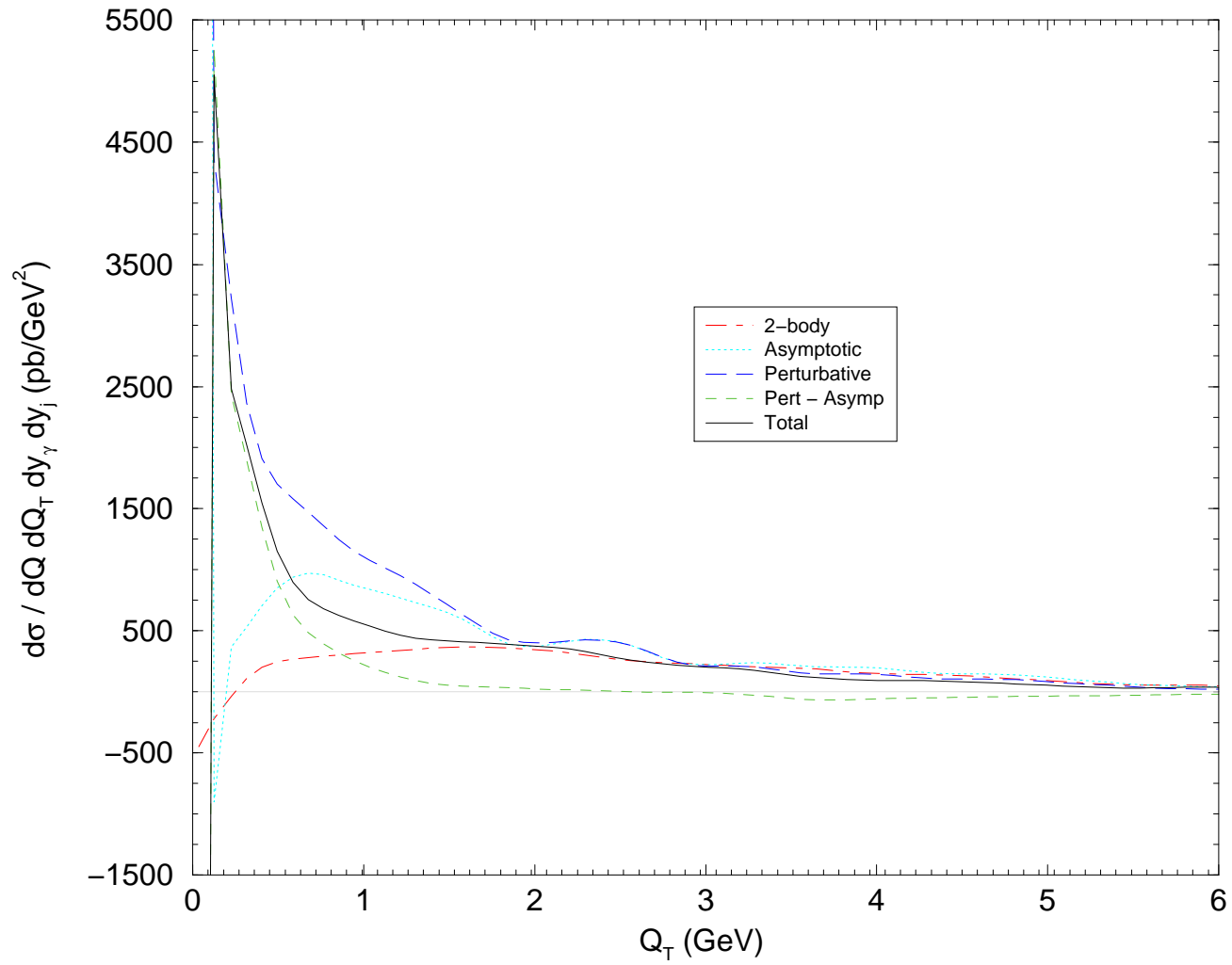


Figure 7.19. Q_T -distribution : Final-state pieces.

At present we know of no data for the Q_T distribution of a photon/jet system, which as just as well, as there are caveats associated with predicting Q_T -distributions in our current calculation.

As can be seen in Chapter 6, in order to extract the logarithms of Q/Q_T for resummation, we needed to analytically integrate over the rapidity y_3 of the third final-state particle. However, our jet definition depended upon y_3 . We were forced to approximate the kinematics as well as the matrix elements, thus removing this y_3 -dependence. For the initial-state pieces, we took $Q_T = p_3$ everywhere, even though radiation inside the jet cone would have resulted in $Q_T = 0$. This doesn't cause much of a problem for small cone width. For the final-state pieces, we treated the soft terms differently than the collinear, and this can cause a mismatch even outside the cone. For example, if a 3-body event comes along for which p_3^μ is soft and just outside the cone, we have the following scenario:

Table 7.1. Anomaly at low Q_T .

Piece	...looks like:	...but gets binned at:
3-body Pert.	SC	$Q_T = p_3$
$m = 2$ (Soft - SC)	0	$Q_T = p_3$
$m = 2$ Coll.	SC	$Q_T = 0$

Here **SC** stands for “Soft-Collinear”. The 3-body perturbative piece and the $m = 2$ asymptotic collinear piece both give roughly the same weight, but the asymptotic collinear is always binned at $Q_T = 0$, while the perturbative piece isn't. If the bin width in Q_T is larger than this p_3 , the cancellation will take place. If not, it won't.

In figure 7.20, we show a comparison of Q_T distributions for the $m = 2$ finite (perturbative - asymptotic) piece, one curve corresponding to the approximated jet definition we were forced to use, the other curve showing what would result were we able to use the non-approximate version. The latter tends nicely to zero as $Q_T \rightarrow 0$,

$$p \text{ Be} \rightarrow \gamma + j + X$$

Final-State Pieces : JetDef Comparison

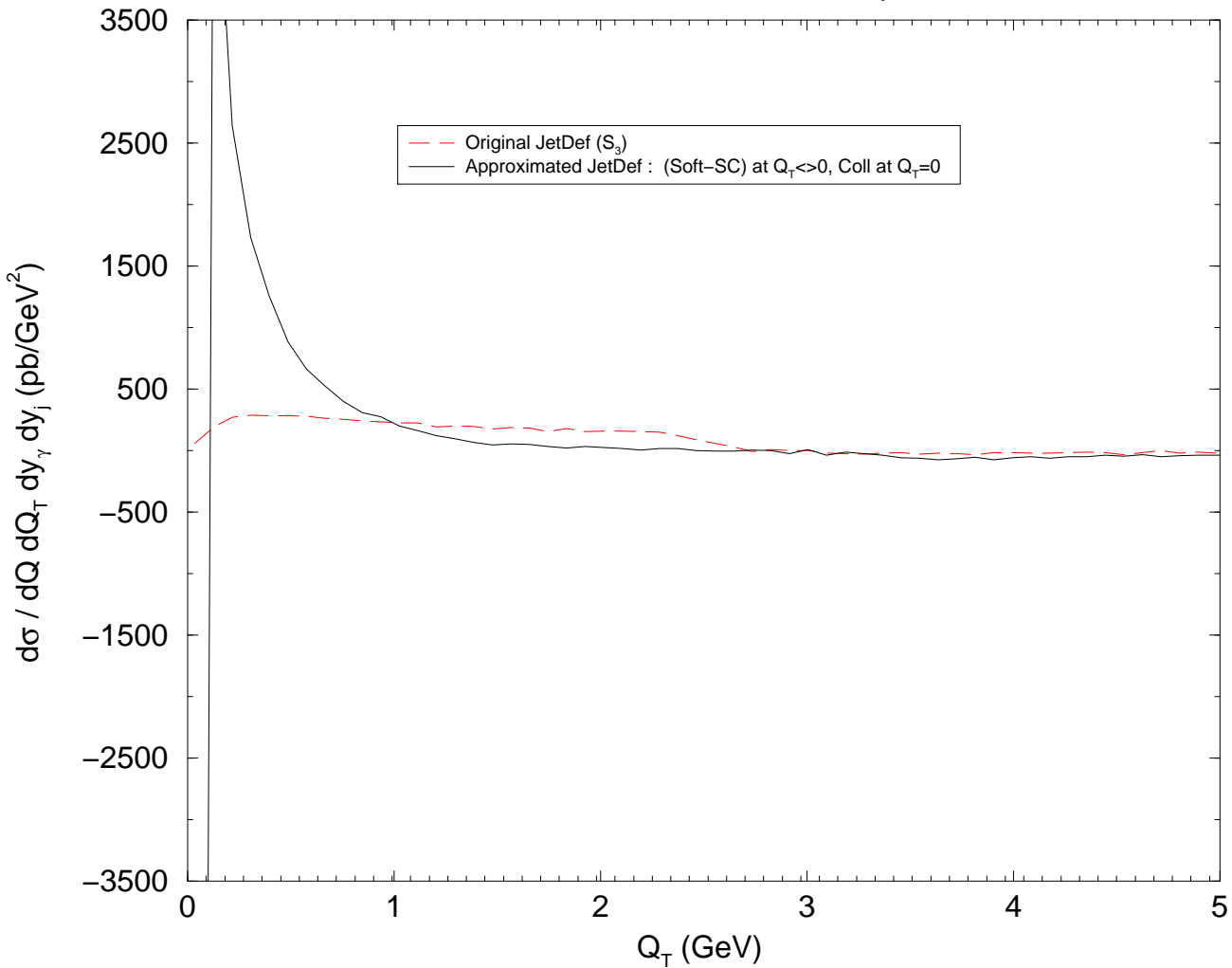


Figure 7.20. Comparison of full and approximate jet definition results.

while the former retains a steep increase and is only counteracted in the first bin by the large, subtracted collinear contribution.

The result is a non-continuous Q_T distribution, and so further work is required in order to deal properly with these final-state terms. Eventually, of course, we'd like to resum these pieces, and to do so in a way that is independent of the particular jet definition in use. For the present, integration over Q_T , as in the preceding inclusive p_γ -distributions, gives a good, unambiguous result.

7.3 Conclusions and Future Improvements

We have seen the means by which soft radiative corrections can be resummed to all orders, and the significant effect such contributions have on the direct photon p_T spectrum. In principle, any steeply-falling spectrum is a candidate for this procedure, including most single-particle inclusive transverse momentum distributions. As contributions from all orders are included, resummation improves agreement with data as compared to fixed-order calculations. Thus there is the potential for a significant impact on the prediction of a wide variety of processes.

In this work, we have also seen that direct photon data can play a role in constraining the nonperturbative function; in particular we have seen evidence of a dependence on the color structure of the subprocess, in the form of mass-independent Gaussians for each structure. The nonperturbative parametrization is thus far from pinned-down, and it is likely that further exploration of perturbative methods can aid in probing the nonperturbative region.

Proper matching of the resummed to fixed-order result has been shown to be important, especially at fixed-target energies. The matching procedure outlined in this work accomplishes this task in a flexible and automatic manner, without influencing the result in any way when not required.

The FORTRAN program written concurrently with this dissertation, and from which the results of this chapter were produced, is available upon request. It is capable of producing either NLO or resummed output, as the user desires.

Without significantly altering the adopted procedure, it should be possible to avoid problems associated with jet definitions by looking at photon plus pion final states, for which there are a good amount of data [83]. Furthermore, Q_T and p_{out} distributions exist for these data, providing a more sensitive base upon which to examine nonperturbative parametrizations.

Inclusion of threshold effects is also possible, as indicated by the recent work of Laenen, Sterman, and Vogelsang [88]. This method involves both Fourier and Mellin transforms, and looks, though complicated, to be quite powerful.

APPENDIX A

DIAGRAMS AND MATRIX ELEMENTS FOR NLO PHOTON HADROPRODUCTION

In this appendix, we include Feynman diagrams of the contributions to photon production by hadrons, first to leading order, then to next-to-leading order.

Figure A.1 shows the basic couplings involved. The first is a QED-like photon-quark coupling of strength e_{QED} . The second is the analogous QCD gluon-quark coupling, this time of strength g_s . The third, a gluon-gluon coupling, has no QED analogue. In general, all non-Abelian theories (such as QCD) will have self-couplings among the gauge fields. Note that in QCD there is another gluon coupling (with four attached propagators), but as it is of order g_s^2 , it will not be needed here.

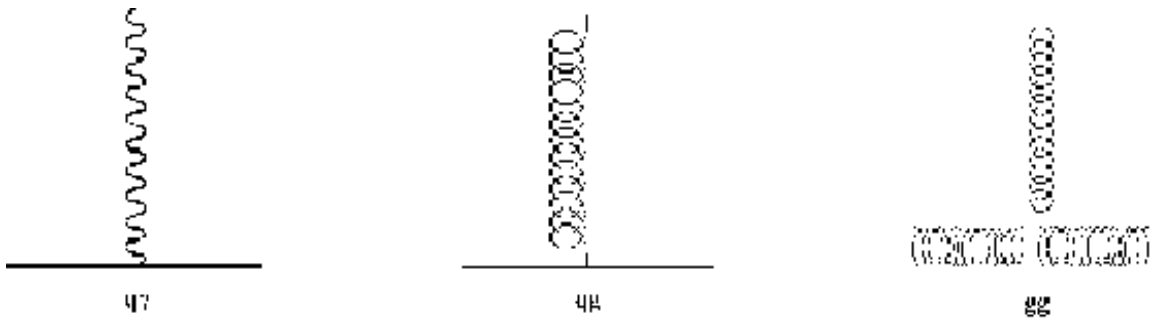


Figure A.1. $q\gamma$, qg , and gg vertices.

To find the leading-order contributions to photon hadroproduction, we need to put these vertices together (along with suitable propagators and external legs) in all possible combinations consistent with the following conditions:

1. There must be one final-state photon.
2. There must be two incoming particles, each either a quark or gluon.
3. Each diagram must be *simply-connected* and maintain momentum conservation.
4. Each diagram must use as few vertices as possible.
5. Each diagram must be topologically distinct.

These conditions constrain us to the diagrams shown in figure A.2.

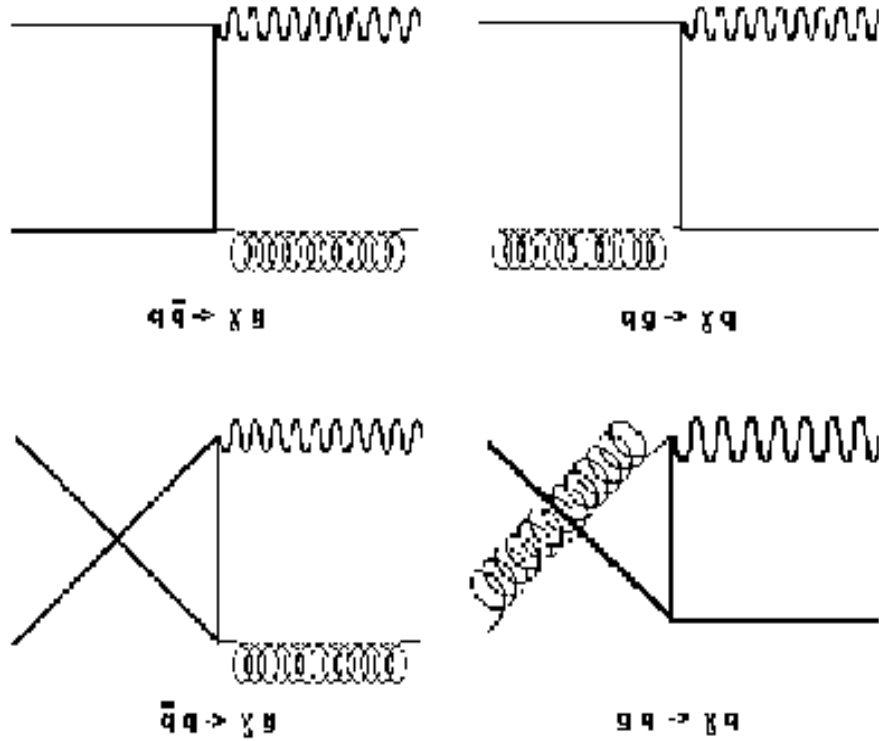


Figure A.2. Leading order photon hadroproduction diagrams.

Now we go to next-to-leading-order (NLO). We first seek the basic simply-connected Green's functions (that is, tree diagrams) which include one photon-quark vertex and two vertices from the set $\{gg, gg\}$. Given the “connected” constraint, we rule out two gg vertices, and arrive at the following four diagrams (fig. A.3).

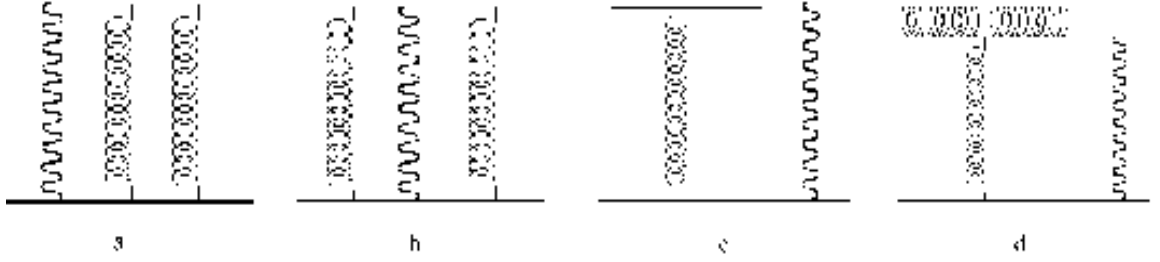


Figure A.3. $qq\gamma gg$ (a, b and d), and $qq\gamma qq$ time-independent Feynman diagrams.

Note that we have not yet shown any time direction. That is, we have not assigned any of the external lines to "incoming" or "outgoing" legs. Figures A.4 and A.5 show the range of such associations, given that the incoming particles (on the left) must be either quarks or gluons (this is *hadroproduction*, after all), and the photon must be outgoing. In addition, we will have next-to-leading order virtual contributions, as shown in figure A.6.

Finally, there will be Bremsstrahlung contributions, which arise when one final-state parton in a purely QCD subprocess fragments and a photon is produced. The signature for such an event is a non-isolated photon (one with hadronic energy deposited in a small cone about the photon axis) and a jet in the opposite direction. The purely QCD 2-body subprocesses are as follows; diagrams for these, as well as the derivation of their matrix elements, can be found in Ellis and Sexton (1986) [89].

$$\begin{aligned}
q\bar{q} &\rightarrow gg & qq &\rightarrow qq \\
gq &\rightarrow qg & gq &\rightarrow q\bar{q} \\
gg &\rightarrow gg & qq &\rightarrow qq \\
q\bar{q} &\rightarrow q\bar{q} & q\bar{q} &\rightarrow \bar{q}q \\
qq' &\rightarrow qq' & qq' &\rightarrow q'q \\
q\bar{q} &\rightarrow q'\bar{q}' & &
\end{aligned} \tag{A.1}$$

A.1 Two-Body Matrix Elements

For dimension $D = 4 - 2\epsilon$, and with the definitions

$$\begin{aligned}
\hat{s} &\equiv (p_1^\mu + p_2^\mu)^2 \\
\hat{t} &\equiv (p_1^\mu - p_3^\mu)^2 \\
\hat{u} &\equiv (p_1^\mu - p_4^\mu)^2 \\
K'_{q\bar{q}} &\equiv \frac{1}{3} \\
K'_{qg} = K'_{gq} &\equiv \frac{1}{8(1-\epsilon)} \\
\omega_{2\gamma} &\equiv 2(4\pi)^2 C_F \alpha_s \mu^{4\epsilon} \\
\omega_{2Q} &\equiv 2(4\pi)^2 C_F \alpha_s^2 \mu^{4\epsilon}
\end{aligned} \tag{A.2}$$

we can write the two-body matrix elements as [89–91]:

A.1.1 $q(p_1)\bar{q}(p_2) \rightarrow \gamma(p_3)g(p_4)$

$$\bar{\Sigma}|M|_{q\bar{q} \rightarrow \gamma g}^2 = K'_{q\bar{q}} Q_q^2 \omega_{2\gamma} (1-\epsilon) \left[(1-\epsilon) \left(\frac{\hat{t}}{\hat{u}} + \frac{\hat{u}}{\hat{t}} \right) - 2\epsilon \right] \tag{A.3}$$

A.1.2 $q(p_1)g(p_2) \rightarrow \gamma(p_3)q(p_4)$

$$\bar{\Sigma}|M|_{qg \rightarrow \gamma q}^2 = -K'_{qg} Q_q^2 \omega_{2\gamma} (1-\epsilon) \left[(1-\epsilon) \left(\frac{\hat{t}}{\hat{s}} + \frac{\hat{s}}{\hat{t}} \right) - 2\epsilon \right] \tag{A.4}$$

A.1.3 $g(p_1)q(p_2) \rightarrow \gamma(p_3)q(p_4)$

$$\bar{\Sigma}|M|_{gq \rightarrow \gamma q}^2 = -K'_{gq} Q_q^2 \omega_{2\gamma} (1-\epsilon) \left[(1-\epsilon) \left(\frac{\hat{u}}{\hat{s}} + \frac{\hat{s}}{\hat{u}} \right) - 2\epsilon \right] \tag{A.5}$$

A.1.4 $q(p_1)\bar{q}(p_2) \rightarrow g(p_3)g(p_4)$

$$\bar{\Sigma}|M|_{q\bar{q} \rightarrow gg}^2 = \frac{K'_{q\bar{q}}}{2} \omega_{2Q} (1-\epsilon) \left[\frac{\hat{u}^2 + \hat{t}^2}{\hat{s}^2} - \epsilon \right] \left[C_F \frac{\hat{s}^2}{\hat{t}\hat{u}} - N_C \right] \tag{A.6}$$

A.1.5 $q(p_1)g(p_2) \rightarrow q(p_3)g(p_4)$

$$\bar{\Sigma}|M|_{qg \rightarrow qg}^2 = -K'_{qg}\omega_{2Q}(1-\epsilon)\left[\frac{\hat{u}^2 + \hat{s}^2}{\hat{t}^2} - \epsilon\right]\left[C_F\frac{\hat{t}^2}{\hat{s}\hat{u}} - N_C\right] \quad (\text{A.7})$$

A.1.6 $g(p_1)q(p_2) \rightarrow q(p_3)g(p_4)$

$$\bar{\Sigma}|M|_{gq \rightarrow qg}^2 = -K'_{qg}\omega_{2Q}(1-\epsilon)\left[\frac{\hat{t}^2 + \hat{s}^2}{\hat{u}^2} - \epsilon\right]\left[C_F\frac{\hat{u}^2}{\hat{s}\hat{t}} - N_C\right] \quad (\text{A.8})$$

A.1.7 $g(p_1)g(p_2) \rightarrow q(p_3)\bar{q}(p_4)$

$$\bar{\Sigma}|M|_{gg \rightarrow q\bar{q}}^2 = \frac{K'_{qg}}{2C_F}\omega_{2Q}\left[\frac{\hat{t}^2 + \hat{u}^2}{\hat{s}^2} - \epsilon\right]\left[C_F\frac{\hat{s}^2}{\hat{u}\hat{t}} - N_C\right] \quad (\text{A.9})$$

A.1.8 $g(p_1)g(p_2) \rightarrow g(p_3)g(p_4)$

$$\bar{\Sigma}|M|_{gg \rightarrow gg}^2 = \frac{K'_{qg}}{2}9N_C\omega_{2Q}\left[3 - \frac{\hat{t}\hat{u}}{\hat{s}^2} - \frac{\hat{s}\hat{u}}{\hat{t}^2} - \frac{\hat{s}\hat{t}}{\hat{u}^2}\right] \quad (\text{A.10})$$

A.1.9 $q(p_1)q(p_2) \rightarrow q(p_3)q(p_4)$

$$\bar{\Sigma}|M|_{qq \rightarrow qq}^2 = \frac{K'_{q\bar{q}}}{4}\omega_{2Q}\left[\frac{\hat{s}^2 + \hat{u}^2}{\hat{t}^2} + \frac{\hat{s}^2 + \hat{t}^2}{\hat{u}^2} - 2\epsilon - \frac{2(1-\epsilon)}{N_C}\left(\frac{\hat{s}^2}{\hat{t}\hat{u}} + \epsilon\right)\right] \quad (\text{A.11})$$

A.1.10 $q(p_1)\bar{q}(p_2) \rightarrow q(p_3)\bar{q}(p_4)$

$$\bar{\Sigma}|M|_{q\bar{q} \rightarrow q\bar{q}}^2 = \frac{K'_{q\bar{q}}}{2}\omega_{2Q}\left[\frac{\hat{s}^2 + \hat{u}^2}{\hat{t}^2} + \frac{\hat{u}^2 + \hat{t}^2}{\hat{s}^2} - 2\epsilon - \frac{2(1-\epsilon)}{N_C}\left(\frac{\hat{u}^2}{\hat{t}\hat{s}} + \epsilon\right)\right] \quad (\text{A.12})$$

A.1.11 $q(p_1)\bar{q}(p_2) \rightarrow \bar{q}(p_3)q(p_4)$

$$\bar{\Sigma}|M|_{q\bar{q} \rightarrow \bar{q}q}^2 = \frac{K'_{q\bar{q}}}{2}\omega_{2Q}\left[\frac{\hat{s}^2 + \hat{t}^2}{\hat{u}^2} + \frac{\hat{t}^2 + \hat{u}^2}{\hat{s}^2} - 2\epsilon - \frac{2(1-\epsilon)}{N_C}\left(\frac{\hat{t}^2}{\hat{u}\hat{s}} + \epsilon\right)\right] \quad (\text{A.13})$$

$$\mathbf{A.1.12} \quad q(p_1)q'(p_2) \rightarrow q(p_3)q'(p_4)$$

$$\bar{\Sigma}|M|_{qq' \rightarrow qq'}^2 = \frac{K'_{q\bar{q}}}{2}\omega_{2Q}[(1-\epsilon) - 2\frac{\hat{u}\hat{s}}{\hat{t}^2}] \quad (\text{A.14})$$

$$\mathbf{A.1.13} \quad q(p_1)q'(p_2) \rightarrow q'(p_3)q(p_4)$$

$$\bar{\Sigma}|M|_{qq' \rightarrow q'q}^2 = \frac{K'_{q\bar{q}}}{2}\omega_{2Q}[(1-\epsilon) - 2\frac{\hat{t}\hat{s}}{\hat{u}^2}] \quad (\text{A.15})$$

$$\mathbf{A.1.14} \quad q(p_1)\bar{q}(p_2) \rightarrow q'(p_3)\bar{q}'(p_4)$$

$$\bar{\Sigma}|M|_{q\bar{q} \rightarrow q'\bar{q}'}^2 = \frac{K'_{q\bar{q}}}{2}\omega_{2Q}[(1-\epsilon) - 2\frac{\hat{t}\hat{u}}{\hat{s}^2}] \quad (\text{A.16})$$

Note that in the text, we will often use the definition

$$K'T'_{f\bar{f}}(v) \equiv \frac{\bar{\Sigma}|\mathcal{M}|^2}{\omega_{2Q}}, \quad (\text{A.17})$$

in which $v \equiv -\hat{u}/\hat{s}$. Use of either K or $T_{f\bar{f}}$ **without** the prime refers to the $\epsilon \rightarrow 0$ limit thereof. Here and in the text, $C_F = 4/3$ and $N_C = 3$.

A.2 Three-Body Matrix Elements

With the definitions

$$\begin{aligned} s_{12} &\equiv (p_1^\mu + p_2^\mu)^2 \\ t_{13} &\equiv (p_1^\mu - p_3^\mu)^2 \\ t_{14} &\equiv (p_1^\mu - p_4^\mu)^2 \\ t_{15} &\equiv (p_1^\mu - p_5^\mu)^2 \\ t_{23} &\equiv (p_2^\mu - p_3^\mu)^2 \\ t_{24} &\equiv (p_2^\mu - p_4^\mu)^2 \\ t_{25} &\equiv (p_2^\mu - p_5^\mu)^2 \\ s_{34} &\equiv (p_3^\mu + p_4^\mu)^2 \end{aligned}$$

$$\begin{aligned}
s_{35} &\equiv (p_3^\mu + p_5^\mu)^2 \\
s_{45} &\equiv (p_4^\mu + p_5^\mu)^2 \\
K'_{q\bar{q}} &\equiv \frac{1}{3} \\
K'_{qg} = K'_{gq} &\equiv \frac{1}{8(1-\epsilon)} \\
\omega_3 &\equiv 4(4\pi)^3 C_F \alpha_s^2 \mu^{6\epsilon}
\end{aligned} \tag{A.18}$$

we can write the 3-body matrix elements as follows [91]:

$$\mathbf{A.2.1} \quad q(p_1)\bar{q}(p_2) \rightarrow \gamma(p_3)g(p_4)g(p_5)$$

We need:

$$\begin{aligned}
M_{qqg} &(s_{12}, t_{13}, t_{14}, t_{15}, t_{23}, t_{24}, t_{25}, s_{34}, s_{35}, s_{45}) \\
&\equiv \left[\left(C_F - \frac{N_C}{2} \right) \frac{s_{12}}{t_{15}t_{25}} + \frac{N_C}{2} \frac{t_{14}}{t_{15}s_{45}} + \frac{N_C}{2} \frac{t_{24}}{t_{25}s_{45}} \right] \\
&\times \left\{ (1-\epsilon)^2 \left[\frac{t_{13}^2 + t_{23}^2}{t_{14}t_{24}} + \frac{t_{14}^2 + t_{24}^2}{t_{13}t_{23}} + \frac{t_{15}t_{25}(t_{15}^2 + t_{25}^2)}{t_{13}t_{23}t_{14}t_{24}} \right] \right. \\
&+ \epsilon(1-2\epsilon) \left[\frac{(t_{14}-t_{24})(t_{15}-t_{25})}{t_{14}t_{24}} + \frac{(t_{13}-t_{23})(t_{15}-t_{25})}{t_{13}t_{23}} \right. \\
&\quad \left. \left. + \frac{t_{13}t_{23}}{t_{15}t_{25}(t_{13}-t_{23})(t_{14}-t_{24})} \right] \right. \\
&+ \epsilon(2+\epsilon) \left[\frac{t_{13}t_{23}}{t_{14}t_{24}} + \frac{t_{14}t_{24}}{t_{13}t_{23}} + \frac{t_{15}^2 t_{25}^2}{t_{13}t_{23}t_{14}t_{24}} \right] \\
&\left. - 2\epsilon(4-\epsilon) \left[1 + \frac{t_{15}t_{25}}{t_{13}t_{23}} + \frac{t_{15}t_{25}}{t_{14}t_{24}} \right] \right\}, \tag{A.19}
\end{aligned}$$

from which we obtain

$$\bar{\Sigma}|M|_{q\bar{q} \rightarrow \gamma gg}^2 = \frac{K'_{q\bar{q}}}{2} Q_q^2 \omega_3 M_{qqg}(s_{12}, t_{13}, t_{14}, t_{15}, t_{23}, t_{24}, t_{25}, s_{34}, s_{35}, s_{45}). \tag{A.20}$$

$$\mathbf{A.2.2} \quad q(p_1)g(p_2) \rightarrow \gamma(p_3)q(p_4)g(p_5)$$

$$\bar{\Sigma}|M|_{qg \rightarrow \gamma qg}^2 = -K'_{qg} Q_q^2 \omega_3 M_{qqg}(t_{14}, t_{13}, s_{12}, t_{15}, s_{34}, t_{24}, s_{45}, t_{23}, s_{35}, t_{25}). \tag{A.21}$$

A.2.3 $g(p_1)q(p_2) \rightarrow \gamma(p_3)q(p_4)g(p_5)$

$$\bar{\Sigma}|M|_{gg \rightarrow \gamma qg}^2 = -K'_{gq} Q_q^2 \omega_3 M_{qqgg}(t_{24}, t_{23}, s_{12}, t_{25}, s_{34}, t_{14}, s_{45}, t_{13}, s_{35}, t_{15}) . \quad (\text{A.22})$$

A.2.4 $g(p_1)g(p_2) \rightarrow \gamma(p_3)q(p_4)\bar{q}(p_5)$

$$\bar{\Sigma}|M|_{gg \rightarrow \gamma q\bar{q}}^2 = \frac{K'_{gq}}{2C_F(1-\epsilon)} Q_q^2 \omega_3 M_{qqgg}(s_{45}, s_{35}, t_{25}, t_{15}, s_{34}, t_{24}, t_{14}, t_{23}, t_{13}, s_{12}) . \quad (\text{A.23})$$

A.2.5 $q(p_1)q(p_2) \rightarrow \gamma(p_3)q(p_4)q(p_5)$

With

$$\begin{aligned} M_0 &= \frac{-s_{12}}{t_{13}t_{23}} + \frac{t_{25}}{t_{23}s_{35}} + \frac{t_{24}}{t_{23}s_{34}} + \frac{t_{14}}{t_{13}s_{34}} - \frac{s_{45}}{s_{35}s_{34}} + \frac{t_{15}}{t_{13}s_{35}} \\ M_1 &= \frac{s_{12}^2 + t_{25}^2 + t_{14}^2 + s_{45}^2}{t_{24}t_{15}} \\ M_2 &= \frac{s_{12}^2 + t_{24}^2 + t_{15}^2 + s_{45}^2}{t_{25}t_{14}} \\ M_3 &= (s_{12} + s_{45}) \frac{(t_{25} + t_{14})}{t_{24}t_{15}} \\ M_4 &= (s_{12} + s_{45}) \frac{(t_{24} + t_{15})}{t_{25}t_{14}} \\ M_5 &= (s_{12}^2 + s_{45}^2)(2s_{12}s_{45} - 2t_{25}t_{14} - 2t_{24}t_{15} - (t_{25} + t_{14})(t_{24} + t_{15})) \\ &\quad + (s_{12} - s_{45})^2(2(t_{25} + t_{14})(t_{24} + t_{15}) + t_{25}t_{14} + t_{24}t_{15}) \\ &\quad + ((t_{25} + t_{24})^2 - (t_{14} + t_{15})^2)(t_{15}t_{14} - t_{25}t_{24}) \\ &\quad - t_{15}t_{24}(t_{24} - t_{15})^2 - t_{14}t_{25}(t_{14} - t_{25})^2 - t_{15}t_{25}(t_{15} + t_{25})^2 - t_{24}t_{14}(t_{14} + t_{24})^2 \\ &\quad + 8t_{25}t_{24}t_{14}t_{15} + (t_{24} - t_{25})(t_{15} - t_{14})(t_{24}t_{25} + t_{14}t_{15}) \end{aligned} \quad (\text{A.24})$$

and the further definition

$$\begin{aligned} M_{qqqq} &= (s_{12}, t_{13}, t_{14}, t_{15}, t_{23}, t_{24}, t_{25}, s_{34}, s_{35}, s_{45}) \\ &\equiv \begin{cases} 2M_0(M_1 + M_2 - 2\epsilon) \end{cases} \end{aligned}$$

$$\begin{aligned}
& - 4\epsilon \left[\left(\frac{t_{24}}{t_{23}s_{34}} + \frac{t_{15}}{t_{13}s_{35}} \right) (M_1 + M_3 - 2) \right. \\
& + \left. \left(\frac{t_{14}}{t_{13}s_{34}} + \frac{t_{25}}{t_{23}s_{35}} \right) (M_2 + M_4 - 2) \right] \\
& - 2\epsilon \left[\left(\frac{-s_{12}}{t_{13}t_{23}} + \frac{t_{25}}{t_{23}s_{35}} + \frac{t_{14}}{t_{13}s_{34}} - \frac{s_{45}}{s_{35}s_{34}} \right) \right. \\
& \times \left(\frac{\frac{1}{2}(s_{12} - s_{45})^2 + \frac{1}{2}(t_{14} - t_{25})^2}{t_{24}t_{15}} + M_1 + M_3 - 2 \right) \\
& + \left(\frac{-s_{12}}{t_{13}t_{23}} + \frac{t_{24}}{t_{23}s_{34}} - \frac{s_{45}}{s_{35}s_{34}} + \frac{t_{15}}{t_{13}s_{35}} \right) \\
& \times \left. \left(\frac{\frac{1}{2}(s_{12} - s_{45})^2 + \frac{1}{2}(t_{15} - t_{24})^2}{t_{25}t_{14}} + M_2 + M_4 - 2 \right) \right] \\
& - 2(1 - \epsilon) \frac{M_0}{N_C} \left[\frac{(s_{12}^2 + s_{45}^2)(s_{12}s_{45} - t_{14}t_{25} - t_{15}t_{24})}{t_{25}t_{24}t_{14}t_{15}} + 4\epsilon \right] \\
& + \frac{2\epsilon}{N_C} \left[\frac{s_{35}(s_{12}s_{34} - t_{23}t_{14} - t_{24}t_{13})}{t_{25}t_{23}t_{13}t_{15}} + \frac{s_{34}(s_{12}s_{35} - t_{25}t_{13} - t_{23}t_{15})}{t_{23}(-s_{45}t_{13} + t_{14}s_{35} + s_{34}t_{15})} \right. \\
& - \left. \frac{t_{23}t_{24}t_{14}t_{13}}{t_{14}s_{34}s_{35}t_{15}} \right] \\
& + \left. \frac{\epsilon}{N_C} \frac{M_0 M_5}{t_{25}t_{24}t_{15}t_{14}} \right\}, \tag{A.25}
\end{aligned}$$

we can write

$$\bar{\Sigma} |M|_{qq \rightarrow \gamma qq}^2 = \frac{K'_{gg}}{4} C_F Q_q^2 \omega_3 M_{qqqq}(s_{12}, t_{13}, t_{14}, t_{15}, t_{23}, t_{24}, t_{25}, s_{34}, s_{35}, s_{45}). \tag{A.26}$$

A.2.6 $q(p_1)\bar{q}(p_2) \rightarrow \gamma(p_3)q(p_4)\bar{q}(p_5)$

$$\bar{\Sigma} |M|_{q\bar{q} \rightarrow \gamma q\bar{q}}^2 = \frac{K'_{gg}}{2} C_F Q_q^2 \omega_3 M_{qqqq}(t_{15}, t_{13}, t_{14}, s_{12}, s_{35}, s_{45}, t_{25}, s_{34}, t_{23}, t_{24}). \tag{A.27}$$

A.2.7 $q(p_1)q'(p_2) \rightarrow \gamma(p_3)q(p_4)q'(p_5)$

We begin with the definitions

$$\begin{aligned}
M_0 &= \frac{-s_{12}}{t_{13}t_{23}} + \frac{t_{24}}{t_{23}s_{34}} - \frac{s_{45}}{s_{35}s_{34}} + \frac{t_{15}}{t_{13}s_{35}} \\
M_1 &= \frac{\frac{1}{2}(s_{12} - s_{45})^2 + \frac{1}{2}(t_{15} - t_{24})^2}{t_{25}t_{14}}
\end{aligned}$$

$$\begin{aligned}
M_2 &= \frac{s_{12}^2 + t_{24}^2 + t_{15}^2 + s_{45}^2}{t_{25}t_{14}} \\
M_3 &= Q_q^2 \frac{t_{14}}{t_{13}s_{34}} + Q_{q'}^2 \frac{t_{25}}{t_{23}s_{35}} \\
M_4 &= \frac{(s_{12} + s_{45})(t_{24} + t_{15})}{t_{25}t_{14}}
\end{aligned} \tag{A.28}$$

$$\begin{aligned}
M_{ppq} &= (s_{12}, t_{13}, t_{14}, t_{15}, t_{23}, t_{24}, t_{25}, s_{34}, s_{35}, s_{45}) \\
&= 2(M_2 - 2\epsilon)(Q_q Q_{q'} M_0 + M_3) - 4\epsilon(M_2 + M_4 - 2)M_3 \\
&- 2\epsilon(M_1 + M_2 + M_4 - 2)Q_q Q_{q'} M_0 .
\end{aligned} \tag{A.29}$$

and arrive at

$$\bar{\Sigma} |M|_{qq' \rightarrow \gamma qq'}^2 = \frac{K'_{qg}}{2} C_F \omega_3 M_{ppq}(s_{12}, t_{13}, t_{14}, t_{15}, t_{23}, t_{24}, t_{25}, s_{34}, s_{35}, s_{45}) . \tag{A.30}$$

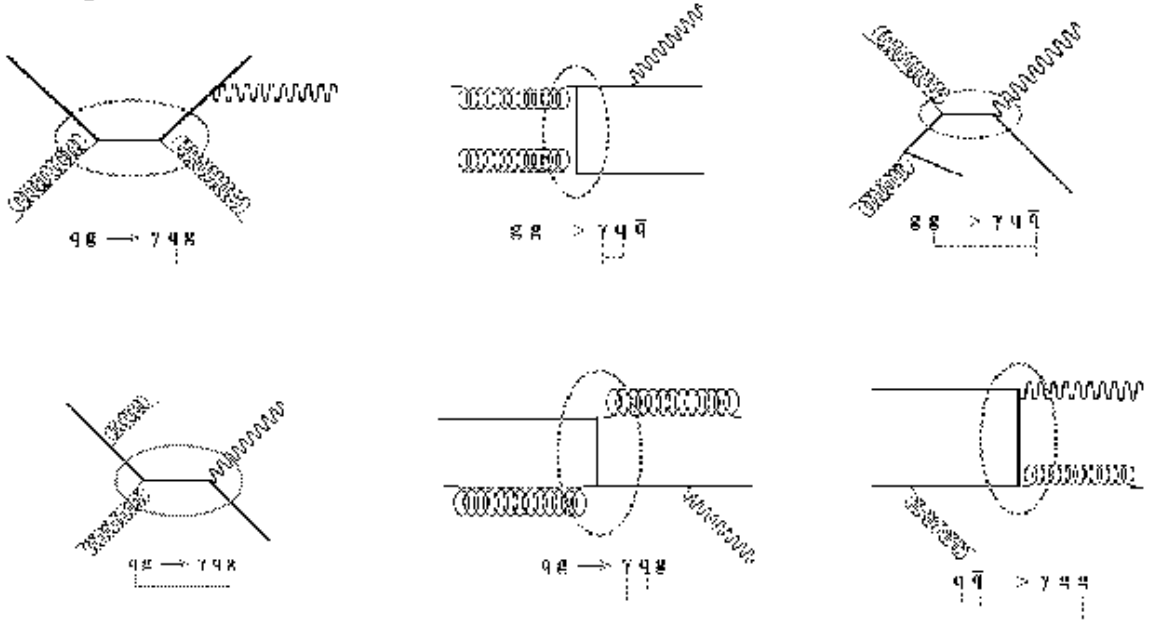
$$\mathbf{A.2.8} \quad q(p_1) \bar{q}'(p_2) \rightarrow \gamma(p_3) q(p_4) \bar{q}'(p_5)$$

$$\bar{\Sigma} |M|_{q\bar{q}' \rightarrow \gamma q\bar{q}'}^2 = \frac{K'_{qg}}{2} C_F \omega_3 M_{ppq}(t_{15}, t_{13}, t_{14}, s_{12}, s_{35}, s_{45}, t_{25}, s_{34}, t_{23}, t_{24}) . \tag{A.31}$$

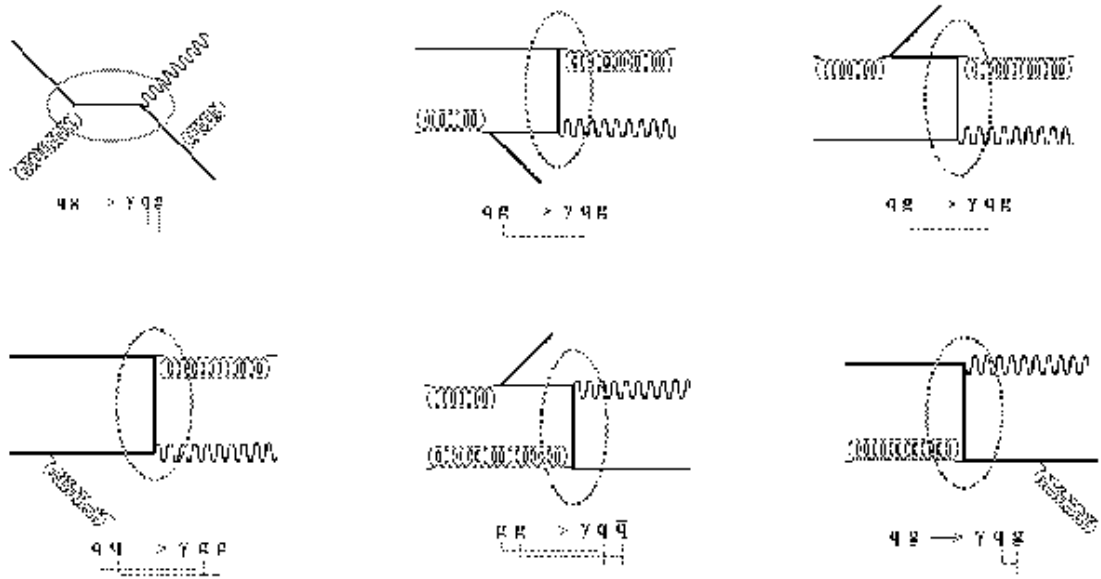
$$\mathbf{A.2.9} \quad q(p_1) \bar{q}(p_2) \rightarrow \gamma(p_3) q'(p_4) \bar{q}'(p_5)$$

$$\bar{\Sigma} |M|_{q\bar{q} \rightarrow \gamma q'\bar{q}'}^2 = \frac{K'_{qg}}{2} C_F \omega_3 M_{ppq}(t_{14}, t_{13}, s_{12}, t_{15}, s_{34}, t_{24}, s_{45}, t_{23}, s_{35}, t_{25}) . \tag{A.32}$$

Diagrams from (a)



Diagrams from (b)

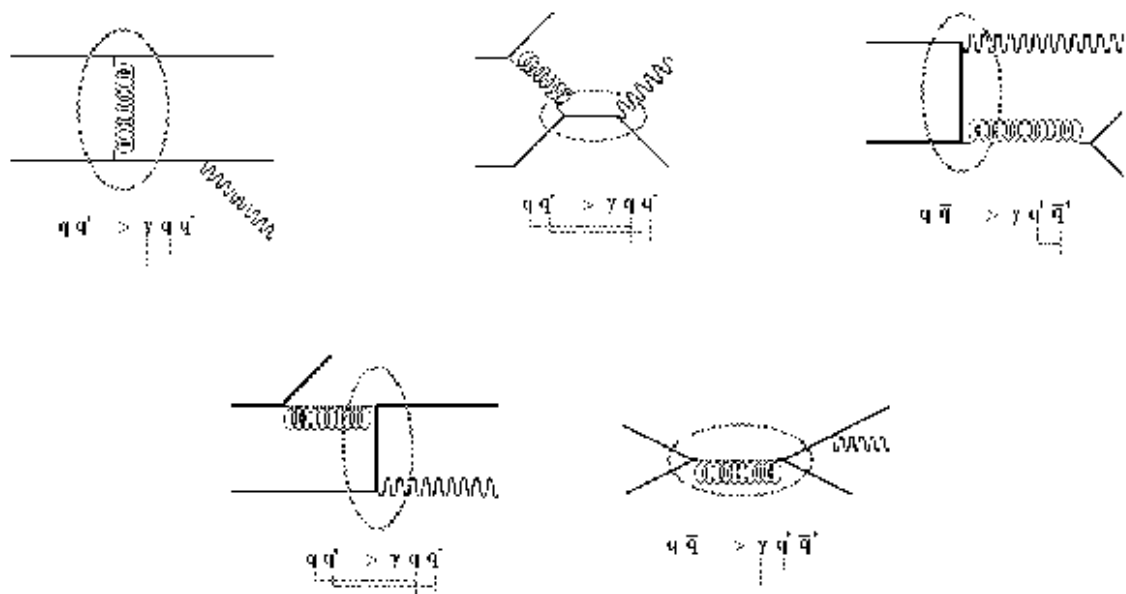


Incoming particles are on the left. Shaded ovals indicate the 2-body subprocesses referred to in the text.

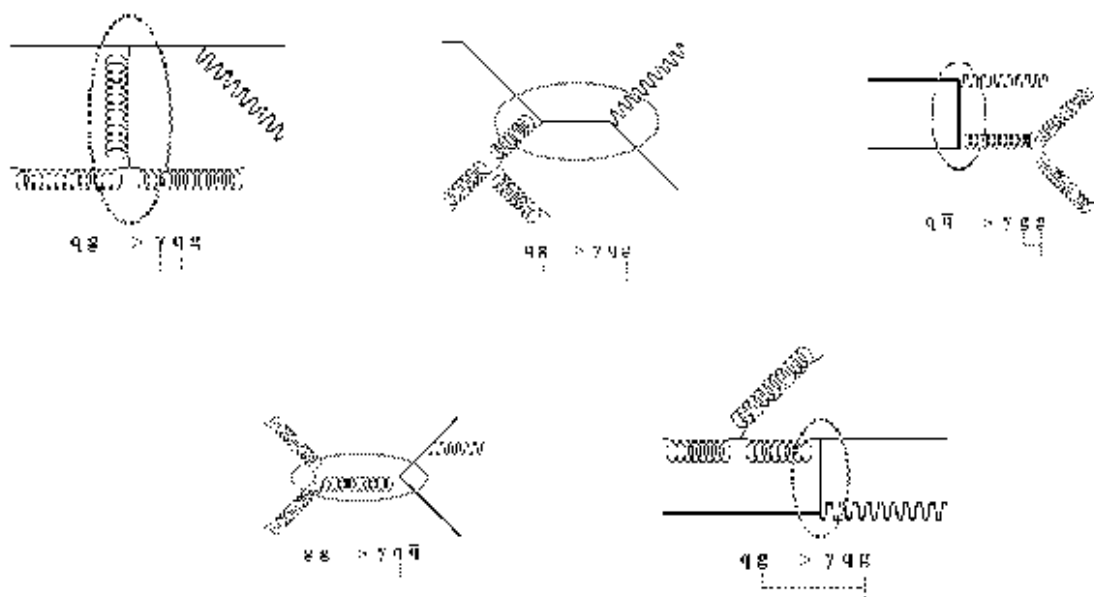
Key: quark ——— photon $\sim\sim\sim\sim$ gluon |||||

Figure A.4. Time-ordered Feynman diagrams from (a) and (b)

Diagrams from (c)



Diagrams from (d)



Horizontal bars underneath a process label indicate the potential collinearities.

The longest vertical bar indicates the particle referred to as "extra" in the text.

Figure A.5. Time-ordered Feynman diagrams from (c) and (d)

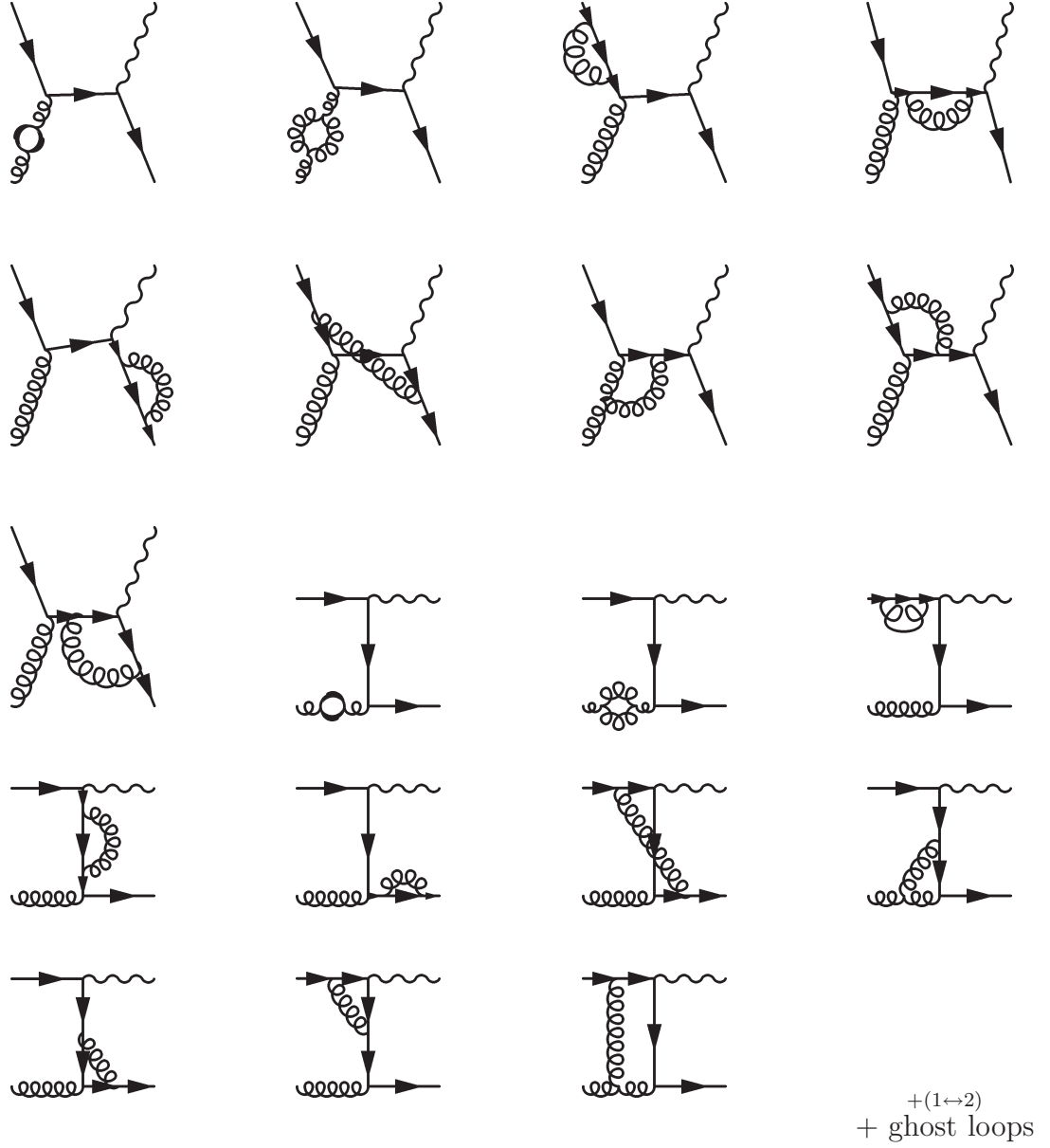


Figure A.6. Virtual Contributions.

APPENDIX B

USEFUL INTEGRALS

Here we collect the details of the y_3 and ϕ_3 integrals used in Chapter 6. Certain sub-integrals have been found in the tables of Gradshteyn and Ryzhik (G.R.) [92].

B.1 I_{ab}

$$\begin{aligned}
 I_{ab}(x) &\equiv \int_{-y_{3m}^b}^{y_{3m}^a} dy_3 \frac{e^{y_3}}{e^{y_3} + x e^{-y_3}} \\
 &= \int_{-y_{3m}^b}^{y_{3m}^a} dy_3 \frac{1}{1 + x e^{-2y_3}} \\
 &= \left[y_3 + \frac{1}{2} \ln(1 + x e^{-2y_3}) \right]_{-y_{3m}^b}^{y_{3m}^a} \quad (\text{G.R. 2.313.1}) \\
 &= y_{3m}^a + y_{3m}^b + \frac{1}{2} \ln \frac{1 + x e^{-2y_{3m}^a}}{1 + x e^{2y_{3m}^b}} .
 \end{aligned} \tag{B.1}$$

Similarly,

$$\begin{aligned}
 I_{ba}(x) &\equiv \int_{-y_{3m}^b}^{y_{3m}^a} dy_3 \frac{1}{1 + x e^{2y_3}} \\
 &= y_{3m}^a + y_{3m}^b + \frac{1}{2} \ln \frac{1 + x e^{-2y_{3m}^b}}{1 + x e^{2y_{3m}^a}} .
 \end{aligned} \tag{B.2}$$

B.2 I_{a2}, I_{b2}

$$I_{a2}(x) \equiv \int_{-y_{3m}^b}^{y_{3m}^a} dy_3 \frac{e^{\Delta y}}{x e^{-\Delta y} + \cosh \Delta y - \cos \Delta \phi}$$

$$= \int_{-y_{3m}^b - y_2}^{y_{3m}^a - y_2} d\Delta y \frac{e^{\Delta y}}{x e^{-\Delta y} + \cosh \Delta y - \cos \Delta \phi}, \quad (\text{B.3})$$

with $\Delta y \equiv y_3 - y_2$, $\Delta \phi \equiv \phi_3 - \phi_2$. With the change of variable $\eta \equiv e^{\Delta y}$ ($\eta_{LO} = e^{-y_{3m}^b - y_2}$, $\eta_{HI} = e^{y_{3m}^a - y_2}$) we can write this as

$$\begin{aligned} \int_{\eta_{LO}}^{\eta_{HI}} \frac{2\eta d\eta}{\eta^2 - 2\eta \cos \Delta \phi + (1 + 2x)} &= \int_{\eta_{LO}}^{\eta_{HI}} \frac{2\eta d\eta}{\eta^2 + (1 + 2x)} \\ &+ \int_0^\infty d\eta \left[\frac{2\eta}{\eta^2 - 2\eta \cos \Delta \phi + (1 + 2x)} - \frac{2\eta}{\eta^2 + (1 + 2x)} \right], \end{aligned} \quad (\text{B.4})$$

where the new limits are justified because in either the soft or collinear regions, $\{y_{3m}^a, y_{3m}^b, \eta\}$ all go to infinity, and the second integrand above goes to zero.

The first term is easy:

$$\int_{\eta_{LO}^2}^{\eta_{HI}^2} \frac{d\eta^2}{\eta^2 + (1 + 2x)} = \ln \frac{e^{2(y_{3m}^a - y_2)} + (1 + 2x)}{e^{-2(y_{3m}^b + y_2)} + (1 + 2x)}, \quad (\text{B.5})$$

while the second term, after defining $\cos \alpha \equiv \cos \Delta \phi / \sqrt{1 + 2x}$, can be partial-fractioned as

$$\begin{aligned} \int_0^\infty d\eta \left[\frac{2\eta}{2i \sin \alpha \sqrt{1 + 2x}} \right. &\left. \left[\frac{1}{\eta - e^{i\alpha} \sqrt{1 + 2x}} - \frac{1}{\eta - e^{-i\alpha} \sqrt{1 + 2x}} \right] \right. \\ &\left. - \left[\frac{1}{\eta - i\sqrt{1 + 2x}} + \frac{1}{\eta + i\sqrt{1 + 2x}} \right] \right]. \end{aligned} \quad (\text{B.6})$$

The first set of fractions has the form $z - z^* = 2i\mathcal{IM}(z)$ for complex z , while the second set looks like $z + z^* = 2\mathcal{RE}(z)$. In this way, we can rewrite the integral as

$$\int_0^\infty d\eta \frac{2}{\sqrt{1 + 2x} \sin \alpha} \mathcal{IM} \left[\frac{\eta}{\eta - e^{i\alpha} \sqrt{1 + 2x}} \right] - \int_0^\infty d\eta 2\mathcal{RE} \left[\frac{1}{\eta - i\sqrt{1 + 2x}} \right], \quad (\text{B.7})$$

where

$$\mathcal{IM}\left[\frac{\eta}{\eta - e^{i\alpha}\sqrt{1+2x}}\right] = \mathcal{IM}\left[1 + \frac{e^{i\alpha}\sqrt{1+2x}}{\eta - e^{i\alpha}\sqrt{1+2x}}\right] = \mathcal{IM}\left[\frac{e^{i\alpha}\sqrt{1+2x}}{\eta - e^{i\alpha}\sqrt{1+2x}}\right], \quad (\text{B.8})$$

and so

$$\begin{aligned} \int_0^\infty d\eta \frac{2}{\sqrt{1+2x} \sin \alpha} \mathcal{IM}\left[\frac{\eta}{\eta - e^{i\alpha}\sqrt{1+2x}}\right] &= 2\mathcal{IM}\left[\frac{e^{i\alpha}}{\sin \alpha} \int_0^\infty \frac{d\eta}{\eta - e^{i\alpha}\sqrt{1+2x}}\right] \\ &= 2\mathcal{IM}\left[\frac{e^{i\alpha}}{\sin \alpha} \ln(\eta - e^{i\alpha}\sqrt{1+2x})\right] \Big|_0^\infty. \end{aligned} \quad (\text{B.9})$$

Meanwhile,

$$\int_0^\infty d\eta 2\mathcal{RE}\left[\frac{1}{\eta - i\sqrt{1+2x}}\right] = 2\mathcal{RE}\left[\ln(\eta - i\sqrt{1+2x})\right]_0^\infty, \quad (\text{B.10})$$

So, since

$$\begin{aligned} e^{i\alpha} &= \cos \alpha + i \sin \alpha \\ \ln(\eta - e^{i\alpha}\sqrt{1+2x}) &= \ln \sqrt{(\eta - e^{i\alpha}\sqrt{1+2x})(\eta - e^{-i\alpha}\sqrt{1+2x})} \\ &\quad + i \tan^{-1}\left[\frac{-\sqrt{1+2x} \sin \alpha}{\eta - \sqrt{1+2x} \cos \alpha}\right], \end{aligned} \quad (\text{B.11})$$

we have

$$\begin{aligned} \mathcal{IM}\left[e^{i\alpha} \ln(\eta - e^{i\alpha}\sqrt{1+2x})\right] &= \sin \alpha \ln \sqrt{\eta^2 + (1+2x) - 2\eta\sqrt{1+2x} \cos \alpha} \\ &\quad + \cos \alpha \tan^{-1}\left[\frac{-\sqrt{1+2x} \sin \alpha}{\eta - \sqrt{1+2x} \cos \alpha}\right] \\ 2\mathcal{RE} \ln(\eta - i\sqrt{1+2x}) &= 2 \ln \sqrt{(\eta - i\sqrt{1+2x})(\eta + i\sqrt{1+2x})} \\ &= \ln(\eta^2 + (1+2x)). \end{aligned} \quad (\text{B.12})$$

Putting it all together, we obtain

$$\begin{aligned} \left[\ln \frac{\eta^2 + (1+2x) - 2\eta\sqrt{1+2x}\cos\alpha}{\eta^2 + (1+2x)} \right]_0^\infty &+ 2 \left[\cot\alpha \tan^{-1} \frac{-\sqrt{1+2x}\sin\alpha}{\eta - \sqrt{1+2x}\cos\alpha} \right]_0^\infty \\ &= 2 \cot\alpha [\pi - \alpha] , \end{aligned} \quad (\text{B.13})$$

and so

$$I_{a2}(x) = \ln \left[\frac{e^{2(y_{3m}^a - y_2)} + (1+2x)}{e^{2(-y_{3m}^b - y_2)} + (1+2x)} \right] + 2 \cot\alpha [\pi - \alpha] . \quad (\text{B.14})$$

$I_{b2}(x)$ will be similar. We here have

$$I_{b2}(x) \equiv \int_{y_2+y_{3m}^b}^{y_2-y_{3m}^a} d\Delta y \frac{e^{-\Delta y}}{xe^{\Delta y} + \cosh \Delta y - \cos \Delta \phi} , \quad (\text{B.15})$$

which, by comparison with equation B.3, can be obtained via the negative of I_{a2} with the signs of the limits reversed. We then get

$$I_{b2}(x) = \ln \left[\frac{e^{2(y_{3m}^b + y_2)} + (1+2x)}{e^{2(-y_{3m}^a + y_2)} + (1+2x)} \right] + 2 \cot\alpha [\pi - \alpha] . \quad (\text{B.16})$$

Again, $\cos\alpha \equiv \cos\Delta\phi/\sqrt{1+2x}$.

B.3 $I_{2a,2b}$

$$I_{2a}(x) \equiv \int_{-\infty}^{\infty} d\Delta y \frac{1}{\cosh \Delta y - \cos \Delta \phi} \left[\frac{x}{xe^{-\Delta y} + \cosh \Delta y - \cos \Delta \phi} - 1 \right] . \quad (\text{B.17})$$

To start, consider the first term, which can be partial fractioned as follows:

$$\begin{aligned} \tilde{I}_{2a}(x) &\equiv \int_{-\infty}^{\infty} d\Delta y \left[\frac{e^{\Delta y}}{\cosh \Delta y - \cos \Delta \phi} - \frac{e^{\Delta y}}{xe^{-\Delta y} + \cosh \Delta y - \cos \Delta \phi} \right] \\ &= 2 \int_0^\infty d\eta \left[\frac{\eta}{\eta^2 - 2\eta \cos \Delta \phi + 1} - \frac{\eta}{\eta^2 - 2\eta \cos \Delta \phi + (1+2x)} \right] , \end{aligned} \quad (\text{B.18})$$

in which we've defined $\eta \equiv e^{\Delta y}$. Each of these terms can itself be partial-fractioned and simplified as follows:

$$\begin{aligned}
\frac{\eta}{\eta^2 - 2\eta \cos \Delta\phi + 1} &= \frac{\eta}{(\eta - e^{i\Delta\phi})(\eta - e^{-i\Delta\phi})} \\
&= \frac{1}{2i \sin \Delta\phi} \left[\frac{\eta}{\eta - e^{i\Delta\phi}} - \frac{\eta}{\eta - e^{-i\Delta\phi}} \right] \\
&= \frac{1}{\sin \Delta\phi} \mathcal{IM} \left[\frac{\eta}{\eta - e^{i\Delta\phi}} \right]; \tag{B.19}
\end{aligned}$$

... while, with the designation $\cos \alpha \equiv \cos \Delta\phi / \sqrt{1+2x}$, we also have

$$\begin{aligned}
\frac{\eta}{\eta^2 - 2\eta \cos \Delta\phi + (1+2x)} &= \frac{\eta}{(\eta - \sqrt{1+2x}e^{i\alpha})(\eta - \sqrt{1+2x}e^{-i\alpha})} \\
&= \frac{1}{2i \sin \alpha \sqrt{1+2x}} \left[\frac{\eta}{\eta - \sqrt{1+2x}e^{i\alpha}} - \frac{\eta}{\eta - \sqrt{1+2x}e^{-i\alpha}} \right] \\
&= \frac{1}{\sin \alpha \sqrt{1+2x}} \mathcal{IM} \left[\frac{\eta}{\eta - \sqrt{1+2x}e^{i\alpha}} \right]. \tag{B.20}
\end{aligned}$$

We're now left with the simple integrals

$$\begin{aligned}
\int_0^\infty d\eta \frac{\eta}{(\eta - e^{i\Delta\phi})} &= \left[(\eta - e^{i\Delta\phi}) + e^{i\Delta\phi} \ln(\eta - e^{i\Delta\phi}) \right]_0^\infty \\
\int_0^\infty d\eta \frac{\eta}{(\eta - \sqrt{1+2x}e^{i\Delta\phi})} &= \left[(\eta - \sqrt{1+2x}e^{i\Delta\phi}) + \sqrt{1+2x}e^{i\Delta\phi} \ln(\eta - \sqrt{1+2x}e^{i\Delta\phi}) \right]_0^\infty, \tag{B.21}
\end{aligned}$$

the imaginary parts of which we now evaluate (before taking limits). Of use will be the identities

$$\begin{aligned}
e^{\pm i\phi} &= \cos \phi \pm i \sin \phi \\
\ln z &= \frac{1}{2} \ln z z^* + i \tan^{-1} \left[\frac{\mathcal{IM}(z)}{\mathcal{RE}(z)} \right], \tag{B.22}
\end{aligned}$$

which lead to

$$\mathcal{IM} \left[(\eta - e^{i\Delta\phi}) + e^{i\Delta\phi} \ln(\eta - e^{i\Delta\phi}) \right]$$

$$\begin{aligned}
&= -\sin \Delta\phi + \frac{1}{2} \sin \Delta\phi \ln(\eta^2 - 2\eta \cos \Delta\phi + 1) \\
&+ \cos \Delta\phi \tan^{-1} \left[\frac{-\sin \Delta\phi}{\eta - \cos \Delta\phi} \right]
\end{aligned} \tag{B.23}$$

$$\begin{aligned}
\mathcal{IM} \left[(\eta - \sqrt{1+2x}e^{i\Delta\phi}) + \sqrt{1+2x}e^{i\Delta\phi} \ln(\eta - \sqrt{1+2x}e^{i\Delta\phi}) \right] \\
&= \frac{\sqrt{1+2x} \sin \alpha}{2} \ln(\eta^2 - 2\eta\sqrt{1+2x} \cos \alpha + (1+2x)) \\
&- \sqrt{1+2x} \sin \alpha \\
&+ \sqrt{1+2x} \cos \alpha \tan^{-1} \left[\frac{-\sqrt{1+2x} \sin \alpha}{\eta - \sqrt{1+2x} \cos \alpha} \right].
\end{aligned} \tag{B.24}$$

Adding these two results, with the proper coefficients from equation B.19, and taking the indicated limits results in:

$$\tilde{I}_{2a}(x) = \ln(1+2x) + 2 \cot \Delta\phi (\pi - \Delta\phi) - 2 \cot \alpha (\pi - \alpha). \tag{B.25}$$

From equation B.17, we see that we still need the integral

$$\begin{aligned}
\hat{I}_{2a}(x) &\equiv \int_{-\infty}^{\infty} \frac{d\Delta y}{\cosh \Delta y - \cos \Delta\phi} \\
&= 2 \int_0^{\infty} \frac{d\eta}{\eta^2 - 2\eta \cos \Delta\phi + 1} \\
&= 2 \int_0^{\infty} \frac{d\eta}{2i \sin \Delta\phi} \left[\frac{1}{\eta - e^{i\Delta\phi}} - \frac{1}{\eta - e^{-i\Delta\phi}} \right] \\
&= \frac{2}{\sin \Delta\phi} \mathcal{IM} \int_0^{\infty} \frac{d\eta}{\eta - e^{i\Delta\phi}} \\
&= \frac{2}{\sin \Delta\phi} \mathcal{IM} \ln(\eta - e^{i\Delta\phi}) \Big|_0^{\infty} \\
&= \frac{2}{\sin \Delta\phi} \tan^{-1} \left[\frac{-\sin \Delta\phi}{\eta - \cos \Delta\phi} \right] \Big|_0^{\infty} \\
&= \frac{2}{\sin \Delta\phi} (\pi - \Delta\phi).
\end{aligned} \tag{B.26}$$

This then makes

$$\begin{aligned}
I_{2a}(x) &= \tilde{I}_{2a}(x) - \hat{I}_{2a}(x) \\
&= \ln(1+2x) + 2 \frac{(\cos \Delta\phi - 1)}{\sin \Delta\phi} (\pi - \Delta\phi) - 2 \cot \alpha (\pi - \alpha) . \quad (\text{B.27})
\end{aligned}$$

Since I_{2b} is the same as I_{2a} with $\Delta y \rightarrow -\Delta y$, but both are symmetric with respect to this transformation, we have $I_{2b}(x) = I_{2a}(x)$.

B.4 I_2^c

$$\begin{aligned}
\int d^{1-2\epsilon} \phi_3 I_2^c(\phi_3) &\equiv \int d^{1-2\epsilon} \phi_3 \frac{2(\pi - \Delta\phi)}{\sin \Delta\phi} \\
&= \int d^{1-2\epsilon} \Delta\phi \left[\frac{2(\pi - \Delta\phi)(1 - \cos \Delta\phi)}{\sin \Delta\phi} + \frac{2(\pi - \Delta\phi) \cos \Delta\phi}{\sin \Delta\phi} \right] , \quad (\text{B.28})
\end{aligned}$$

where the last term is

$$\int d^{1-2\epsilon} \Delta\phi \frac{2(\pi - \Delta\phi) \cos \Delta\phi}{\sin \Delta\phi} = 2 \int d\Omega_{1-2\epsilon} \int_0^\pi d\Delta\phi \sin^{-1-2\epsilon} \Delta\phi \cos \Delta\phi (\pi - \Delta\phi) . \quad (\text{B.29})$$

Now, since $\cos \Delta\phi$ is odd around $\pi/2$, we have

$$\pi \int_0^\pi d\Delta\phi \sin^{-1-2\epsilon} \Delta\phi \cos \Delta\phi = 0 , \quad (\text{B.30})$$

while

$$\int_0^\pi d\Delta\phi \sin^{-1-2\epsilon} \Delta\phi \cos \Delta\phi \Delta\phi$$

can be integrated by parts to give

$$\frac{\Delta\phi}{-2\epsilon} \sin^{-2\epsilon} \Delta\phi \Big|_0^\pi - \int_0^\pi d\Delta\phi \frac{\sin^{-2\epsilon}}{-2\epsilon} = \frac{\sqrt{\pi} \Gamma(\frac{1}{2} - \epsilon)}{2\epsilon \Gamma(1 - \epsilon)} . \quad (\text{B.31})$$

Since

$$\begin{aligned}\int d\Omega_{1-2\epsilon} &= \frac{2\pi^{1/2-\epsilon}}{\Gamma(\frac{1}{2}-\epsilon)} \\ \int d^{1-2\epsilon}\phi &\equiv \int d\Omega_{2-2\epsilon} = \frac{2\pi^{1-\epsilon}}{\Gamma(1-\epsilon)},\end{aligned}\tag{B.32}$$

it follows that

$$\int d^{1-2\epsilon}\Delta\phi \frac{2(\pi - \Delta\phi) \cos \Delta\phi}{\sin \Delta\phi} = -\frac{1}{\epsilon} \int d^{1-2\epsilon}\phi_3, \tag{B.33}$$

and thus, in the sense of a distribution,

$$\int d^{1-2\epsilon}\phi_3 I_2^c(\phi_3) = \int d^{1-2\epsilon}\phi_3 \left[\frac{2(\pi - \Delta\phi)(1 - \cos \Delta\phi)}{\sin \Delta\phi} - \frac{1}{\epsilon} \right]. \tag{B.34}$$

It will be useful to perform this integral fully as well. Concentrating on the first term, we can choose a change of variable $w \equiv (1 + \cos \Delta\phi)/2$, which leads to

$$\begin{aligned}\sin^2 \Delta\phi &= 4w(1-w) \\ dw &= -\frac{1}{2} \sin \Delta\phi d\Delta\phi \\ \Delta\phi &= -2i \ln(\sqrt{w} + i\sqrt{1-w}),\end{aligned}\tag{B.35}$$

and the integral

$$\begin{aligned}\int d^{1-2\epsilon}\phi_3 \frac{2(\pi - \Delta\phi)(1 - \cos \Delta\phi)}{\sin \Delta\phi} &= \int_0^1 dw 4^{-\epsilon} w^{-1-\epsilon} (1-w)^{-\epsilon} \\ &\times \left(\pi + 2i \ln(\sqrt{w} + i\sqrt{1-w}) \right).\end{aligned}\tag{B.36}$$

The log term can be integrated by parts. With

$$\begin{aligned}u &\equiv \ln(\sqrt{w} + i\sqrt{1-w}) \\ dv &\equiv dw w^{-1-\epsilon} (1-w)^{-\epsilon},\end{aligned}\tag{B.37}$$

we find both $du = -\frac{i dw}{2\sqrt{w}\sqrt{1-w}}$ and

$$v = \int dw w^{-1-\epsilon}(1-w)^{-\epsilon} = -\frac{w^{-\epsilon}(1-w)^{-\epsilon}}{\epsilon} - \int dw w^{-\epsilon}(1-w)^{-1-\epsilon}, \quad (\text{B.38})$$

the latter term of which is $\int dw w^{-1-\epsilon}(1-w)^{-\epsilon} + \frac{1}{\epsilon}w^{-\epsilon}(1-w)^{-\epsilon}$ by symmetry. We then have

$$v = -\frac{w^{-\epsilon}(1-w)^{-\epsilon}}{\epsilon}, \quad (\text{B.39})$$

so that

$$\begin{aligned} \int_0^1 dw w^{-1-\epsilon}(1-w)^{-\epsilon} \ln(\sqrt{w} + i\sqrt{1-w}) &= \\ -\frac{w^{-\epsilon}(1-w)^{-\epsilon}}{\epsilon} \ln(\sqrt{w} + i\sqrt{1-w}) \Big|_0^1 &- \frac{i}{2\epsilon} \int_0^1 dw w^{-\frac{1}{2}-\epsilon}(1-w)^{-\frac{1}{2}-\epsilon} \\ &= -\frac{i\pi}{2\epsilon} 16^\epsilon \frac{\Gamma(1-2\epsilon)}{\Gamma^2(1-\epsilon)}. \end{aligned} \quad (\text{B.40})$$

This gives, finally,

$$\begin{aligned} \int d^{1-2\epsilon} \phi_3 \frac{2(\pi - \Delta\phi)(1 - \cos \Delta\phi)}{\sin \Delta\phi} &= \frac{1}{\epsilon} \left[1 - \frac{16^{-\epsilon} \Gamma^4(1-\epsilon)}{\Gamma^2(1-2\epsilon)} \right] \frac{2\pi^{1-\epsilon}}{\Gamma(1-\epsilon)} \\ &= \frac{1}{\epsilon} \left[1 - \frac{16^{-\epsilon} \Gamma^4(1-\epsilon)}{\Gamma^2(1-2\epsilon)} \right] \int d^{1-2\epsilon} \phi_3, \end{aligned} \quad (\text{B.41})$$

from which

$$\int d^{1-2\epsilon} \phi_3 I_2^c(\phi_3) = -\frac{16^{-\epsilon}}{\epsilon} \frac{\Gamma^4(1-\epsilon)}{\Gamma^2(1-2\epsilon)} \int d^{1-2\epsilon} \phi_3 \quad (\text{B.42})$$

follows by addition of equation B.33.

B.5 $I_{2a}^{2b}(x) - I_2^c$

This integral is not used in the text, but may be useful to those interested in treating all final-state pieces with a common $Q_T = 0$ definition. The crucial integral here is

$$\begin{aligned}
\int d^{1-2\epsilon} \Delta\phi(\pi - \alpha) \cot \alpha &= \int d\Omega_{1-2\epsilon} \int_0^\pi d\Delta\phi(\pi - \alpha) \cot \alpha \sin^{-2\epsilon} \Delta\phi \\
&\equiv I_1(I_2 - 2\epsilon I_3)
\end{aligned} \tag{B.43}$$

to $\mathcal{O}(\epsilon)$, where

$$\begin{aligned}
I_1 &\equiv \int d\Omega_{1-2\epsilon} = \frac{2}{(4\pi)^\epsilon} \frac{\Gamma(1-\epsilon)}{\Gamma(1-2\epsilon)} = \frac{4^{-\epsilon}}{\pi} \frac{\Gamma^2(1-\epsilon)}{\Gamma(1-2\epsilon)} \int d^{1-2\epsilon} \phi \\
I_2 &\equiv \int_0^\pi d\Delta\phi(\pi - \alpha) \cot \alpha \\
I_3 &\equiv \frac{\pi}{2} h(x), \quad \text{where} \\
h(x) &\equiv \frac{2}{\pi} \int_0^\pi d\Delta\phi(\pi - \alpha) \cot \alpha \ln \sin \Delta\phi.
\end{aligned} \tag{B.44}$$

I_2 can be evaluated as follows:

$$\begin{aligned}
d \cos \alpha &= -\sin \alpha d\alpha = -\frac{\sin \Delta\phi d\Delta\phi}{\sqrt{1+2x}} \\
\sin \Delta\phi &= \sqrt{1 - \cos^2 \Delta\phi} = \sqrt{1+2x} \sqrt{\sin^2 \alpha - \frac{2x}{1+2x}} \\
\alpha(\Delta\phi = 0) &= \cos^{-1}\left(\frac{1}{\sqrt{1+2x}}\right) \\
\alpha(\Delta\phi = \pi) &= \cos^{-1}\left(\frac{-1}{\sqrt{1+2x}}\right),
\end{aligned} \tag{B.45}$$

and so

$$I_2 = \int_{\cos^{-1}(1/\sqrt{1+2x})}^{\cos^{-1}(-1/\sqrt{1+2x})} \frac{d\alpha(\pi - \alpha) \cos \alpha}{\sqrt{\sin^2 \alpha - \frac{2x}{1+2x}}}. \tag{B.46}$$

Now, with $\pi - \alpha = \frac{\pi}{2} + (\frac{\pi}{2} - \alpha)$, this can be broken up into two terms, the first of which is odd about $\pi/2$ and the second even. Since our limits of integration straddle $\pi/2$ evenly, integration over the first term gives zero, while the second term gives the same integral from $\cos^{-1}(\frac{1}{\sqrt{1+2x}}) \leq \alpha \leq \frac{\pi}{2}$ as it does from $\frac{\pi}{2} \leq \alpha \leq \cos^{-1}(\frac{1}{\sqrt{1+2x}})$. Thus

$$I_2 = 2 \int_{\cos^{-1}(1/\sqrt{1+2x})}^{\pi/2} d\alpha \frac{(\frac{\pi}{2} - \alpha) \cos \alpha}{\sqrt{\sin^2 \alpha - \frac{2x}{1+2x}}} . \quad (\text{B.47})$$

The first term here can be evaluated using the change of variable $y \equiv \sin \alpha$, which yields

$$\begin{aligned} dy &= \cos \alpha d\alpha \\ y_0 \equiv y(\alpha_0) &= \sin \cos^{-1}\left(\frac{1}{\sqrt{1+2x}}\right) = \sqrt{\frac{2x}{1+2x}} \end{aligned} \quad (\text{B.48})$$

and thus

$$\pi \int_{y_0}^1 \frac{dy}{\sqrt{y^2 - y_0^2}} = \pi \ln 2 \left(y + \sqrt{y^2 - y_0^2} \right) \Big|_{y_0}^1 = \pi \ln \frac{1 + \sqrt{1+2x}}{\sqrt{2x}} \quad (\text{B.49})$$

by G.R. 2.261. The second term can be obtained via G.R. 3.842.2 with $u \equiv \cos^{-1}(1/\sqrt{1+2x})$:

$$2 \int_u^{\pi/2} \frac{d\alpha \cos \alpha}{\sqrt{\sin^2 \alpha - \frac{2x}{1+2x}}} = \pi \ln(1 + \cos u) = \pi \ln \frac{1 + \sqrt{1+2x}}{\sqrt{1+2x}} . \quad (\text{B.50})$$

Thus

$$I_2 = \pi \ln \frac{1 + \sqrt{1+2x}}{\sqrt{2x}} - \pi \ln \frac{1 + \sqrt{1+2x}}{\sqrt{1+2x}} = \frac{\pi}{2} \ln \frac{1+2x}{2x} , \quad (\text{B.51})$$

and so, to $\mathcal{O}(\epsilon)$

$$\int d^{1-2\epsilon} \Delta \phi(\pi - \alpha) \cot \alpha = 4^{-\epsilon} \frac{\Gamma^2(1-\epsilon)}{\Gamma(1-2\epsilon)} \left[\frac{1}{2} \ln \frac{1+2x}{2x} - \epsilon h(x) \right] \int d^{1-2\epsilon} \phi . \quad (\text{B.52})$$

Now, from equations 6.80 and 6.81, we find that

$$\int d^{1-2\epsilon} \phi_3(I_{2a}(x) - I_2^c)$$

$$\begin{aligned}
&= \int d^{1-2\epsilon} \Delta \phi \left[\ln(1+2x) - 2 \frac{(\pi - \Delta \phi)(1 - \cos \Delta \phi)}{\sin \Delta \phi} - 2(\pi - \alpha(x)) \cot \alpha(x) \right] \\
&= \left[\ln(1+2x) - \frac{1}{\epsilon} + \frac{16^{-\epsilon}}{\epsilon} \frac{\Gamma^4(1-\epsilon)}{\Gamma^2(1-2\epsilon)} - 4^{-\epsilon} \frac{\Gamma^2(1-\epsilon)}{\Gamma(1-2\epsilon)} \left(\ln \frac{1+2x}{2x} - 2\epsilon h(x) \right) \right] \\
&\times \int d^{1-2\epsilon} \phi \\
&\simeq \left[(\ln 2x - \ln 16) + \epsilon \left(2h(x) + \ln 4 \ln \frac{1+2x}{2x} + \frac{1}{2} \ln^2 16 - \frac{\pi^2}{3} \right) \right] \int d^{1-2\epsilon} \phi \text{(B.53)}
\end{aligned}$$

APPENDIX C

DETAILED NLO RESULTS

If we write out our Γ_{mn} factors from Chapter 6 grouped by Q_T -dependence (and including poles):

$$\begin{aligned}
\Gamma_{mn} \equiv & \delta(Q_T) \left(\frac{{}_2\Gamma_{mn}}{\epsilon^2} + \frac{{}_1\Gamma_{mn}}{\epsilon} \right) + \delta(Q_T) {}_\delta C_{mn} \\
& + \delta(Q_T) \left[\sum_{\bar{a}} \int_{x_a}^1 \frac{dz}{z} \frac{H(x_a/z, x_b)}{H(x_a, x_b)} {}_{\bar{a}}C_{mn}(z) \right. \\
& + \left. \sum_{\bar{b}} \int_{x_b}^1 \frac{dz}{z} \frac{H(x_a, x_b/z)}{H(x_a, x_b)} {}_{\bar{b}}C_{mn}(z) \right] \\
& - 4A_{mn} \left[\frac{\ln Q_T/Q}{Q_T} \right]_+ + 2B_{mn} \left[\frac{1}{Q_T} \right]_+ \\
& + \left[\frac{2}{Q_T} \right]_+ \left[{}_a D_{mn} \sum_{\bar{a}} \int_{x_a}^1 \frac{dz}{z} \frac{H(x_a/z, x_b)}{H(x_a, x_b)} P_{a\bar{a}}^+(z) \right. \\
& + \left. {}_b D_{mn} \sum_{\bar{b}} \int_{x_b}^1 \frac{dz}{z} \frac{H(x_a, x_b/z)}{H(x_a, x_b)} P_{b\bar{b}}^+(z) \right], \tag{C.1}
\end{aligned}$$

then each Γ_{mn} is specified by writing out $\{{}_2\Gamma, {}_1\Gamma, {}_\delta C, {}_{\bar{a}}C, {}_{\bar{b}}C, A, B, {}_a D, {}_b D\}$ for each $\{mn\}$. On the next few pages, we'll lay out our findings for these parameters. As usual, $C_F = 4/3$, $N_C = 3$, and N_f is the number of participating flavors at the appropriate renormalization scale μ . In general, each Γ_{mn} will depend on the subprocess under consideration, labeled in the text by the index i , or more specifically by indices $\{a, b, d\}$ over the types of partons participating in the subprocess $ab \rightarrow \gamma d$, for instance $qg \rightarrow \gamma q$. For the virtual contributions, each $\Gamma_{(i)}$ is presented independently. The rest are expressed in terms of constants $C(f)$ and $\gamma(f)$, where

$$\begin{aligned}
C(q) &\equiv C_F \\
C(g) &\equiv N_C \\
\gamma(q) &\equiv \frac{3}{2}C_F \\
\gamma(g) &\equiv \frac{11N_C - 2N_f}{6}
\end{aligned} \tag{C.2}$$

For example, $C(a) + C(b) - C(d)$ for $q\bar{q} \rightarrow \gamma g$ is $2C_F - N_C$.

C.1 Γ_{Virt}

$${}_2\Gamma_{Virt}^{(q\bar{q} \rightarrow \gamma g)} = -(2C_F + N_C) \tag{C.3}$$

$${}_1\Gamma_{Virt}^{(q\bar{q} \rightarrow \gamma g)} = -3C_F - \frac{(11N_C - 2N_f)}{6} + (2C_F - N_C) \ln \frac{\hat{s}}{M_f^2} + N_C \ln \frac{\hat{t}\hat{u}}{M_f^4} \tag{C.4}$$

$$A_{Virt}^{(q\bar{q} \rightarrow \gamma g)} = 0 \tag{C.5}$$

$$B_{Virt}^{(q\bar{q} \rightarrow \gamma g)} = 0 \tag{C.6}$$

$${}_\delta C_{Virt}^{(q\bar{q} \rightarrow \gamma g)} = \left[A_{0\nu} + \frac{B_\nu}{T_0} \right]_{(q\bar{q} \rightarrow \gamma g)} - (2C_F + N_C) \frac{\pi^2}{6} \tag{C.7}$$

$${}_a C_{Virt}^{(q\bar{q} \rightarrow \gamma g)} = 0 \tag{C.8}$$

$${}_b C_{Virt}^{(q\bar{q} \rightarrow \gamma g)} = 0 \tag{C.9}$$

$${}_a D_{Virt}^{(q\bar{q} \rightarrow \gamma g)} = 0 \tag{C.10}$$

$${}_b D_{Virt}^{(q\bar{q} \rightarrow \gamma g)} = 0 \tag{C.11}$$

where

$$\begin{aligned}
A_{0\nu}^{(q\bar{q} \rightarrow \gamma g)} &= -2 \left(C_F + \frac{N_C}{2} \right) \left[-\frac{\pi^2}{6} + \frac{1}{2} \ln^2 \frac{M_f^2}{\hat{s}} \right] - \frac{(11N_C - 2N_f)}{6} \ln \frac{\hat{s}}{\mu^2} \\
&- \left[3C_F + \frac{(11N_C - 2N_f)}{6} + N_C \ln \left| \frac{\hat{s}^2}{\hat{t}\hat{u}} \right| \right] \ln \frac{M_f^2}{\hat{s}} \\
&+ \left(2C_F - \frac{N_C}{2} \right) \frac{\pi^2}{3} - 7C_F + C_F \left(\ln^2 \left| \frac{\hat{t}}{\hat{s}} \right| + \ln^2 \left| \frac{\hat{u}}{\hat{s}} \right| \right)
\end{aligned}$$

$$- \frac{N_C}{2} \ln^2 \frac{\hat{s}^2}{\hat{t}\hat{u}} \quad (C.12)$$

$$\begin{aligned} B_\nu^{(q\bar{q} \rightarrow \gamma g)} &= 3C_F \left| \frac{\hat{t}}{\hat{u}} \right| \ln \left| \frac{\hat{u}}{\hat{s}} \right| \\ &+ \left(C_F - \frac{N_C}{2} \right) \left[\left(2 + \left| \frac{\hat{u}}{\hat{t}} \right| \right) \ln^2 \left| \frac{\hat{s}}{\hat{u}} \right| + \left(2 + \left| \frac{\hat{t}}{\hat{u}} \right| \right) \ln^2 \left| \frac{\hat{s}}{\hat{t}} \right| \right] \\ &+ 3C_F \left| \frac{\hat{u}}{\hat{t}} \right| \ln \left| \frac{\hat{t}}{\hat{s}} \right| + 2 \left(C_F - \frac{N_C}{2} \right) \ln \left| \frac{\hat{t}\hat{u}}{\hat{s}^2} \right| \end{aligned} \quad (C.13)$$

$$T_0^{(q\bar{q} \rightarrow \gamma g)} = \frac{\hat{t}}{\hat{u}} + \frac{\hat{u}}{\hat{t}} \quad (C.14)$$

and

$$\Gamma_{Virt}^{(qg \rightarrow \gamma q)} = \Gamma_{Virt}^{(q\bar{q} \rightarrow \gamma g)}(\hat{s} \leftrightarrow \hat{u}) \quad (C.15)$$

$$\Gamma_{Virt}^{(gq \rightarrow \gamma q)} = \Gamma_{Virt}^{(q\bar{q} \rightarrow \gamma g)}(\hat{s} \leftrightarrow \hat{t}) . \quad (C.16)$$

C.2 $\Gamma_{ab}^{\text{soft}}$

$${}_2\Gamma_{ab} = \frac{C(a) + C(b) - C(d)}{2} \quad (C.17)$$

$${}_1\Gamma_{ab} = \frac{C(a) + C(b) - C(d)}{2} \left[\ln \frac{M_f^2}{p_j^2} - \ln \frac{(1-x_a)^2 S x_b}{x_a p_j^2} \right] \quad (C.18)$$

$$A_{ab} = \frac{C(a) + C(b) - C(d)}{2} \quad (C.19)$$

$$B_{ab} = \frac{C(a) + C(b) - C(d)}{2} \ln \frac{(1-x_a)^2 S x_b}{x_a Q^2} \quad (C.20)$$

$${}_\delta C_{ab} = \frac{C(a) + C(b) - C(d)}{2} \left[\frac{1}{2} \ln^2 \frac{M_f^2}{p_j^2} - \ln \frac{M_f^2}{p_j^2} \ln \frac{(1-x_a)^2 S x_b}{x_a p_j^2} + \frac{\pi^2}{6} \right] \quad (C.21)$$

$${}_{\bar{a}} C_{ab} = 0 \quad (C.22)$$

$${}_{\bar{b}} C_{ab} = 0 \quad (C.23)$$

$${}_a D_{ab} = 0 \quad (C.24)$$

$${}_b D_{ab} = 0 \quad (C.25)$$

C.3 $\Gamma_{ba}^{\text{soft}}$

$${}_2\Gamma_{ba} = \frac{C(a) + C(b) - C(d)}{2} \quad (\text{C.26})$$

$${}_1\Gamma_{ba} = \frac{C(a) + C(b) - C(d)}{2} \left[\ln \frac{M_f^2}{p_j^2} - \ln \frac{(1-x_b)^2 S x_a}{x_b p_j^2} \right] \quad (\text{C.27})$$

$$A_{ba} = \frac{C(a) + C(b) - C(d)}{2} \quad (\text{C.28})$$

$$B_{ba} = \frac{C(a) + C(b) - C(d)}{2} \ln \frac{(1-x_b)^2 S x_a}{x_b Q^2} \quad (\text{C.29})$$

$${}_{\delta}C_{ba} = \frac{C(a) + C(b) - C(d)}{2} \left[\frac{1}{2} \ln^2 \frac{M_f^2}{p_j^2} - \ln \frac{M_f^2}{p_j^2} \ln \frac{(1-x_b)^2 S x_a}{x_b p_j^2} + \frac{\pi^2}{6} \right] \quad (\text{C.30})$$

$${}_{\bar{a}}C_{ba} = 0 \quad (\text{C.31})$$

$${}_{\bar{b}}C_{ba} = 0 \quad (\text{C.32})$$

$${}_aD_{ba} = 0 \quad (\text{C.33})$$

$${}_bD_{ba} = 0 \quad (\text{C.34})$$

C.4 $\Gamma_{a2}^{\text{soft}}$

$${}_2\Gamma_{a2} = \frac{C(a) - C(b) + C(d)}{2} \quad (\text{C.35})$$

$${}_1\Gamma_{a2} = \frac{C(a) - C(b) + C(d)}{2} \times \left[\ln \frac{M_f^2}{p_j^2} - \ln \frac{(1-x_a)^2 S(1-v)}{(2-v)p_j^2} - 2(\pi - \alpha_a) \cot \alpha_a + 2y_j \right] \quad (\text{C.36})$$

$$A_{a2} = \frac{C(a) - C(b) + C(d)}{2} \quad (\text{C.37})$$

$$B_{a2} = \frac{C(a) - C(b) + C(d)}{2} \times \left[\ln \frac{(1-x_a)^2 S(1-v)}{(2-v)Q^2} + 2(\pi - \alpha_a) \cot \alpha_a - 2y_j \right] \quad (\text{C.38})$$

$${}_{\delta}C_{a2} = \frac{C(a) - C(b) + C(d)}{2} \left[\frac{1}{2} \ln^2 \frac{M_f^2}{p_j^2} - \ln \frac{M_f^2}{p_j^2} \left[\ln \frac{(1-x_a)^2 S(1-v)}{(2-v)p_j^2} + 2(\pi - \alpha_a) \cot \alpha_a - 2y_j \right] + \frac{\pi^2}{6} \right] \quad (\text{C.39})$$

$$\tilde{a}C_{a2} = 0 \quad (C.40)$$

$$\tilde{b}C_{a2} = 0 \quad (C.41)$$

$$_aD_{a2} = 0 \quad (C.42)$$

$$_bD_{a2} = 0 \quad (C.43)$$

where $v \equiv -\hat{u}/\hat{s}$, $\alpha_a \equiv \alpha(\frac{1}{2(1-v)})$ and $2y_j = \ln \frac{x_a(1-v)}{x_b v}$.

C.5 $\Gamma_{b2}^{\text{soft}}$

$$_2\Gamma_{b2} = \frac{-C(a) + C(b) + C(d)}{2} \quad (C.44)$$

$$\begin{aligned} _1\Gamma_{b2} &= \frac{-C(a) + C(b) + C(d)}{2} \\ &\times \left[\ln \frac{M_f^2}{p_j^2} - \ln \frac{(1-x_b)^2 S v}{(1+v)p_j^2} - 2(\pi - \alpha_b) \cot \alpha_b - 2y_j \right] \end{aligned} \quad (C.45)$$

$$A_{b2} = \frac{-C(a) + C(b) + C(d)}{2} \quad (C.46)$$

$$B_{b2} = \frac{-C(a) + C(b) + C(d)}{2} \left[\ln \frac{(1-x_b)^2 S v}{(1+v)Q^2} + 2(\pi - \alpha_b) \cot \alpha_b + 2y_j \right] \quad (C.47)$$

$$\begin{aligned} _\delta C_{b2} &= \frac{-C(a) + C(b) + C(d)}{2} \left[\frac{1}{2} \ln^2 \frac{M_f^2}{p_j^2} \right. \\ &\quad \left. - \ln \frac{M_f^2}{p_j^2} \left[\ln \frac{(1-x_b)^2 S v}{(1+v)p_j^2} + 2(\pi - \alpha_b) \cot \alpha_b + 2y_j \right] + \frac{\pi^2}{6} \right] \end{aligned} \quad (C.48)$$

$$\tilde{a}C_{b2} = 0 \quad (C.49)$$

$$\tilde{b}C_{b2} = 0 \quad (C.50)$$

$$_aD_{b2} = 0 \quad (C.51)$$

$$_bD_{b2} = 0 \quad (C.52)$$

where $\alpha_b \equiv \alpha(\frac{1}{2v})$ and $2y_j = \ln \frac{x_a(1-v)}{x_b v}$.

C.6 $\Gamma_{2a}^{\text{soft}}$

$$_2\Gamma_{2a} = 0 \quad (C.53)$$

$$\begin{aligned}
{}_1\Gamma_{2a} &= \frac{C(a) - C(b) + C(d)}{2} \\
&\times \left[\ln \frac{1-v}{2-v} + 2 \frac{(\pi - \Delta\phi)}{\sin \Delta\phi} (1 - \cos \Delta\phi) + 2(\pi - \alpha_a) \cot \alpha_a \right] \quad (C.54)
\end{aligned}$$

$$A_{2a} = 0 \quad (C.55)$$

$$\begin{aligned}
B_{2a} &= \frac{C(a) - C(b) + C(d)}{2} \\
&\times \left[\ln \frac{2-v}{1-v} - 2 \frac{(\pi - \Delta\phi)}{\sin \Delta\phi} (1 - \cos \Delta\phi) - 2(\pi - \alpha_a) \cot \alpha_a \right] \quad (C.56)
\end{aligned}$$

$$\begin{aligned}
{}_\delta C_{2a} &= \frac{C(a) - C(b) + C(d)}{2} \ln \frac{p_j^2}{M_f^2} \\
&\times \left[\ln \frac{2-v}{1-v} - 2 \frac{(\pi - \Delta\phi)}{\sin \Delta\phi} (1 - \cos \Delta\phi) - 2(\pi - \alpha_a) \cot \alpha_a \right] \quad (C.57)
\end{aligned}$$

$${}_{\bar{a}}C_{2a} = 0 \quad (C.58)$$

$${}_{\bar{b}}C_{2a} = 0 \quad (C.59)$$

$${}_aD_{2a} = 0 \quad (C.60)$$

$${}_bD_{2a} = 0 \quad (C.61)$$

where $\alpha_a \equiv \alpha(\frac{1}{2(1-v)})$ and $\Delta\phi \equiv \text{MOD}(\|\phi_q - \phi_j - \pi\|/\pi)$.

C.7 $\Gamma_{2b}^{\text{soft}}$

$${}_2\Gamma_{2b} = 0 \quad (C.62)$$

$$\begin{aligned}
{}_1\Gamma_{2b} &= \frac{-C(a) + C(b) + C(d)}{2} \\
&\times \left[\ln \frac{v}{1+v} + 2 \frac{(\pi - \Delta\phi)}{\sin \Delta\phi} (1 - \cos \Delta\phi) + 2(\pi - \alpha_b) \cot \alpha_b \right] \quad (C.63)
\end{aligned}$$

$$A_{2b} = 0 \quad (C.64)$$

$$\begin{aligned}
B_{2b} &= \frac{-C(a) + C(b) + C(d)}{2} \\
&\times \left[\ln \frac{1+v}{v} - 2 \frac{(\pi - \Delta\phi)}{\sin \Delta\phi} (1 - \cos \Delta\phi) - 2(\pi - \alpha_b) \cot \alpha_b \right] \quad (C.65)
\end{aligned}$$

$$\begin{aligned}
{}_\delta C_{2b} &= \frac{-C(a) + C(b) + C(d)}{2} \ln \frac{p_j^2}{M_f^2} \\
&\times \left[\ln \frac{1+v}{v} - 2 \frac{(\pi - \Delta\phi)}{\sin \Delta\phi} (1 - \cos \Delta\phi) - 2(\pi - \alpha_b) \cot \alpha_b \right] \quad (C.66)
\end{aligned}$$

$$\bar{a}C_{2b} = 0 \quad (\text{C.67})$$

$$\bar{b}C_{2b} = 0 \quad (\text{C.68})$$

$$_aD_{2b} = 0 \quad (\text{C.69})$$

$$_bD_{2b} = 0 \quad (\text{C.70})$$

where $\alpha_b \equiv \alpha(\frac{1}{2v})$ and $\Delta\phi \equiv \text{MOD}(\|\phi_q - \phi_j - \pi\|/\pi)$.

C.8 Γ_a^{coll}

$$_2\Gamma_a = 0 \quad (\text{C.71})$$

$$_1\Gamma_a = \gamma(a) + 2C(a) \ln \frac{1-x_a}{x_a} - \sum_{\bar{a}} \int_{x_a}^1 \frac{dz}{z} \frac{H(x_a/z, x_b)}{H(x_a, x_b)} P_{a\bar{a}}^+(z) \quad (\text{C.72})$$

$$A_a = 0 \quad (\text{C.73})$$

$$B_a = -\gamma(a) - 2C(a) \ln \frac{1-x_a}{x_a} \quad (\text{C.74})$$

$$_\delta C_a = \ln \frac{M_f^2}{p_j^2} \left[\gamma(a) + 2C(a) \ln \frac{1-x_a}{x_a} \right] \quad (\text{C.75})$$

$$\bar{a}C_a = P_{a\bar{a}}^+(z) \ln \frac{p_j^2}{M_f^2} - P_{a\bar{a}}^1 \quad (\text{C.76})$$

$$\bar{b}C_a = 0 \quad (\text{C.77})$$

$$_aD_a = 1 \quad (\text{C.78})$$

$$_bD_a = 0 \quad (\text{C.79})$$

C.9 Γ_b^{coll}

$$_2\Gamma_b = 0 \quad (\text{C.80})$$

$$_1\Gamma_b = \gamma(b) + 2C(b) \ln \frac{1-x_b}{x_b} - \sum_{\bar{b}} \int_{x_b}^1 \frac{dz}{z} \frac{H(x_a, x_b/z)}{H(x_a, x_b)} P_{b\bar{b}}^+(z) \quad (\text{C.81})$$

$$A_b = 0 \quad (\text{C.82})$$

$$B_b = -\gamma(b) - 2C(b) \ln \frac{1-x_b}{x_b} \quad (\text{C.83})$$

$$\delta C_b = \ln \frac{M_f^2}{p_j^2} \left[\gamma(b) + 2C(b) \ln \frac{1-x_b}{x_b} \right] \quad (\text{C.84})$$

$$\bar{a} C_b = 0 \quad (\text{C.85})$$

$$\bar{b} C_b = P_{b\bar{b}}^+(z) \ln \frac{p_j^2}{M_f^2} - P_{b\bar{b}}^1 \quad (\text{C.86})$$

$$_a D_b = 0 \quad (\text{C.87})$$

$$_b D_b = 1 \quad (\text{C.88})$$

C.10 Γ_a^{CT}

$$_2 \Gamma_a^{CT} = 0 \quad (\text{C.89})$$

$$_1 \Gamma_a^{CT} = \sum_{\bar{a}} \int_{x_a}^1 \frac{dz}{z} \frac{H(x_a/z, x_b)}{H(x_a, x_b)} P_{a\bar{a}}^+(z) \quad (\text{C.90})$$

$$A_a^{CT} = 0 \quad (\text{C.91})$$

$$B_a^{CT} = 0 \quad (\text{C.92})$$

$$\delta C_a^{CT} = 0 \quad (\text{C.93})$$

$$\bar{a} C_a^{CT} = 0 \quad (\text{C.94})$$

$$\bar{b} C_a^{CT} = 0 \quad (\text{C.95})$$

$$_a D_a^{CT} = 0 \quad (\text{C.96})$$

$$_b D_a^{CT} = 0 \quad (\text{C.97})$$

C.11 Γ_b^{CT}

$$_2 \Gamma_b^{CT} = 0 \quad (\text{C.98})$$

$$_1 \Gamma_b^{CT} = \sum_{\bar{b}} \int_{x_b}^1 \frac{dz}{z} \frac{H(x_a, x_b/z)}{H(x_a, x_b)} P_{b\bar{b}}^+(z) \quad (\text{C.99})$$

$$A_b^{CT} = 0 \quad (\text{C.100})$$

$$B_b^{CT} = 0 \quad (\text{C.101})$$

$$\delta C_b^{CT} = 0 \quad (\text{C.102})$$

$$\tilde{a}C_b^{CT} = 0 \quad (\text{C.103})$$

$$\tilde{b}C_b^{CT} = 0 \quad (\text{C.104})$$

$$_aD_b^{CT} = 0 \quad (\text{C.105})$$

$$_bD_b^{CT} = 0 \quad (\text{C.106})$$

C.12 Γ_2^{coll}

$$_2\Gamma_2 = C(d) \quad (\text{C.107})$$

$$_1\Gamma_2 = \gamma(d) - C(d) \left[2 \frac{(\pi - \Delta\phi)}{\sin \Delta\phi} (1 - \cos \Delta\phi) - \ln \frac{M_f^2}{p_j^2} \right] \quad (\text{C.108})$$

$$A_2 = 0 \quad (\text{C.109})$$

$$B_2 = 0 \quad (\text{C.110})$$

$$\begin{aligned} \delta C_2 &= -\gamma(d) \left[2 \frac{(\pi - \Delta\phi)}{\sin \Delta\phi} (1 - \cos \Delta\phi) - \ln \frac{M_f^2}{p_j^2} \right] + \delta_{dg} \frac{(17N_C - 23N_f)}{18} \\ &- C(d) \left[2 \frac{(\pi - \Delta\phi)}{\sin \Delta\phi} (1 - \cos \Delta\phi) \ln \frac{M_f^2}{p_j^2} \right. \\ &- \left. \frac{1}{2} \ln^2 \frac{M_f^2}{p_j^2} + \left(\frac{2\pi^2}{3} - \frac{13}{2} \right) - \frac{\pi^2}{6} \right] \end{aligned} \quad (\text{C.111})$$

$$\tilde{a}C_2 = 0 \quad (\text{C.112})$$

$$\tilde{b}C_2 = 0 \quad (\text{C.113})$$

$$_aD_2 = 0 \quad (\text{C.114})$$

$$_bD_2 = 0 \quad (\text{C.115})$$

where $\Delta\phi \equiv \text{MOD}(\|\phi_q - \phi_j - \pi\|/\pi)$.

One can easily verify that the poles all cancel; that is, the sums $\sum_{mn} {}_2\Gamma_{mn}$ and $\sum_{mn} {}_1\Gamma_{mn}$ both equal 0. Additional cancellations will occur upon summing the remaining pieces, and further simplification arises upon integration over ϕ_q . In particular,

$$\int_0^{2\pi} d\phi_q 2 \frac{(\pi - \Delta\phi)}{\sin \Delta\phi} (1 - \cos \Delta\phi) = 2\pi \ln 16, \quad (\text{C.116})$$

$$\int_0^{2\pi} d\phi_q 2(\pi - \alpha(x_i)) \cot \alpha(x_i) = 2\pi \ln \frac{1+2x_i}{2x_i}. \quad (\text{C.117})$$

Thus, for example, terms involving $\cot \alpha(\frac{1}{2(1-v)})$ will cancel corresponding $\ln(2-v)$ terms, and $\cot \alpha(\frac{1}{2v})$ terms will get rid of $\ln(1+v)$ pieces.

As it is, we have the initial-state and final-state sums:

$$\begin{aligned} A_{init} &\equiv A_{Virt} + A_{ab} + A_{ba} + A_{a2} + A_{b2} + A_a^{\text{coll}} + A_b^{\text{coll}} + A_a^{CT} + A_b^{CT} \\ &= C(a) + C(b) \end{aligned} \quad (\text{C.118})$$

$$\begin{aligned} A_{final} &\equiv A_{2a} + A_{2b} + A_2^{\text{coll}} \\ &= 0 \end{aligned} \quad (\text{C.119})$$

$$\begin{aligned} B_{init} &\equiv B_{Virt} + B_{ab} + B_{ba} + B_{a2} + B_{b2} + B_a^{\text{coll}} + B_b^{\text{coll}} + B_a^{CT} + B_b^{CT} \\ &= C(a) \left[\frac{1}{2} \ln \frac{1+v}{2-v} \frac{v}{1-v} + \ln \frac{\hat{s}}{Q^2} + (\pi - \alpha_a) \cot \alpha_a - (\pi - \alpha_b) \cot \alpha_b \right] \\ &+ C(b) \left[\frac{1}{2} \ln \frac{2-v}{1+v} \frac{1-v}{v} + \ln \frac{\hat{s}}{Q^2} - (\pi - \alpha_a) \cot \alpha_a + (\pi - \alpha_b) \cot \alpha_b \right] \\ &+ C(d) \left[\frac{1}{2} \ln \frac{v(1-v)}{(2-v)(1+v)} + (\pi - \alpha_a) \cot \alpha_a + (\pi - \alpha_b) \cot \alpha_b \right] \\ &- (\gamma(a) + \gamma(b)) \end{aligned} \quad (\text{C.120})$$

$$\begin{aligned} B_{final} &\equiv B_{2a} + B_{2b} + B_2^{\text{coll}} \\ &= C(a) \left[\frac{1}{2} \ln \frac{2-v}{1+v} \frac{v}{1-v} - (\pi - \alpha_a) \cot \alpha_a + (\pi - \alpha_b) \cot \alpha_b \right] \\ &+ C(b) \left[\frac{1}{2} \ln \frac{1+v}{2-v} \frac{1-v}{v} + (\pi - \alpha_a) \cot \alpha_a - (\pi - \alpha_b) \cot \alpha_b \right] \\ &+ C(d) \left[\frac{1}{2} \ln \frac{(2-v)(1+v)}{v(1-v)} - (\pi - \alpha_a) \cot \alpha_a - (\pi - \alpha_b) \cot \alpha_b \right] \\ &- 2 \frac{(\pi - \Delta\phi)}{\sin \Delta\phi} (1 - \cos \Delta\phi) \end{aligned} \quad (\text{C.121})$$

$$\delta C_{init} = C(a) \left[\frac{1}{2} \ln^2 \frac{M_f^2}{p_j^2} - \frac{1}{2} \ln \frac{M_f^2}{p_j^2} \left[\ln \frac{1+v}{2-v} \frac{v}{1-v} + 2 \ln \frac{\hat{s}}{p_j^2} \right] \right]$$

$$\begin{aligned}
& + 2(\pi - \alpha_a) \cot \alpha_a - 2(\pi - \alpha_b) \cot \alpha_b \Big] \\
& + C(b) \left[\frac{1}{2} \ln^2 \frac{M_f^2}{p_j^2} - \frac{1}{2} \ln \frac{M_f^2}{p_j^2} \left[\ln \frac{2-v}{1+v} \frac{1-v}{v} + 2 \ln \frac{\hat{s}}{p_j^2} \right. \right. \\
& \left. \left. - 2(\pi - \alpha_a) \cot \alpha_a + 2(\pi - \alpha_b) \cot \alpha_b \right] \right] \\
& - \frac{C(d)}{2} \ln \frac{M_f^2}{p_j^2} \left[\ln \frac{v(1-v)}{(2-v)(1+v)} + 2(\pi - \alpha_a) \cot \alpha_a + 2(\pi - \alpha_b) \cot \alpha_b \right] \\
& + (\gamma(a) + \gamma(b)) \ln \frac{M_f^2}{p_j^2} + A_{0\nu} + \frac{B_\nu}{T_0} - C(d) \frac{\pi^2}{6} \tag{C.122}
\end{aligned}$$

$$\begin{aligned}
\delta C_{final} &= \frac{C(a)}{2} \ln \frac{M_f^2}{p_j^2} \left[\ln \frac{1+v}{2-v} \frac{1-v}{v} + 2(\pi - \alpha_a) \cot \alpha_a - 2(\pi - \alpha_b) \cot \alpha_b \right] \\
&+ \frac{C(b)}{2} \ln \frac{M_f^2}{p_j^2} \left[\ln \frac{2-v}{1+v} \frac{v}{1-v} - 2(\pi - \alpha_a) \cot \alpha_a + 2(\pi - \alpha_b) \cot \alpha_b \right] \\
&+ C(d) \left[\frac{1}{2} \ln \frac{M_f^2}{p_j^2} \left[\ln \frac{v(1-v)}{(2-v)(1+v)} \right. \right. \\
&+ 2(\pi - \alpha_a) \cot \alpha_a + 2(\pi - \alpha_b) \cot \alpha_b + 4 \frac{(\pi - \Delta\phi)}{\sin \Delta\phi} (1 - \cos \Delta\phi) \Big] \\
&- \frac{1}{2} \ln \frac{M_f^2}{p_j^2} \left[4 \frac{(\pi - \Delta\phi)}{\sin \Delta\phi} (1 - \cos \Delta\phi) \right] + \frac{1}{2} \ln^2 \frac{M_f^2}{p_j^2} - \left(\frac{2\pi^2}{3} - \frac{13}{2} \right) + \frac{\pi^2}{6} \Big] \\
&- \gamma(d) \left[2 \frac{(\pi - \Delta\phi)}{\sin \Delta\phi} (1 - \cos \Delta\phi) - \ln \frac{M_f^2}{p_j^2} \right] + \delta_{dg} \frac{17N_C - 23N_f}{18} \tag{C.123}
\end{aligned}$$

$$\bar{a}C_{init} + \bar{b}C_{init} = - \left[P_{a\bar{a}}^1 + P_{b\bar{b}}^1 \right] - \ln \frac{M_f^2}{p_j^2} \left(P_{a\bar{a}}^+ + P_{b\bar{b}}^+ \right) \tag{C.124}$$

$$\bar{a}C_{final} + \bar{b}C_{final} = 0 \tag{C.125}$$

$${}_aD_{init} = 1 \tag{C.126}$$

$${}_bD_{init} = 1 \tag{C.127}$$

$${}_aD_{final} = 0 \tag{C.128}$$

$${}_bD_{final} = 0 \tag{C.129}$$

Calculation of the CSS $\{A, B, C\}$ parameters from these results is outlined in Section 6.5.

For the $m = 1$ Bremsstrahlung contributions, we derive (to order 1):

$$\begin{aligned}
p_j \Gamma_1^{\text{coll}} &= -\frac{1}{\epsilon} \sum_q P_{\gamma q}^+ + \sum_q \left[\left(\frac{2(\pi - \Delta\phi)}{\sin \Delta\phi} (1 - \cos \Delta\phi) + 2 \ln \frac{\tilde{z}(1 - \tilde{z})p_j}{M_f} \right) \hat{P}_{\gamma q}(\hat{z}) - P_{\gamma q}^1(\hat{z}) \right] \\
p_j \Gamma_1^{\text{CT}} &= \frac{1}{\epsilon} \sum_q P_{\gamma q}^+(\tilde{z}) ,
\end{aligned} \tag{C.130}$$

where $\tilde{z} = (p_j - Q_T)/p_j$, $\Delta\phi = \phi_q - \phi_j - \pi$. The poles cancel.

APPENDIX D

THE MONTE CARLO METHOD IN HIGH ENERGY PHYSICS

D.1 Basic Theory

Monte Carlo is, at its essence, a numerical method of performing integrations. Compared with other methods, it has certain features which make it particularly well-suited to the types of problems encountered in high energy physics. The fundamental theorem is based upon the recognition that the average of a function over a domain V can be expressed as the average of a set of discrete samples of the integrand, in the limit that the number of samples goes to infinity [93]:

$$\langle f \rangle = \frac{\int_V d^n x f(\vec{x})}{V = \int d^n x} = \lim_{N \rightarrow \infty} \frac{1}{N} \sum_{j=1}^N f(\vec{x}_j) . \quad (\text{D.1})$$

Here \vec{x}_j is a particular vector in the domain V of dimension n , and N is the number of samples, each generated randomly by computer.

In practice, the generally available random number generators choose values on a $0 \rightarrow 1$ scale, and the function to be integrated is then re-expressed in terms of variables y_i which have been thus scaled. Now (for each variable),

$$\int_{x_{min}}^{x_{max}} f(x) dx \quad \text{becomes} \quad \int_0^1 f(y) dy, \quad \text{where} \quad (\text{D.2})$$

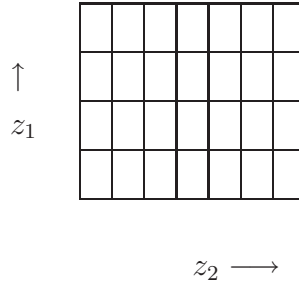
$$y = \frac{(x - x_{min})}{(x_{max} - x_{min})} \quad \text{and the volume} \quad V = \prod_{i=1}^n \left[\int_0^1 dy_i \right] = 1^n = 1 . \quad (\text{D.3})$$

The theorem is then expressed as

$$\int d^n y f(\vec{y}) = \lim_{N \rightarrow \infty} \frac{1}{N} \sum_{j=1}^N f(\vec{y}_j) . \quad (\text{D.4})$$

Often there will be variables \vec{z} in f that are not integrated over, but are not fixed. They define a desired distribution $\int d\vec{y} f(\vec{y}, \vec{z})$. Instead of stepping through values of \vec{z}_j and calculating $\int d\vec{y} f(\vec{y}, \vec{z}_j)$ at each, we can define *bins* in \vec{z} and expand our definition of the volume V to include the domain of \vec{z} . Each evaluation $f(\vec{y}_j, \vec{z}_j)$ is then added to the appropriate bin in \vec{z} , and the result $\int d\vec{y} f(\vec{y}, \{\vec{z}\}_k)$ for bin k is calculated by dividing by the number of evaluations N .

Further integrations can be done from here. For instance, if \vec{z} consists of two variables z_1 and z_2 , we have a two dimensional grid of bins in \vec{z} -space:



Integration over z_1 then consists of summing the contents of each column of bins into a new one-dimensional set of bins in z_2 :



While evaluating an integral, Monte Carlo can also be used to compute derivatives of this integral with respect to a variable. If Δx is a region in the domain V , then the derivative with respect to x is found by binning in x and dividing by the width of the bin [94]:

$$\frac{dI}{dx} = \lim_{\Delta x \rightarrow 0} \left(\frac{\Delta I}{\Delta x} \right), \quad (\text{D.5})$$

where ΔI is the sum of those weights Vf/N which fall in the range Δx . In practice, we find the approximate derivative $\frac{\Delta I}{\Delta x}$, as we can't take the limit. In fact, decreasing Δx increases the uncertainty since fewer points fall into each bin. Note that we can differentiate with respect to any variables, not just the ones being used to evaluate the integral, as long as the former are expressible in terms of the latter.

D.2 Advantages of Monte Carlo for High Energy Physics

Among the many quantities of interest in high energy physics, surely the one most frequently evaluated through numerical integration is the cross section σ for a particular reaction. The integrand is a *differential* cross section $\frac{d\sigma}{d\{p_i\}}$ which, depending on the order of the calculation, may be a function of many four-momenta $\{p_i\}$, and of course each four-vector has four components. Integrating over all of these variables would yield one number – the total cross section; but often we will want to leave one or more unintegrated so as to see the distribution in these variables. Also, some variables may be fixed by the associated experiment (like the center-of-mass energy), or there may be complicated relations among the variables which fix one of them with respect to others. These things would all tend to reduce the number of integrations required, but in practice it is not always clear at the outset which variables will be of interest. Furthermore, some of the integrations may be impossible analytically, either due to the iterative nature of the integrand (as in the case of parton distributions) or to the complicated, discontinuous domains of integration that can arise when experimental constraints are applied. It is of necessity, then, to seek the fastest, simplest, and most flexible tool for the job.

The fundamental theorem of Monte Carlo integration allows us to think of the situation in the following way: We have a space V of randomly selected points \vec{x} , each point carrying a contribution $Vf(\vec{x})/N$ to the total integral, and each section of

our program, from selection of the points, through application of the cuts, evaluation of the weight, and finally binning, can carve up this space in its own way, with its own variables. The following considerations should make this advantage clear.

Speed. For integrals over many variables, Monte Carlo converges faster than other methods. For example, to do an n dimensional integral with N -point Gaussian Quadrature, the integrand would need to be evaluated N^n times. Using N randomly distributed vectors, by contrast, requires only N evaluations.

Variable Transformations. Analytically, if one has calculated a distribution (say $\frac{d\sigma}{dx_1 dx_2}$), and one now wants this as a distribution in the related set $dyd\tau$, one must calculate the Jacobian function for the transformation:

$$\frac{d\sigma}{dyd\tau} = \frac{d\sigma}{dx_1 dx_2} \left| \begin{array}{cc} \frac{\partial y}{\partial x_1} & \frac{\partial y}{\partial x_2} \\ \frac{\partial \tau}{\partial x_1} & \frac{\partial \tau}{\partial x_2} \end{array} \right|. \quad (\text{D.6})$$

In Monte Carlo, one simply bins in the new variables, modifying the bin sizes if desired. That is, the weights σ may still be evaluated using random $\{x_1, x_2\}$ values; one need now only insert the calculation of $\{y, \tau\}$, and use these values instead to decide on the bin.

Discontinuous Domains. There are times when an integral we wish to evaluate has a domain that is not analytically expressible, is discontinuous, or is more easily expressed in variables other than the ones which provide the simplest form for the integrand. In a typical high energy cross section, it may be that each Lorentz-invariant piece is simplest in a different frame, and experimental cuts may be most easily expressed in yet another frame or coordinate system. There may be regions of the detector which are blind by design or damage, and which therefore should be similarly removed from the theoretical calculation. Creating these types of “holes” in the domain would violate the principles upon which Gaussian quadrature and Simpson’s Rule are based; in Monte Carlo the evaluation of the integrand at any two points is divorced from continuity constraints between these points, and the integral becomes possible.

The trick is to use a larger volume \acute{V} which contains V , and simply ask, for each random vector \vec{x} in \acute{V} , whether or not it is in V . This prescription allows us to perform the random selections x_i within a conveniently continuous space, within one subroutine, and leave until later (a different subroutine) the question of whether a particular point \vec{x} is in the desired domain V . The condition (or *cut*) can be described using any quantities calculable from \vec{x} , with the result being a decision on inclusion of the point's weight in the integral:

$$\text{If } \vec{x} \in V \text{ then WEIGHT} = f(\vec{x})\acute{V}/N$$

$$\text{If } \vec{x} \notin V \text{ then WEIGHT} = 0$$

To minimize the uncertainty, the volume \acute{V} should be as close to V as possible.

Estimate of Precision. In contrast with Gaussian Quadrature, Monte Carlo integration directly produces an uncertainty estimate. For large N (the number of sampled points), the variance is given by [94]:

$$\sigma = \sqrt{\frac{\langle w^2 \rangle - \langle w \rangle^2}{N - 1}}, \quad (\text{D.7})$$

$$\text{where} \quad \langle w \rangle = \frac{1}{N} \sum_{i=1}^N f(\vec{x}_i), \quad \langle w^2 \rangle = \frac{1}{N} \sum_{i=1}^N f^2(\vec{x}_i). \quad (\text{D.8})$$

Having a numerical value for the statistical variance of an integral is a first step toward trying to decrease it, as we will see.

Event Generation. Monte Carlo can be used as an event simulator in particle physics. The fact that a particular randomly chosen event \vec{x}_i yields an evaluation $f(\vec{x}_i)$ proportional to its probability of occurrence can be turned around – once we know which regions of phase space give the greatest weights, we can generate sets of four-vectors (events \vec{x}_i) with frequency $f(\vec{x}_i)\triangle V$ [95]. Such simulators (e.g. PYTHIA, HERWIG, ISAJET) are helpful in determining background rates for unwanted processes. This “cross-referencing” of the weights to the points usually turns out to be necessary anyway, for reasons discussed below.

D.3 Importance Sampling

Monte Carlo with uniformly chosen ordinates has one major drawback: the frequency with which a region ΔV is sampled depends only on the size of ΔV , not on the size of the integrand there. Thus just as much computing time is spent generating contributions in regions of low weight as in high-weight regions. Avoiding this inefficiency is especially important for most particle physics cross sections, which are rapidly falling functions of their arguments. If the function f were simple enough, certain changes of variable might sufficiently flatten it [96], but particle physics cross sections are rarely simple, and for good results some means of *importance sampling* is usually required.

If we select our points \vec{x} with a different density $\rho(\vec{x})$ in each region of space, we will be more efficient; but if we expect to get the same answer for the integral, then those regions with more points should count less. In other words, normalization will require that the size of the volume element ΔV about point \vec{x} go as $1/\rho(\vec{x})$, and in the above formula $f(\vec{x})$ is replaced with $f(\vec{x})/\rho(\vec{x})$. It can be shown that the uncertainty is minimized when the density has the same shape as the absolute value of the integrand:

$$\text{“Best”} \quad \rho(\vec{x}) = \frac{|f(\vec{x})|}{\int_V |f(\vec{x})| dV} \quad (\text{D.9})$$

Of course, if we could calculate this, all our work would be done already; we can't, but there are certain means of approximating the best density on an iterative basis. If one divides the integration volume into smaller volumes, then as implied above there are two ways of modifying the density of selected points – either have equal subvolumes with a different number of points in each, or have varying subvolume sizes each with the same number of points. The latter method, called *stratified sampling*, is used in most of the common algorithms, such as VEGAS and SHEP [97]. Initially, the subvolumes are of equal size. At each iteration, a two-point Monte Carlo integration is performed in each subvolume, generating a contribution to the

total integral and to the variance. This information is then used to redefine the subvolume sizes for the next iteration, such that concentrations of small subvolumes are built up in regions where the variance was initially largest. The overall variance is thus decreased at each iteration until no significant change occurs. The better algorithms are able to use the integral information from each step, not just the last.

D.4 Program Structure and Example

Here we will outline the main sections of a Monte Carlo program, using hadronic two-photon production as our example. At Born level, a quark from one hadron annihilates with an antiquark from the other, to emit two photons whose momenta we detect. At higher orders, we may have additional particles in the final state, for example gluons that are radiated from the incoming quark legs. We'll stick with one-gluon emission here, and ask the question, "How much transverse momentum will this extra gluon impart to the two-photon system?" Without the gluon, the photon system has zero transverse momentum, as there is none coming in (the quarks are assumed collinear). With the additional kick, the question makes sense, but so do many others, so we want to keep as many of the photon variables unintegrated as possible. In other words, we look at:

$$d\sigma(AB \rightarrow 2\gamma + X) = \sum_f \int_0^1 dx_A \int_0^1 dx_B [q_f(x_A)q_{\bar{f}}(x_B) + (f \leftrightarrow \bar{f})] d\hat{\sigma}(f\bar{f} \rightarrow 2\gamma) , \quad (\text{D.10})$$

where

$$d\hat{\sigma}(f\bar{f} \rightarrow 2\gamma) \sim \int_g d^4p_g d^4p_{\gamma_1} d^4p_{\gamma_2} \times \delta^{(4)}(p_f^\mu + p_{\bar{f}}^\mu - p_{\gamma_1}^\mu - p_{\gamma_2}^\mu - p_g^\mu) \sum |\mathcal{M}(f\bar{f} \rightarrow \gamma\gamma g)|^2 . \quad (\text{D.11})$$

Note that we are integrating only over the gluon, as we want all photon variables to be free.

Let's see what we can do to get this ready for Monte Carlo integration. We know Monte Carlo doesn't like delta functions, so we get rid of these first. Out of the 20 variables we started with (five 4-vectors, one for each of the two incoming quarks, the outgoing photons, and the gluon), we now are left with 16. Additionally, we are assuming the partons and photons to be massless, which means that one component of each 4-vector is fixed relative to the others. This brings our variable count down to 12. Fixing our \hat{z} -axis along the beam line also helps, as the incoming partons now have no transverse momentum, which gets rid of two variables apiece. Finally, we work at fixed total hadronic center-of-mass energy \sqrt{S} , so we are left with seven variables. Since it takes six to specify the two photons, and these we wish to leave free, we will actually need only one "forced" integration (over one or the other momentum fraction x). Integration over the others (the photons) will be left for the user to decide upon through binning. Whatever is left determines the desired distribution. That is, our total integration volume V is 7-dimensional, as we add the free variables to the volume as discussed in Section D.1. For the purposes of generating the random points in this space, and their weights, we need to choose a set for which we know the kinematic bounds. For binning of these weights, the user may choose any set he or she wishes.

With a bit of analytical work, then, we obtain a simplified expression, each piece of which we will write as a function of the simplest parameters for that piece:

$$\begin{aligned}
d\sigma(AB \rightarrow 2\gamma + X) &\sim \sum_f \int_{\frac{Q^2}{S} e^y}^1 dx [q_f(x, Q^2) q_{\bar{f}}(\tilde{x}, Q^2) + (f \leftrightarrow \bar{f})] P(Q^2, p_T^2, y, \phi_{2\gamma}) \\
&\times \sum |\mathcal{M}(\hat{s}_{12}, \hat{t}_{13}, \hat{t}_{14}, \hat{t}_{15}, \hat{t}_{23}, \hat{t}_{24}, \hat{t}_{25})|^2.
\end{aligned}
\tag{D.12}$$

Here \tilde{x} is a known function of x , given by the massless gluon constraint. Q^2 , p_T^2 , y , and $\phi_{2\gamma}$ are, respectively, the (squared) energy, transverse momentum, rapidity, and azimuthal angle of the two-photon system in the hadronic cm frame (which we take

to be the lab frame – at a collider). P is a function which depends purely on phase space.

The matrix element for the subprocess is most easily written in terms of Mandelstam variables \hat{s}_{ij} and \hat{t}_{ij} . The astute reader will notice that there are seven of these, so they cannot all be independent of the four we’ve already mentioned. With a little extra work, we could choose a frame and rewrite the matrix element in terms of Q^2 , p_T^2 , y , $\phi_{2\gamma}$, x , and two more variables, but the result would not be pretty. And indeed there is no need to. All that matters is that we be able to calculate the 4-vectors of each particle in whatever frame is easiest for that particle, boost them all to the same frame, and calculate the Mandelstam variables.

The best frame for the photons is the rest frame of the two-photon system, in which their momenta are equal and opposite, and their energies are simply $Q/2$ each. The direction of their “momentum line” in this frame can be anywhere from 0 to π in theta, and 0 to 2π in phi. Those three variables completely specify the photon 4-vectors in that frame, and now we’re done seeking variables. We have seven, and know their limits:

$$\begin{aligned}
0 &\leq Q^2 \leq S \\
0 &\leq p_T^2 \leq \frac{(S + Q^2)^2}{4S \cosh^2 y} - Q^2 \\
y_{min} &\leq y \leq y_{max} \\
0 &\leq \phi_{2\gamma} \leq 2\pi \\
0 &\leq \theta_\gamma \leq \pi \\
0 &\leq \phi_\gamma \leq 2\pi \\
\frac{Q^2}{S} e^y &\leq x \leq 1
\end{aligned} \tag{D.13}$$

Note that in reality Q^2 will never approach S (unless the hadrons disappear altogether!). We are taking a larger volume (as discussed in Section D.2) for lack of

a better limit. Here y_{min} and y_{max} are assumed to be given by the user, based on the viable range of the detector. We are now ready to begin writing the code.

In the following, variables entering a subroutine will be denoted by lowercase names, outgoing variables will be in uppercase, and variables which are both inputs and outputs will be italicized. To avoid confusion, we'll show the passed variables only in subroutine definitions, not in calls.

Program MAIN

Initialize fixed values.

Initialize bins

Loop ($i = 1 \dots N$)

 Call EVENT

 Call WEIGHT

 Call BINIT

 Write LABVECS,WEIGHT (optional)

end Loop

Here we read our fixed values (e.g. S , y_{min} , y_{max} , etc.), make sure our bins are empty, and then process N randomly selected events. For each event, we find the four-vectors (EVENT), calculate this event's contribution (WEIGHT), put the weight in the appropriate bin (BINIT), and optionally, send the event out to a file.

Subroutine EVENT (fixed, LABVECS[5,0:3], UNSCALED, VOLUME)

Random selection of scaled vars (e.g. $XQ2=RAND(SEED)$, $XPT=RAND(SEED)$, etc.)

Scaled vars \rightarrow Unscaled vars (e.g. $Q2=S*XQ2$) & VOLUME

Find photon cm 4-vecs (using Q^2 , θ_γ , ϕ_γ)

Find boost parameters (using Q^2 , p_T^2 , y , $\phi_{2\gamma}$)

Boost photons to lab frame

Find parton 4-vecs in lab (from S, x, \tilde{x})

Find gluon 4-vec ($= p_f^\mu + p_{\bar{f}}^\mu - p_{\gamma 1}^\mu - p_{\gamma 2}^\mu$)

return

Remember that we can't randomly choose (what I call) the “unscaled” variables $[Q^2, p_T^2, y, \phi_{2\gamma}, \theta_\gamma, \phi_\gamma, x]$ directly; our random number generator picks between the limits 0 and 1. So we define a “scaled” variable (e.g. `XQ2` in the code) for each, choose it randomly, and then calculate the unscaled variables from them. The volume V is the product of the unscaled variables' domains, and this will be multiplied by the integrand in evaluation of the weight for this event. Once we find the four-vectors for all the particles of the subprocess, we'll be able to calculate the matrix element; we also send out the unscaled variables, as they may be more directly useful for the phase space factor, cuts, and binning.

Subroutine WEIGHT (fixed, labvecs, unscaled, volume, WEIGHT)

Implement CUTS (using labvecs, unscaled), e.g. `IF(P5(0).LT.0.75) GOTO REJECT`

Calculate MANDELSTAM vars t_{ij} (using labvecs)

Calculate MATRIX ELEMENT (using t_{ij})

Calculate PARTON DISTRIBUTIONS $q_f(x, Q^2)$

Calculate PHASE SPACE FACTOR P (using unscaled)

$\text{INTEGRAND} = (\text{partons}) \times (\text{phase space}) \times (\text{matrix element})$

$\text{WEIGHT} = (\text{volume}) \times (\text{integrand}) / (N)$

return

REJECT:

$\text{WEIGHT} = 0$

return

The first section here (CUTS) is open to user modification. The user has access to all of the variables that describe the event, and may invent new variables as needed, all in order to define IF statements which either accept or deny this event as valid. If denied, control is passed to the REJECT line, where the weight is set to zero. This CUTS section may be put in the binning routine instead, but this just wastes time, as the weight will be unnecessarily calculated.

Subroutine BINIT (fixed, labvecs, unscaled, $BIN[1:100]$, WEIGHT)

Decide upon and calculate binning variable(s) (e.g. the pair PT in our case)

$BIN\# = INT((PT-LO)/STEP) + 1$

$BIN(BIN\#)=BIN(BIN\#) + WEIGHT/STEP$

return

Again, the first section here is user-accessible, for the purpose of defining whatever variables are of interest. The user may wish to look at the transverse momentum of the photon pair (as we do), rapidity differences between the photons, or single photon spectra (in which case each photon might contribute to a different bin). Here we assume a one-dimensional bin array, corresponding to $\frac{d\sigma}{dp_T}$, but the generalization to higher dimensions is trivial, and affects no other subroutine. Note that our WEIGHT corresponds to $d\sigma$, so if we want $\frac{d\sigma}{dp_T}$, we must divide by the bin width (STEP) – see the discussion on differentiation in Section D.1.

In figure D.1 we present results for two-photon production in π^-p collisions, to first order in α_s . The fixed quantities are: $S=526.33 \text{ GeV}^2$, $\Lambda_{QCD}=0.2305 \text{ GeV}$, $STEP=0.08 \text{ GeV}$. The cuts that were used are the following:

1. The photon of higher p_T must have $p_T \geq 3.00\text{GeV}$.
2. The photon of lower p_T must have $p_T \geq 2.75\text{GeV}$.
3. The quantity $zz = -(\vec{p_{T\gamma_1}} \cdot \vec{p_{T\gamma_2}}) / \max(p_{T\gamma_1}, p_{T\gamma_2})$ must exceed 2.75.

and the code that took care of these cuts:

```
C --- CUTS ON LAB VARS ---  
PT3=DSQRT(P3(1)**2.D0+P3(2)**2.D0)  
PT4=DSQRT(P4(1)**2.D0+P4(2)**2.D0)  
ZZ=-1.D0*(P3(1)*P4(1)+P3(2)*P4(2))/DMAX1(PT3,PT4)  
IF (DMAX1(PT3,PT4).LT.3.D0) GOTO REJECT  
IF (DMIN1(PT3,PT4).LT.2.75D0) GOTO REJECT  
IF (ZZ.LE.2.75D0) GOTO REJECT
```

On the graph, the p_T distribution of the photon pair is shown. The dashed line is the perturbative 1-gluon result; the solid line is the result of resumming the soft gluons.

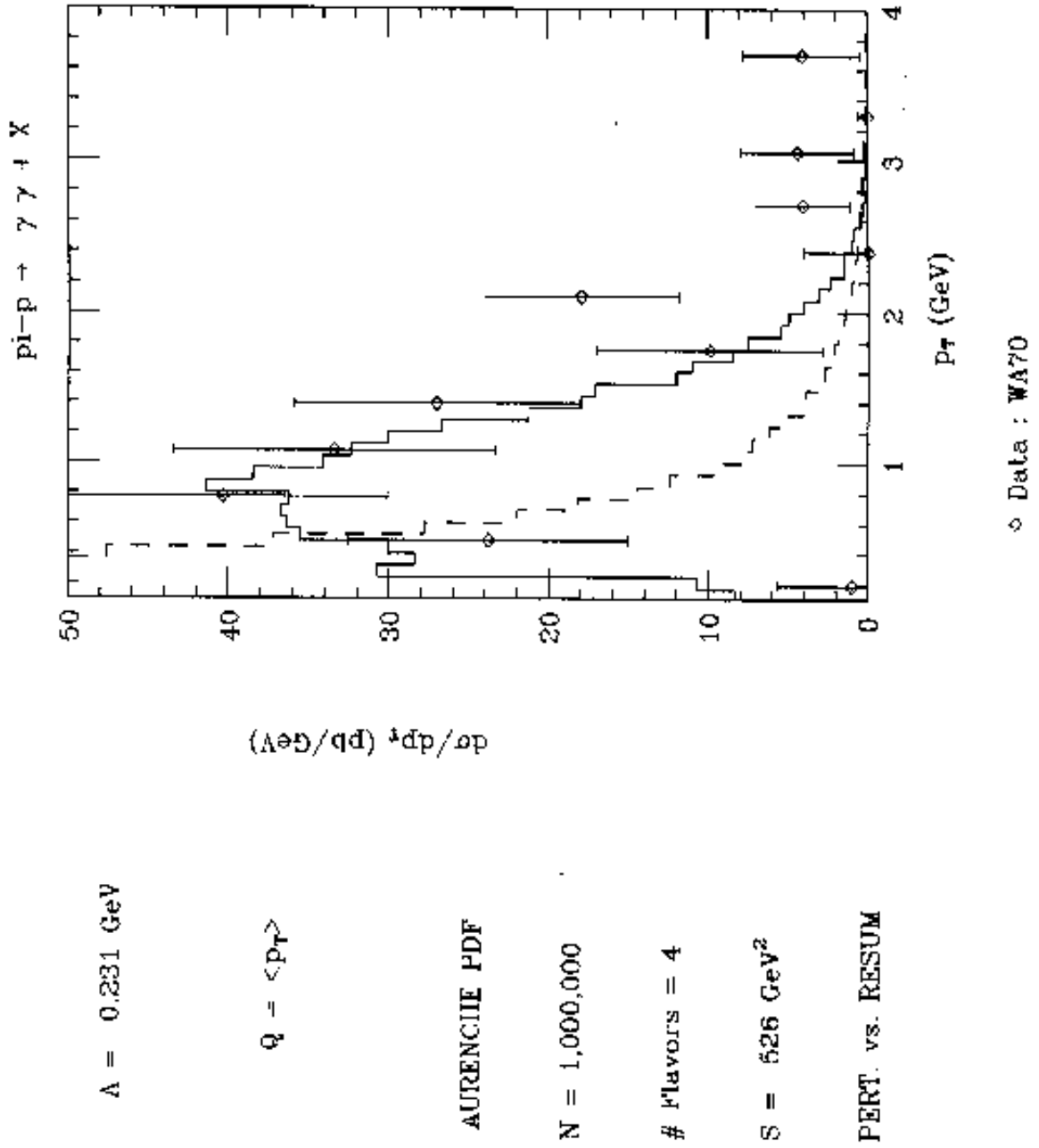


Figure D.1. $\pi^- p \rightarrow \gamma \gamma X$ pair p_T distribution.

REFERENCES

- [1] M. Gell-Mann, Phys. Lett. **8** (1964) 214.
- [2] G. Zweig, Preprints CERN-TH **401** and **412** (1964).
- [3] M. Han and Y. Nambu, Phys. Rev. **139B** (1965) 1006.
- [4] O.W. Greenberg, Phys. Rev. Lett. **13** (1964) 598.
- [5] M. Gell-Mann, Acta Phys. Austriaca Suppl. **9** (1972) 733.
- [6] J.D. Bjorken, Phys. Rev. **179** (1969) 1547.
- [7] W.K.H. Panovsky, *Proc. 14th Int. Conf. on High Energy Physics*, CERN Scientific Information Service, 1968, p.23.
- [8] G. 't Hooft, unpublished comments. See *Proc. Colloquium on Renormalization of Yang-Mills Fields and Applications to Particle Physics*, ed. C.P. Korthals-Altes, Marseilles, 1972.
- [9] D.J. Gross and F. Wilczek, Phys. Rev. Lett. **30** (1973) 1343.
- [10] H.D. Politzer, Phys. Rev. Lett. **30** (1973) 1346.
- [11] A. Zee, Phys. Rev. **D7** (1973) 3630.
- [12] H. Fritzsch and M. Gell-Mann, *Proc. XVI Int. Conf. on High Energy Physics*, eds. J.D. Jackson and A. Roberts, Fermilab, 1972, Vol. 2, p.135.
- [13] H. Fritzsch, M. Gell-Mann, and H. Leutwyler, Phys. Lett. **47B** (1973) 365.
- [14] R.P. Feynman, Phys. Rev. Lett. **23** (1969) 1415.
- [15] K.G. Wilson, Phys. Rev. **D14** (1974) 2455.
- [16] J. Kogut and L. Susskind, Phys. Rev. **D9** (1974) 697, 3391.
- [17] H.D. Politzer, Phys. Lett. **70B** (1977) 430.
- [18] A.P. Contogouris, S. Papadopoulos and J. Ralston, Phys. Lett. **104B** (1981) 70.; Phys. Rev **D26** (1982) 1280.

- [19] S.D. Drell and T.M. Yan, Phys. Rev. Lett. **25** (1970) 316.
- [20] S.D. Drell and T.M. Yan, Ann. Phys. **66** (N.Y. 1971) 578.
- [21] G. Sterman and S. Weinberg, Phys. Rev. Lett. **39** (1977) 1436.
- [22] T. Kinoshita, J. Math. Phys. **3** (1962) 650.
- [23] T.D. Lee and M. Nauenberg, Phys. Rev. **133B** (1964) 1549.
- [24] F. Bloch and H. Nordsiek, Phys. Rev. **52** (1937) 54.
- [25] H.D. Politzer, Nucl. Phys. **B129** (1977) 301.
- [26] R.K. Ellis *et al.*, Nucl. Phys. **B152** (1979) 285.
- [27] D. Amati, R. Petronzio and G. Veneziano, Nucl. Phys. **B140** (1978) 54; **B146** (1978) 29.
- [28] G. Altarelli and G. Parisi, Nucl. Phys. **B126** (1977) 298.
- [29] G. Altarelli, G. Parisi and R. Petronzio, Phys. Lett. **76B** (1978) 351,356.
- [30] CTEQ Collaboration, Rev. Mod. Phys. **67** (1995) 157.
- [31] C.T. Sachrajda, Phys. Lett. **73B** (1978) 185.
- [32] G. Altarelli, R.K. Ellis and G. Martinelli, Nucl. Phys. **B143** (1978) 521.
- [33] G. Altarelli, R.K. Ellis and G. Martinelli, Nucl. Phys. **B157** (1979) 461.
- [34] J. Kubar-André and F.E. Paige, Phys. Rev. **D19** (1979) 221.
- [35] C.G. Callan, Jr., and D.J. Gross, Phys. Rev. **D8** (1973) 4383.
- [36] G. Parisi, Nuc. Phys. **B59** (1973) 641.
- [37] J.K. Yoh *et al.*, Phys. Rev. Lett. **41** (1978) 684.
- [38] J. Kogut, Phys. Lett. **65B** (1976) 377.
- [39] J. Hinchcliffe and C. Llewellyn Smith, Phys. Lett. **66B** (1977) 281.
- [40] R. P. Feynman, R. D. Field and G.C. Fox, Phys. Rev. **D18** (1978) 3320.
- [41] K. Kajantie and R. Raitio, Nucl. Phys. **B139** (1978) 72.
- [42] H. Firtzsch and P. Minkowski, Phys. Lett. **73B** (1978) 80.
- [43] K. Kajantie, J. Lindfors and R. Raitio, Phys. Lett. **74B** (1978) 384.

- [44] Y. L. Dokshitzer, D.I. D'yakonov and S.I. Troyan, Phys. Lett. **79B** (1978) 269.
- [45] G. Parisi and R. Petronzio, Nucl. Phys. **B154** (1979) 427.
- [46] G. Curci and M. Greco, Phys. Lett. **92B** (1980) 175.
- [47] J.C. Collins and D.E. Soper, Nucl. Phys. **B193** (1981) 381; errata **B213** (1983) 545, **B197** (1982) 446.
- [48] G. Altarelli, R.K. Ellis, M. Greco and G. Martinelli, Nucl. Phys. **B246** (1984) 12.
- [49] J.C. Collins, D.E. Soper and G. Sterman, Nucl.Phys. **B250** (1985) 199.
- [50] B. Bailey, J.F. Owens and J. Ohnemus, Phys. Rev. **D46** (1992) 2018.
- [51] G. Curci, M. Greco and R. Srivastava, Phys. Rev. Lett. **43** (1979) 834; Nucl. Phys. **B159** (1979) 451.
- [52] P. Chiappetta, R. Fergani and J.Ph. Guillet, Phys. Lett. **B348** (1995) 646.
- [53] C. Balázs, E. Berger, S. Mrenna, C.-P. Yuan, Phys. Rev. **D57** (1998) 6934.
- [54] J.M. Hammersley and D.C. Handscomb, *Monte Carlo Methods*, Chaps. 3,5, Methuen (London, 1964).
- [55] A.H. Stroud, *Approximate Calculation of Multiple Integrals*, Chap. 6, Prentice-Hall (N.J., 1971).
- [56] H. Baer, J. Ohnemus and J.F. Owens, Phys. Rev. **D42** (1990) 61.
- [57] T. Muta, *Foundations of Quantum Chromodynamics*, World Scientific, Singapore, 1987.
- [58] M.E. Peskin and D.V. Schroeder, *An Introduction to Quantum Field Theory*, Addison-Wesley, Reading, 1995.
- [59] C.G. Callan, Phys. Rev. **D2** (1970) 1541.
- [60] K. Symanzik, Comm. Math. Phys. **18** (1970) 227.
- [61] J.F. Owens, Phys. Lett. **76B** (1978) 85.
- [62] R. Blankenbecker and S.J. Brodsky, Phys. Rev. **D10** (1974) 2973.
- [63] B.L. Combridge, J. Kripfganz, and J. Ranft, Phys. Lett. **70B** (1977) 234.
- [64] J.F. Owens, E. Reya, and M. Glück, Phys. Rev. **D18** (1978) 1501.

- [65] Cornell and J.F. Owens, Phys. Rev. **D22** (1980) 7.
- [66] H.L. Lai, J. Botts, J. Huston, J.G. Morfin, J.F. Owens, J. Qiu, W.K. Tung and H. Weerts; Preprint MSU-HEP/**41024**, CTEQ **404**.
- [67] J.C. Collins, D.E. Soper, and G. Sterman, in *Perturbative Quantum Chromodynamics*, ed. A.H. Mueller, World Scientific, Singapore, 1989.
- [68] H. Contopanagos, E. Laenen, and G. Sterman, Preprint **hep-ph/9604313** (1996).
- [69] J.C. Collins and D.E. Soper, Nuc. Phys. **B197** (1982) 446.
- [70] Landinsky, Yuan; Phys. Rev. **D50** (1994) 4239.
- [71] F. Landry, R. Brock, G. Ladinsky and C.P. Yuan, Preprint **hep-ph/9905391** (1999).
- [72] Davies, Webber, Stirling; Nucl. Phys. **B256** (1985) 413.
- [73] Ellis, Ross, Veseli, Preprint **hep-ph/9704239** (1997).
- [74] P.B. Arnold and R.P. Kaufmann, Nucl. Phys. **B349** (1991) 381.
- [75] Y. L. Dokshitzer, D.I. D'yakonov and S.I. Troyan, Phys. Lett. **78B** (1978) 290.
- [76] M.A. Kimber, A.D. Martin, and M.G. Ryskin, Preprint **hep-ph/9911379** (1999).
- [77] R.K. Ellis and S. Veseli, Preprint Fermilab-Pub-**97/207-T** (1997).
- [78] D.W. Duke and J.F. Owens, Phys. Rev. **D26** (1982) 1600.
- [79] S.D. Ellis, Z. Kunszt and D.E. Soper, Phys. Rev. **D40** (1989) 2188.
- [80] Z. Kunszt and D.E. Soper, Phys. Rev. **D46** (1992) 192.
- [81] R. Kauffman, Phys. Rev. **D44** (1991) 1415.
- [82] The Fermilab D0 Collaboration, Preprint **hep-ex/9912017** (1999).
- [83] The Fermilab E706 Collaboration, Preprint **hep-ex/9711017** (1997).
- [84] CTEQ Collaboration, Preprint **hep-ph/9903282** (1999).
- [85] C. Balázs and C.P. Yuan, Preprint **hep-ph/9704258** (1997).
- [86] The Fermilab E605 Collaboration, Phys. Rev **D43** (1991) 2815.

- [87] The CERN R209 Collaboration, Phys. Rev. Lett. **48** (1982) 302.
- [88] E. Laenen, G. Sterman, and W. Vogelsang, Preprint **hep-ph/0002078** (2000).
- [89] R.K. Ellis and J.C. Sexton, Nucl. Phys. **B269** (1986) 445.
- [90] J.F. Owens, Rev.Mod. Phys. **59** (1987) 465.
- [91] P. Aurenche, R. Baier, A. Douiri, M. Fontannaz and D. Schiff, Nuc. Phys. **B87** (1986) 553.
- [92] I.S. Gradshteyn and I.M. Ryzhik, *Table of Integrals, Series, and Products*, Academic Press, Inc., 1965.
- [93] V.D. Barger and R.J.N. Phillips, *Collider Physics*, Chap. 11, Addison-Wesley (1987).
- [94] L.J. Bergmann, Ph.D. Thesis, Florida State University (1979) Chap. 3.
- [95] M. Seymour, Notes from the CTEQ Summer School on QCD, CLRC (Lake Geneva, WI., 1997).
- [96] W.H. Press, B.P. Flannery, S.A. Teukolsky, W.T. Vetterling, *Numerical Recipes*, Chap. 7, Cambridge University Press (1989).
- [97] G.P. LePage, J. Comp. Phys. **27** (1978) 192.

BIOGRAPHICAL SKETCH

Christopher Edmond Fink

Personal

Date of Birth: **December 25, 1964.**
Place of Birth: **Milwaukee, WI., U.S.A.**
Marital Status: **Single.**
Languages: **English and Spanish.**
Nationality: **U.S.A.**

Education

2001 **Ph.D. in physics**, specialization in theoretical high energy physics, Florida State University.
Dissertation: “Transverse Resummation for Direct Photon Production”.
1995 **M.S. in physics**, Florida State University.
1987 **B.S., physics and philosophy**, University of Wisconsin, Madison.

Experience

1995 to present **Research Assistant**, High Energy Physics Dept., Florida State University.
1994 to 1995 **Teaching Assistant**, Department of Physics, Florida State University.
1987 to 1994 **Information Systems Analyst**, Temperature Control Specialties, Middleton, WI.

Research Interests

Theoretical high energy physics, particularly precision tests of QCD and application of renormalization group methods to extend the region of applicability of perturbation theory. Additional interests include grand unification, physics education, quantum coherence and computing, symbolic logic, and computational methods.

Ph.D. Dissertation Advisor

Joseph F. Owens at Florida State University.

Additional Research Advisors

Howard Baer, Vasken Hagopian, Elbio Dagotto, Jack Quine, all at Florida State University.